# THE DEVELOPMENT AND APPLICATION OF VERSATILE INTERACTING PEPTIDE (VIP) TAGS FOR ADVANCED IMAGING

By

**Julia Kim Doh**

## A DISSERTATION

Presented to the Department of Chemical Physiology and Biochemistry

and the Oregon Health & Science University

School of Medicine

in partial fulfillment of the requirements for the degree of Doctor of Philosophy

April 30 2020

## School of Medicine

## Oregon Health & Science University

---

Certificate of Approval

This is to certify that the Ph. D. dissertation of

**Julia Kim Doh**

has been approved.

_____
Kimberly Beatty, PhD (Mentor)

_____
Francis Valiyaveetil, PhD (Committee Chair)

_____
Caroline Enns, PhD

_____
Carsten Schultz, PhD

_____
Jim Korkola, PhD

_____
Claudia López, PhD

# TABLE OF CONTENTS

# ACKNOWLEDGEMENTS

Thank you to the generous funders that have supported me or my work. The Oregon Chapter of ARCS supported me directly from 2014-2017. I was awarded an OHSU Tartar Trust award in 2017. The work from this thesis from 2017 to present day was funded by NIGMS.

Thank you to Dr. Caroline Enns, whom I consider my co-mentor, and who welcomed me in her lab for lab meetings, training, and research assistance. Caroline shared a wealth of experience with me, be it professional or scientific, and has long been involved in my research endeavors and served on my dissertation advisory committee. Caroline's investment in the development of VIP tags allowed me to demonstrate some of the most exciting applications of my thesis research.

Thank you to my other committee members, including Dr. Francis Valiyaveetil, Dr. Carsten Schultz, and Dr. Jim Korkola. All of whom were generous in their time and advising. Francis and Carsten have both supported my research efforts with resources and expertise from their own labs. I thank Jim especially for his collaborations with our lab and his role in my day to day at the OCSSB, from reviewing my qualifying exam, running the RLSB journal club with Kimberly, and kind encouragement in the hallways.

Thank you to Dr. Claudia Lopez, who trained me for many hours over the years in electron microscopy. Claudia was also a kind mentor who was invested in my success and a source of positive reinforcement when I needed it most. I was invited to speak at Microscopy and Microanalysis 2019 and won a student scholar award and was proud to represent OHSU and the Multiscale Microscopy Core that day.

Thank you to Dr. Stephanie Kaech-Petrie and Dr. Crystal Chaw at the Advanced Light Microscopy Core. Their patience and enthusiastic assistance made fluorescent imaging a fun and integral part of my research endeavors.

Thank you to Dr. Cheryl Maslen and Crystal Paredes, who showed me empathy and helped me during an unforeseen situation in my first year. Their swift aid affirmed to me that I made the right choice in attending OHSU and that this was a graduate program that cared for the well-being of its students.

Thank you to Dr. Samantha Levine, Dr. Katie Tallman, Dr. Hannah Zane, and Dr. Jon White. In the earlier years of the Beatty group, I relied heavily on the expertise of those senior to me and they were all patient, enthusiastic and helpful in my journey as a graduate student.

Thank you to Savannah Tobin, whom I consider my best ever coworker (to-date). Savannah is a dedicated, conscientious and practical scientist, and an endless source of encouragement in the lab. I am proud to be a co-first authors on our recent manuscript and look forward to becoming colleagues in our future careers.

Thank you to my family, my mother, Kim, and my sister, Leah, for always having a home for me to return to. To my mother especially for her parentage, for inspiring me to invest in my education and independence, and for teaching me that a happy and fulfilled life is my right.

Thank you to Emilio and William, for their enduring friendship, love and care. These gifts carried my mind and body through the challenging years of earning my doctorate.

Finally, thank you to Dr. Kimberly Beatty, my mentor, for training me into the scientist I am today. For sharing her enthusiasm for ambitious and rigorous science, for her positive and kind management, and for her optimistic yet practical outlook. I consider myself as having a successful PhD experience and it was in no small part due to her mentorship.

# LIST OF TABLES

# LIST OF FIGURES AND SCHEMES

# ABSTRACT

Microscopy allows researchers to detect and track proteins in their endogenous cellular environment and thus interrogate protein structure, function, distribution, and interactions. A protein must be tagged by a reporter to generate contrast between itself and its environment, with different types of reporters corresponding to different microscopy methods. We have developed a new type of genetically-encoded protein tag, called Versatile Interacting Peptides (VIP) tags. VIP tags use a heterodimeric coiled-coil interaction to label proteins. The probe peptide can be covalently linked to either fluorescent or electron-dense reporters, making the VIP technology compatible with imaging across different platforms and size scales. VIPs are small (<7 kDa), offering a substantial size reduction from commonly used protein tags such as fluorescent proteins. VIP tags label protein targets specifically for analysis in vitro or in cells, by flow cytometry, light microscopy, and electron microscopy. New tags were validated using a number of model proteins, including cytoplasmic targets (e.g., actin, histone 2B, and TOMM20) and membrane receptors, such as transferrin receptor 1 (TfR1). We demonstrated that VIP tags can be used for a number of applications, including visualizing multiple targets in one cell. VIP tags can also be combined within the cell to artificially dimerize targets and change a protein's localization. The development and validation of the VIP Y/Z, VIPER and MiniVIPER tags are detailed in Chapters 2, 3, and 4. Detailed step-by-step methods regarding probe peptide production, fluorescence imaging, and correlative light and electron microscopy are described in Appendices A, B, and C. Appendix D details preliminary work using VIP tags to elucidate mechanisms used by cells to sense and respond to iron levels.

# Chapter 1: Labeling strategies for imaging cellular proteins


## Abstract

Biological imaging relies on the ability to generate contrast between the target of interest and the cell. Proteins are specifically labeled with reporters compatible with either light microscopy or electron microscopy or both. This chapter provides a broad overview of methods for protein labeling for imaging and a description of Versatile Interacting Peptide (VIP) tags, a new technology for labeling proteins for microscopy. VIP tags are discussed herein in the context of: 1) peptide tags for imaging and 2) tags for electron microscopy. VIP tags are part of an effort to develop small peptide tags (<7 kDa), without sacrificing specificity or utility. VIP tags are also a new genetically-encoded tag for electron microscopy, which has far fewer options compared to protein tags for fluorescent imaging.


## Background

Microscopy is an integral tool for biology due to the ability to interrogate biomolecules in their native cellular environment. Insights made available by imaging include trafficking, structure, abundance, and interactions with other biomolecules. The field of cell biology relies heavily on light and electron microscopy (EM). In recent years, high resolution imaging methods such as super-resolution microscopy (SRM)[1–4] and correlative light and electron microscopy (CLEM)[5–10] have enabled new discoveries of the localization, interactions and architecture of cellular proteins.

Proteins are a common target of study by imaging. However, visualizing proteins can be challenging due to their lack of inherent contrast with their cellular environment. Therefore, a common strategy is to attach a reporter molecule with the desired physical properties in order to highlight the protein of study. For light-based imaging this reporter should “light up” in the dark, either by generating bioluminescence or fluorescence in response to illumination. For EM, the reporter should be electron-dense, and often employs the use of heavy metals.

This chapter will contextualize the work presented in this thesis by discussing two topics in detail: genetically-encoded peptide tags for fluorescence imaging and genetically-encoded tags for EM. In order to provide context for these two topics, a broad overview of labeling methods used for biological imaging will be discussed first. These methods include immunolabeling, fluorescent proteins, and self-labeling enzymes, which are all widely implemented solutions to labeling proteins. Next, peptide tags will be introduced as a strategy to address some of the shortcomings of large protein tags. This group of tags can be further divided based on the strategy employed: enzyme-modified peptides, peptide detection by a protein domain, and labeling via coiled-coil dimer formation. Lastly, developing tags for EM remains a nascent field relative to advances made in labeling proteins for fluorescence. The final section of this chapter discusses genetically-encoded tags for EM imaging. These EM-compatible tags include proteins that chelate metal, enzymes that generate singlet oxygen for polymerization of diaminobenzidine, and VIP tags, which enable nanoparticle attachment via a coiled-coil.

## 1.1 Immunolabeling

A commonly used method for labeling proteins for either light or EM is immunolabeling. Antibodies, such as immunoglobulin G (IgG), have high affinity for the target protein and can be modified in vitro with a number of different reporters. The antibody that binds the target (the primary antibody) can be labeled directly with the reporter. Reporter flexibility can be further enabled by secondary detection, whereby the primary antibody binds the target protein, and a secondary antibody carrying the reporter binds the primary antibody. There is a wide variety of reporter-labeled secondary antibodies, maximizing the imaging applications for the researcher. Antibodies are typically functionalized in vitro with reporter probes through reaction between primary amines (lysines) and N-hydroxysuccinimide (NHS) esters. The site of modification is not specific and often results in multiple fluorophores per antibody.

Although antibodies are commonly used and widely accepted for specific labeling of proteins, they have a number of important drawbacks. Firstly, IgG is a comparatively large biomolecule, weighing 155 kDa and measuring 14.5 nm × 8.5 nm × 4.0 nm[11]. This

presents logistical challenges, such as steric hindrances and the difficulty of introducing such a large molecule into living cells. Reaching intracellular targets with a large antibody is often in conflict with preservation of cellular structures since it requires permeabilization of the cell membrane, often using strong detergents. As a result, antibodies are inappropriate for live, intracellular labeling. Another consideration against antibodies, as biologists adopt more high resolution techniques, are the resolution artifacts resulting from the antibody size. With secondary detection, the reporter is displaced up to 60 nm away from the protein target[12]. This would negate any resolution benefits of SRM or EM techniques that can resolve <50 nm. Lastly, one of the key disadvantages of antibodies is that their performance varies from antibody to antibody. Antibodies can have low efficiency[13–15], meaning that a low percentage of target protein will be successfully labeled. Antibodies can also have cross-reactivity[16–18], meaning that they can bind incorrect targets or create non-specific labeling. A failure to validate antibodies beforehand creates issues downstream when research using these antibodies is unable to be reproduced[17].

Antibody fragments address the large size of IgG[19,20]. A “conventional” antibody (e.g. IgG) is made of two heavy chains and two light chains that are held together by disulfide bonds (**Figure 1.1**). The heavy and light chains both contribute an identical copy of the antigen binding site, named VH and VL (heavy and light). The upper half of the antibody that binds the antigen is made up by heavy and light chain domains and is known as the Fab (antibody fragment). The heavy chain-only lower half of the antibody does not participate in antigen recognition and is known as Fc (crystallizable fragment, from early protein crystal studies). The antibody molecule can be fragmented so that only the antigen-binding domain is preserved for labeling proteins. These fragments can then be reporter-labeled for imaging. These fragments include using the Fab alone (50 kDa) or scFv, which is made of only VH and VL (30 kDa)[19,20]. A peptide linker is used to keep the VH and VL fragments of the scFv together in the absence of the cysteine bonds found in the intact antibody.

Recently, antibodies from camelid or shark species have been used to make even smaller immunolabeling reagents (**Figure 1.1**). These antibodies are comprised of the heavy chain only, making the Fab smaller than that of heavy and light chain IgG

antibodies[19–22]. Nanobodies are single domain antibody fragments derived from the VHH antigen-binding domain of heavy chain only of camelid antibodies. Nanobodies are small, ~15 kDa[22], and can be modified with fluorescent reporters, allowing them to be used for imaging.

Despite the benefits of antibody fragments, they are not as common as full-sized IgGs. This is partially due to their recent discovery[21,22] and their unusual animal origin (camelids compared to rodent, goat, or rabbit). Antibody fragments, like full size antibodies, vary from product to product, but do not inherently have greater or lower affinity[20,23] than full size antibodies. Antibody fragments and nanobodies share the same need for prior validation in order to account for variability in target labeling efficiency and cross-reactivity. Nevertheless antibody fragments represent an upcoming paradigm shift in immunolabeling.

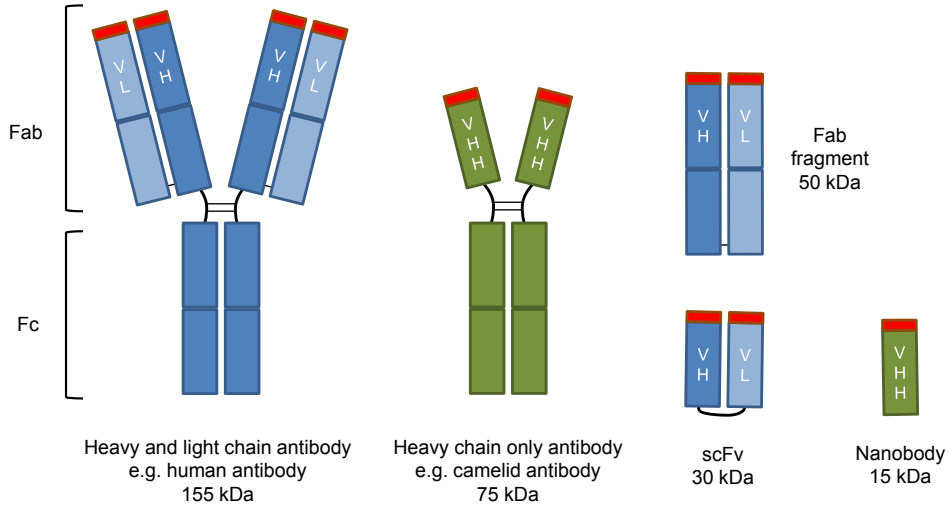


**Figure 1.1. Comparing full length IgG antibodies with antibody fragments.** Components that make up the heavy chain in the human IgG antibody are depicted in dark blue, and the light chain is depicted as light blue. The camelid antibody, which is heavy-chain only, is depicted in green. The antigen binding site is depicted in red. VH and VL are the heavy (H) and light (L) chain domains of the antigen binding portion of a heavy and light chain antibody. VHH is the antigen binding domain of a heavy chain only antibody.

## 1.2 Genetically-encoded protein tags

A major solution to the variable specificity of antibodies is a genetically-encoded tag. By employing a genetic fusion to the protein of interest, the protein tag is therefore covalently attached to the target protein during translation. The field of genetically-

encoded protein tags for imaging is reaching 50 years, with a truly wide and varied stable of options at the biologist's disposal[24,25].

The most widely employed and well-known protein tag for imaging is the green fluorescent protein (**Figure 1.2**). Originally discovered as a by-product of purifying aequorin from jellyfish[26,27], the green fluorescent protein spawned the development of genetically-encoded fluorescent proteins in various colors and for functional applications[25,28,29]. The major advantage to fluorescent proteins is that tagged proteins are automatically fluorescent due to the chromophore that forms within the barrel structure of the fluorescent protein. This aspect revolutionized live cell imaging applications, allowing biologists to image proteins inside live cells over time. This first generation of imaging protein tags, however, was limited by a key element: the fluorescent protein's chromophore. The chromophore, which is formed by internal residues within the beta-barrel hollow of the fluorescent protein, requires oxygen for maturation and has limited optical properties. This limits the brightness, photostability, and applications of fluorescent proteins.

Self-labeling proteins are a subsequent generation of imaging protein tags that address the disadvantages of the fluorescent protein chromophore. This is done by combining the specificity of a genetically-encoded tag with the wide array of optical properties afforded by small molecule fluorophores. Functionally, target proteins are tagged with a protein that allows them to be specifically labeled with small molecule fluorophores.

The first approach is a self-labeling enzyme, whereby a protein domain is fused to an enzyme that specifically reacts with fluorophore substrates (**Figure 1.2B**). The most well-employed versions of this strategy are HaloTag (33 kDa)[30] and SNAP (19 kDa)[31] (and its orthogonal partner, CLIP[32]); see **Table 1.1**. A non-covalent version of this strategy includes the DHFR tag (18 kDa) which binds trimethoprim ligands[33,34] (**Figure 1.2C**). There are additionally protein tags where the protein tag binds the fluorogenic ligand in a non-covalent manner and causes fluorescence to turn on. This includes fluorogen activating proteins (FAPs)[35,36] and Fluorescence-Activating and absorption-Shifting Tag (FAST) [37,38]. One drawback of these protein tags, however, is

that their size (14-33 kDa) does not offer substantial improvement compared to a fluorescent protein (27 kDa).

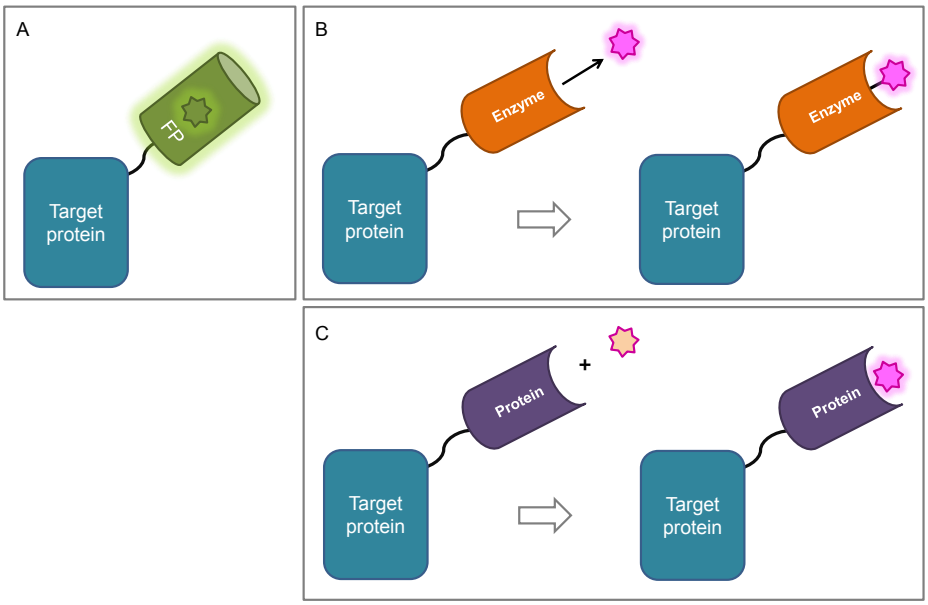


**Figure 1.2. Commonly used protein tags for labeling proteins for fluorescence.** These approaches include: (**A**) endogenously fluorescent proteins (FP), such as the green fluorescent protein; (**B**) enzymes that covalently react with a fluorophore molecule (i.e., SNAP or HaloTag); or (**C**) protein tags that bind a fluorophore or fluorogenic ligand (latter is depicted).

## Table 1.1. Properties of genetically-encoded protein tags.

| Protein Tag | Size (kDa) | Fluorophore | Ligand Binding |
|---|---|---|---|
| GFP[26,27] | 27 | Post-translationally formed chromophore | N/A |
| SNAP[31,39] | 19 | $O^6$-benzylguanine derivatives | Covalent |
| CLIP[32] | 19 | $O^2$-benzylcytosine derivatives | Covalent |
| HaloTag[30,40] | 33 | Chloroalkane derivatives | Covalent |
| DHFR[33,34] | 18 | Trimethoprim derivatives | Non-Covalent |
| Fluorogen Activating Proteins[35] | 26 | Malachite green or thiazole orange | Non-covalent |
| Fluorescence-Activating and absorption-Shifting Tag (FAST)[37] | 14 | 4-hydroxybenzylidene-rhodanine or 4-hydroxy-3-methylbenzylidene-rhodanine | Non-covalent |

## 1.3 Peptide Tags

There is another approach to using genetically-encoded tag proteins with a chemical fluorophore that relies on peptide tags. For the purposes of this chapter, a peptide is defined here as <7 kDa. Peptide tags appeal to the biological imaging community because their smaller size makes them less likely to perturb the biological function of proteins in cells.

Peptide tags rely on a diversity of mechanisms which will be covered in further detail in this section. The tetracysteine, tetraserine and hexahistidine tags are unique, and will be described first. From there, there are three additional strategies for labeling a peptide-tagged protein for imaging (**Figure 1.3**). The first method is covalent attachment of the fluorophore to the peptide via an exogenous enzyme (**Figure 1.3A**). This takes advantage of the chemoselectivity of enzymes in order to specifically modify the tag with a substrate for imaging. The second approach uses tags that are recognized and bound by a reporter domain (**Figure 1.3B**). These include epitope tags and tags that bind to non-antibody proteins. The final class of peptide tags is the coiled-coil tags, which include the VIP tags (**Figure 1.4**).

A summary of the peptide tags discussed in this chapter is provided in **Table 1.2**.

## Table 1.2. Properties of genetically-encoded peptide tags.

| Peptide Tag† | Amino acid sequence | Tag size (kDa) | Recognition partner | Final size (minus the reporter, kDa) |
|---|---|---|---|---|
| Tetraserine tag[41,42] | SSPGSS | 0.5 | RhoBO | 0.5 |
| Tetracysteine tag[40] | CCPGCC | 0.6 | FlAsH-EDT2 or ReAsH-EDT2 | 0.6 |
| Hexahistidine[43,44] | HHHHHH | 0.8 | HisZiFiT[45] or antibody | 0.8 (HisZiFiT) or ~155 (antibody) |
| FLAG tag[46,47] | DYKDDDDK | 1.0 | Antibody | ~155 |
| HA tag[48] | YPYDVPDYA | 1.1 | Antibody | ~155 |
| Myc tag | EQKLISEEDL | 1.2 | Antibody | ~155 |
| Sfp Tag[49] | GDSLSWLLRLLN | 1.4 | probe-CoA conjugate | 1.4 |
| AcpS Tag[49] | GDSLDMLEWSLM | 1.4 | probe-CoA conjugate | 1.4 |
| BC2 (Spot) Tag[50] | PDRKAAVSHWQQ | 1.4 | BC2 (Spot) Nanobody (15.0 kDa) | 16.4 |
| SnoopTag[51] | KLGDIEFIKVNK | 1.4 | SnoopCatcher (14.9 kDa) | 16.3 |
| SpyTag[52] | AHIVMVDAYKPTK | 1.5 | SpyCatcher (15.3 kDa) | 16.8 |
| ALFA Tag[53] | SRLEEELRRRLTE | 1.7 | ALFA Nanobody (15.0 kDa) | 17.7 |
| Moon Tag (per gp41 unit)[54] | KNEQELLELDKWASL | 1.8 | gp41 GFP Nanobody (47.4 kDa) | 49.2 |
| $GFP_{11}$ (tag)[55–57] | RDHMVLHEYVNAAGIT | 1.8 | $GFP_{1-10}$ (24.0 kDa) | 25.8 |
| AviTag[58,59] | GLNDIFEAQKIEWHE | 1.8 | biotin-probe | 1.8 |
| LAP Tag[60] | DEVLVEIETDKAVLEVPGEEE | 2.3 | lipoic acid probe | 2.3 |
| CCE3 (tag)[61] | EVAALEKEVAALEKEVAALEK | 2.2 | CCK3 (probe) (2.2 kDa) | 4.4 |
| E3 (tag)[62–65] | EIAALEKEIAALEKEIAALEK | 2.3 | K3 (probe) (2.3 kDa) or acyl transfer reaction[64,65] | 4.6 (K3) or 2.3 (acyl transfer) |
| SunTag (per GCN4 unit)[66] | EELLSKNYHLENEVARKLKK | 2.4 | scFV-GFP (71.8 kDa) | 74.2 |
| MiniE (tag) | LEIEAAFLERENTALETRVAELRQRVQRLRNEYGPL | 4.3 | MiniR (probe) (7.3 kDa) | 11.6 |
| MiniR (tag) | LEIRVAFLRQRNTALRTEVAELEQEVQRLENRYGPL | 4.3 | MiniE (probe) (7.3 kDa) | 11.6 |
| CoilE (tag)[67] | LEIEAAFLERENTALETRVAELRQRVQRLRNRVSQY RTRYGPL | 5.2 | CoilR (probe) (7.5 kDa) | 12.7 |
| ZIP Dimer (tag)[68–70] | WGALKKELEAAKKELEALKKELAGGCGGALEKELEA LEKEAEALEKELA | 5.3 | ZIP Monomer (probe) (2.3 kDa) | 7.6 |
| CoilY (tag)[71] | NTVKELKNYIQELEERNAELKNLKEHLKFAKAELEF ELAAHKFE | 5.3 | CoilZ (probe) (8.7 kDa) | 14.0 |
| CoilZ (tag)[71] | QKVAQLKNRVAYKLKENAKLENIVARLENDNANLEK DIANLEKDIANLERDVAR | 6.2 | CoilY (probe) (7.8 kDa) | 14.0 |

† Tags are color-coded: Gray = six-residue metal/metalloid binding tag; Orange = Enzyme-modified tags; Dark Blue = epitope tags; Light Blue = peptide targeting tag + binding protein; Green = coiled-coil peptide tags.

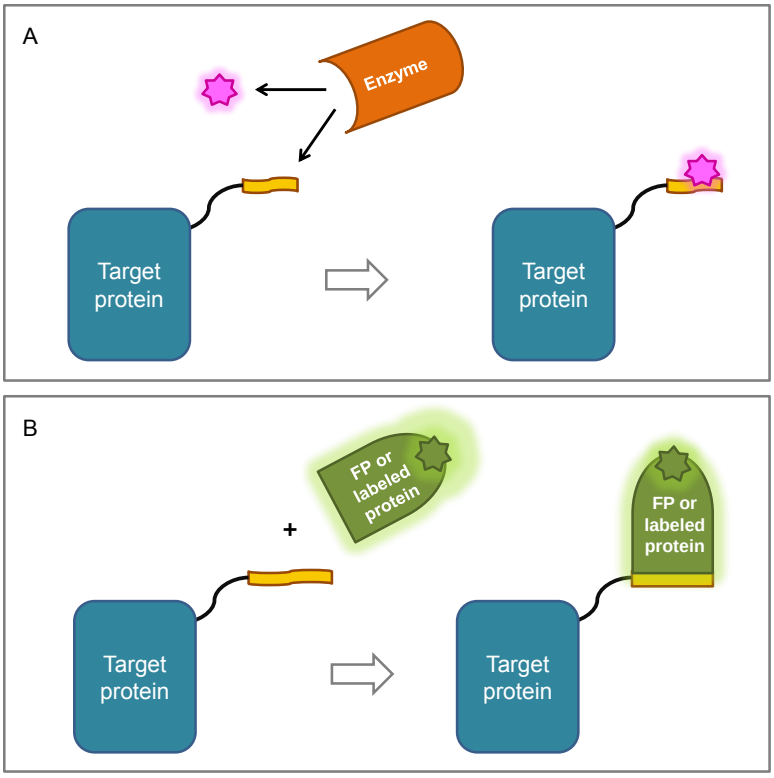


**Figure 1.3. Strategies using peptide targeting tags.** (**A**) Tagging with a peptide sequence that is selectively modified with a fluorophore via an enzymatic reaction. (**B**) Tagging with a peptide sequence that targets it for binding by either a fluorescent protein or a fluorophore-labeled protein.

### Peptide Tags: Metal or metalloid binding tags

The smallest tags are the 6-residue tags that bind a fluorescent ligand that coordinates a metal or metalloid. These tags uniquely feature residue repetition as part of their design: hexahistidine, tetracysteine, and tetraserine. These are distinctive tags that make use of coordination complexes, allowing the residues of the peptide tag to bind the metal or metalloid in a specific geometry.

The first example, the hexahistine tag (HHHHHH), is unique because the histidine residues can bind copper, nickel, or cobalt that is chelated by nitrilotriacetic acid (NTA)[43,44]. Chelated metals can be functionalized with fluorophores to create a cell-impermeable imaging probe to detect hexahistidine-tagged receptors. This was demonstrated by the Tsien group with HisZiFiT[45]. The hexahistidine tag can also be recognized with antibodies[72,73], albeit with some known variability in specificity[74].

The next two examples bind either a bi-arsenical or bis-boronic fluorescent ligand. The first demonstration was the tetracysteine tag, which was developed by the Tsien group (UC San Diego) and consists of the peptide sequence: CCPGCC. The particular arrangement of the sulfhydryl groups in this tag enables it to bind bi-arsenical ligands, namely FlASH or ReASH, which are fluorescein and resorufin-based fluorophores, respectively[41,42]. In cells, these bi-arsenical fluorophores can experience cross-reactivity with cysteine-rich proteins and the toxicity of arsenic requires administration of the ligand with an antidote. Since binding is dependent on the spatial geometry of the sulfhydryls and biarsenics, the choice of fluorophores is limited to those derived from the xanthene structure. An analogous strategy to tetracysteine that overcomes the cross-reactivity with cysteine-rich proteins was designed by the Schepartz group (Yale). This group designed a tetraserine motif (SSPGSS) that complexes a bis-boronic rhodamine derivative (RhoBo)[40].

**Peptide Tags: Enzyme-modified tags**

There are a number of peptide targeting tags that employ the enzymatic modification method. This includes the AviTag (GLNDIFEAQKIEWHE) from the Ting group (Stanford). Proteins tagged with AviTag are recognized and specifically biotinylated by biotin ligase, BirA. The biotinylated protein is then detected by streptavidin-conjugated reporters[58,59]. Ting and coworkers additionally designed the LAP tag (DEVLVEIETDKAVLEVPGEEE). Proteins expressing the LAP tag are modified with lipoic acid-attached fluorophores[60] or “clickable” reactive-handles[75] by lipoic acid ligase. The Walsh group (Harvard) employed similar approaches using phosphopantetheinyl-transferases to modify a short sequence with CoA-derived fluorescent probes[49]. These included the Sfp tag (GDSLSWLLRLLN) and AcpS tag (GDSLDMLEWSLM). Indeed, the co-opting of enzymatic chemoselectivity is a reliable strategy for labeling proteins via direction of a peptide targeting tag. There are, however, some experimental restrictions to this enzyme-mediated labeling strategy. Labeling by BirA or Sfp/AcpS can be slow (about 1 hour), due to the reliance on accumulated enzymatic activity to generate appreciable imaging signal. This can limit applications aiming to study processes that happen on a faster timescale. Additionally, these

methods can be restricted to cell surface-exposed targets. The LAP tag is the only tag in this class that has fast labeling (10 min) and can label targets inside cells, albeit the reporter choice is restricted to coumarin (blue) or resorufin (red).

**Peptide tags: Peptide-binder tags**

The second class of peptide targeting tags, referred here as peptide-binder tags, are tags that bind a larger, more structured molecule (>10 kDa) that is fluorescent. This approach contrasts the previous method in that the peptide tag carries the bulk of the protein binding component at the time of imaging. These binders are reporter-labeled either due to fusion to a fluorescent protein, conjugation to a small molecule fluorophore (e.g., fluorescent antibodies), or are fluorescent proteins themselves (**Figure 1.3B)**.

The main benefit of peptide-binder tags is their small size. They are smaller than coiled-coil tags, which are discussed in the next sub-section of this chapter. These experimental systems require the addition of an exogenous protein however, whether it is an enzyme, fluorescent protein or fluorescently-labeled antibody. These labeling proteins have varying sizes, from 12 kDa (nanobody[52,55,74]) to 14,000 kDa (multiple copies of scFv-GFP[69]). If the binding component is large, it can result in cellular perturbations as a result of co-expression or introducing the exogenous component inside or on living cells. Lastly, any peptide tags with lysine residues in their sequences are sensitive to amine-based chemical cross-linking and might be incompatible with fixed-cell applications.

The first example of the peptide-binder strategy is epitope tags. These are small tags between 6 and 10 residues that are recognized by an antibody. They have the benefit of being one of the smaller tags discussed in this chapter while accessing the diversity of reporters afforded by antibody labeling. The FLAG tag is one of the earliest and most widely adopted epitope tags (DYKDDDDK), being intentionally designed for antibody detection[46,47]. The HA tag (YPYDVPDYA)[48] and myc tag (EQKLISEEDL)[77] are additional epitope tags using this strategy. Since these tags rely on antibody detection, the issues previously discussed with regards to antibody specificity and size still apply. These tags are more frequently used for affinity-based purification of proteins in cell lysates than they are used for fluorescent imaging[78].

Another example is the SunTag, which is an epitope tag derived from GCN4 that was developed by the Vale group (UC San Francisco). The SunTag (EELLSKNYHLENEVARKLKK) is bound by an antibody single chain variable fragment (scFv) that is genetically fused to a fluorescent protein[66]. Tandem repeats of GCN4 can be employed, whereby up to 24 GCN4 peptides could be added to a target protein, thus attaching 24 copies of scFV-GFP per peptide tag. Tandem epitope tagging results in bright, photostable fluorescence. A sister system has since been developed, named the Moon tag, that makes use of a nanobody-fused fluorescent protein or HaloTag that binds a 15 amino acid gp41 peptide tag (KNEQELLELDKWASL)[54].

On the topic of antibody fragments, the epitope tag and antibody fragment binding approach has continued to evolve by using smaller binding fragments compared to scFv. Another example was the 12-residue BC2 tag (PDRKAAVSHWQQ), a short peptide recognized by a nanobody[50,76] that was developed by the Rothbauer group (Eberhard Karls University Tuebingen). A similar tag, the ALFA tag (SRLEEELRRRLTE), is a small helical peptide recognized by the ALFA nanobody[53] that was developed by Opazo and Frey (Nanotag Biotechnologies). Both the BC2 tag and ALFA tag have demonstrated use with super-resolution microscopy[50,53].

Peptide-binder tags can also be detected using non-antibody protein reporters. The SpyTag is a 13 residue peptide tag (AHIVMVDAYKPTK) that forms a covalent bond with SpyCatcher (12.3 kDa)[52]. SpyTag was developed by the Howarth group (University of Oxford). SpyCatcher is fluorescently labeled in vitro to allow for imaging of Spytagged proteins. SpyCatcher and SpyTag were developed from split engineering of the CnaB2 domain of FbaB protein in *Streptococcus pyogenes* (*S. py*). Orthogonal systems based on the same principles have been developed, including SnoopCatcher/SnoopTag[51] (derived from RrgA protein in *Streptococcus pneumoniae*).

The final peptide-binder tag makes use of split-FP methodology that was developed by the Huang group (UC San Francisco). Fluorescent proteins are barrels constructed of beta sheets, where interior residues react to form the fluorescent chromophore. The 11$^{th}$ beta-strand of GFP ($GFP_{11}$) can be removed from the protein structure and fused to a protein of interest to act as a peptide tag. When this peptide tag encounters strands 1-10 of GFP ($GFP_{1-10}$), the full protein and fluorescent chromophore

is formed[55–57]. Similarly to the SunTag, tandem repeats of $GFP_{11}$ can be used to attach multiple GFPs to a molecule, resulting in bright labeling.

There are drawbacks to using the peptide tag and binder approach. For methods relying on binders that are conjugated to chemical fluorophores, the applications are restricted to imaging targets on the cell surface. Targets can be imaged in live cells if the binder is fused to a fluorescent protein (such as scFv-GFP or SpyCatcher-GFP) or is a fragment of a fluorescent protein ($GFP_{1-10}$). However the trade-off is now the target protein is modified by a large protein, diminishing the benefit of using a small peptide tag.

**Peptide Tags: Coiled-coil peptide tags**

Coiled-coil peptide tags differ from peptide targeting tags in that the genetic tag is a peptide (2.2-6.2 kDa) and the exogenously added probe is also a peptide (2.2-8.7 kDa). The probe peptide can be conjugated to a fluorophore or template a proximity-induced reaction that labels the peptide tag directly with a fluorophore[79]. One of the benefits of this approach is that the binding probe is also a small peptide, compared to a large protein (e.g., $GFP_{1-10}$ or scFV-GFP).

The rationale for this strategy is that high specificity can be afforded by a longer sequence, resulting in mutually high affinity between the tag and the probe. This results in a fast labeling time (15 min or less)[79]. Many of these tags were used to image fast processes, such as receptor trafficking. By the same token, coiled-coil labeling can also be restricted to imaging the cell surface due to the cell-membrane impermeance of the probe peptides in living cells.

Coiled-coils are a well-studied protein motif made of interacting alpha helices. Dimerizing coiled-coils rely on a repeat heptad motif, $(abcdefg)_n$, where each position has a defined role in coiled-coil structure and formation[80,81]. The *a* and *d* positions are occupied by hydrophobic residues that form the core of the coiled-coil interaction. The *e* and *g* positions are occupied by charged residues that form salt bridges across the hydrophobic core. These salt bridges contribute to the stability and specificity of the dimer as well as the orientation of the two coils (parallel or antiparallel). Given the

simple design principles of coiled-coils, there have been a number of published coiled-coil sequences designed rationally by hand[82–86] or computationally[87–91].

The most straightforward use of coiled-coil tagging is labeling a coiled-coil peptide tag with the cognate probe peptide that is reporter-labeled (**Figure 1.4A**). This method frequently employs previously-published coiled-coil designs. The E3-K3[82] peptide pair ($K_D$ = 70 nM) is well-represented in this approach, and several research groups have used this peptide pair to label many different proteins on the cell surface[62,83,92,93]. E3-K3 was first used by the Matsuzaki group (Kyoto University) to image membrane receptors[63]. E3 was used as the peptide tag while K3 or K4 were used as the probe to deliver the reporter.

The Xia group (Chinese University of Hong Kong) used the CCE-CCK coils they designed to label tagged proteins in a similar manner, however they also included the formation of a thioether bond to covalently link the peptides upon coiled-coil dimerization[61].

The Versatile Interacting Peptide (VIP) tags, discussed at length in this thesis, were also sourced from existing coiled-coils and are introduced in depth in the final section of this chapter. VIP Y/Z[71] (comprised of CoilY and CoilZ) was designed from heterodimeric coiled-coil sequences published by the Keating group ($K_D$ < 15 nM)[88,89]. VIPER[67] (comprised of CoilE tag and CoilR probe) was designed from a sequence published by the Vinson group ($K_D$ < 13 pM)[84]. The Beatty group (OHSU) designed MiniVIPER[94] (comprised of MiniE and MiniR) by truncating the VIPER sequence (among other changes). The VIP coiled-coil tags will be discussed in more detail in Section 1.5.

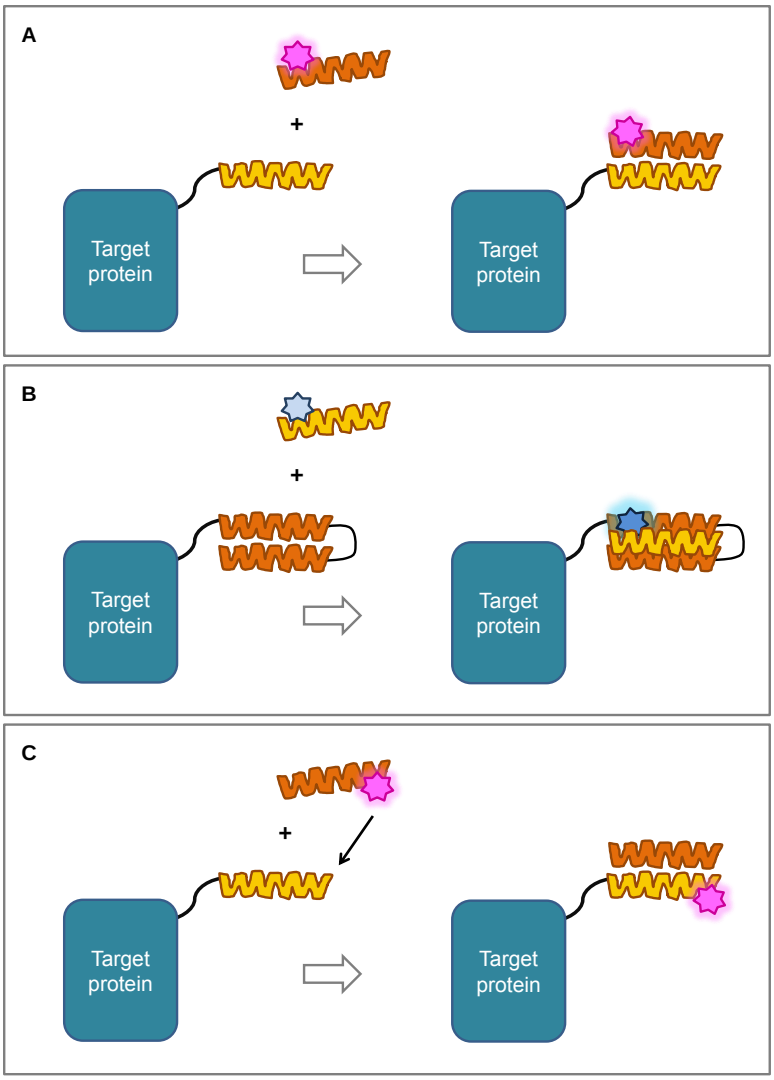


**Figure 1.4. Types of coiled-coil peptide tags. (A)** Tagging with a coiled-coil peptide tag that non-covalently binds a fluorophore-labeled probe peptide. This is the strategy used for VIP tags. **(B)** Tagging with a fluorogenic peptide trimer. The protein is tagged with a dimer that binds a third probe peptide that carries an environmentally-sensitive fluorophore that "turns on" upon binding. **(C)** Tagging with a coiled-coil peptide tag that templates a reaction that transfers the fluorophore from the probe peptide to the tag peptide.

The Tamamura group (Tokyo Medical and Dental University) developed a fluorogenic coiled-coil ZIP system made of a peptide trimer[68] (**Figure 1.4B**). The ZIP probe peptide carries a 4-nitrobenzo-2-oxa-1,3-diazole (NBD), which is an environmentally sensitive fluorophore that experiences an increase in fluorescence in a hydrophobic environment. The ZIP peptide tag is two alpha-helical anti-parallel coiled-coils that bind the probe peptide to form the completed trimer. Upon binding the peptide

tag pair, the NBD fluorophore becomes buried in the hydrophobic binding interface and blue fluorescence is detected. The Tamamura group later showed that this interaction can be further stabilized with the addition of a disulfide bridge[69]. They have used the ZIP system inside cells by addition of a cell penetrating peptide on the peptide probe[70].

Some coiled-coil tags mediate a proximity-induced covalent reaction between the tagged protein and the reporter molecule (**Figure 1.4C**). The Seitz group (Humboldt University of Berlin) employed an acyl transfer reaction between the coil tag and a probe peptide to label proteins of study with fluorophores[64,65,95]. This system made use of the E3-K3 pair. The E3 peptide acts as a tag and carries an N-terminal cysteine. The Cys-E3 binds a K3 probe peptide conjugated to a reporter via a thioester bond. The formation of the coiled-coil dimer induces a proximity induced acyl transfer reaction where the fluorophore is then transferred to the E3 peptide tag. The Seitz group argued that this tag is therefore even smaller than other coiled-coil tag pairs because the peptide tag is directly labeled. Although the E3/K3 dissociation was detectable by SDS-PAGE, other groups using E3/K3 have observed sustained labeling over time in live cells, suggesting K3 would not necessarily dissociate from E3 in cells.

A common problem shared by a number of the coiled-coil tags is the restriction of labeling to the cell surface. This is due to inability of the exogenous portion, the probe peptide, to cross the cell membrane. In some cases this can be an advantage, if the application is focused solely on transmembrane receptor biology. Some groups have overcome this challenge in order to image targets within cells. For example, the Tamamura group used cell penetrating peptides[70]. Meanwhile, our group relied on hollow gold nanoshell delivery systems in order to introduce VIP probes into cells[96] (discussed in Section 1.5).

## 1.4 Genetically-encoded tags for electron microscopy

Developing genetically-encoded tags for EM is challenging, as reflected in the narrower selection of tags compared to fluorescence imaging. The addition of electron density relies on metal particles, metal chelation, or the oxidation of metal-binding polymers. This field narrows even more when considering only small, peptide-based tags or tags that can also enable combined fluorescence and EM imaging (i.e. CLEM).

As a result of these difficulties, most CLEM studies rely heavily on immunolabeling with antibody-nanoparticle conjugates for imaging proteins.

There are three major approaches for labeling a protein for electron microscopy: 1) metal chelation; 2) polymerization of diaminobenzidine (DAB) with singlet oxygen; and 3) particle-based detection. A summary of EM tags described in this chapter is provided in **Table 1.3**.

**Table 1.3. Properties of genetically-encoded EM tags.**

| Tag | Size during imaging (kDa) | Mechanism | Compatible with fluorescent imaging? |
|---|---|---|---|
| Metallotheinin[97,98] | 7 | Metal chelation | No |
| Bacterioferritin[99] | 467 | Iron chelation | No |
| Ferritag[100] | 494 | Iron chelation | Yes (when fused to a fluorescent protein |
| APEX | 28 | Singlet oxygen generation (enzymatic) | Yes (when fused to a fluorescent protein) |
| FLIPPER | 72 | Singlet oxygen generation (enzymatic) | Yes |
| Tetracysteine tag[41] | 0.6 | Singlet oxygen generation by ReAsH (photoconversion) | Yes |
| MiniSOG[101] | 15.3 | Singlet oxygen generation (photoconversion) | Yes |
| VIP Tags (VIPER)[67] | 12.7 (CoilE tag: 5.2 + CoilR probe: 7.5) | Biotinylated probe peptide detection by a streptavidin-nanoparticle | Yes |

The first approach is metal chelating tags (**Figure 1.5**). These are tags that chelate metals such as zinc, iron, or copper. The tags based on metallotheinin[97,98] are small (<7 kDa) but have a poor signal to noise ratio and are not widely used in EM. The tags that are based on ferritin[99,100], an iron storage structure, are large (>400 kDa). The tag based on bacterioferritin can only be used in bacteria and can lead to aggregation of the target[99]. Ferritag[100] is a rapamycin-inducible assembly of ferritin to a protein of interest in mammalian cells. None of these metal-chelating tags are fluorescent on their

own and would need to be combined with immunolabeling or a fluorescent tag in order to be used for CLEM.

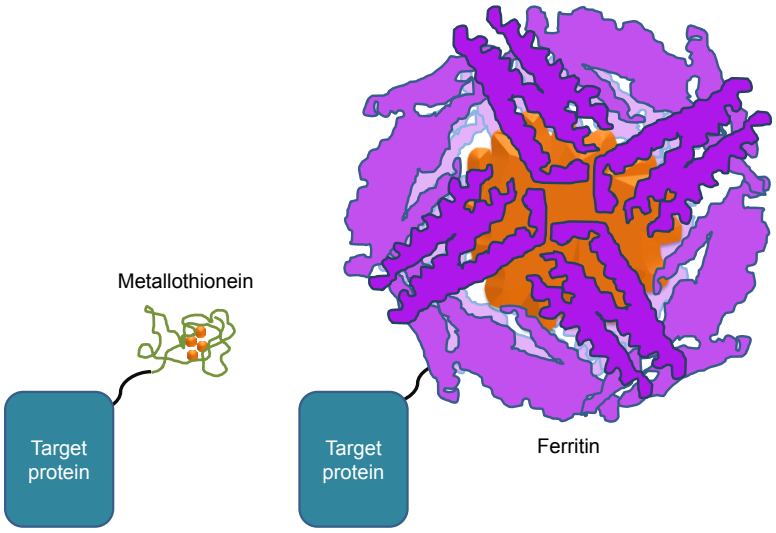


**Figure 1.5. Labeling proteins for electron microscopy with metal-chelating tags.** Proteins can be attached to metal-chelating proteins such as metallothionein (PDB: 2KAK[102]) or ferritin (PDB: 1MFR[103]) in order to append electron density contrast to a target.

The second approach involves using singlet oxygen generation to polymerize diaminobenzidine (DAB), which forms a polymer that can be stained with osmium tetroxide (**Figure 1.6**). This can be done using a genetically-encoded peroxidase enzyme. The Ting group (Stanford) developed a genetically-encoded EM tag by engineering ascorbate peroxidase into the APEX tag[104]. The Giepmans group (UMC Groningen) developed FLIPPER, a genetically-encoded tag for CLEM by fusing a fluorescent protein to horseradish peroxidase (HRP)[105]. Many "colors" of FLIPPER were designed by fusing different fluorescent proteins to HRP. These tags are relatively large, as APEX is 28 kDa and FLIPPER is 72 kDa.

The Tsien group (UC San Diego) engineered smaller EM tags. The 6-residue tetracysteine tag has demonstrated CLEM capability[106–108]. The ReAsH ligand can be imaged by fluorescence and used to generate singlet oxygen to polymerize DAB for localized EM staining. The Tsien group also developed MiniSOG[101], a 15.3 kDa fluorescent flavoprotein that acts as a genetically-encoded CLEM tag. This protein tag is green fluorescent upon binding endogenous flavin and it generates singlet oxygen to oxidize DAB.

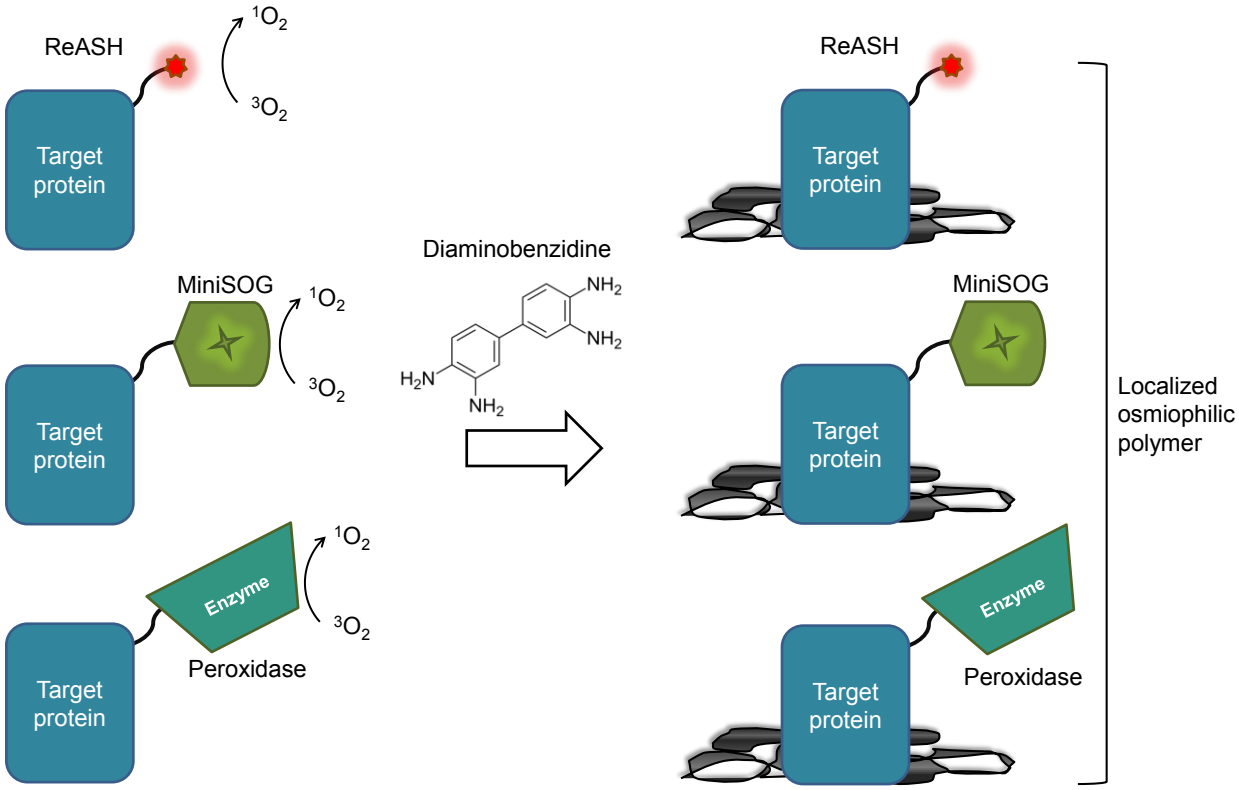


**Figure 1.6. Labeling proteins by oxidation of diaminobenzidine.** Proteins can be appended to singlet oxygen generators, such as ReAsH (by tetracysteine tag), MiniSOG or a peroxidase. Singlet oxygen polymerizes diaminobenzidine, which can be stained with osmium tetroxide.

Approaches that depend on creating a heavy metal deposit are qualitative and are more suitable for imaging abundant targets. These methods are also only used for labeling one protein at a time, since only one contrast reagent (DAB) is used. To overcome this issue, the Tsien and Ellisman groups (UC San Diego) have succeeded in precipitating DAB in multiple "colors" in order to image more than one target at once[109]. DAB was combined with chemical structures that could chelate lanthanide metals (Ln-DAB). When this Ln-DAB was deposited by either MiniSOG-based or ReASH-based oxidation, the deposits could then be imaged by EM. An electron energy-loss spectra (EELS) unit was used to differentiate between two different lanthanide deposits and thus two different protein targets.

The remaining EM labeling approach is particle-based labeling, whereby the protein of study is labeled with an electron-dense nanoparticle (1 nm – 500 nm) (**Figure 1.7**). These particles can be made of metals (e.g., gold, silver, and platinum) or semi-

conductor nanocrystals, such as Qdots. Since there is a variety of particles available, nanoparticle labeling can be “multi-color”, where different sizes and shapes can be used to label different targets[106,110,111]. Ellisman, Deerinck and Giepmans pioneered the use of Qdots for multicolor CLEM, demonstrating immunolabeling of three protein targets in mouse cerebellum. Particles can also be counted, allowing for quantitative imaging of proteins, such as counting transferrin receptor 1 (TfR1)[67] or receptor tyrosine kinases (e.g., HER2[112,113]) on the cell surface.

Attaching nanoparticles to proteins in a specific manner is challenging. The most commonly used method is immunolabeling, where nanoparticles are attached to antibodies. This method frequently makes use of secondary antibody detection. Immunolabeling, while commonly used, is frequently inefficient, labeling <50% of targets available[14,114]. Additionally, the large size of antibodies can introduce resolution artifacts, as discussed in Section 1.1.

Implementing smaller tags with nanoparticle labeling is thus appealing for reaping the benefits of nanoparticles while overcoming the drawbacks of antibody labeling. When VIPER was introduced, we showed that it was a capable genetically-encoded tag for fluorescence and EM imaging. Target protein was labeled with a biotinylated probe peptide and then detected with streptavidin-conjugated Qdots[67] (discussed in Section 1.5).

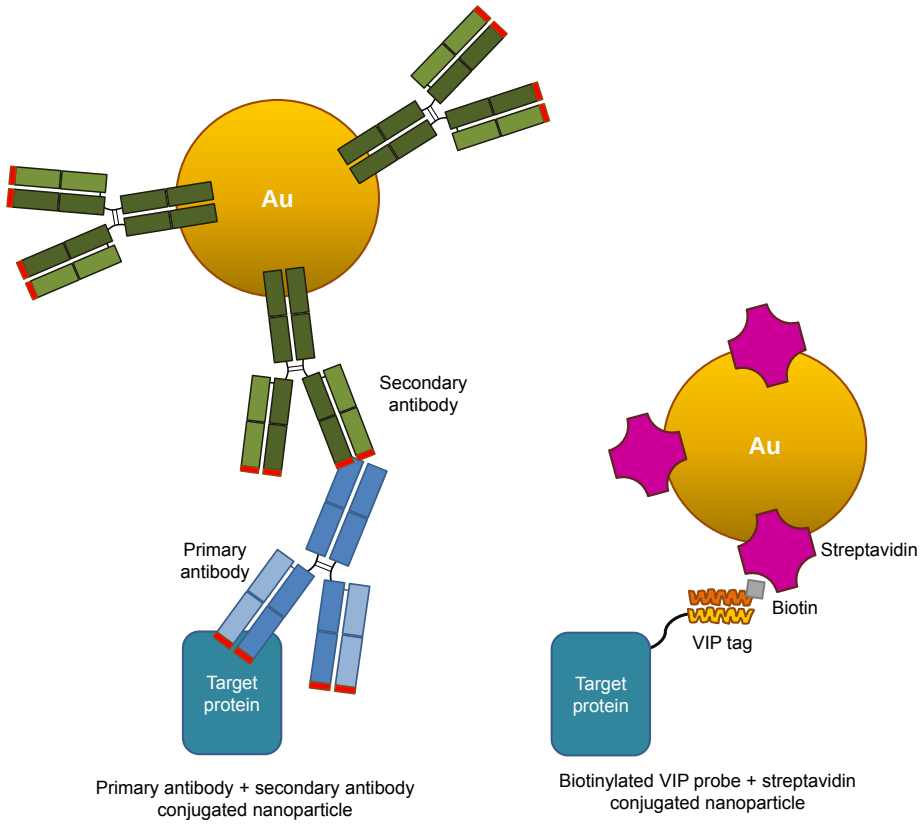


**Figure 1.7. Methods for labeling proteins with electron-dense particles.** Proteins can be labeled for EM by immunolabeling whereby a protein target is detected with primary antibodies and then labeled with secondary antibodies attached to a nanoparticle. An alternate approach is detection of a VIP-tagged protein by a biotinylated probe peptide with subsequent labeling with a streptavidin bound nanoparticle.

## 1.5 Versatile Interacting Peptide (VIP) Tags

Given the considerations and needs of the imaging community and the drawbacks of existing protein labeling strategies introduced in this chapter, our group has developed Versatile Interacting Peptide (VIP) tags (**Figure 1.8**). VIP tags are a set of coiled-coil dimers where the protein of interest is tagged with one VIP tag and then subsequently binds a reporter-labeled VIP probe peptide (see Section **1.3**). VIP tags are also genetically-encoded tags for EM imaging (see Section **1.4**). To date, the existing VIP tags are VIP Y/Z[71], VIPER[67], and MiniVIPER[94]. VIP tags are small (4.3-6.2 kDa) and the probe peptide can be modified (e.g., via thiol or lysine bioconjugation chemistry). We have used a diversity of spectrally distinct fluorophores (Alexa Fluor 488, Oregon Green 488, Cy3, TAMRA, Cy5, Alexa Fluor 647, Qdot655, etc.) to image VIP-tagged

proteins[67,71,115]. Biotinylated peptide probes allowed for detection with fluorescent streptavidin or streptavidin-functionalized nanoparticles.

VIP Y/Z[71] was the first demonstration of the specificity and efficacy of VIP tags for labeling cellular proteins, and is described in **Chapter 2** of this thesis. VIP Y/Z is comprised of CoilY and CoilZ. The selectivity of VIP tags was demonstrated in cell lysates via membrane detection and on live cells by flow cytometry and fluorescence imaging. VIP Y/Z was bi-directional; either CoilY or CoilZ could serve as the peptide tag. This allowed us to label two targets simultaneously in a single experiment. For four-color imaging we used membrane-anchored fluorescent proteins as model targets.

VIPER was the second introduced VIP tag and is described in **Chapter 3** of this thesis. VIPER consists of a CoilE tag and CoilR probe peptide. VIPER was used in fixed and permeabilized cells to label proteins in the nucleus (histone 2B), mitochondria (via a Cox8 fragment), and cytoskeleton (actin). Labeling was target-specific, showing no interaction with endogenous proteins in cells. VIPER was also used to image a trans-membrane receptor, transferrin receptor 1 (TfR1), in live cell applications. Labeling was stable over time, allowing time-lapse imaging of VIP-tagged TfR1 with fluorescent transferrin as they trafficked into the cell via clathrin-mediated endocytosis (**Figure 1.8B**).

We demonstrated a novel use of coiled-coil peptide tagging for CLEM imaging. The tag was detected by biotinylated VIP probes with streptavidin-conjugated Qdots. The dual fluorescent and electron-dense properties of Qdots allowed for the fluorescence detection of TfR1 by light microscopy, as well as quantification of labeled TfR1 by scanning EM (**Figure 1.8C**). In a comparison against immunolabeling, the VIPER tag showed a greater labeling efficiency than 3 out of 4 anti-TfR1 antibodies tested. These results showed that VIPER can enable new opportunities for EM imaging of targets lacking good antibodies.

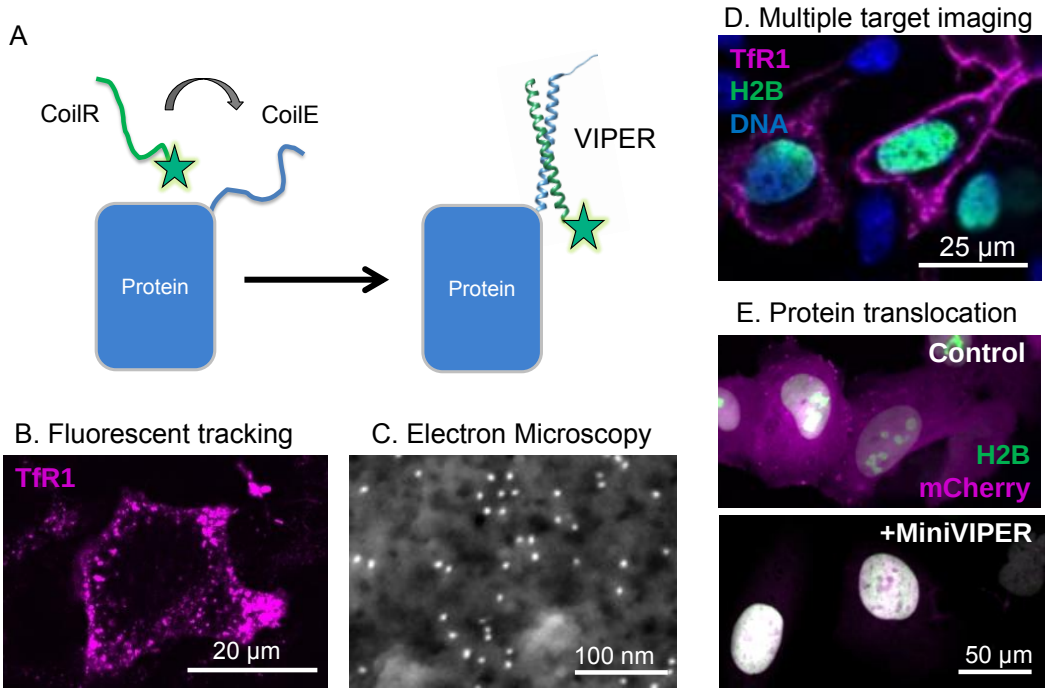


**Figure 1.8. The capabilities of Versatile Interacting Peptide (VIP) Tags.** (**A**) Schematic demonstrating the principle of VIP tagging. (**B**) Live fluorescence tracking of TfR1-CoilE with CoilR-Cy5. (**C**) Electron microscopy of the cell surface and imaging TfR1-CoilE labeled with Qdot nanoparticles. (**D**) Tracking of two targets at once in cells by labeling TfR1-MiniR with MiniE-Cy5 and H2B-CoilE with CoilR-AF488. (**E**) Translocation of a fluorescent protein to the nucleus via artificial dimerization of H2B-MiniR-mEmerald and MiniE-mCherry.

MiniVIPER is a shorter, more charge-balanced variant of VIPER. It is discussed in detail in **Chapter 4**. Either MiniR or MiniE could serve as the peptide tag with the cognate coil serving as the probe peptide. We validated MiniVIPER as a specific and versatile tag by imaging TfR1, H2B (nucleus), and TOMM20 (mitochondria). Using MiniVIPER, we demonstrated two new applications for combining VIP tags. We simultaneously labeled and imaged a cytosolic protein (H2B or TOMM20) and TfR1 by combining two VIP tags in cells (**Figure 1.8D**). In a separate application, we showed that VIP coiled-coil pairs can be used to translocate proteins. This was demonstrated by fusing cognate VIP tags on a soluble mCherry and H2B in order to translocate mCherry to the nucleus (**Figure 1.8E**).

Like other coiled-coil peptide tags, VIP tags are cell membrane impermeant unless modified with a cell penetrating peptide. This means that the majority of live cell

applications discussed in this chapter were restricted to extracellular targets (e.g., TfR1), while imaging intracellular targets required fixation and permeabilization. To overcome this drawback, we collaborated with the Reich group (UC Santa Barbara) to use hollow gold nanoshells (HGNs) to deliver VIP probes into live cells[96]. The HGNs were functionalized with cell penetrating peptides and fluorescent CoilR probe. After the HGNs were internalized by the cells, the CoilR cargo could be released with 2-photon excitation. This method was used to label VIP-tagged proteins in the mitochondria (via Cox8 fragment) or the nucleus (H2B) and track them over time in live cells.

## Conclusions

Developing tools for imaging requires combining expertise in protein engineering, chemistry, cellular biology, and imaging technologies. A great deal of progress has been made since the introduction of the green fluorescent protein. The wide array of optical properties afforded by the ever expanding collection of small molecule fluorophores is only limited by options for specifically attaching them to proteins.

The ideal protein tag is traceless, versatile, and universally compatible with any protein or any detection method. While this ideal tag is still theoretical, many strides have been made in the development of peptide tags in an attempt to address this community desire. For peptide tags, their small size and use of small molecule fluorophores address many of the shortcomings of the previous generation of genetically-encoded protein tags.

We developed VIP tags with the needs of the imaging community in mind. In particular, this includes the need for more functionally diverse peptide tags and the need for more genetically-encoded tags for EM. This chapter introduced VIP tags as an ongoing effort to reduce the size of the tag, without sacrificing specificity and flexibility. VIP tags work by relying on the specificity of coiled-coil heterodimers, where the peptide tag is bound by a peptide probe.

The current stable of protein tags for EM is small compared to those for fluorescence, with even less genetically-encoded tags compatible with CLEM. An exciting application of VIP tags is the ability to enable CLEM imaging. VIP tags offer

new opportunities to see proteins with nanoparticles that are otherwise not detectable by immunolabeling.

Many of the peptide tags discussed here have been demonstrated for fluorescence imaging only, while many of the EM tags are larger than 7 kDa. Given the current field of genetically-encoded tags for fluorescence or tags for EM, VIP tags occupy a unique niche in their varied number of applications for their small size.

## Works Cited


1. Bates, M., Huang, B. & Zhuang, X. Super-resolution microscopy by nanoscale localization of photo-switchable fluorescent probes. *Curr. Opin. Chem. Biol.* **12**, 505–514 (2008).
2. Huang, B., Wang, W., Bates, M. & Zhuang, X. Three-Dimensional Super-Resolution Imaging by Stochastic Optical Reconstruction Microscopy. *Science* **319**, 810–813 (2008).
3. Han, B., Zhou, R., Xia, C. & Zhuang, X. Structural organization of the actin-spectrin–based membrane skeleton in dendrites and soma of neurons. *Proc. Natl. Acad. Sci.* **114**, E6678–E6685 (2017).
4. Nixon-Abell, J. *et al.* Increased spatiotemporal resolution reveals highly dynamic dense tubular matrices in the peripheral ER. *Science* **354**, aaf3928 (2016).
5. Ellisman, M. H., Deerinck, T. J., Shu, X. & Sosinsky, G. E. Picking Faces out of a Crowd. in *Methods in Cell Biology* vol. 111 139–155 (Elsevier, 2012).
6. Shahmoradian, S. H. *et al.* Lewy pathology in Parkinson's disease consists of crowded organelles and lipid membranes. *Nat. Neurosci.* **22**, 1099–1109 (2019).
7. Sochacki, K. A., Dickey, A. M., Strub, M.-P. & Taraska, J. W. Endocytic proteins are partitioned at the edge of the clathrin lattice in mammalian cells. *Nat. Cell Biol.* **19**, 352–361 (2017).
8. Hoffman, D. P. *et al.* Correlative three-dimensional super-resolution and block-face electron microscopy of whole vitreously frozen cells. *Science* **367**, (2020).
9. Vassilopoulos, S., Gibaud, S., Jimenez, A., Caillol, G. & Leterrier, C. Ultrastructure of the axonal periodic scaffold reveals a braid-like organization of actin rings. *Nat. Commun.* **10**, 1–13 (2019).
10. Bowler, M. *et al.* High-resolution characterization of centriole distal appendage morphology and dynamics by correlative STORM and electron microscopy. *Nat. Commun.* **10**, 1–15 (2019).
11. Edmundson, A. B., Guddat, L. W. & Andersen, K. N. Crystal Structures of Intact IgG Antibodies. *ImmunoMethods* **3**, 197–210 (1993).
12. Hermann, R., Walther, P. & Müller, M. Immunogold labeling in scanning electron microscopy. *Histochem. Cell Biol.* **106**, 31–39 (1996).
13. Griffiths, G. & Lucocq, J. M. Antibodies for immunolabeling by light and electron microscopy: not for the faint hearted. *Histochem. Cell Biol.* **142**, 347–360 (2014).
14. Griffiths, G. & Hoppeler, H. Quantitation in immunocytochemistry: correlation of immunogold labeling to absolute number of membrane antigens. *J. Histochem. Cytochem. Off. J. Histochem. Soc.* **34**, 1389–1398 (1986).
15. Schnell, U., Dijk, F., Sjollema, K. A. & Giepmans, B. N. G. Immunolabeling artifacts and the need for live-cell imaging. *Nat. Methods* **9**, 152–158 (2012).
16. Baker, M. Reproducibility crisis: Blame it on the antibodies. *Nature* **521**, 274–276 (2015).
17. Berglund, L. *et al.* A genecentric Human Protein Atlas for expression profiles based on antibodies. *Mol. Cell. Proteomics MCP* **7**, 2019–2027 (2008).
18. Bradbury, A. & Plückthun, A. Reproducibility: Standardize antibodies used in research. *Nat. News* **518**, 27 (2015).
19. Bannas, P., Hambach, J. & Koch-Nolte, F. Nanobodies and Nanobody-Based Human Heavy Chain Antibodies As Antitumor Therapeutics. *Front. Immunol.* **8**, (2017).
20. Nelson, A. L. Antibody fragments. *mAbs* **2**, 77–83 (2010).
21. Barelle, C., Gill, D. S. & Charlton, K. Shark Novel Antigen Receptors—The Next Generation of Biologic Therapeutics? in *Pharmaceutical Biotechnology* (eds. Guzmán, C. A. & Feuerstein, G. Z.) 49–62 (Springer, 2009). doi:10.1007/978-1-4419-1132-2_6.
22. Harmsen, M. M. & De Haard, H. J. Properties, production, and applications of camelid single-domain antibody fragments. *Appl. Microbiol. Biotechnol.* **77**, 13–22 (2007).

23. Boder, E. T., Midelfort, K. S. & Wittrup, K. D. Directed evolution of antibody fragments with monovalent femtomolar antigen-binding affinity. *Proc. Natl. Acad. Sci.* **97**, 10701–10705 (2000).
24. Giepmans, B. N. G., Adams, S. R., Ellisman, M. H. & Tsien, R. Y. The Fluorescent Toolbox for Assessing Protein Location and Function. *Science* **312**, 217–224 (2006).
25. Day, R. N. & Davidson, M. W. The fluorescent protein palette: tools for cellular imaging. *Chem. Soc. Rev.* **38**, 2887–2921 (2009).
26. Shimomura, O., Johnson, F. H. & Saiga, Y. Extraction, purification and properties of aequorin, a bioluminescent protein from the luminous hydromedusan, Aequorea. *J. Cell. Comp. Physiol.* **59**, 223–239 (1962).
27. Shimomura, O. Structure of the chromophore of Aequorea green fluorescent protein. *FEBS Lett.* **104**, 220–222 (1979).
28. Cranfill, P. J. *et al.* Quantitative assessment of fluorescent proteins. *Nat. Methods* **13**, 557–562 (2016).
29. Costantini, L. M. & Snapp, E. L. Fluorescent proteins in cellular organelles: serious pitfalls and some solutions. *DNA Cell Biol.* **32**, 622–627 (2013).
30. Los, G. V. *et al.* HaloTag: A Novel Protein Labeling Technology for Cell Imaging and Protein Analysis. *ACS Chem. Biol.* **3**, 373–382 (2008).
31. Keppler, A. *et al.* A general method for the covalent labeling of fusion proteins with small molecules in vivo. *Nat. Biotechnol.* **21**, 86–89 (2003).
32. Gautier, A. *et al.* An engineered protein tag for multiprotein labeling in living cells. *Chem. Biol.* **15**, 128–136 (2008).
33. Miller, L. W., Cai, Y., Sheetz, M. P. & Cornish, V. W. In vivo protein labeling with trimethoprim conjugates: a flexible chemical tag. *Nat. Methods* **2**, 255–257 (2005).
34. Chen, Z., Jing, C., Gallagher, S. S., Sheetz, M. P. & Cornish, V. W. Second-generation covalent TMP-tag for live cell imaging. *J. Am. Chem. Soc.* **134**, 13692–13699 (2012).
35. Szent-Gyorgyi, C. *et al.* Fluorogen-activating single-chain antibodies for imaging cell surface proteins. *Nat. Biotechnol.* **26**, 235–240 (2008).
36. Yan, Q. *et al.* Localization microscopy using noncovalent fluorogen activation by genetically encoded fluorogen-activating proteins. *Chemphyschem Eur. J. Chem. Phys. Phys. Chem.* **15**, 687–695 (2014).
37. Plamont, M.-A. *et al.* Small fluorescence-activating and absorption-shifting tag for tunable protein imaging in vivo. *Proc. Natl. Acad. Sci.* **113**, 497–502 (2016).
38. Pimenta, F. M. *et al.* Chromophore Renewal and Fluorogen-Binding Tags: A Match Made to Last. *Sci. Rep.* **7**, 1–8 (2017).
39. Gautier, A., Johnsson, K. & O'Hare, H. AGT/SNAP-Tag: A Versatile Tag for Covalent Protein Labeling. in *Probes and Tags to Study Biomolecular Function* 89–107 (John Wiley & Sons, Ltd, 2008). doi:10.1002/9783527623099.ch5.
40. Halo, T. L., Appelbaum, J., Hobert, E. M., Balkin, D. M. & Schepartz, A. Selective recognition of protein tetraserine motifs with a cell-permeable, pro-fluorescent bis-boronic acid. *J. Am. Chem. Soc.* **131**, 438–439 (2009).
41. Griffin, B. A., Adams, S. R. & Tsien, R. Y. Specific Covalent Labeling of Recombinant Protein Molecules Inside Live Cells. *Science* **281**, 269–272 (1998).
42. Adams, S. R. *et al.* New Biarsenical Ligands and Tetracysteine Motifs for Protein Labeling in Vitro and in Vivo: Synthesis and Biological Applications. *J. Am. Chem. Soc.* **124**, 6063–6076 (2002).
43. Hochuli, E., Döbeli, H. & Schacher, A. New metal chelate adsorbent selective for proteins and peptides containing neighbouring histidine residues. *J. Chromatogr. A* **411**, 177–184 (1987).

44. Hochuli, E., Bannwarth, W., Döbeli, H., Gentz, R. & Stüber, D. Genetic Approach to Facilitate Purification of Recombinant Proteins with a Novel Metal Chelate Adsorbent. *Bio/Technology* **6**, 1321–1325 (1988).
45. Hauser, C. T. & Tsien, R. Y. A hexahistidine-Zn2+-dye label reveals STIM1 surface exposure. *Proc. Natl. Acad. Sci.* **104**, 3693–3697 (2007).
46. Hopp, T. P. *et al.* A Short Polypeptide Marker Sequence Useful for Recombinant Protein Identification and Purification. *Bio/Technology* **6**, 1204–1210 (1988).
47. Einhauer, A. & Jungbauer, A. The FLAG peptide, a versatile fusion tag for the purification of recombinant proteins. *J. Biochem. Biophys. Methods* **49**, 455–465 (2001).
48. Field, J. *et al.* Purification of a RAS-responsive adenylyl cyclase complex from Saccharomyces cerevisiae by use of an epitope addition method. *Mol. Cell. Biol.* **8**, 2159–2165 (1988).
49. Zhou, Z. *et al.* Genetically Encoded Short Peptide Tags for Orthogonal Protein Labeling by Sfp and AcpS Phosphopantetheinyl Transferases. *ACS Chem. Biol.* **2**, 337–346 (2007).
50. Virant, D. *et al.* A peptide tag-specific nanobody enables high-quality labeling for dSTORM imaging. *Nat. Commun.* **9**, 1–14 (2018).
51. Veggiani, G. *et al.* Programmable polyproteams built using twin peptide superglues. *Proc. Natl. Acad. Sci.* **113**, 1202–1207 (2016).
52. Zakeri, B. *et al.* Peptide tag forming a rapid covalent bond to a protein, through engineering a bacterial adhesin. *Proc. Natl. Acad. Sci.* **109**, E690–E697 (2012).
53. Götzke, H. *et al.* The ALFA-tag is a highly versatile tool for nanobody-based bioscience applications. *Nat. Commun.* **10**, 1–12 (2019).
54. Boersma, S. *et al.* Multi-Color Single-Molecule Imaging Uncovers Extensive Heterogeneity in mRNA Decoding. *Cell* **178**, 458-472.e19 (2019).
55. Kamiyama, D. *et al.* Versatile protein tagging in cells with split fluorescent protein. *Nat. Commun.* **7**, 11046 (2016).
56. Leonetti, M. D., Sekine, S., Kamiyama, D., Weissman, J. S. & Huang, B. A scalable strategy for high-throughput GFP tagging of endogenous human proteins. *Proc. Natl. Acad. Sci.* **113**, E3501–E3508 (2016).
57. Feng, S. *et al.* Improved split fluorescent proteins for endogenous protein labeling. *Nat. Commun.* **8**, 370 (2017).
58. Howarth, M., Takao, K., Hayashi, Y. & Ting, A. Y. Targeting quantum dots to surface proteins in living cells with biotin ligase. *Proc. Natl. Acad. Sci. U. S. A.* **102**, 7583–7588 (2005).
59. Howarth, M. & Ting, A. Y. Imaging proteins in live mammalian cells with biotin ligase and monovalent streptavidin. *Nat. Protoc.* **3**, 534–545 (2008).
60. Fernández-Suárez, M. *et al.* Re-directing lipoic acid ligase for cell surface protein labeling with small-molecule probes. *Nat. Biotechnol.* **25**, 1483–1487 (2007).
61. Wang, J., Yu, Y. & Xia, J. Short Peptide Tag for Covalent Protein Labeling Based on Coiled Coils. *Bioconjug. Chem.* **25**, 178–187 (2014).
62. Yano, Y. *et al.* Coiled-Coil Tag−Probe System for Quick Labeling of Membrane Receptors in Living Cells. *ACS Chem. Biol.* **3**, 341–345 (2008).
63. Yano, Y. & Matsuzaki, K. Tag–probe labeling methods for live-cell imaging of membrane proteins. *Biochim. Biophys. Acta BBA - Biomembr.* **1788**, 2124–2131 (2009).
64. Reinhardt, U. *et al.* Peptide-Templated Acyl Transfer: A Chemical Method for the Labeling of Membrane Proteins on Live Cells. *Angew. Chem. Int. Ed.* **53**, 10237–10241 (2014).
65. Reinhardt, U., Lotze, J., Mörl, K., Beck-Sickinger, A. G. & Seitz, O. Rapid Covalent Fluorescence Labeling of Membrane Proteins on Live Cells via Coiled-Coil Templated Acyl Transfer. *Bioconjug. Chem.* **26**, 2106–2117 (2015).

66. Tanenbaum, M. E., Gilbert, L. A., Qi, L. S., Weissman, J. S. & Vale, R. D. A protein-tagging system for signal amplification in gene expression and fluorescence imaging. *Cell* **159**, 635–646 (2014).
67. Doh, J. K. *et al.* VIPER is a genetically encoded peptide tag for fluorescence and electron microscopy. *Proc. Natl. Acad. Sci.* 201808626 (2018) doi:10.1073/pnas.1808626115.
68. Tsutsumi, H. *et al.* Fluorogenically active leucine zipper peptides as tag-probe pairs for protein imaging in living cells. *Angew. Chem. Int. Ed Engl.* **48**, 9164–9166 (2009).
69. Nomura, W. *et al.* Development of crosslink-type tag-probe pairs for fluorescent imaging of proteins. *Biopolymers* **94**, 843–852 (2010).
70. Nomura, W., Ohashi, N., Mori, A. & Tamamura, H. An in-cell fluorogenic Tag-probe system for protein dynamics imaging enabled by cell-penetrating peptides. *Bioconjug. Chem.* **26**, 1080–1085 (2015).
71. Zane, H. K., Doh, J. K., Enns, C. A. & Beatty, K. E. Versatile interacting peptide (VIP) tags for labeling proteins with bright chemical reporters. *ChemBioChem* (2017) doi:10.1002/cbic.201600627.
72. Müller, K. M., Arndt, K. M., Bauer, K. & Plückthun, A. Tandem Immobilized Metal-Ion Affinity Chromatography/Immunoaffinity Purification of His-tagged Proteins— Evaluation of Two Anti-His-Tag Monoclonal Antibodies. *Anal. Biochem.* **259**, 54–61 (1998).
73. Kaufmann, M. *et al.* Crystal Structure of the Anti-His Tag Antibody 3D5 Single-chain Fragment Complexed to its Antigen. *J. Mol. Biol.* **318**, 135–147 (2002).
74. Debeljak, N., Feldman, L., Davis, K. L., Komel, R. & Sytkowski, A. J. Variability in the immunodetection of His-tagged recombinant proteins. *Anal. Biochem.* **359**, 216–223 (2006).
75. Uttamapinant, C. *et al.* Fast, Cell-compatible Click Chemistry with Copper-chelating Azides for Biomolecular Labeling. *Angew. Chem. Int. Ed Engl.* **51**, 5852–5856 (2012).
76. Braun, M. B. *et al.* Peptides in headlock--a novel high-affinity and versatile peptide-binding nanobody for proteomics and microscopy. *Sci. Rep.* **6**, 19211 (2016).
77. Evan, G. I., Lewis, G. K., Ramsay, G. & Bishop, J. M. Isolation of monoclonal antibodies specific for human c-myc proto-oncogene product. *Mol. Cell. Biol.* **5**, 3610–3616 (1985).
78. Vandemoortele, G., Eyckerman, S. & Gevaert, K. Pick a Tag and Explore the Functions of Your Pet Protein. *Trends Biotechnol.* (2019) doi:10.1016/j.tibtech.2019.03.016.
79. Yano, Y. & Matsuzaki, K. Live-cell imaging of membrane proteins by a coiled-coil labeling method—Principles and applications. *Biochim. Biophys. Acta BBA - Biomembr.* **1861**, 1011–1017 (2019).
80. Hodges, R. S. De novo design of α-helical proteins: basic research to medical applications. *Biochem. Cell Biol.* **74**, 133–154 (1996).
81. Lupas, A. Coiled coils: new structures and new functions. *Trends Biochem. Sci.* **21**, 375–382 (1996).
82. O'Shea, E. K., Lumb, K. J. & Kim, P. S. Peptide 'Velcro': design of a heterodimeric coiled coil. *Curr. Biol. CB* **3**, 658–667 (1993).
83. Litowski, J. R. & Hodges, R. S. Designing Heterodimeric Two-stranded α-Helical Coiled-coils EFFECTS OF HYDROPHOBICITY AND α-HELICAL PROPENSITY ON PROTEIN FOLDING, STABILITY, AND SPECIFICITY. *J. Biol. Chem.* **277**, 37272–37279 (2002).
84. Moll, J. R., Ruvinov, S. B., Pastan, I. & Vinson, C. Designed heterodimerizing leucine zippers with a ranger of pIs and stabilities up to 10−15 M. *Protein Sci. Publ. Protein Soc.* **10**, 649–655 (2001).
85. Acharya, A., Ruvinov, S. B., Gal, J., Moll, J. R. & Vinson, C. A Heterodimerizing Leucine Zipper Coiled Coil System for Examining the Specificity of a Position Interactions: Amino Acids I, V, L, N, A, and K. *Biochemistry* **41**, 14122–14131 (2002).
86. Thomas, F., Boyle, A. L., Burton, A. J. & Woolfson, D. N. A Set of de Novo Designed Parallel Heterodimeric Coiled Coils with Quantified Dissociation Constants in the Micromolar to Sub-nanomolar Regime. *J. Am. Chem. Soc.* **135**, 5161–5166 (2013).

87. Negron, C. & Keating, A. E. A Set of Computationally Designed Orthogonal Antiparallel Homodimers that Expands the Synthetic Coiled-Coil Toolkit. *J. Am. Chem. Soc.* **136**, 16544–16556 (2014).
88. Reinke, A. W., Grant, R. A. & Keating, A. E. A Synthetic Coiled-Coil Interactome Provides Heterospecific Modules for Molecular Engineering. *J. Am. Chem. Soc.* **132**, 6025–6031 (2010).
89. Thompson, K. E., Bashor, C. J., Lim, W. A. & Keating, A. E. SYNZIP Protein Interaction Toolbox: *in Vitro* and *in Vivo* Specifications of Heterospecific Coiled-Coil Interaction Domains. *ACS Synth. Biol.* **1**, 118–129 (2012).
90. Boyken, S. E. *et al.* De novo design of protein homo-oligomers with modular hydrogen bond network-mediated specificity. *Science* **352**, 680–687 (2016).
91. Chen, Z. *et al.* Programmable design of orthogonal protein heterodimers. *Nature* **565**, 106–111 (2019).
92. Ono, S., Yano, Y. & Matsuzaki, K. Improvement of probe peptides for coiled-coil labeling by introducing phosphoserines. *Biopolymers* **98**, 234–238 (2012).
93. Yamashita, H., Yano, Y., Kawano, K. & Matsuzaki, K. Oligomerization–function relationship of EGFR on living cells detected by the coiled-coil labeling and FRET microscopy. *Biochim. Biophys. Acta BBA - Biomembr.* **1848**, 1359–1366 (2015).
94. Doh, J. K., Tobin, S. & Beatty, K. E. MiniVIPER is a peptide tag for imaging and translocating proteins in cells. (2020).
95. Lotze, J. *et al.* Time-Resolved Tracking of Separately Internalized Neuropeptide Y2 Receptors by Two-Color Pulse-Chase. *ACS Chem. Biol.* (2017) doi:10.1021/acschembio.7b00999.
96. Morgan, E., Doh, J. K., Beatty, K. E. & Reich, N. O. VIPERnano : Improved live cell intracellular protein tracking. *ACS Appl. Mater. Interfaces* (2019) doi:10.1021/acsami.9b12679.
97. Mercogliano, C. P. & DeRosier, D. J. Concatenated metallothionein as a clonable gold label for electron microscopy. *J. Struct. Biol.* **160**, 70–82 (2007).
98. Morphew, M. k. *et al.* Metallothionein as a clonable tag for protein localization by electron microscopy of cells. *J. Microsc.* **260**, 20–29 (2015).
99. Wang, Q., Mercogliano, C. P. & Löwe, J. A ferritin-based label for cellular electron cryotomography. *Struct. Lond. Engl. 1993* **19**, 147–154 (2011).
100. Clarke, N. I. & Royle, S. J. FerriTag is a new genetically-encoded inducible tag for correlative light-electron microscopy. *Nat. Commun.* **9**, 2604 (2018).
101. Shu, X. *et al.* A Genetically Encoded Tag for Correlated Light and Electron Microscopy of Intact Cells, Tissues, and Organisms. *PLoS Biol.* **9**, e1001041 (2011).
102. Peroza, E. A., Schmucki, R., Güntert, P., Freisinger, E. & Zerbe, O. The beta(E)-domain of wheat E(c)-1 metallothionein: a metal-binding domain with a distinctive structure. *J. Mol. Biol.* **387**, 207–218 (2009).
103. Ha, Y., Shi, D., Small, G. W., Theil, E. C. & Allewell, N. M. Crystal structure of bullfrog M ferritin at 2.8 A resolution: analysis of subunit interactions and the binuclear metal center. *J. Biol. Inorg. Chem. JBIC Publ. Soc. Biol. Inorg. Chem.* **4**, 243–256 (1999).
104. Martell, J. D. *et al.* Engineered ascorbate peroxidase as a genetically encoded reporter for electron microscopy. *Nat. Biotechnol.* **30**, 1143–1148 (2012).
105. Kuipers, J. *et al.* FLIPPER, a combinatorial probe for correlated live imaging and electron microscopy, allows identification and quantitative analysis of various cells and organelles. *Cell Tissue Res.* **360**, 61–70 (2015).
106. Gaietta, G. *et al.* Multicolor and electron microscopic imaging of connexin trafficking. *Science* **296**, 503–507 (2002).

107. Gaietta, G. M. *et al.* Golgi twins in late mitosis revealed by genetically encoded tags for live cell imaging and correlated electron microscopy. *Proc. Natl. Acad. Sci.* **103**, 17777–17782 (2006).
108. Gaietta, G. M., Deerinck, T. J. & Ellisman, M. H. Correlated Live Cell Light and Electron Microscopy Using Tetracysteine Tags and Biarsenicals. *Cold Spring Harb. Protoc.* **2011**, pdb.top94 (2011).
109. Adams, S. R. *et al.* Multicolor Electron Microscopy for Simultaneous Visualization of Multiple Molecular Species. *Cell Chem. Biol.* **0**, (2016).
110. Giepmans, B. N. G., Deerinck, T. J., Smarr, B. L., Jones, Y. Z. & Ellisman, M. H. Correlated light and electron microscopic imaging of multiple endogenous proteins using Quantum dots. *Nat. Methods* **2**, 743–749 (2005).
111. Deerinck, T. J., Giepmans, B. N. G., Smarr, B. L., Martone, M. E. & Ellisman, M. H. Light and electron microscopic localization of multiple proteins using quantum dots. *Methods Mol. Biol. Clifton NJ* **374**, 43–53 (2007).
112. Peckys, D. B., Korf, U. & Jonge, N. de. Local variations of HER2 dimerization in breast cancer cells discovered by correlative fluorescence and liquid electron microscopy. *Sci. Adv.* **1**, e1500165 (2015).
113. Peckys, D. B., Hirsch, D., Gaiser, T. & de Jonge, N. Visualisation of HER2 homodimers in single cells from HER2 overexpressing primary formalin fixed paraffin embedded tumour tissue. *Mol. Med.* **25**, 42 (2019).
114. Howell, K. E., Reuter-Carlson, U., Devaney, E., Luzio, J. P. & Fuller, S. D. One antigen, one gold? A quantitative analysis of immunogold labeling of plasma membrane 5'-nucleotidase in frozen thin sections. *Eur. J. Cell Biol.* **44**, 318–327 (1987).
115. Doh, J., Tobin, S. & Beatty, K. Generation of CoilR Probe Peptides for VIPER-labeling of Cellular Proteins. *BIO-Protoc.* **9**, (2019).

# Chapter 2: Versatile interacting peptide (VIP) tags for labeling proteins with bright chemical reporters

Hannah K. Zane*, **Julia K. Doh***, Caroline A. Enns, and Kimberly E. Beatty

**authors contributed equally to the work*

*This work is adapted from a manuscript originally published by Chembiochem on January 4, 2017 in volume 18, issue 15, pages 470-474 (Copyright 2017 John Wiley & Sons, Inc). It has been adapted for this dissertation and reprinted with permission.*

## Abstract

Fluorescence microscopy is an essential tool for the biosciences, enabling the direct observation of proteins in their cellular environment. New methods that facilitate attachment of photostable synthetic fluorophores with genetic specificity are needed to advance the frontiers of biological imaging. Here we describe a new set of small, selective, genetically-encoded tags for proteins based on a heterodimeric coiled-coil interaction between two peptides: CoilY and CoilZ. Proteins expressed as a fusion to CoilZ were selectively labeled with the complementary CoilY fluorescent probe peptide. Fluorophore-labeled target proteins were readily detected in cell lysates with high specificity and sensitivity. We found that these versatile interacting peptide (VIP) tags allowed rapid and specific delivery of bright organic dyes or quantum dots to proteins displayed on living cells. Additionally, we validated that either CoilY or CoilZ could serve as the VIP tag, which enabled us to observe two distinct cell-surface protein targets with this one heterodimeric pair.

## Introduction

Fluorescent labeling of proteins enables the evaluation of protein function, interactions, dynamics, and sub-cellular localization[1–3]. The fluorescent proteins (e.g., GFP and mCherry) are useful tools for microscopy, but their large sizes (~28 kDa) can disrupt protein function, trafficking, stability, and sub-cellular morphology[4–6]. The tripeptide-derived fluorescent protein chromophores are formed spontaneously, but have a restricted range of photophysical properties. Faced with these limitations, chemical biologists designed genetically-encoded protein tags that bind synthetic fluorophore ligands[7,8]. These include tags based on DNA alkyl transferases (SNAP[9] and CLIP tags[10]), dehalogenases (HaloTag[11]), dihydrofolate reductase (TMP tag[12]), and antibody fragments (e.g., fluorogen-activating proteins[13]). The introduction of synthetic chemical reporters improves the palette of fluorophores and enables new applications in cellular imaging such as multi-color super-resolution imaging[14–17]. Still, these protein tags remain relatively large, adding 18 to 33 kDa to the protein of interest.

In contrast to the protein tags, short peptide tags facilitate fluorophore labeling with a minimal increase in the target protein's molecular weight. The tetracysteine tag[18,19] was the first peptide tag but its fluorescent biarsenical reporter is toxic and prone to labeling cysteine-rich cellular proteins[20,21]. Another approach exploits ligase variants to append biotin[22], coumarin[23,24], or resorufin[25] to short (<2 kDa) peptide tags. These peptide tags utilize the specificity and speed of enzymatic catalysis but are relatively complicated and limited in scope. Thus, despite over 15 years of community development, there are few versatile peptide tags and those tags have little spectral diversity compared to fluorescent proteins.

An ideal genetically-encoded peptide tag would be small, target-specific, easy to use, and compatible with diverse chemical reporters. We report herein two peptide tags, CoilY and CoilZ, with all of these features. These peptides heterodimerize to form a structured motif called an α-helical coiled-coil (**Scheme 2.1**). We used the strong interaction between CoilY and CoilZ to fluorescently label proteins in cell lysates and on live cells. Our approach achieves spectral diversity through the delivery of a range of biophysical probes, including bright organic fluorophores and quantum dots (Qdots).

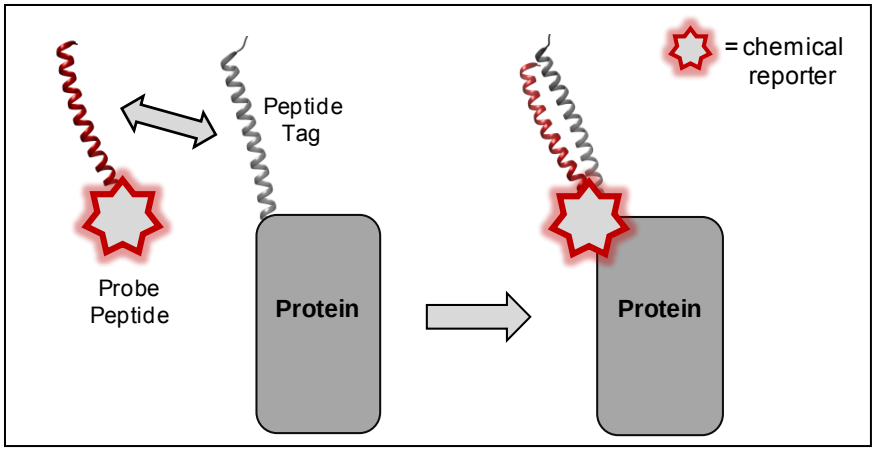


**Scheme 2.1** CoilY and CoilZ facilitate the fluorescent labeling of cellular proteins through heterodimerization.

## Design of VIP Y/Z

We initiated this project by identifying candidate heterodimers from the literature[26–36]. We considered the E3/K3 pair described by Litowski and Hodges[26], and adapted for imaging by Matsuzaki[27] and Seitz[35]. But this pair lacked bi-directionality—only the basic peptide could be used to deliver a fluorescent label. Therefore we sought a heterodimeric pair with strong affinity and better isoelectric properties. We were inspired by a report from Keating and coworkers, which described 27 coiled-coils designed for synthetic biology applications[28]. From among those peptides, we selected SYNZIP-5 and SYNZIP-6, a high affinity coiled-coil pair (KD < 15 nM) that does not homodimerize. These peptides are small (5-6 kDa), biocompatible, and have a good balance of basic (K/R) and acidic (E/D) residues[28,29].

We used this pair to create our CoilY and CoilZ peptide tags. We added a short linker adjacent to each coil to create genetically-encoded peptide tags (see Table S1 for sequences and properties). Further modifications were needed to make the CoilY and CoilZ probe peptides. We used gene assembly PCR to enable recombinant expression of the peptides in E. coli. We included a short linker (GGGAAA) before a cysteine residue, which we included for site-specific conjugation to fluorescent reporters. A C-terminal hexahistidine tag was introduced for affinity purification of the peptides. We analyzed the solution phase structures of the peptides by circular dichroism (CD) spectroscopy and found that both had α-helical structures. A CoilY/CoilZ mixture also

had a coiled-coil structure (**Figure 2.1**), consistent with the crystal structure of SYNZIP-5/SYNZIP-6 published by Keating et al. (structure available: 3HE4.pdb)[28].

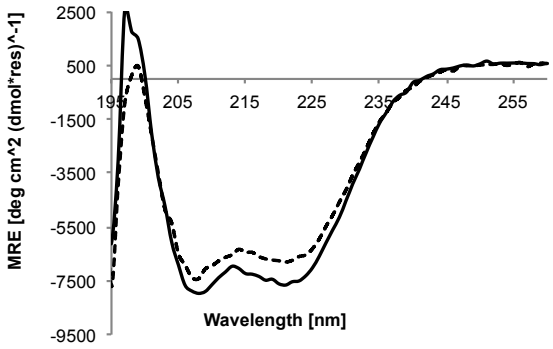


**Figure 2.1. CD spectra of CoilY/CoilZ peptide mixture.** CoilY and CoilZ (50 μM total peptide) were analyzed at 25 °C (solid line) and 37 °C (dotted line) in PBS (pH 7.4).

## In-vitro analysis of VIP Y/Z using membrane detection

The CoilY and CoilZ probe peptides were assessed for their ability to label tagged proteins in cell lysates (Figure **2.2**). Peptide-tagged proteins were genetically-encoded in a pDisplay vector[22], which anchored model proteins on the cell surface via the transmembrane (TM) domain of platelet-derived growth factor receptor. The CoilY tag was fused near the N-terminus of mCherry (CoilY-mCherry-TM) and the CoilZ tag was fused near the N-terminus of enhanced GFP (CoilZ-EGFP-TM). Sequences of these constructs are described in the ESI (Table S2). Transfected human embryonic kidney (HEK) 293FT cell lysates contained tagged (lanes 2 and 4) or untagged (lanes 1 and 3) proteins. Cell extracts were denatured, subjected to polyacrylamide gel electrophoresis (PAGE), and transferred to a polyvinylidene difluoride (PVDF) membrane. The PVDF membrane was incubated sequentially with CoilZ-fluorescein and then CoilY-rhodamine. Fluorescence imaging demonstrated that only CoilY-mCherry-TM and CoilZ-EGFP-TM were labeled by their corresponding probe peptides (lanes 2 and 4). Homodimerization, which would appear as red fluorescence in lane 2 or green fluorescence in lane 4, was not observed. The probe peptides did not label untagged EGFP-TM, mCherry-TM, or other cellular proteins, demonstrating their specificity and selectivity. Additionally, our results indicated that either coil could be used as the genetically-encoded peptide tag for protein labeling in vitro.

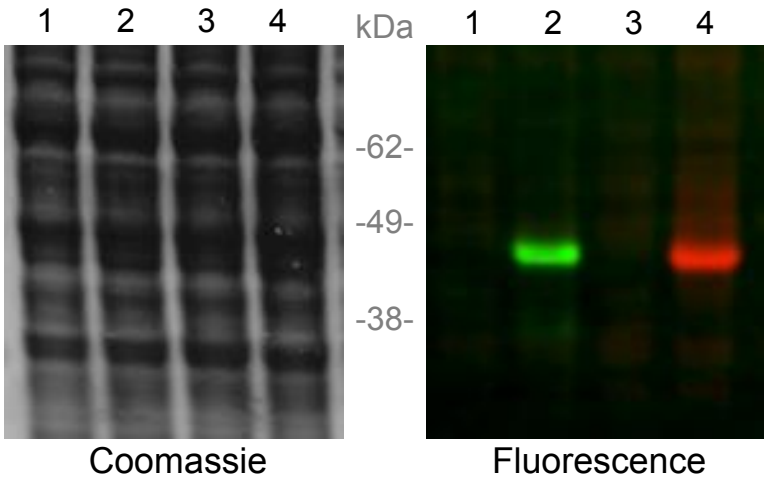


**Figure 2.2 Selective fluorophore labeling of peptide-tagged proteins.** Lysates were resolved by SDS-PAGE, transferred to a membrane, and then incubated with CoilZ-fluorescein (green) and then CoilY-rhodamine (red). Fluorescence imaging revealed green-fluorescent CoilY-mCherry-TM (lane 2) and red-fluorescent CoilZ-EGFP-TM (lane 4). GFP-TM (lane 3) and mCherry-TM (lane 1) were not labeled by either probe peptide.

This membrane assay enabled us to evaluate our probe peptide labeling as an alternative to fluorescent immunoblotting (i.e., Western blotting). For this experiment we used purified His6-CoilY-mCherry (400 ng to 0.8 ng). The sensitivity of direct detection using CoilZ-fluorescein was compared with an Alexa Fluor (AF) 488-labeled anti-His antibody (**Figure 2.3**). CoilZ-fluorescein could detect as little as 3 ng of His6-CoilY-mCherry, while detection by immunolabeling required 8-fold more protein. Anti-His antibodies often exhibit low sensitivity and selectivity[37]. However we used a penta-His antibody from Qiagen, which is one of the best available commercially. Many proteins lack good antibodies, and we posit that our detection method offers a sensitive alternative to immunolabeling.

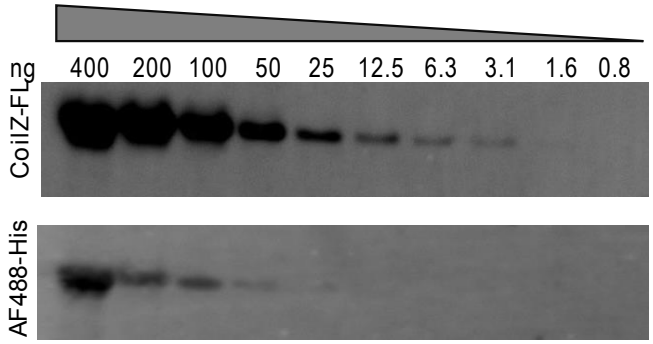


**Figure 2.3. Detection limit comparison between peptide and immunolabeling.** Serial dilutions of CoilY-mCherry (400 ng to 0.8 ng) were run on two identical SDS-PAGE gels before transfer to a PVDF membrane. The first membrane (top) was treated with CoilZ-fluorescein (CoilZ-FL) and imaged (ex 475/42 nm; em 537/35 nm). The second membrane (bottom) was labeled using an AF488-conjugated anti-His antibody "AF488-His" (QIAGEN, product number 35310) and imaged (475/42 nm excitation, 537/35 nm emission).

## Flow analysis of VIP Y/Z labeling on live cells

We translated our results from cell lysates to living cells. Flow cytometry was used to evaluate protein labeling in live human osteosarcoma (U-2 OS) cells expressing CoilZ-EGFP-TM, CoilY-EGFP-TM, or untagged EGFP-TM. Cells were treated with 500 nM AF647-conjugated probe peptide before analysis and gated for EGFP expression. We found that both peptide tags, CoilY and CoilZ, enabled selective protein labeling via heterodimerization (**Figure 2.4**). Treatment of cells expressing CoilZ-EGFP-TM with CoilY-AF647 resulted in bright, selective protein labeling with a greater than 40-fold enhancement. Non- specific labeling of untagged EGFP-TM and homodimerization with CoilY-EGFP-TM were minimal for cells exposed to CoilY-AF647. Cells expressing CoilY-EGFP-TM were labeled with CoilZ-AF647, but with only a 4-fold enhancement. Non-specific labeling was slightly higher for cells treated with CoilZ-AF647, and we suspect that this positively charged probe might interact with the negatively charged cell surface resulting in a higher non-specific signal.

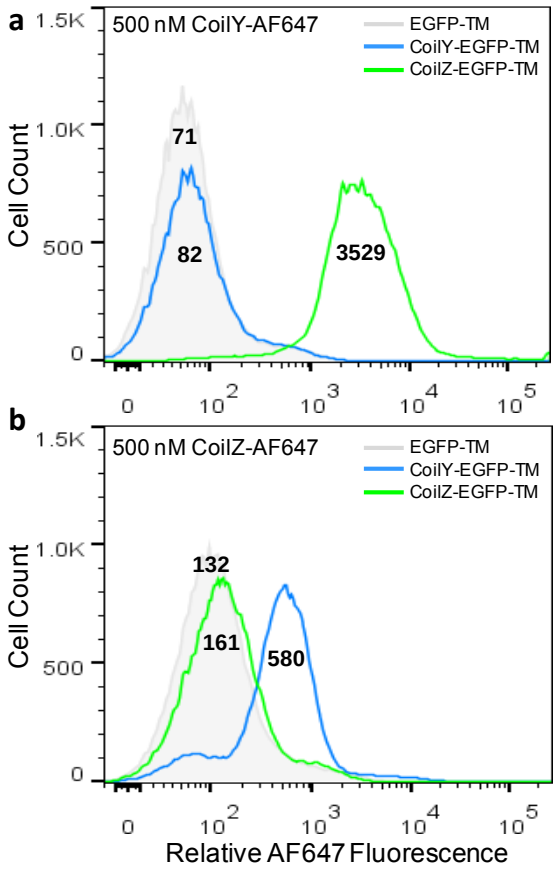


**Figure 2.4. Histograms of AF647 fluorescence from flow cytometry.** Cells were gated for green fluorescence and analyzed for labeling with Coil5-AF647 (a) or Coil6-AF647 (b). Transfected cells expressed Coil6-EGFP-TM (green), Coil5-EGFP-TM (blue), or untagged EGFP-TM (gray). Values in bold indicate the median AF647 fluorescence for each cell population.

We assessed protein labeling as a function of CoilY-AF647 concentration. Live cells expressing CoilZ-EGFP-TM or untagged EGFP-TM were treated with a range of CoilY-AF647 concentrations (50 to 1000 nM) for 30 min at room temperature. Flow cytometry showed that the median AF647 signal increased with increasing concentration of probe peptide (**Figure 2.5**). Cells had 21- to 44-fold higher median fluorescence compared to cells expressing untagged protein. Treatment with 300 nM AF647-CoilY gave optimal labeling, with 98% of cells labeled and a 35-fold increase in AF647 fluorescence. Treatment with an excess of probe peptide (i.e., 1000 nM) enhanced the AF647 signal, but at the cost of a small increase in non-specific labeling.

These results demonstrate that a range of concentrations could be used successfully to label tagged proteins.

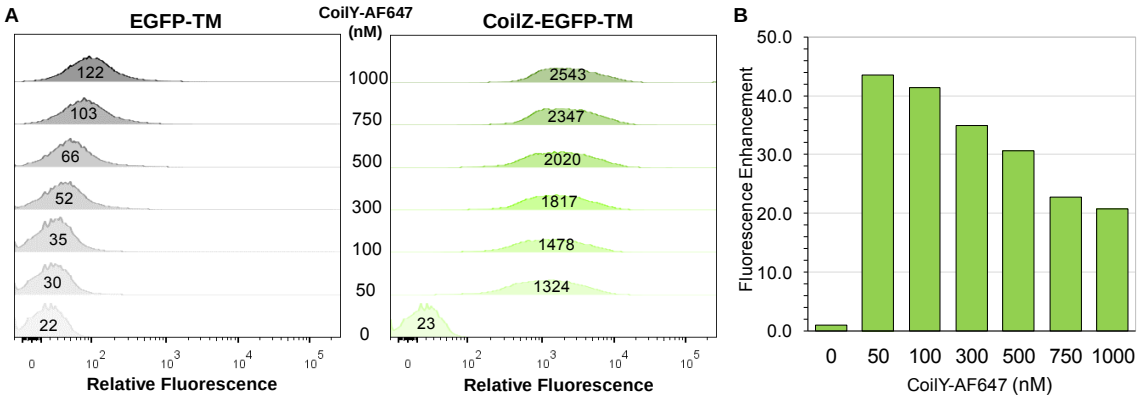


**Figure 2.5. Flow analysis of cells treated with CoilY-AF647. A.** U-2 OS cells were transfected with EGFP-TM or CoilZ-EGFP-TM and treated with increasing concentrations of CoilY-AF647. Single, live, green fluorescent cells expressing untagged (left) or tagged (right) EGFP-TM were counted and analyzed for labeling without probe peptide (0 nM) or with CoilY-AF647 (50, 100, 300, 500, 750, or 1000 nM). Values within each histogram indicate the median AF647 fluorescence for each cell population. Data analyzed included between 26,000 and 35,000 live, singlet GFP+ cells. **B.** Median fluorescence enhancement as a function of CoilY-AF647 concentration.

## Live cell fluorescence microscopy using VIP Y/Z

We used confocal fluorescence microscopy to assess protein labeling in transfected U-2 OS cells (**Figure 2.6**). Again, we relied on our CoilZ-EGFP-TM, CoilY-EGFP-TM, and untagged EGFP-TM constructs, which allowed us to track protein targets based on their green fluorescence. After transfection, EGFP fluorescence was observed both within cells and at the cell surface, where the peptide tag would be accessible to extracellular labeling by probe peptides. Live cells were blocked with 10% serum and 6% BSA to reduce non-specific labeling, and nuclei were stained with Hoechst 33342. Cells were selectively labeled with probe peptide at 37 ˚C, and we found that the EGFP-TM protein was rapidly internalized at this temperature (data not shown). Therefore, we opted to chill cells on ice to minimize endocytosis before treatment with a cold solution of probe peptide (300 nM). Unbound probe was removed by washing. We acquired optically-sectioned images at room temperature within 10 min

of probe peptide labeling. Fluorescent micrographs showed that labeling was tag-dependent and AF647 (magenta) and tagged EGFP (green) signal was colocalized (white) at the cell surface. Again, we observed no homodimerization and untagged EGFP-TM was not labeled. Protein-specific labeling was also observed with cells that were fixed prior to imaging (**Figure 2.8**).

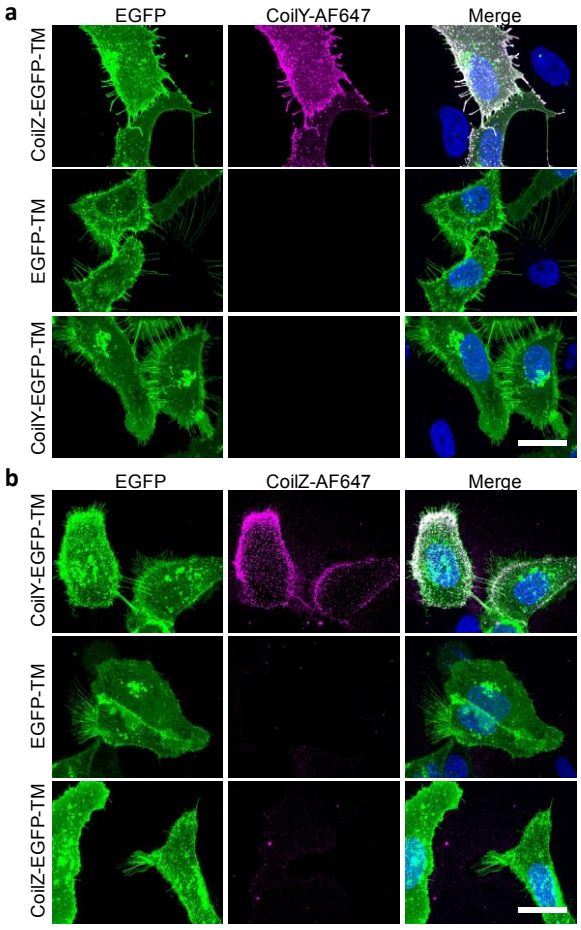


**Figure 2.6. Selective fluorescent labeling of cell-surface EGFP using CoilY and CoilZ.** (a) Cells treated with CoilY-AF647. (b) Cells treated with CoilZ-AF647. In both (a) and (b), labeling was only observed upon heterodimer formation with peptide tagged EGFP-TM. The merged images include EGFP (green), AF647 (magenta), and nuclear stain (blue). Colocalization of green and magenta appears as white in the merged image. Scale bars represent 25 μm. Individual slices from the Z-projections are available **Figure 2.7**

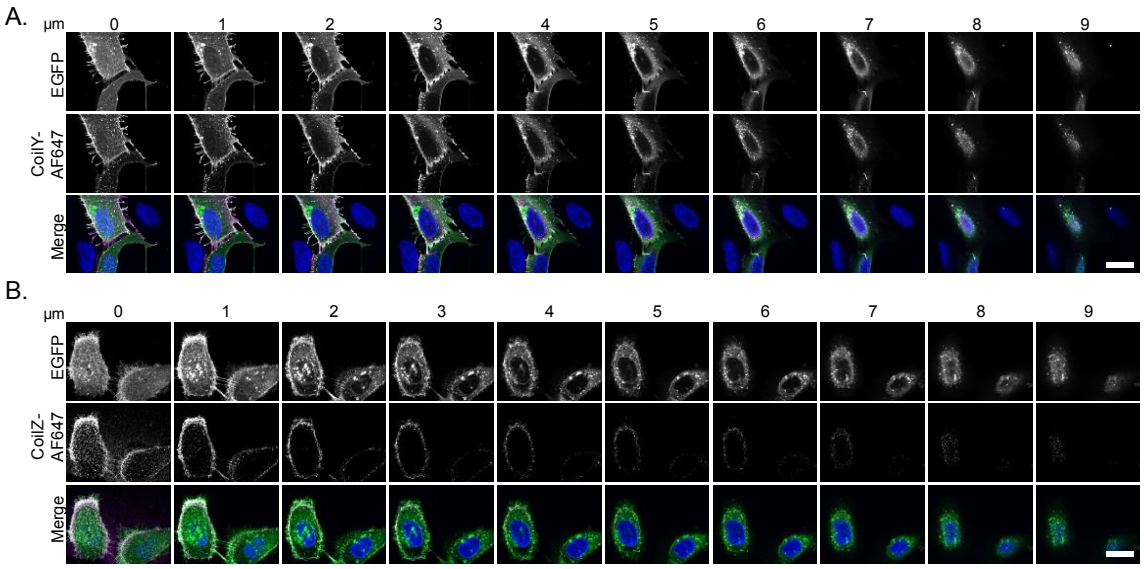


**Figure 2.7**. **Single microscopy slices showing specific peptide labeling of tagged EGFP-TM using CoilY/Z in live cells.** Single (1 μm-thick) optical slices used to create the Z projections in **Figure 3.** Micrographs show CoilY-AF647 specifically labeling CoilZ-EGFP-TM (**A**) or CoilZ-AF647 labeling CoilY-EGFP-TM (**B**). The merged image includes EGFP (green), AF647 (magenta), and Hoechst nuclear stain (blue). Scale bars represent 25 μm.

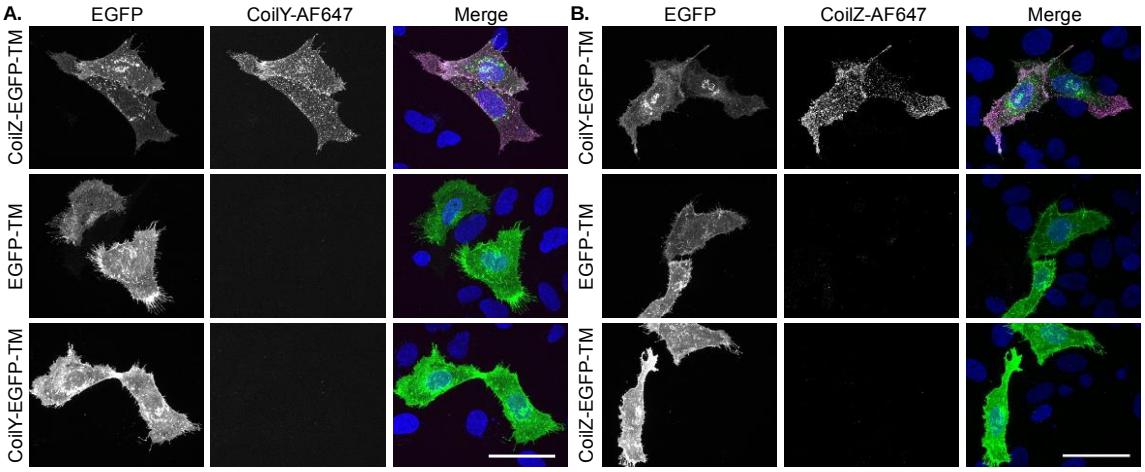


**Figure 2.8**. **Specific peptide labeling of tagged EGFP-TM using CoilY/Z in fixed cells. A.** CoilZ-EGFP-TM in live U-2 OS cells was selectively labeled with CoilY-AF647 (300 nM) before fixation and imaging. **B.** CoilY-EGFP-TM in live cells was selectively labeled with CoilZ-AF647 (300 nM) before fixation and imaging. In both A and B, labeling was only observed upon heterodimer formation. The merged image includes EGFP (green), AF647 (magenta), and Hoechst nuclear stain (blue). Scale bar represents 50 μm.

We observed that the probe peptides were membrane-impermeant towards living cells, as expected. Therefore AF647-labeling was limited to the subset of EGFP-TM localized to the cell surface at the time of treatment. We anticipate that this property will make VIP tags useful for monitoring endocytosis or recycling of cell-surface receptors. While we have not yet undertaken such studies, we did find that tagged proteins could be observed by time-lapse imaging (**Figure 2.9**).

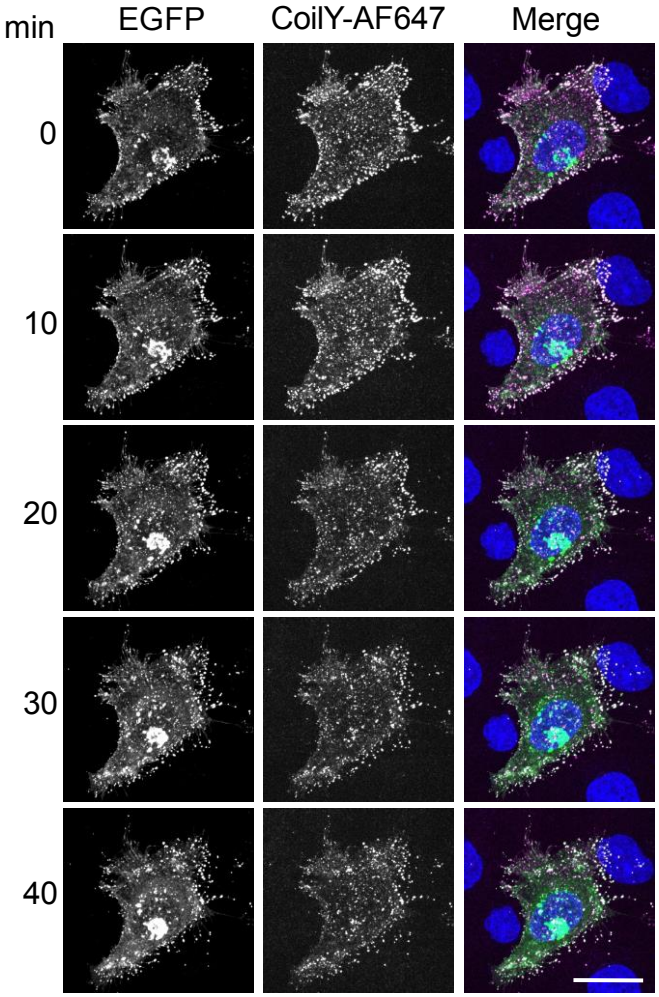


**Figure 2.9. Time-lapse imaging (0 to 40 min) of CoilY/Z labeling in live cells.** CoilZ-EGFP-TM was selectively labeled with 300 nM CoilY-AF647 and imaged every 10 min at room temperature. Overlay includes Hoechst (blue), EGFP (green), AF647 (magenta). Scale bar represents 25 μm.

In prior work, Matsuzaki and coworkers used an E3-K3 heterodimer for protein labeling and reported that the acidic (i.e., negatively charged) E3 peptide (pI = 4.5) could not be used to label K3-tagged proteins. The lysine-rich K3 peptide had a pI of

9.7[27]. In contrast, we found that both our basic CoilZ (pI = 8.0) and acidic CoilY (pI = 6.4) enabled selective labeling. We attribute this bi-directionality to the better overall charge balance of CoilY and CoilZ compared to E3 and K3. Although our data suggest that CoilZ is a better genetically-encoded tag than CoilY, it is notable that either peptide could be used to fluorophore-label proteins.

## VIP Y/Z's bi-directionality enables 4-color, 2-target imaging

We took advantage of CoilY and CoilZ's bi-directionality to observe two different protein targets simultaneously. Cells expressing CoilY-mCherry-TM were combined with cells expressing CoilZ-EGFP-TM to demonstrate the target-specific fluorophore labeling of distinct cell populations (**Figure 2.10**). Live cells were blocked and then cooled to halt endocytosis. Cells were labeled sequentially with CoilZ-biotin (500 nM; 15 min) and CoilY-AF647 (500 nM; 15 min). After fixation, cells were treated with Qdot565-conjugated streptavidin to Qdot-label CoilZ-biotin. To assess specificity, we used the same protocol to label cells expressing untagged EGFP-TM or mCherry-TM. Four-color fluorescence imaging revealed that CoilY and CoilZ could be used concurrently for tagging two distinct cell populations. When exposed to a mixture of cells displaying either CoilY or CoilZ tags, CoilY-AF647 and CoilZ-biotin correctly heterodimerized with their respective targets at the cell surface. We observed the expected colocalization of AF647 with EGFP and Qdot565 with mCherry, indicative of highly specific protein labeling. There was no cross-reactivity or labeling of untagged proteins. Therefore, this one heterodimeric pair unambiguously distinguished between two distinct protein targets at once.

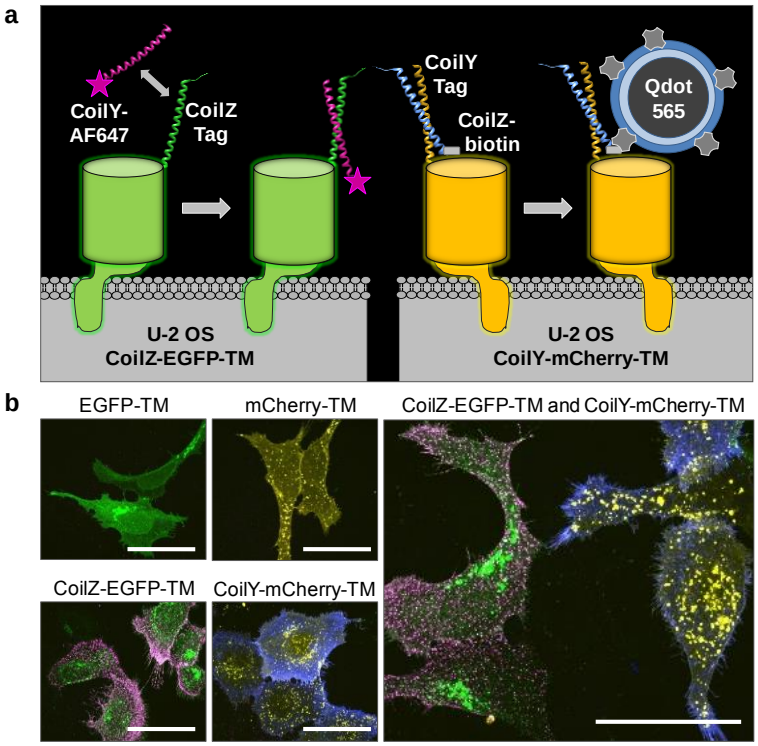


**Figure 2.10. Four-color imaging reveals heterodimer-mediated protein labeling in a mixed population of cells**. (a) Schematic of cell labeling protocol used to distinguish cells expressing Coil6-EGFP-TM from those expressing Coil5-mCherry-TM. (b) Confocal projections show Coil6-EGFP-TM (green) colocalized with Coil5-AF647 (magenta) and fluorescence from Coil5-mCherry-TM (yellow) colocalized with Qdot565 (blue). Qdot-labeling was mediated by binding of streptavidin-Qdot565 to Coil6-biotin. Untagged proteins did not colocalize with AF647 or Qdot565 signal, and homodimerization was not observed. See the **Figure 2.11** for individual channels. Scale bars represent 50 μm.

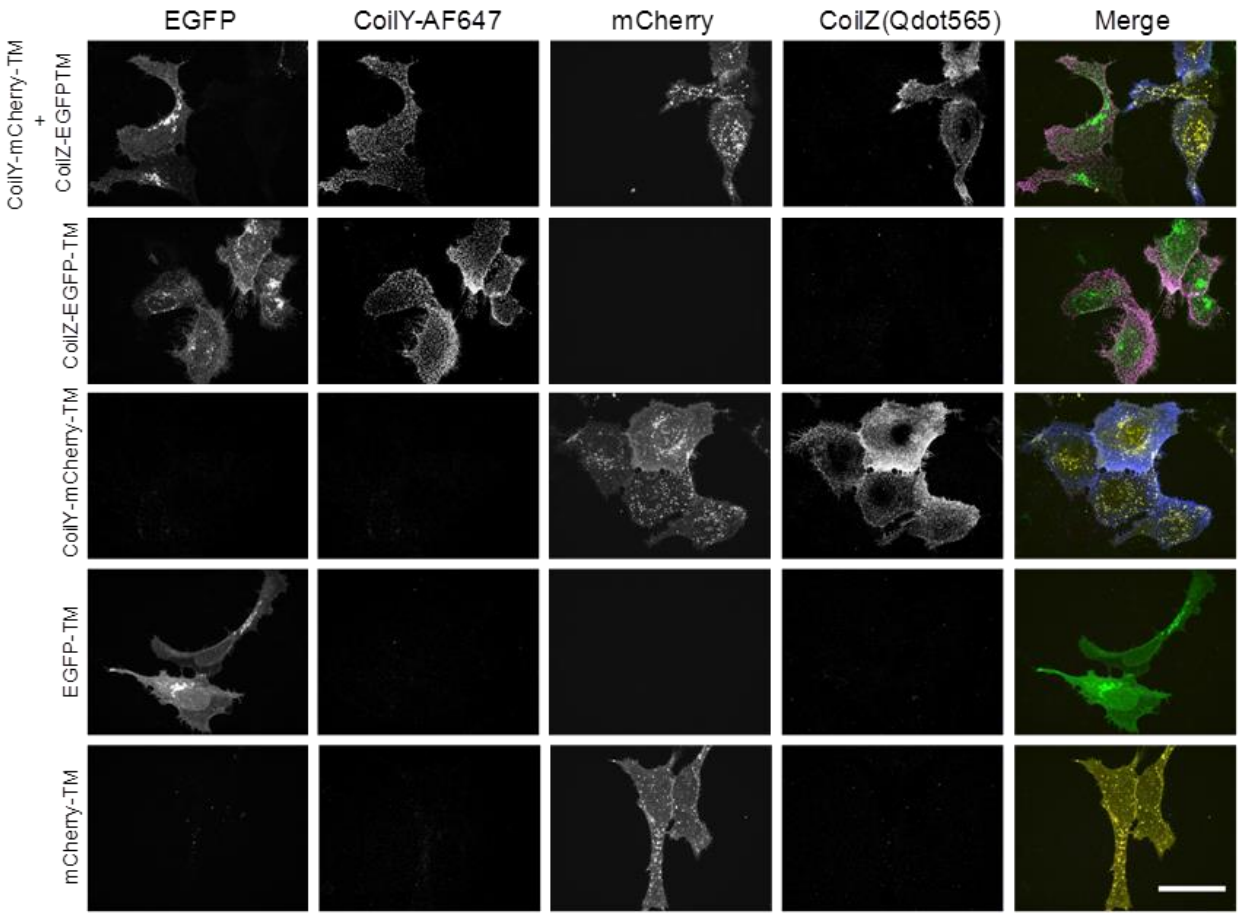


**Figure 2.11. Four-color imaging of CoilY/Z-mediated protein labeling in a mixed population of cells.** U-2 OS cells were transiently-transfected to express model proteins as indicated. Single channels of **Figure 2.10** showing fluorescence from CoilZ-EGFP-TM (green) colocalized with CoilY-AF647 (magenta), and fluorescence from CoilY-mCherry-TM (yellow) colocalized with Qdot565 (blue). Qdot-labeling was mediated by binding of streptavidin-Qdot565 to CoilZ-biotin. Untagged proteins did not colocalize with AF647 or Qdot565 signal, and homodimerization was not observed. Scale bar represents 50 μm.

## Conclusion

In summary, we demonstrated that CoilY and CoilZ are two new genetically-encoded peptide tags that enable the selective fluorescent labeling of target proteins in vitro and on the cell-surface. Fluorescent labeling of proteins in cells was analyzed by flow cytometry and confocal fluorescence microscopy, and we confirmed that this one heterodimeric pair could be used to detect two proteins simultaneously in a mixed cell population. These two genetically-encoded tags offer significant advantages over

extant protein and peptide tags. Labeling was rapid (15 to 30 min) and cells could be imaged either live or post-fixation. CoilY and CoilZ are small, target-specific, easy to use, and compatible with diverse chemical reporters. In the current work, we labeled proteins with bright organic fluorophores (fluorescein, rhodamine, and AF647) and Qdots (Qdot565). The reporter chemistry can be selected and optimized for different applications, which makes this technology highly versatile. We look forward to developing other selective heterodimeric coiled-coils into new VIP tags in future work.

## Acknowledgements

We are grateful to Drs. L. Lavis, J. Gray, S. Kaech-Petrie, J. Garay, and G. Sahay for helpful discussions. We thank Dr. U. Shinde for the use of his CD spectrometer and Dr. S. Gibbs for the use of her inverted light microscope. We are grateful to Drs. S. Levine and K. Tallman for advice and assistance. J.K.D. was partially supported by the Oregon chapter of the Achievement Rewards for College Scientists (ARCS) Foundation. Plasmids were provided by Dr. A. Ting (Addgene # 20861) and Drs. R. Tsien and M. Davidson (Addgene # 54630). Funding for K.E.B. was generously provided by the OHSU School of Medicine and the OHSU Knight Cancer Institute.

## Materials and Methods

The sequence and properties of CoilY, CoilZ, SYNZIP-5, and SYNZIP-6 are described in **Table 2.1**. Protein and peptide construct sequences are listed in **Table 2.2**. Bacterial strains and plasmids are summarized in **Table 2.3**. Oligonucleotides were purchased from Integrated DNA Technologies (IDT; **Table 2.4**). All SDS-PAGE separations used pre-cast Criterion XT Bis-Tris gels (Bio-Rad) with XT-MES buffer (Bio-Rad).

### Construction of CoilY-pET28b(+) and CoilZ-pET28b(+)

The CoilY and CoilZ genes were constructed using gene synthesis PCR with primers designed using DNAWorks (v3.2.3). Primers were designed to introduce a *Nco*I cut site at the 5' end and a *Hind*III cut sites at the 3' end of the gene for insertion to the multiple cloning site of pET28b(+). The CoilY gene was assembled by PCR from 8 primers: CoilY 1F, CoilY 2R, CoilY 3F, CoilY 4R, CoilY 5F, CoilY 6R, CoilY 7F, and CoilY 8R (**Table 2.4**). Following gene assembly, the gene was amplified by PCR (using the CoilY 1F and CoilY 8R primer). Amplified CoilY was inserted into a pET28b(+) vector using the *Nco*I and *Hind*III sites, and transformed into DH5α competent *E. coli* cells. Sequences were confirmed by DNA sequencing (OHSU Vollum DNA Sequencing Core). For peptide production, the CoilY-pET28b(+) construct was transformed into BL21(DE3) *E. coli.*

CoilZ was gene synthesized using the same approach with 10 primers: CoilZ 1F, CoilZ 2R, CoilZ 3F, CoilZ 4R, CoilZ 5F, CoilZ 6R, CoilZ 7F, CoilZ 8R, CoilZ 9F, and CoilZ 10R (**Table 2.4**). The gene was amplified using CoilZ 1F and CoilZ 10R primers before insertion into pET28b(+).

### Expression and purification of the CoilY and CoilZ probe peptides

A starter culture (5 mL) in LB-Kan of CoilY-pET28b(+) or CoilZ-pET28b(+) in BL21(DE3) *E. coli* was grown O/N at 37 °C, 225 rpm. A 1 L culture in LB-Kan was inoculated with the starter culture (1:200 dilution) and grown to an O.D. of 0.8. Expression of CoilY-$His_6$ was induced with 0.1 mM IPTG and grown for 1 h at 37 °C.

Expression of CoilZ-$His_6$ was induced with 0.6 mM IPTG and grown for 3 h at 37 °C. The cells were pelleted by centrifugation and frozen at -20 °C.

The $His_6$–tagged peptides were purified under denaturing conditions. Frozen cells were thawed on ice and re-suspended in 45 mL of denaturing lysis buffer (20 mM sodium phosphate, 500 mM NaCl, 8 M urea, 1 mM DTT, pH 7.5). Re-suspended cells were sonicated on ice with a 0.5" horn for 8 min with 30 s on/30 s off (Branson A-450; duty cycle, 80% and output control, 8). The lysate was transferred to a 50 mL centrifuge tube and clarified by centrifugation at 10,000*g* for 10 min. Clarified lysate was transferred to a fresh 50 mL conical tube with 1 mL of Ni-NTA resin (QIAGEN; pre-equilibrated with lysis buffer). The lysate/resin mixture was incubated at 4 °C on a rotating mixer for 1 h. The resin was then loaded into an Econo-Pac® Chromatography Column (Bio-Rad) and washed with 10 mL lysis buffer containing 20 mM imidazole and 10 mL lysis buffer containing 50 mM imidazole. The $His_6$-tagged peptides were eluted from the resin with 20 mL lysis buffer containing 500 mM imidazole. Fractions containing the desired peptides were combined, concentrated, and buffer exchanged into a low imidazole buffer (20 mM sodium phosphate, 500 mM NaCl, 10 mM imidazole, 1 mM DTT pH 7.5, 8 M Urea) using centrifugal filters (3000 MWCO Amicon Ultra, Millipore).

The peptides were further purified on a HisTrap FF 1 mL column (GE Healthcare) via FPLC (GE Äkta Purifier). The peptides were eluted with a linear gradient of 20 mM to 500 mM imidazole in lysis buffer over 20 column volumes. Fractions (1 mL) were collected throughout the gradient and analyzed by SDS-PAGE (**Figures 2.12 and 2.13**). Fractions containing purified peptides were combined, concentrated, and buffer exchanged into 1x TBS/Urea (50 mM Tris pH 8, 150 mM NaCl, 6 M urea) with 10% glycerol using centrifugal filters.

Peptide concentration (c) was determined using the equation $c = A_{280}/(\varepsilon * l)$, where $A_{280}$ is the absorbance at 280 nm, ε is the extinction coefficient of the protein, and l is the pathlength. The extinction coefficient was predicted using the ExPASy ProtParam tool (http://web.expasy.org/cgi-bin/protparam/protparam). The yield of purified CoilY-$His_6$ was 6.5 mg/L of culture. The yield of CoilZ-$His_6$ was 1.13 mg/L of culture.

**SDS-PAGE analysis**

Protein samples were combined with SDS-PAGE loading dye (final concentration: 50 mM Tris-HCl, 100 mM DTT, 2% SDS, 0.1% Bromophenol Blue, 10% glycerol pH 6.9) and boiled (10 min). Samples were centrifuged before analyzing on a 12% gel. Proteins were stained with Coomassie Brilliant Blue.

**Circular Dichroism (CD) Spectroscopy**

CD Spectra were recorded using a JASCO J-810 spectropolarimeter. CD spectra were measured at 50 μM total peptide concentration in PBS (8.2 mM $Na_2HPO_4$, 1.8 mM $K_2HPO_4$, 137 mM NaCl, pH 7.4) at 25 °C and 37 °C in 1 mm quartz cuvettes at 3 sec/nm scanning speed (**Figure 2.1**). We are grateful to Prof. Ujwal Shinde (OHSU) for the use of his instrument.

**Fluorophore labeling of CoilY-$His_6$ and CoilZ-$His_6$**

Purified peptides (100 nmol) were reduced with 5 mM TCEP in 1 mL degassed denaturing buffer (DenBf: Tris-Buffered Saline pH 7.0 with 6−8 M urea) at 50 °C for 30 min. The reduced peptides were diluted 5-fold with the same buffer and incubated with 0.5 mL pre-equilibrated Ni-NTA resin for 30 min at 4 °C. The resin was loaded on an Econo-Pac® Chromatography column (Bio-Rad) and washed once with DenBf supplemented with 1 mM TCEP. The maleimide containing fluorophore (0.1 mM, 100 equiv.) in degassed DenBf was added to the column for on-bead labeling. The flow-through was reloaded onto the column multiple times to improve labeling efficiency. The resin was washed with fresh DenBf and the labeled peptide eluted with DenBf containing 200 mM imidazole. Labeled peptide was buffered exchanged into DenBf (without imidazole) and stored in aliquots at -20 °C.

Peptide concentration (c) was calculated as $c = [A_{280} - (A_{fl}*CF)]/\varepsilon$, where $A_{280}$ is the absorbance at 280 nm, $A_{fl}$ is the absorbance at the maximum absorbance wavelength of the fluorophore, CF is the correction factor for the dye's absorbance at 280 nm, and ε is the extinction coefficient of the peptide (calculated as above). Labeling efficiency was calculated as $[A_{fl} / (\varepsilon_{fl}*c)]$ where $A_{fl}$ and c are as defined previously and $\varepsilon_{fl}$ is the

extinction coefficient of the fluorophore. See **Table 2.7** for fluorophores used and relevant values.

### Size exclusion chromatography analysis of CoilY-CoilZ dimerization

A Superdex 75 3.2/30 column (GE Healthcare) on an FPLC (GE ÄktaPurifier) was calibrated using the Gel Filtration Calibration Kit (GE) which contains blue dextran (2,000 kDa), albumin (66 kDa), carbonic anhydrase (29 kDa), cytochrome C (12.4 kDa) and aprotinin (6.5 kDa). ROX-labeled CoilY and CoilZ were prepared separately (25 μM) or as a 1:1 mixture (25 μM each) in TBS (pH 7.7). Peptides were incubated at room temperature for 2 h. 50 μL of each sample was resolved on the Superdex column with a flow rate of 0.05 mL/min in 20 mM Tris, 150 mM NaCl, pH 7.7. Absorbance was monitored at 280 nm (**Figure 2.14**). UNICORN software (Version 5.31 GE Healthcare) was used to analyze the elution profiles. The molecular masses for monomers and dimers were calculated from the calibration curve.

### Genetic construction of CoilY-mCherry-pBad

In-Fusion primers were designed following the manufacturer's protocol (In-Fusion HD, *Cloning Kit User Manual,* Takara Clontech). Briefly, the 5' end of the primers contained a sequence homologous to the linear mCherry-pBad vector (Addgene # 54630; depositing labs: Michael Davidson, Roger Tsien), including the restriction sites, *Nhe*I and *Sac*I, while the 3' end of the primer were specific to the CoilY gene (**Table 2.4**). The CoilY In-Fusion gene product was PCR amplified in using CloneAmp HiFi PCR Premix with 6 pmol of each primer (**Table 2.4**) and 1 ng of CoilY-pET28b(+) as the template. A touchdown PCR program was used with an initial denaturation step at 98 °C for 30 s, and 10 cycles of 98 °C for 10 s, 72 °C for 15 s, and 72 °C for 5 s, with the annealing temperature dropping 1 °C/cycle, followed by 15 cycles with the annealing temperature at 62 °C and finishing with a final elongation step at 72 °C. Products were analyzed on a 2% agarose gel in TAE Buffer and purified with Nucleospin PCR clean-up columns (Takara Clontech).

mCherry-pBad (Addgene # 54630) in DH5-α *E. coli* was grown in LB-ampicillin (LB-Amp) overnight at 37 °C for plasmid isolation. mCherry-pBad was isolated using a

FastPlasmid Mini Kit (5 Prime) following the manufacturer's instructions and doubly-digested with *Nhe*I-HF and *Sac*I in CutSmart™ Buffer (NEB) for 2 h at 37 °C. Linearized mCherry-pBad was purified via spin column and eluted in 15 µL EB buffer (10 mM Tris-Cl pH 8.5).

In-Fusion HD reactions were set up in 10 µL reaction volumes with 5X In-Fusion HD Enzyme mix, 100 ng of linearized vector and 150 ng of PCR amplified CoilY. The reaction was incubated at 50 °C for 15 min followed by transformation into TOP10 competent *E. coli* cells. Recombinant colonies were screened with colony PCR. CoilY-mCherry-pBad plasmid was isolated from positive hits with the FastPlasmid kit (5 Prime) and its identity confirmed via DNA sequencing (OHSU Vollum DNA Sequencing Core).

**Genetic construction of mCherry-TM, CoilY-mCherry-TM and CoilZ-mCherry-TM**

In-Fusion primers were designed as above (mCherry-pDisplay-F, mCherry-pDisplay-R, CoilY-mCherry-pDisplay-F; **Table 2.4**). The In-Fusion gene products were PCR amplified using in 25 µL reactions using the 2x CloneAmp HiFi PCR Premix following the protocol outlined in the previous section. Products were analyzed on a 1% agarose gel in TAE and purified with a spin column.

pDisplay-AP-CFP-TM (Addgene # 20861; depositing lab: Alice Ting) in DH5$\alpha$ was grown in 5 mL LB-Amp cultures overnight at 37 °C for plasmid isolation. pDisplay-AP-CFP-TM was isolated following the manufacturer's instructions with the FastPlasmid Mini Kit (5 Prime). Plasmid DNA (5 µg) was digested with *Bgl*II in Buffer 3 (NEB) at 37 °C for 3 h, followed by spin column purification. *Bgl*II digested pDisplay-AP-CFP-TM was then sequentially digested with *Sac*II in CutSmart™ buffer (NEB) at 37 °C for 3 h followed by purification from a 1% agarose gel using the Zymoclean Gel DNA Recovery Kit.

In-Fusion HD reactions were set up with a 1:3 molar ratio of linearized vector to InFusion PCR product. The reactions were incubated at 50 °C for 15 min followed by transformation into TOP10 competent *E. coli* cells. Recombinant colonies were screened with colony PCR. Plasmid was isolated from positive hits and its identity confirmed via DNA sequencing (OHSU DNA Services Core).

The CoilZ-mCherry-TM plasmid was constructed using the above protocol with the primers CoilZ-mCherry-pDisplay-F, CoilZ-mCherry-pDisplay-R (**Table 2.4**) and the *Bgl*II linearized pDisplay-mCherry plasmid. Plasmid was isolated and confirmed via DNA sequencing (OHSU DNA Services Core).

**Genetic construction of cell surface-displayed EGFP-TM, CoilY-EGFP-TM, and CoilZ-EGFP-TM**

In-Fusion primers were designed as above for EGFP-TM (EGFP-pDisp-F, EGFP-pDisp-R; **Table 2.4**). The In-Fusion gene products were PCR amplified using the 2x CloneAmp HiFi PCR Premix following the protocol outlined above. Products were analyzed on a 1% agarose gel in TAE and purified with a spin column.

AP-CFP-pDisplay in DH5$\alpha$ was grown in 5 mL LB-Amp cultures overnight at 37°C for plasmid isolation. AP-CFP-pDisplay was isolated using the FastPlasmid Mini Kit (5 Prime). DNA (5 µg) was digested with *Bgl*II in Buffer 3 at 37 °C for 3 h, followed by spin column purification. *Bgl*II digested AP-CFP-pDisplay was then sequentially digested with *Sac*II at 37 °C for 3 hours followed by purification from a 1% agarose gel using the Zymoclean Gel DNA Recovery Kit (89 ng/µl).

In-Fusion HD reactions were performed with 89 ng of linearized vector and 250 ng of InFusion PCR product. The reactions were incubated at 50 °C for 15 min followed by transformation into TOP10 competent *E. coli* cells. Recombinant colonies were screened with colony PCR. Plasmid was isolated from positive hits and its identity confirmed via DNA sequencing (OHSU DNA Services Core).

Next, we generated constructs for cell surface-displayed CoilY-EGFP-TM and CoilZ-EGFP-TM In-Fusion primers were designed as above (CoilY-EGFP-pDisp-F, CoilY-EGFP-pDisp-R, CoilZ-EGFP-pDisp-F, CoilZ-EGFP-pDisp-R; **Table 2.4**). The In-Fusion gene products were PCR amplified using in 25 µl reactions using the 2x CloneAmp HiFi PCR Premix following the protocol outlined in the "Methods" section: "Construction of CoilY-mCherry-pBad." Products were analyzed on a 1% agarose gel in TAE and purified with a spin column.

EGFP-pDisplay in DH5$\alpha$ was grown in 5 mL LB-Amp cultures overnight at 37 °C for plasmid isolation. EGFP-pDisplay was isolated using the FastPlasmid Mini Kit (5 Prime).

DNA (5 µg) was digested with *Bgl*II in Buffer 3 (NEB) at 37 °C for 3 h, followed by spin column purification. *Bgl*II digested AP-CFP-pDisplay was then sequentially digested with *Sac*II in CutSmart™ Buffer (NEB) at 37 °C for 3 h followed by purification from a 1% agarose gel using the Zymoclean Gel DNA Recovery Kit.

The In-Fusion cloning reactions were set up in 10 µl reaction volume with 5X In-Fusion HD Enzyme mix, 89 ng of linearized vector and 250 ng EGFP InFusion PCR product. The reaction was incubated at 50 °C for 15 min followed by transformation into TOP10 competent *E. coli* cells. Recombinant colonies were screened with colony PCR. Plasmid was isolated from positive hits and identities were confirmed via DNA sequencing (OHSU DNA Services Core).

**Expression and purification of $His_6$-mCherry and $His_6$-CoilY-mCherry**

A 5 mL starter culture in LB-Amp of mCherry-pBad or CoilY-mCherry-pBad in TOP10 *E. coli* was grown overnight at 37 °C, 225 rpm. A 1 L culture in LB-Amp was inoculated with 5 mL of the starter culture (1:200 dilution) and grown to an O.D. of 0.6. Protein expression was induced with 0.02% L-arabinose and grown for 4 h at 37 °C. The cells were pelleted by centrifugation. Cells were frozen at -20 °C prior to purification.

$His_6$-mCherry and $His_6$-CoilY-mCherry were purified under denaturing conditions. Frozen cells were thawed on ice and resuspended in 45 mL of denaturing lysis buffer. Resuspended cells were sonicated (Branson sonifier) on ice for 4 min (20 sec on/40 sec off). The lysate was clarified by centrifugation at 10,000*g* for 10 min to remove cellular debris and insoluble material. The supernatant was transferred to a new 50 mL conical tube and incubated with 1 mL of pre-washed Ni-NTA resin (QIAGEN) at 4 °C. After 1 h, the lysate/resin mixture was loaded onto an Econo-Pac® Chromatography column (Bio-Rad) and washed with 10 mL lysis buffer with 20 mM imidazole and 10 mL lysis buffer with 50 mM imidazole. $His_6$-mCherry and $His_6$-CoilY-mCherry were eluted with 20 mL lysis buffer containing 500 mM imidazole in 5 mL fractions. Fractions were analyzed by SDS-PAGE on a 10% gel.

The combined fractions containing $His_6$-mCherry or $His_6$-CoilY-mCherry were concentrated to <1.0 mL and buffer exchanged into Akta Buffer A (20 mM phosphate,

500 mM NaCl, 10 mM imidazole, 8M Urea, pH 7.5) using 10 kDa MWCO Amicon Ultra Centrifugal Filters (Millipore). The concentrated protein solution was purified on an ÄktaPurifier using a HisTrap FF 1 mL column (GE Healthcare). $His_6$-mCherry and $His_6$-CoilY-mCherry were eluted using a linear gradient of 20 mM to 500 mM imidazole over 20 column volumes. Fractions (1 mL) were analyzed by SDS-PAGE (**Figures 2.15** and **2.16**). Fractions containing purified protein were combined, concentrated, and buffer exchanged into 1x TBS + 10% glycerol. Protein concentration was determined using the calculated extinction coefficient at 280 nm (http://web.expasy.org/cgi-bin/protparam/protparam).

**Cell culture and transient expression of constructs in HEK 293FT cells**

HEK293-FT cells were generously provided by Prof. Joseph Gray (OHSU). HEK293-FT were maintained in alpha modification Eagle's medium ($\alpha$MEM) supplemented with 10% fetal bovine serum (FBS) and 100 U/mL penicillin and 100 µg/mL streptomycin in 5% $CO_2$ at 37 °C. For transfection, 4 x $10^5$ cells were seeded into each well of a 12-well plate and grown overnight. Transfection was performed using Lipofectamine 2000 (ThermoFisher Scientific) following the manufacturer's instructions. The transfection mixture contained 1.2 µg plasmid DNA (mCherry-TM, CoilY-mCherry-TM, CoilZ-mCherry-TM, EGFP-TM, CoilY-EGFP-TM, or CoilZ-EGFP-TM), 1.2 µL Lipofectamine 2000, and 200 µL Opti-MEM. Cell transfection was assessed on a Carl Zeiss Primo Vert inverted microscope 24 h after transfection using a 40x/0.75 NA lens with appropriate excitation and emission filters (mCherry: ex 545/25 nm, em 605/70 em, EGFP: ex 470/40, em 525/50). We are grateful to Prof. Summer Gibbs (OHSU) for the use of her inverted light microscope.

**Cell culture and transient expression of constructs in U-2 OS cells**

U-2 OS cells were generously provided by Prof. Xiaolin Nan (OHSU). Cells were maintained in Dulbecco's modified Eagle's medium (DMEM) with 10% FBS with 100 U/mL penicillin and 100 µg/mL streptomycin in 5% $CO_2$ at 37 °C. For imaging experiments, 1 x $10^5$ cells were plated in a 12 well plate and grown overnight. Transfection was carried out using Lipofectamine 2000 (ThermoFisher Scientific) following the manufacturer's instructions. The transfection mixture contained 100 µL

Opti-MEM, 1 µL Lipofectamine 2000 and 1 µg plasmid DNA (mCherry-TM, CoilY-mCherry-TM, EGFP-TM, CoilY-EGFP-TM, or CoilZ-EGFP-TM).

For flow cytometry, 1 x $10^7$ cells were plated on 10 cm tissue culture dishes and transfection was carried out using 1 mL of Opti-MEM with 15 µL Lipofectamine 2000 and 15 µg plasmid DNA. Transfected cells were used in experiments 24 h after transfection.

**Fluorescent detection of labeled proteins *in vitro* via a membrane transfer assay**

HEK293-FT were harvested 24 h after transfection with mCherry-TM, CoilY-mCherry-TM, EGFP-TM, or CoilZ-EGFP-TM. Cells were resuspended and incubated in modified RIPA buffer (10 mM Tris-Cl, 1 mM EDTA, 1% Triton X-100, 0.1% SDS, 140 mM NaCl, and 1 mM PMSF pH 8.0) for 5 min on ice. Crude lysates were clarified by centrifugation and analyzed by SDS-PAGE. Proteins were transferred from the gel onto polyvinylidene difluoride (PVDF) membrane (Immobilon-P, Millipore) at 80 V for 75 min. The PVDF membrane was blocked with 5% dehydrated milk in TBST (TBS with 0.1% Tween20) for 1 h. For CoilY-mCherry detection, the membrane was incubated with CoilZ-fluorescein (CoilZ-Fl) (250 nM in TBST with 5% BSA) for 1 h. The membrane was washed with TBST. For subsequent CoilZ-EGFP detection, the same membrane was then incubated with CoilY-ROX (250 nM in TBST with 5% BSA) for 1 h. The membrane was washed twice with TBST and twice with TBS (20 mM Tris, 150 mM NaCl). The membrane was imaged on a FluorChem Q system (GE Healthcare). CoilZ-Fl was imaged with the blue channel (475/42 nm excitation, 537/35 nm emission) and CoilY-ROX was imaged using the green channel (534/30 nm excitation, 606/62 nm emission). See **Figure 2.2**. We are grateful to Prof. Joe Gray for the use of his imager.

**Detection sensitivity comparison**

Purified $His_6$-mCherry and $His_6$-CoilY-mCherry were loaded on a 10% SDS-PAGE gel for separation. Electrophoresis occurred at 165 V for 1 h. The proteins were transferred from the gel onto a PVDF membrane (Immobilon-P, Millipore) at 80 V for 75 min. The membrane was blocked in 5% milk in TBST for 1 h. CoilZ-Fluorescein was diluted to 250 nM in 5% BSA in TBST and incubated with the membrane for 1 h.

Fluorescent images were collected using FluorChem Q (blue channel: 475/42 nm excitation, 537/35 nm emission) imaging system after washing two times with TBST and twice with TBS.

Decreasing quantities of purified CoilY-mCherry (400 ng to 0.8 ng) were resolved by SDS-PAGE and transferred to a PVDF membrane. The membrane was blocked in 5% milk in TBST for 1 h. CoilY-mCherry was detected by blotting with anti-pentahistidine mouse antibody conjugated to AlexaFluor488 (1:5000, QIAGEN; product number 35310). Fluorescent images were collected using FluorChem Q (blue channel: 475/42 excitation, 537/35 emission) imaging system after washing twice with TBST and twice with TBS (**Figure 2.3**).

**Flow cytometry analysis of CoilY and CoilZ labeling of tagged EGFP-TM in live cells**

U-2 OS cells (1 x $10^7$ cells/sample) expressing EGFP-TM, CoilY-EGFP-TM or CoilZ-EGFP-TM were detached using PBS with 10 mM EDTA. Cells were pelleted (500*g*, 10 min) and resuspended in 500 µL DMEM with 10% serum, and 10 mM HEPES. Cells were incubated for 30 min at room temperature with either CoilY-AF647, CoilZ-AF647, or without probe peptide. Cells were then washed three times with cold PBS and resuspended in 500 µL of Live Cell Imaging Solution (Molecular Probes, 140 mM NaCl, 2.5 mM KCl, 1.8 mM $CaCl_2$, 1 mM $MgCl_2$, 20 mM HEPES) and transferred to 5 mL polystyrene round-bottom tubes (Falcon). Cells were analyzed using a LSR II Flow Cytometer (BD Biosciences) and gated for live, singlet, EGFP positive cells. EGFP and AF647 were excited by 480 and 633 nm lasers and detected through 530/30 and 660/20 nm emission filters (see **Figures 2.4 and 2.5**).

Flow data was analyzed using FlowJo software (Version X.07). A scatterplot of forward scatter width versus forward scatter area (FSC-W/FSC-H) was used to gate for single cell events, and a scatterplot of side scatter area versus forward scatter area (SSC-A/FSC-A) was used to gate for live cells. Transfected cells were then gated using their green fluorescence intensity (ex 488 nm; em 530/30 nm), and cells greater than 500 relative fluorescence units were deemed GFP-positive. Live, singlet, and GFP-positive cells were then displayed on a histogram of AF647 fluorescence intensity (ex

633 nm; em 660/20 nm). Cells with AF647 fluorescence greater than 200 relative fluorescence units were deemed AF647-positive. The median AF647 fluorescence and percent of GFP-positive cells deemed AF647-positive of each cell population was determined (**Tables 2.5** and **2.6)**.

**CoilY/CoilZ-labeling and fluorescence imaging of tagged EGFP-TM in live cells**

Transiently transfected U-2 OS cells expressing EGFP-TM, CoilY-EGFP-TM or CoilZ-EGFP-TM were seeded in an 8-well chambered glass coverslip (Cellvis) at 5 x $10^4$ cells/well and allowed to adhere overnight. Cells were incubated with 1 µg/mL Hoechst 33342 (ThermoFisher Scientific) in DMEM with 10% FBS and 6% BSA for 30 min at 37 ºC. This step was included to stain the nuclei and reduce nonspecific binding of probe peptides. The cells were cooled on ice to halt endocytosis and then incubated with CoilY-AF647 or CoilZ-AF647 (300 nM probe peptide in ice-cold DMEM with 10% FBS and 10 mM HEPES). After 30 min, cells were washed thrice with ice-cold PBS and then placed in 200 µL of Live Cell Imaging Solution.

Fluorescent images were acquired as a Z-stack (1 µm slices; 10 slices acquired) on a Zeiss Yokogawa CSU-X1 spinning disk confocal microscope (OHSU ALMC Core). Temperature control was enabled by a temperature-controlled chamber around the microscope. Images were acquired with either a 40x/0.95 NA air or a 63x/1.4 NA oil immersion lens. Three color (**blue**: Hoechst, ex 405 nm, em 450/50 nm; **green**: EGFP, ex 488 nm, em 525/50 nm; **far-red**: AF647, ex 638 nm, em 690/650 nm) images were acquired with identical settings for all channels (**Figures 2.6, 2.7,** and **2.9**).

**CoilY/CoilZ labeling and fluorescence imaging of tagged EGFP-TM in fixed cells.**

Transiently transfected U-2 OS cells expressing EGFP-TM, CoilY-EGFP-TM or CoilZ-EGFP-TM were plated on an 8-well glass chambered coverslips (Cellvis) at 5 x $10^4$ cells/well and allowed to adhere overnight. The cells were initially incubated with 1 µg/mL Hoechst in DMEM with 10% FBS and 6% BSA for 30 min at 37 ºC. The cells were placed on ice to halt endocytosis and then incubated for 30 min with CoilY-AF647 or CoilZ-AF647 (300 nM probe peptide in ice-cold media with 10 mM HEPES. Cells were washed thrice with cold PBS and then fixed for 20 min at room temperature with

4% paraformaldehyde in PBS. Cells were washed twice with PBS before imaging in PBS.

Fluorescent images were acquired at the OHSU Advanced Light Microscopy Core (ALMC). Cells were imaged with optical sectioning on a Zeiss Yokogawa CSU-X1 spinning disk confocal microscope to acquire blue, green, and far-red fluorescence, as described above (see **Figure 2.8**).

**Dual-labeling of tagged-EGFP-TM and tagged-mCherry-TM**

U-2 OS cells were transiently transfected with: CoilZ-EGFP-TM, EGFP-TM, CoilY-mCherry-TM, or mCherry-TM. Cells (5 x $10^4$ total per well) were plated in an 8-well chambered glass coverslip (Cellvis) and grown overnight.

For the dual-labeling experiment, we either plated U-2 OS transfected with one construct or plated a 1:1 mixture of U-2 OS cells transfected with CoilZ-EGFP-TM and CoilY-mCherry-TM. More specifically, control wells were seeded with 5 x $10^4$ transfected U-2 OS expressing CoilZ-EGFP-TM, EGFP-TM, CoilY-mCherry-TM, or mCherry-TM. Experimental wells contained a mixed population (1:1) of CoilZ-EGFP-TM cells and CoilY-mCherry-TM cells and were created by seeding 2.5 x $10^4$ cells of each genotype into the same well; cells were mixed by pipetting immediately after seeding. It is worth noting that we did not observe artificial dimerization of CoilY-mCherry-TM cells with CoilZ-EGFP-TM cells.

Once the cells adhered overnight, all wells were treated following the same protocol. Prior to probe peptide labeling, cells were incubated with DMEM with 10% FBS and 6% BSA for 30 min at 37 ºC and then transferred to ice to stop endocytosis. Cells were incubated with ice-cold CoilZ-biotin (500 nM) in complete media with 10 mM HEPES. After 15 min, the CoilZ-biotin labeling solution was removed and replaced with ice-cold CoilY-AF647 (500 nM) in complete media with 10 mM HEPES for 15 min. Cells were washed thrice with cold PBS and fixed with 4% paraformaldehyde in PBS (20 min; room temperature).

After fixation, cells were washed twice with PBS and blocked (DMEM,10% FBS, 6% BSA) for 1 h at room temperature and then washed again with PBS. Cells were then treated with 1 nM streptavidin-Qdot565 (ThermoFisher Scientific) in PBS with 6% BSA

in order to Qdot-label CoilZ-biotin. Cells were washed two additional times before imaging in PBS.

Images were acquired as a Z-stack on a Zeiss Yokogawa CSU-X1 spinning disk confocal microscope (OHSU ALMC) with a 63x/1.4 NA oil lens. Four-color images (Qdot565: ex 405 nm, em 562/45 nm; EGFP: ex 488 nm, em 525/50 nm; mCherry: ex 561 nm, em 545/50 nm; AF647: ex 638 nm, em 690/50 nm). Acquisition settings were selected to minimize cross-talk between the 4 channels, and images were acquired under identical settings for each channel. Channels were false-colored for merged images (Qdot=blue, AF647=magenta, EGFP=green, mCherry=yellow; **Figure 2.10** and **2.11**).

**Microscopy Image Analysis**

Image analysis was carried out using Fiji Software (Version 2.0.0-rc-46). For each experiment, the Brightness and Contrast (B/C) was adjusted separately for each channel. Each channel was adjusted to the same B/C settings across all samples in an experiment. For example, all images of EGFP fluorescence were set to the same brightness and contrast settings. Grayscale images were false-colored using standard look up tables. Confocal Z-stacks were converted to projection images in Fiji using maximum pixel intensities before B/C optimization.

# Supplementary Tables and Figures

## Table 2.1. Sequence and properties of heterodimerizing peptides.[§]

| Peptide | Sequence | MW (kDa) | pI |
|---|---|---|---|
| CoilY tag (SYNZIP-5) | **NTVKELKNYIQELEERNAELKNLKEHLKFAKAELEFELAAHKFE** | 5.29 | 5.6 |
| CoilZ tag (SYNZIP-6) | **QKVAQLKNRVAYKLKENAKLENIVARLENDNANLEKDIANLEKDIANLERDVAR** | 6.20 | 8.3 |
| CoilY probe peptide | MGSS**NTVKELKNYIQELEERNAELKNLKEHLKFAKAELEFELAAHKFE***GGGAAA*CLGKLAAALEHHHHHH | 7.83 | 6.4 |
| CoilZ probe peptide | MGSS**QKVAQLKNRVAYKLKENAKLENIVARLENDNANLEKDIANLEKDIANLERDVAR***GGGAAA*CLGKLAAALEHHHHHH | 8.74 | 8.0 |

§ Key: **Coil gene sequence**, *linker sequence*, reactive cysteine, pET 28b(+)-derived sequence, $His_6$ tag for purification.

## Table 2.2. Summary of peptide and protein constructs.

| Name | Sequence (CoilY and CoilZ sequences are in **bold**) | Molecular Weight (Daltons) | Isoelectric point (pI) | Expression Vector |
|---|---|---|---|---|
| CoilY Probe Peptide | MGSS**NTVKELKNYIQELEERNAELKNLKEHLKFAKAELEFELAAHKFE**GGGAAACLGKLAAALEHHHHHH | 7,826.85 | 6.43 | pET28b(+) |
| CoilZ Probe Peptide | MGSS**QKVAQLKNRVAYKLKENAKLENIVARLENDNANLEKDIANLEKDIANLERDVAR**GGGAAACLGKLAAALEHHHHHH | 8,743.89 | 7.96 | pET28b(+) |
| $His_6$-CoilY-mCherry | MGGSHHHHHHGMAS**NTVKELKNYIQELEERNAELKNLKEHLKFAKAELEFELAAHKFE**GSSSMVSKGEEDNMAIIKEFMRFKVHMEGSVNGHEFEIEGEGEGRPYEGTQTAKLKVTKGGPLPFAWDILSPQFMYGSKAYVKHPADIPDYLKLSFPEGFKWERVMNFEDGGVVTVTQDSSLQDGEFIYKVKLRGTNFPSDGPVMQKKTMGWEASSERMYPEDGALKGEIKQRLKLDGGHYDAEVKTTYKAKKPQLPGAYNVNIKLDITSHNEDYTIVEQYERAEGRHSTGGMDELYK | 33,583.7 | 5.89 | mCherry-pBad |
| $His_6$-mCherry | MGGSHHHHHHGMASMTGGQQMGRDLYDDDDKDPSSSMVSKGEEDNMAIIKEFMRFKVHMEGSVNGHEFEIEGEGEGRPYEGTQTAKLKVTKGGPLPFAWDILSPQFMYGSKAYVKHPADIPDYLKLSFPEGFKWERVMNFEDGGVVTVTQDSSLQDGEFIYKVKLRGTNFPSDGPVMQKKTMGWEASSERMYPEDGALKGEIKQRLKLDGGHYDAEVKTTYKAKKPQLPGAYNVNIKLDITSHNEDYTIVEQYERAEGRHSTGGMDELYK | 30,624.30 | 5.66 | mCherry-pBad |
| mCherry-TM | METDTLLLWVLLLWVPGSTGDYPYDVPDYAGAQPARSMVSKGEEDNMAIIKEFMRFKVHMEGSVNGHEFEIEGEGEGRPYEGTQTAKLKVTKGGPLPFAWDILSPQFMYGSKAYVKHPADIPDYLKLSFPEGFKWERVMNFEDGGVVTVTQDSSLQDGEFIYKVKLRGTNFPSDGPVMQKKTMGWEASSERMYPEDGALKGEIKQRLKLKDGGHYDAEVKTTYKAKKPVQLPGAYNVNIKLDITSHNEDYTIVEQYERAEGRHSTGGMDELYKPRLQVDEQKLISEEDLNAVGQDTQEVIVVPHSLPFKVVVISAILALVVLTIISLIILIMLWQKKPR | 38,209.72 | 5.26 | pDisplay |
| CoilY-mCherry-TM | METDTLLLWVLLLWVPGSTGDYPYDVPDYAGAQPARS**NTVKELKNYIQELEERNAELKNLKEHLKFAKAELEFELAAHKFE**GSSSMVSKGEEDNMAIIKEFM | 43,797.01 | 5.33 | pDisplay |

| | | | | |
|---|---|---|---|---|
| | RFKVHMEGSVNGHEFEIEGEGEGRPYEGTQTAKLKVTKGGPLPFAWDILSP QFMYGSKAYVKHPADIPDYLKLSFPEGFKWERVMNFEDGGVVTVTQDSSLQ DGEFIYKVKLRGTNFPSDGPVMQKKTMGWEASSERMYPEDGALKGEIKQRL KLKDGGHYDAEVKTTYKAKKPVQLPGAYNVNIKLDITSHNEDYTIVEQYER AEGRHSTGGMDELYKPRLQVDEQKLISEEDLNAVGQDTQEVIVVPHSLPFK VVVISAILALVVLTIISLIILIMLWQKKPR | | | |
| CoilZ-mCherry-TM | METDTLLLWVLLLWVPGSTGDYPYDVPDYAGAQPARSRS**QKVAQLKNRVAY KLKENAKLENIVARLENDNANLEKDIANLEKDIANLERDVAR**GGGRSMVSK GEEDNMAIIKEFMRFKVHMEGSVNGHEFEIEGEGEGRPYEGTQTAKLKVTK GGPLPFAWDILSPQFMYGSKAYVKHPADIPDYLKLSFPEGFKWERVMNFED GGVVTVTQDSSLQDGEFIYKVKLRGTNFPSDGPVMQKKTMGWEASSERMYP EDGALKGEIKQRLKLKDGGHYDAEVKTTYKAKKPVQLPGAYNVNIKLDITS HNEDYTIVEQYERAEGRHSTGGMDELYKPRLQVDEQKLISEEDLNAVGQDT QEVIVVPHSLPFKVVVISAILALVVLTIISLIILIMLWQKKPR | 45,053.45 | 5.59 | pDisplay |
| CoilY-EGFP-TM | METDTLLLWVLLLWVPGSTGDYPYDVPDYAGAQPARS**NTVKELKNYIQELE ERNAELKNLKEHLKFAKAELEFELAAHKFE**GGGRSMVSKGEELFTGVVPIL VELDGDVNGHKFSVSGEGEGDATYGKLTLKFICTTGKLPVPWPTLVTTLTY GVQCFSRYPDHMKQHDFFKSAMPEGYVQERTIFFKDDGNYKTRAEVKFEGD TLVNRIELKGIDFKEDGNILGHKLEYNYNSHNVYIMADKQKNGIKVNFKIR HNIEDGSVQLADHYQQNTPIGDGPVLLPDNHYLSTQSKLSKDPNEKRDHMV LLEFVTAAGITLGMDELYKPRLQVDEQKLISEEDLNAVGQDTQEVIVVPHS LPFKVVVISAILALVVLTIISLIILIMLWQKKPR | 44,169.53 | 5.45 | pDisplay |
| CoilZ-EGFP-TM | METDTLLLWVLLLWVPGSTGDYPYDVPDYAGAQPARSRS**QKVAQLKNRVAY KLKENAKLENIVARLENDNANLEKDIANLEKDIANLERDVAR**GGGRSMVSK GEELFTGVVPILVELDGDVNGHKFSVSGEGEGDATYGKLTLKFICTTGKLP VPWPTLVTTLTYGVQCFSRYPDHMKQHDFFKSAMPEGYVQERTIFFKDDGN YKTRAEVKFEGDTLVNRIELKGIDFKEDGNILGHKLEYNYNSHNVYIMADK QKNGIKVNFKIRHNIEDGSVQLADHYQQNTPIGDGPVLLPDNHYLSTQSKL SKDPNEKRDHMVLLEFVTAAGITLGMDELYKPRLQVDEQKLISEEDLNAVG QDTQEVIVVPHSLPFKVVVISAILALVVLTIISLIILIMLWQKKPR | 45,329.84 | 5.66 | pDisplay |

## Table 2.3. Bacterial strains and plasmids.

| | Characteristics | Source |
|---|---|---|
| *E. coli* strains | | |
| TOP10 | F– mcrA Δ(mrr-hsdRMS-mcrBC) Φ80lacZΔM15 ΔlacX74 recA1 araD139 Δ(ara leu) 7697 galU galK rpsL (StrR) endA1 nupG | ThermoFisher Scientific |
| BL21(DE3) | fhuA2 [lon] ompT gal (λ DE3) [dcm] ΔhsdS λ DE3 = λ sBamHIo ΔEcoRI-B int::(lacI::PlacUV5::T7 gene1) i21 Δnin5 | ThermoFisher Scientific |
| Plasmids | | |
| pET28b(+) | T7 promoter, His-tag coding sequence, MCS, *lacI* coding sequence, (KanR) | Novagen |
| mCherry-pBad | T7 promoter, His-tag coding sequence, mCherry coding sequence, MCS, (AmpR) | Addgene |

| | | |
|---|---|---|
| EGFP-pBad | T7 promoter, His-tag coding sequence, mCherry coding sequence, MCS, (AmpR) | Addgene |
| pDisplay | CMV promoter/enhancer, T7 promoter, Murin Ig κ–chain leader coding sequence, hemagglutinin A epitope, MCS, myc epitope, PDGFR-TM coding sequence, (GeneticinR, AmpR) | Addgene/ThermoFisher Scientific |

**Table 2.4. Oligonucleotide sequences.**

| Primer Name | Sequence (Restriction sites are underlined) |
|---|---|
| CoilY 1F (*Nco*I) | GATATACCATGGGCAGCAGCA |
| CoilY 2R (*Nco*I) | TATAGTTTTTCAACTCTTTCACGGTATTGCTGCTGCCCATGGTAT |
| CoilY 3F | ACCGTGAAAGAGTTGAAAAACTATATTCAGGAGCTGGAAGAACGT |
| CoilY 4R | TCTTTCAGATTTTTCAGCTCCGCATTACGTTCTTCCAGCTCCTGA |
| CoilY 5F | CGGAGCTGAAAAATCTGAAAGAACATCTGAAGTTTGCGAAAGCGG |
| CoilY 6R | ATGTGCCGCCAGTTCAAACTCCAGTTCCGCTTTCGCAAACTTCAG |
| CoilY 7F | TTTGAACTGGCGGCACATAAATTCGAAGGCGGTGGGGCTGCGGCG |
| CoilY 8R (*Hind*III) | GCAAGCTTGCCCAGGCACGCCGCAGCCCCAC |
| CoilZ 1F (*Nco*I) | GATATACCATGGGCAGCAGC |
| CoilZ 2R (*Nco*I) | GATTTTTCAGCTGCGCCACTTTCTGGCTGCTGCCCATGGTATATC |
| CoilZ 3F | GTGGCGCAGCTGAAAAATCGTGTGGCGTATAAACTGAAAGAAAAT |
| CoilZ 4R | GCTACAATATTCTCCAGTTTCGCATTTTCTTTCAGTTTATACGCCACA |
| CoilZ 5F | GCGAAACTGGAGAATATTGTAGCGCGTTTGGAGAACGATAATGCT |
| CoilZ 6R | ATTTGCAATGTCCTTTTCCAGATTAGCATTATCGTTCTCCAAACG |
| CoilZ 7F | ATCTGGAAAAGGACATTGCAAATCTTGAAAAAGATATTGCGAACTTGG |
| CoilZ 8R | TCCACGCGCCACGTCACGTTCCAAGTTCGCAATATCTTTTTCAAG |
| CoilZ 9F (*Hind*III) | GACGTGGCGCGTGGAGGGGGTGCTGCTGCTTGTCTGGGGAAGCTT |
| CoilZ 10R (*Hind*III) | GCAAGCTTCCCCAGACAAGC |
| CoilY-pBad_mCherry (*Nhe*I) F | ACATCATCATGGTATGGCTAGCAATACCGTGAAAGAGTTGAAAAACT |
| CoilY-pBad_mCherry (*Sac*I) R | CTTGCTCACCATGCTCGAGCTCCCTTCGAATTTATGTGCCG |
| mCherry-pDisplay-F (*Bgl*II) | CCAGCCGGCCAGATCTATGGTGAGCAAGGGCGAGGA |
| mCherry-pDisplay-R (*Sac*II) | CGTCGACCTGCAGCCGCGGCTTGTACAGCTCGTCCATGC |
| CoilY-mCherry-pDisplay F (*Bgl*II) | CCAGCCGGCCAGATCTAATACCGTGAAAGAGTTGAAAAA |
| CoilZ-mCherry-pDisplay F (*Bgl*II) | CCAGCCGGCCAGATCTCAGAAAGTGGCGCAGCTGAAAAATC |
| CoilZ-mCherry-pDisplay R (*Bgl*II) | TGCTCACCATAGATCTACCCCCTCCACGCGCCAC |
| EGFP pDisp F (*Bgl*II) | CCAGCCGGCCAGATCTATGGTGAGCAAGGGCGAGGA |
| EGFP pDisp R (*Sac*I) | CGTCGACCTGCAGCCGCGGCTTGTACAGCTCGTCCATGCCGA |
| CoilY-EGFP-pDisp F (*Bgl*II) | CCAGCCGGCCAGATCTAATACCGTGAAAGAGTTGAAAAACTA |
| CoilY-EGFP-pDisp R (*Bgl*II) | TGCTCACCATAGATCTGCTCCCTTCGAATTTATGTGC |
| CoilZ-EGFP-pDisplay F (*Bgl*II) | CCAGCCGGCCAGATCTCAGAAAGTGGCGCAGCTGAAAAATC |

| | |
|---|---|
| CoilZ-EGFP-pDisplay R (*Bgl*II) | TGCTCACCATAGATCTACCCCCTCCACGCGCCAC |

## Table 2.5. Flow cytometry analysis of CoilY/Z protein labeling §

| | U-2 OS cell line | Cell Count | Median AF647 Fluorescence (AU) | AF647+ (percent) |
|---|---|---|---|---|
| Unlabeled | EGFP-TM | 48406 | 22.3 | 0.01 |
| | CoilY-EGFP-TM | 34205 | 21.4 | 0 |
| | CoilZ-EGFP-TM | 41832 | 24.9 | 0.01 |
| 500 nM CoilY-AF647 | EGFP-TM | 46678 | 71.3 | 6.1 |
| | CoilY-EGFP-TM | 34337 | 81.7 | 8.7 |
| | CoilZ-EGFP-TM | 38716 | 3529 | 97.6 |
| 500 nM CoilZ-AF647 | EGFP-TM | 47474 | 132 | 15.1 |
| | CoilY-EGFP-TM | 35922 | 580 | 79 |
| | CoilZ-EGFP-TM | 41875 | 161 | 20 |

§ Data corresponds to the histograms in **Figure S4**. "Cell count" refers to the number of live, single, GFP-positive cells analyzed. "AF647+ (percent)" refers to the percent of GFP-positive cells that were AF647-positive.

## Table 2.6. Flow cytometry analysis of labeling with variable amounts of CoilY-AF647§

| | EGFP-TM | | | CoilZ-EGFP-TM | | |
|---|---|---|---|---|---|---|
| CoilZ-AF647 (nM) | Median AF647 Fluorescence (AU) | AF647+ (percent) | Cell Count | Median AF647 Fluorescence (AU) | AF647+ (percent) | Cell Count |
| 0 | 21.7 | 0.06 | 30064 | 22.5 | 0.08 | 30226 |
| 50 | 30.4 | 0.9 | 30690 | 1324 | 95.5 | 30678 |
| 100 | 35.7 | 2.1 | 34723 | 1478 | 96.1 | 26484 |
| 300 | 52.1 | 5.4 | 30800 | 1817 | 98.2 | 27403 |
| 500 | 66.0 | 8.4 | 30497 | 2020 | 98.2 | 30944 |
| 750 | 103 | 17.8 | 30729 | 2347 | 99.0 | 30925 |
| 1000 | 122 | 23.2 | 30742 | 2534 | 99.0 | 26022 |

§ Data corresponds to **Figure S4.** "Cell count" refers to the number of live, single, GFP-positive cells analyzed. "AF647+ (percent)" refers to the percent of GFP-positive cells that were AF647-positive.

**Table 2.7. Fluorophores used for fluorophore-peptide conjugation of VIP Y/Z**

| Reactive fluorophore | Vendor | $\varepsilon_{fl}$ ($M^{-1}cm^{-1}$) | CF | Labeling efficiency |
|---|---|---|---|---|
| **Fluorescein maleimide** | VWR | 68,000 | 0.3 | 90−98% |
| **5(6)-Carboxy-X-rhodamine-C5 (ROX) maleimide** | VWR | 82,000 | 0.16 | 40−45% |
| **AF647 maleimide** | ThermoFisher | 239,000 | 0.03 | 88−92% |

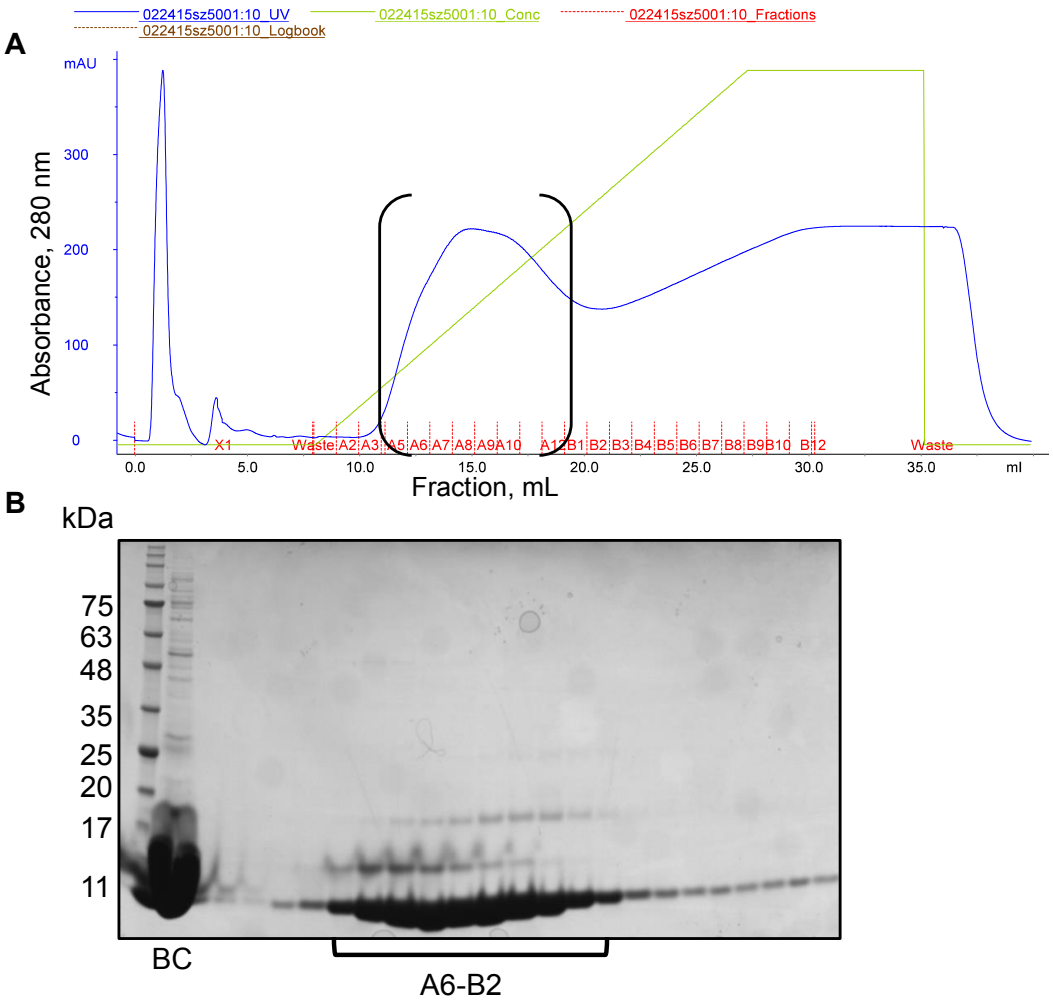


**Figure 2.12. CoilY probe peptide purification.** **A.** Chromatogram of denatured CoilY purification using a His-trap FF column. **B.** SDS-PAGE of 1 mL fractions (Coomassie-stained); bracketed fractions contained purified CoilY. "BC" is the concentrated sample (**b**efore **c**olumn) that was batch purified using Ni-NTA resin before FPLC purification. Some CoilY dimerization, potentially due to disulfide bonding, was observed at these high concentrations during purification.

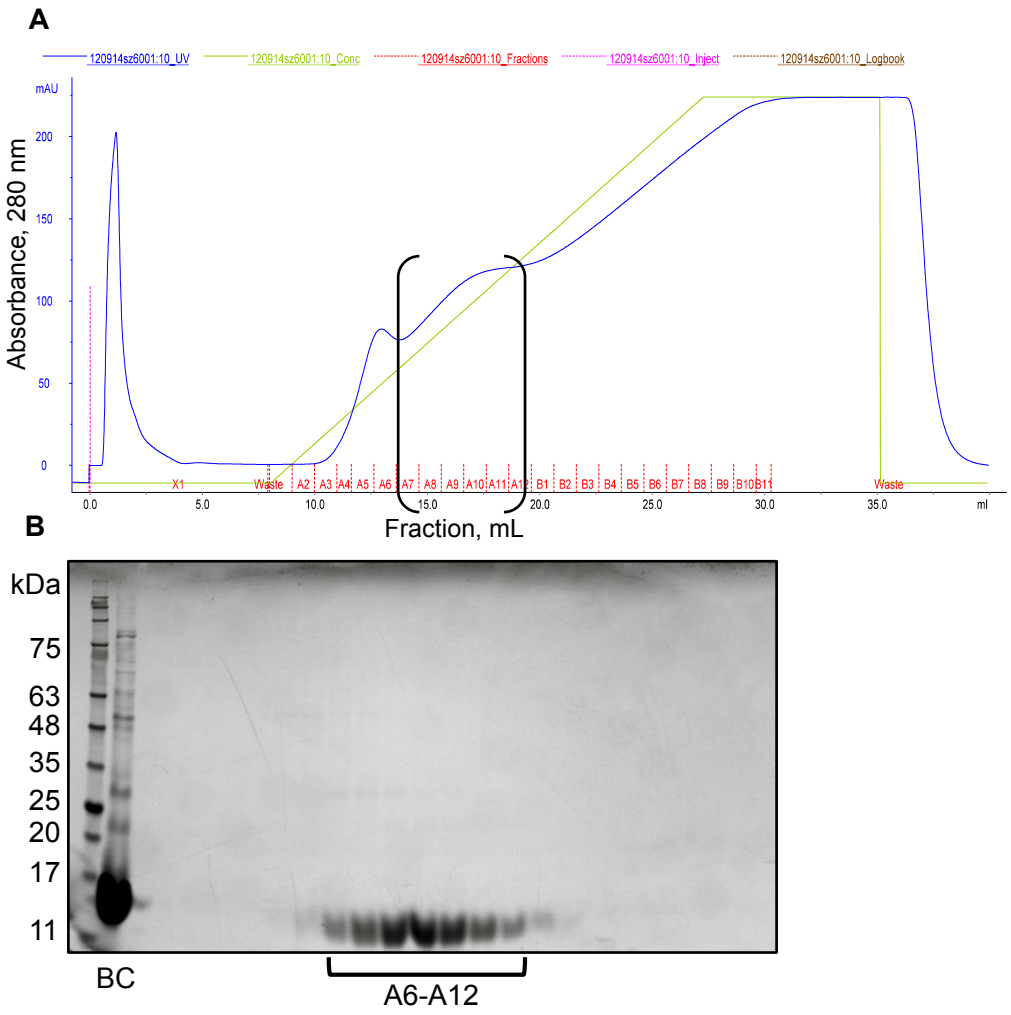


**Figure 2.13. CoilZ probe peptide purification. A.** Chromatogram of denatured CoilZ purification using a His-trap FF column. **B.** SDS-PAGE of 1 mL fractions (Coomassie stained; bracketed fractions contained purified CoilZ. "BC" is the concentrated sample (**b**efore **c**olumn) that was batch purified using Ni-NTA resin before FPLC purification.

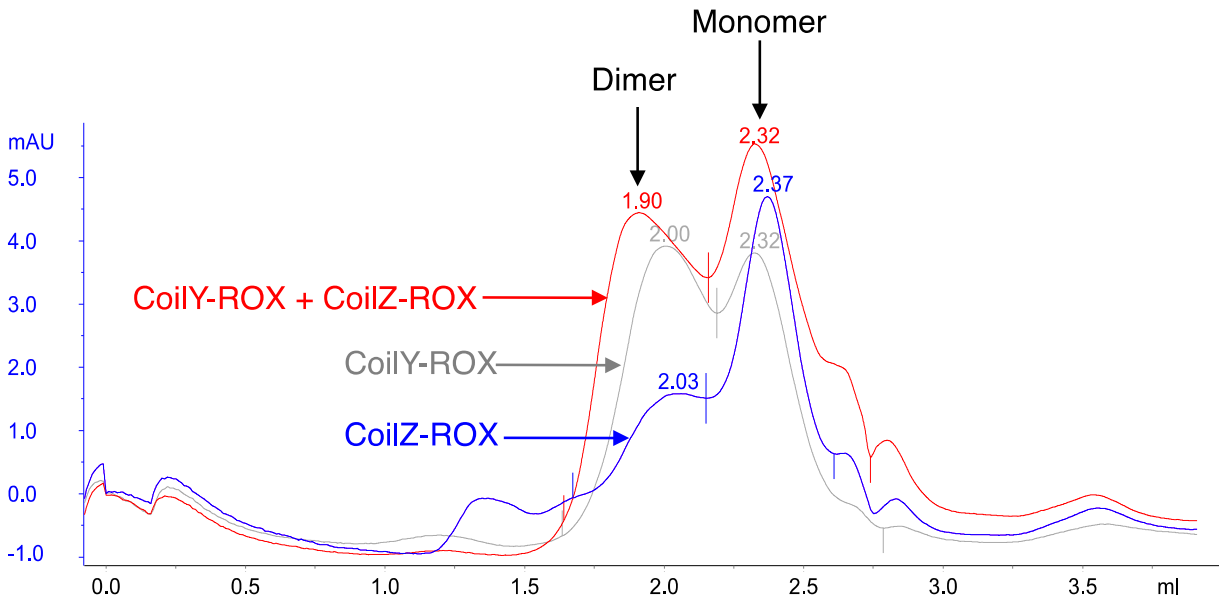


**Figure 2.14. Analysis of dimerization by size-exclusion chromatography.** Superdex 75 size exclusion chromatogram overlay of 25 μM CoilZ-ROX (blue), 25 μM CoilY-ROX (gray) and 25 μM CoilY-ROX + 25 μM CoilZ-ROX (red), monitored at 280 nm. The first peak represents the peptide dimer while the second peak represents the monomer. At the high concentrations needed to detect the peptides at 280 nm some dimerization was observed. The column was calibrated using the Gel Filtration Calibration Kit (GE Healthcare).

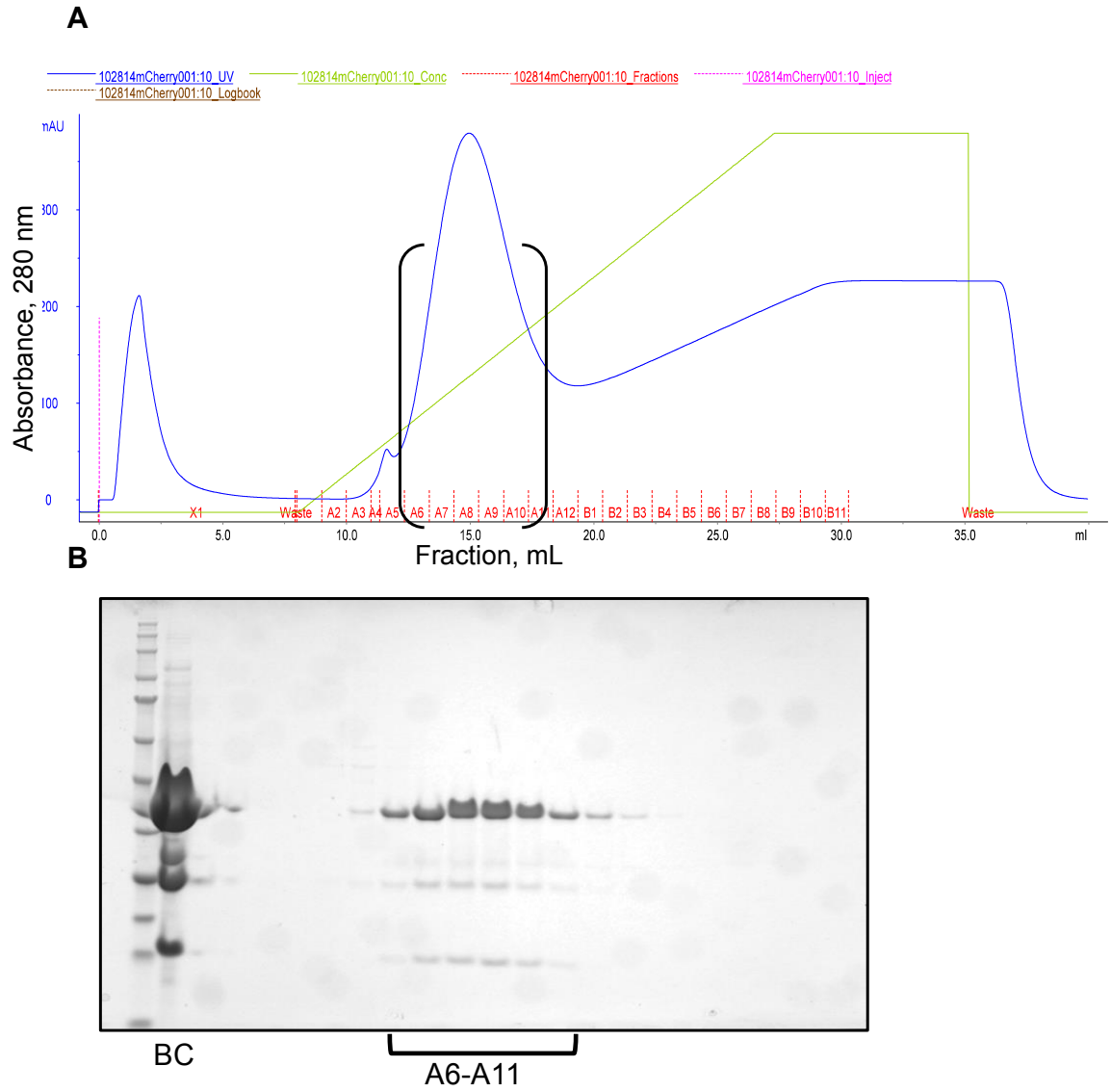


**Figure 2.15**. **FPLC chromatogram of $His_6$-mCherry purification.** **A.** Chromatogram of denatured $His_6$-mCherry purification using a His-trap FF column. **B.** SDS-PAGE of 1 mL fractions (Coomassie-stained); bracketed fractions contained purified $His_6$–mCherry and degradation products. "BC" is the concentrated sample (**b**efore **c**olumn) that was batch purified using Ni-NTA resin before FPLC purification.

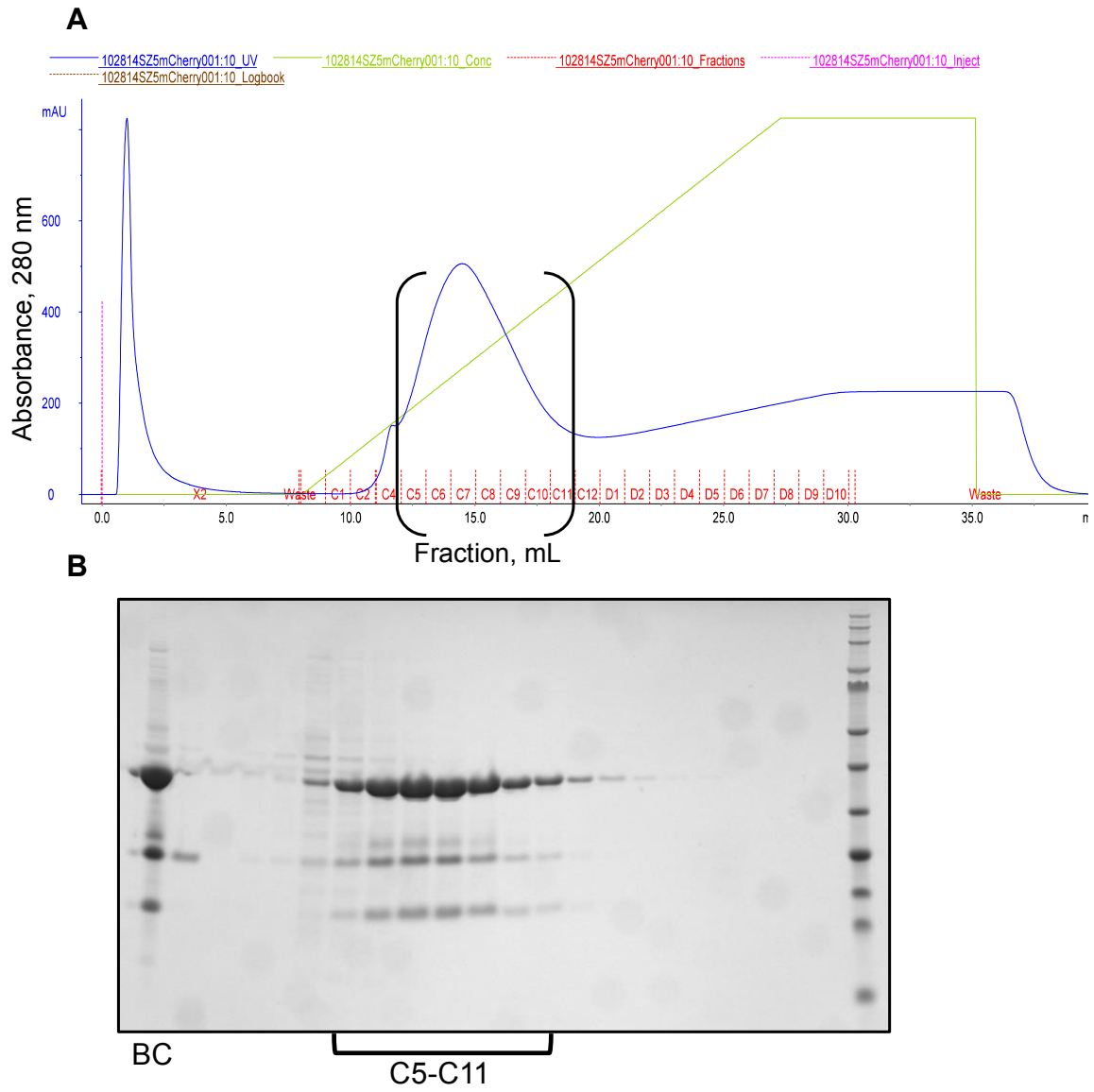


**Figure 2.16. FPLC chromatogram of $His_6$-CoilY-mCherry purification.** **A.** Chromatogram of denatured $His_6$-CoilY-mCherry purification using a His-trap FF column. **B.** SDS-PAGE of 1 mL fractions (Coomassie-stained); bracketed fractions contained purified $His_6$–Coil-5-mCherry and degradation products. "BC" is the concentrated sample (**b**efore **c**olumn) that was batch purified using Ni-NTA resin before FPLC purification.

## Works Cited


1. Dean, K. M. & Palmer, A. E. Advances in fluorescence labeling strategies for dynamic cellular imaging. *Nat. Chem. Biol.* **10**, 512–523 (2014).
2. Liu, Z., Lavis, L. D. & Betzig, E. Imaging live-cell dynamics and structure at the single-molecule level. *Mol. Cell* **58**, 644–659 (2015).
3. Giepmans, B. N. G., Adams, S. R., Ellisman, M. H. & Tsien, R. Y. The Fluorescent Toolbox for Assessing Protein Location and Function. *Science* **312**, 217–224 (2006).
4. Brock, R., Hamelers, I. H. & Jovin, T. M. Comparison of fixation protocols for adherent cultured cells applied to a GFP fusion protein of the epidermal growth factor receptor. *Cytometry* **35**, 353–362 (1999).
5. Huang, L., Pike, D., Sleat, D. E., Nanda, V. & Lobel, P. Potential Pitfalls and Solutions for Use of Fluorescent Fusion Proteins to Study the Lysosome. *PLOS ONE* **9**, e88893 (2014).
6. Costantini, L. M. & Snapp, E. L. Fluorescent proteins in cellular organelles: serious pitfalls and some solutions. *DNA Cell Biol.* **32**, 622–627 (2013).
7. Xue, L., Karpenko, I. A., Hiblot, J. & Johnsson, K. Imaging and manipulating proteins in live cells through covalent labeling. *Nat. Chem. Biol.* **11**, 917–923 (2015).
8. Sunbul, M. & Yin, J. Site specific protein labeling by enzymatic posttranslational modification. *Org. Biomol. Chem.* **7**, 3361 (2009).
9. Keppler, A. *et al.* A general method for the covalent labeling of fusion proteins with small molecules in vivo. *Nat. Biotechnol.* **21**, 86–89 (2003).
10. Heinis, C., Schmitt, S., Kindermann, M., Godin, G. & Johnsson, K. Evolving the substrate specificity of O6-alkylguanine-DNA alkyltransferase through loop insertion for applications in molecular imaging. *ACS Chem. Biol.* **1**, 575–584 (2006).
11. Los, G. V. *et al.* HaloTag: A Novel Protein Labeling Technology for Cell Imaging and Protein Analysis. *ACS Chem. Biol.* **3**, 373–382 (2008).
12. Miller, L. W., Cai, Y., Sheetz, M. P. & Cornish, V. W. In vivo protein labeling with trimethoprim conjugates: a flexible chemical tag. *Nat. Methods* **2**, 255–257 (2005).
13. Szent-Gyorgyi, C. *et al.* Fluorogen-activating single-chain antibodies for imaging cell surface proteins. *Nat. Biotechnol.* **26**, 235–240 (2008).
14. Dempsey, G. T., Vaughan, J. C., Chen, K. H., Bates, M. & Zhuang, X. Evaluation of fluorophores for optimal performance in localization-based super-resolution imaging. *Nat. Methods* **8**, 1027–1036 (2011).
15. Grimm, J. B. *et al.* Synthesis of a Far-Red Photoactivatable Silicon-Containing Rhodamine for Super-Resolution Microscopy. *Angew. Chem. Int. Ed Engl.* **55**, 1723–1727 (2016).
16. Grimm, J. B. *et al.* Bright photoactivatable fluorophores for single-molecule imaging. *Nat. Methods* **13**, 985–988 (2016).
17. Yan, Q. *et al.* Localization microscopy using noncovalent fluorogen activation by genetically encoded fluorogen-activating proteins. *Chemphyschem Eur. J. Chem. Phys. Phys. Chem.* **15**, 687–695 (2014).
18. Griffin, B. A., Adams, S. R. & Tsien, R. Y. Specific Covalent Labeling of Recombinant Protein Molecules Inside Live Cells. *Science* **281**, 269–272 (1998).
19. Gaietta, G. *et al.* Multicolor and electron microscopic imaging of connexin trafficking. *Science* **296**, 503–507 (2002).

20. Langhorst, M. F., Genisyuerek, S. & Stuermer, C. A. Accumulation of FlAsH/Lumio Green in active mitochondria can be reversed by beta-mercaptoethanol for specific staining of tetracysteine-tagged proteins. *Histochem. Cell Biol.* **125**, 743–747 (2006).
21. Crivat, G., Tokumasu, F., Sa, J. M., Hwang, J. & Wellems, T. E. Tetracysteine-Based Fluorescent Tags to Study Protein Localization and Trafficking in Plasmodium falciparum-Infected Erythrocytes. *PLOS ONE* **6**, e22975 (2011).
22. Howarth, M., Takao, K., Hayashi, Y. & Ting, A. Y. Targeting quantum dots to surface proteins in living cells with biotin ligase. *Proc. Natl. Acad. Sci. U. S. A.* **102**, 7583–7588 (2005).
23. Cohen, J. D., Thompson, S. & Ting, A. Y. Structure-Guided Engineering of a Pacific Blue Fluorophore Ligase for Specific Protein Imaging in Living Cells. *Biochemistry* **50**, 8221–8225 (2011).
24. Uttamapinant, C. *et al.* A fluorophore ligase for site-specific protein labeling inside living cells. *Proc. Natl. Acad. Sci.* **107**, 10914–10919 (2010).
25. Liu, D. S. *et al.* Computational design of a red fluorophore ligase for site-specific protein labeling in living cells. *Proc. Natl. Acad. Sci.* **111**, E4551–E4559 (2014).
26. Litowski, J. R. & Hodges, R. S. Designing Heterodimeric Two-stranded α-Helical Coiled-coils EFFECTS OF HYDROPHOBICITY AND α-HELICAL PROPENSITY ON PROTEIN FOLDING, STABILITY, AND SPECIFICITY. *J. Biol. Chem.* **277**, 37272–37279 (2002).
27. Yano, Y. *et al.* Coiled-Coil Tag−Probe System for Quick Labeling of Membrane Receptors in Living Cells. *ACS Chem. Biol.* **3**, 341–345 (2008).
28. Reinke, A. W., Grant, R. A. & Keating, A. E. A Synthetic Coiled-Coil Interactome Provides Heterospecific Modules for Molecular Engineering. *J. Am. Chem. Soc.* **132**, 6025–6031 (2010).
29. Thompson, K. E., Bashor, C. J., Lim, W. A. & Keating, A. E. SYNZIP Protein Interaction Toolbox: *in Vitro* and *in Vivo* Specifications of Heterospecific Coiled-Coil Interaction Domains. *ACS Synth. Biol.* **1**, 118–129 (2012).
30. Wang, J., Yu, Y. & Xia, J. Short Peptide Tag for Covalent Protein Labeling Based on Coiled Coils. *Bioconjug. Chem.* **25**, 178–187 (2014).
31. Tsutsumi, H. *et al.* Fluorogenically active leucine zipper peptides as tag-probe pairs for protein imaging in living cells. *Angew. Chem. Int. Ed Engl.* **48**, 9164–9166 (2009).
32. Bromley, E. H. C., Sessions, R. B., Thomson, A. R. & Woolfson, D. N. Designed α-Helical Tectons for Constructing Multicomponent Synthetic Biological Systems. *J. Am. Chem. Soc.* **131**, 928–930 (2009).
33. Aronsson, C. *et al.* Self-sorting heterodimeric coiled coil peptides with defined and tuneable self-assembly properties. *Sci. Rep.* **5**, (2015).
34. Robson Marsden, H. & Kros, A. Self-Assembly of Coiled Coils in Synthetic Biology: Inspiration and Progress. *Angew. Chem. Int. Ed.* **49**, 2988–3005 (2010).
35. Reinhardt, U. *et al.* Peptide-Templated Acyl Transfer: A Chemical Method for the Labeling of Membrane Proteins on Live Cells. *Angew. Chem. Int. Ed.* **53**, 10237–10241 (2014).
36. Apostolovic, B., Danial, M. & Klok, H.-A. Coiled coils: attractive protein folding motifs for the fabrication of self-assembled, responsive and bioactive materials. *Chem. Soc. Rev.* **39**, 3541–3575 (2010).

37. Debeljak, N., Feldman, L., Davis, K. L., Komel, R. & Sytkowski, A. J. Variability in the immunodetection of His-tagged recombinant proteins. *Anal. Biochem.* **359**, 216–223 (2006).

# Chapter 3: VIPER is a genetically-encoded peptide tag for fluorescence and electron microscopy

**Julia K. Doh**, Jonathan D. White, Hannah K. Zane, Young Hwan Chang, Claudia S. López, Caroline A. Enns, and Kimberly E. Beatty

*This work is adapted from a manuscript originally published by Proceedings of the National Academy of Sciences of the United States of America (PNAS) on December 5, 2018 in Volume 115 (Issue 51) pages 12961-12966 (Copyright 2018 National Academy of Sciences). It has been adapted for this dissertation and reprinted with permission. I was the lead on this project. I made a subset of the materials (probes, genetic constructs) and performed all of the experiments featured in this chapter.*

## Abstract

Many discoveries in cell biology rely on making specific proteins visible within their native cellular environment. There are various genetically-encoded tags, such as fluorescent proteins, developed for fluorescence microscopy (FM). However, there are almost no genetically-encoded tags that enable cellular proteins to be observed by both FM and electron microscopy (EM). Herein, we describe a new technology for labeling proteins with diverse chemical reporters, including bright organic fluorophores for FM and electron dense nanoparticles for EM. Our technology uses Versatile Interacting Peptide (VIP) tags, a new class of genetically-encoded tag. We present VIPER, which consists of a coiled-coil heterodimer formed between the genetic tag, CoilE, and a probe-labeled peptide, CoilR. Using confocal FM, we demonstrate that VIPER can be used to highlight sub-cellular structures or to image receptor-mediated iron uptake. Additionally, we used VIPER to image the iron uptake machinery by correlative light and EM (CLEM). VIPER compared favorably with immunolabeling for imaging proteins by CLEM, and is an enabling technology for protein targets that cannot be immunolabeled. VIPER is the first example, to our knowledge, of a peptide tag that can be used to label and track proteins with diverse chemical reporters observable by both FM and EM instrumentation.

## Introduction

Recent advances in imaging instrumentation and computational analysis have created an exciting opportunity for investigating the molecular basis of diseases with extraordinary detail. For example, in the area of fluorescence microscopy (FM), the development of super-resolution microscopy (SRM)[1–3] has enabled new discoveries on the structure, organization, and dynamics of organelles[4–6]. While SRM offers better resolution than conventional FM, it still falls short of obtaining the ultrastructural detail and cellular context afforded by electron microscopy (EM). EM is therefore more useful for imaging nanoscale sub-cellular features, including neuronal connections[7], chromatin organization[8], or components of the endocytic machinery[9]. Correlative light and EM (CLEM) seeks to combine the best features of both FM and EM[10,11], but there are few methods for labeling and tracking cellular proteins across size scales and imaging platforms. New protein labeling methods for multi-scale microscopy need to be developed in order to fully exploit the potential of these technologies.

How can cellular proteins be labeled to take advantage of these remarkable new technologies? Immunolabeling is one of the only methods compatible with FM, EM, and CLEM. Antibodies can be conjugated to a wide variety of chemical reporters, including fluorophores and nanoparticles (e.g. gold or quantum dots). However, labeling proteins with antibodies has several drawbacks. The large size of antibodies reduces localization precision and labeling protocols can change or disrupt cellular ultrastructure[10]. Low abundance proteins and rare interactions often evade detection because immunolabeling is typically inefficient (<30%)[10–12]. Many antibodies have poor target specificity and cross-reactivity[13,14], which can result in misleading observations. To summarize, issues with immunolabeling have led to widespread interest in having better genetically-encoded tags for imaging cellular proteins.

Genetically-encoded tags are widely available for FM, and a subset are compatible with SRM[1,15]. However, most tags for FM are large, which can have negative consequences on protein folding, trafficking, and function[2,16,17]. Commonly used tags include fusions to fluorescent proteins (30 kDa)[18], DNA alkyltransferases (28 kDa)[19,20], a dehalogenase (33 kDa)[21], DHFR (18 kDa)[22], or antibody fragments (26 kDa)[23].

By comparison, there is a scarcity of genetically-encoded tags for EM. There have been efforts to develop metal-chelating protein tags, but those tags have not been widely adopted due to multimerization, size, toxicity, and a low signal-to-noise ratio[24–29]All other EM tags, including APEX and miniSOG[30–32], use the oxidation of diaminobenzidine (DAB) to form an insoluble polymer that is stained with osmium tetroxide to generate contrast. DAB precipitation is difficult to control, which limits localization precision[33]. APEX uses peroxidase activity to polymerize DAB, but is large (28 kDa)[30,31]. MiniSOG is a 15 kDa photo-oxidizing tag with dim fluorescence for CLEM imaging[32]. The remaining DAB-oxidizing tags are rarely used for EM[34–36]. A drawback with all of these tags is their reliance on the same reporter chemistry.

We report herein a new technology that enables effortless switching from FM to high-resolution EM without changing the genetically-encoded tag. In 2017, we published our first versatile interacting peptide (VIP) tag, named VIP Y/Z[37]. Now we present VIPER, a new tag that has high specificity in a miniaturized size. VIPER uses a heterodimeric coiled-coil between two peptides, CoilE and CoilR, to label cellular proteins with several distinct chemical reporters (**Scheme 3.1**). The genetically-encoded peptide, CoilE, is one of the smallest available tags (5.2 kDa). We validated the specificity and versatility of VIPER by imaging CoilE-tagged proteins by both FM and EM.

## Design of VIPER, a genetically-encoded tag

Most genetically-encoded tags rely on large protein structures to deliver contrast. Due to their inherent structural complexity, it has been challenging and time-intensive to engineer new tags. For example, it took five years to convert SNAP into CLIP[19] and twenty years to develop a satisfactory near-infrared fluorescent protein[38,39]. In contrast, VIP tags are a new class of tag that uses an alpha-helical coiled-coil to label proteins. This is a simple structural motif amenable to design and optimization by protein engineering, with dimerization specificity and affinity dictated by the peptide sequence[40–49]. For our prior VIP tag, VIP Y/Z[37], we adapted a heterodimeric coiled-coil reported by Keating and coworkers[44]. That dimer had a reported dissociation constant ($K_D$) of <15 x 10-9 M[50] and a melting temperature ($T_m$) of 32 ºC[44]. VIP Y/Z precisely

labeled protein targets with various chemical reporters, including fluorophores and quantum dots (Qdots)[37].

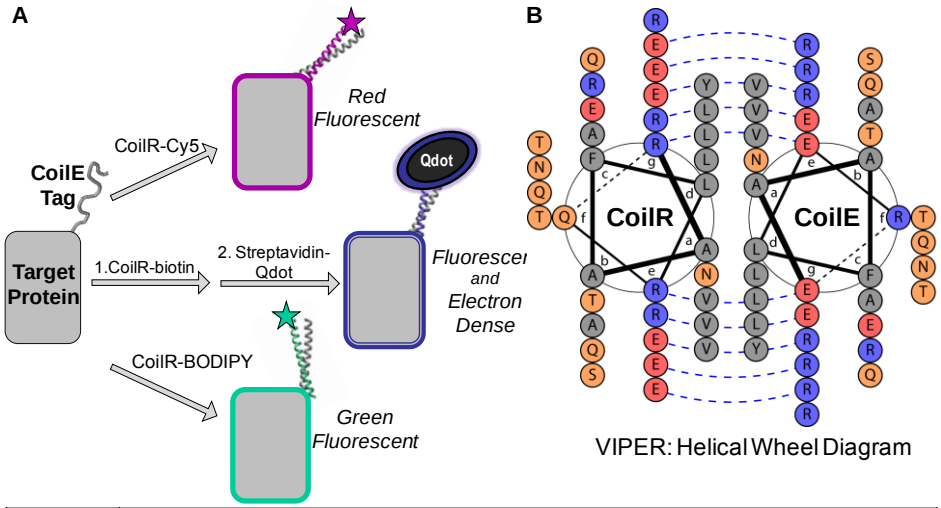


**Scheme 3.1. VIPER is a new technology for multi-scale microscopy. A.** A target protein is genetically-tagged with the CoilE peptide. Then the tagged protein can be labeled by dimerization with a CoilR peptide covalently bound to various chemical reporters, including BODIPY, Sulfo-cyanine5 (Cy5), or biotin for detection by a streptavidin-Qdot. **B.** Helical wheel diagram of VIPER highlighting the hydrophobic interface (a and d positions) and the g↔e' inter-strand salt bridges (dashed lines) between the E and R amino acid side-chains. The diagram was generated using DrawCoil 1.0. Sequences for the CoilE tag and the CoilR probe peptide are provided.

For the current work, we expanded our protein labeling toolkit to include a VIP tag with higher affinity. We selected a heterodimeric pair described by Vinson and coworkers: $RR_{12}EE_{345}L$ and $EE_{12}RR_{345}L$[42]. Dimerization between these two peptides is driven by a hydrophobic interface and optimized inter-strand salt bridges, as shown in Figure 1B. The result is a high affinity dimer ($K_D$ 1.3 x 10-11 M; $T_m$ 73 ºC[42]). We used these two sequences to create a CoilE tag and CoilR probe peptide, which dimerize to produce VIPER.

Homology-based gene assembly was used to introduce the CoilE tag into target proteins. CoilR probe peptides were generated in vitro by recombinant bacterial

expression. The CoilR sequence included a hexahistadine tag for purification and a cysteine for site-specific labeling using thiol-maleimide chemistry[51]. These features enabled us to rapidly generate a set of probe peptides: CoilR-biotin, CoilR-Cy5, and CoilR-BODIPY.

## Localization of VIPER-tagged proteins to distinct sub-cellular structures

Our first priority was to establish that VIPER enabled selective labeling of cellular proteins. We selected three distinctive sub-cellular structures for labeling: the cytoskeleton (β-actin), nucleus (histone 2B; H2B), and the mitochondrial matrix (using a COX8 fragment encoding a localization sequence; "Mito"). We obtained mammalian expression vectors (pcDNA3) that encoded each target protein fused to a monomeric green fluorescent protein, mEmerald[18]. We modified each vector to insert the CoilE sequence intragenically between the target protein and mEmerald (Figure 2A). We transfected human osteosarcoma (U-2 OS) cells with vectors encoding tagged proteins, which we named mEmerald-CoilE-Actin, Mito-CoilE-mEmerald, and H2B-CoilE-mEmerald. We also transfected cells with proteins lacking the CoilE tag (mEmerald-Actin, Mito-mEmerald, H2B-mEmerald). Cells were fixed, permeabilized, and blocked before treatment with the probe peptide CoilR-Cy5.

We used confocal FM to assess VIPER labeling and specificity in cells (**Figure 3.1**). Transfected cells were identified using mEmerald fluorescence. We found that CoilR-Cy5 produced specific fluorescent signal in sub-cellular structures only in cells expressing CoilE-tagged proteins. For example, in cells expressing mEmerald-CoilE-Actin, CoilR-Cy5 fluorescence (magenta) co-localized with mEmerald fluorescence (green) (**Figure 3.1B**). VIPER-labeling consistently highlighted the cytoskeleton, indicating that CoilE-tagged actin localized correctly. Similarly, cells expressing Mito-CoilE-mEmerald or H2B-CoilE-mEmerald had co-localized fluorescence in the mitochondria or nucleus, respectively (**Figure 3.1C, 3.1D**). CoilR-Cy5 signal in cells expressing the untagged mEmerald constructs was nearly undetectable. These results demonstrate that VIPER-labeling was selective and the CoilE tag did not change or disrupt the target protein's localization. Our results showed that VIPER-labeling

occurred with the CoilE tag inserted between two proteins, a useful feature for labeling proteins that do not tolerate tags at the N- or C-terminus.

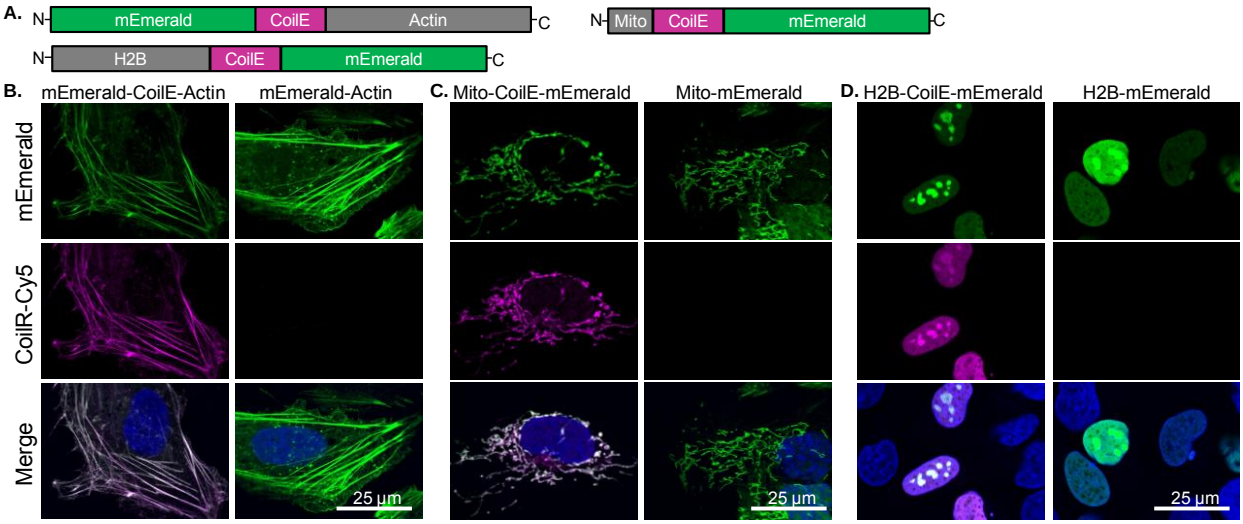


**Figure 3.1. Selective fluorescent labeling of cellular actin, mitochondria, and the nucleus using VIPER.** (**A**) Representation of the CoilE-tagged proteins used to label the cytoskeleton (mEmerald-CoilE-Actin), mitochondria (Mito-CoilE-mEmerald), and the nucleus (H2B-CoilE-mEmerald). Transfected U-2 OS cells were labeled post-fixation by treatment with CoilR-Cy5 (100 nM) and then imaged by confocal FM to observe the cytoskeleton (**B**), mitochondria (**C**), or the nucleus (**D**). CoilR-Cy5 labeling was specific for CoilE-tagged proteins, and the Cy5 (magenta) and mEmerald (green) signal colocalized. Green-magenta overlap appears white in the merged images and the nuclear stain (Hoechst 33342) is false-colored blue. Images are single confocal slices (450 nm depth) acquired at 63X magnification (1.4 NA) with fluorescence signal normalized for each channel.

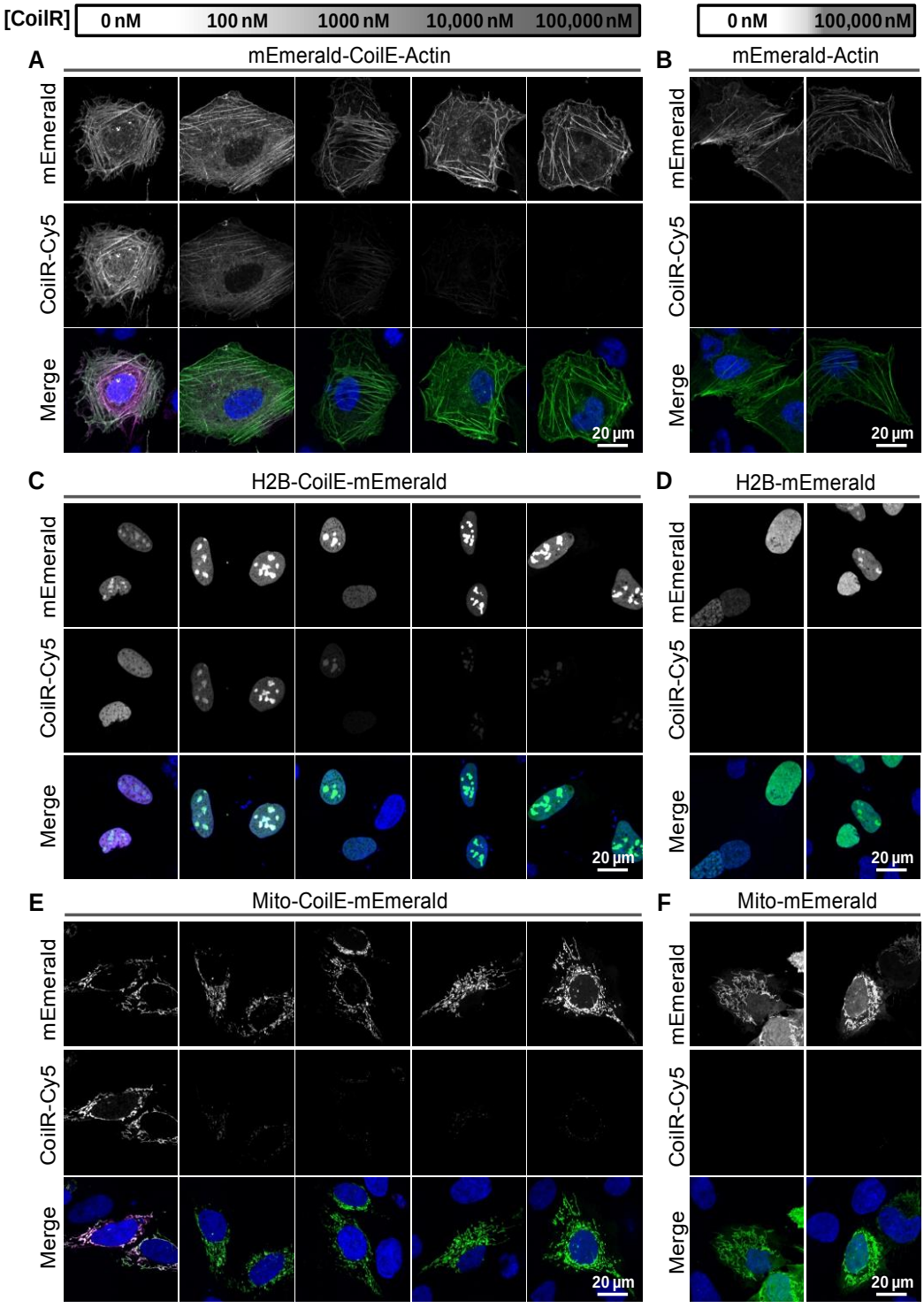


**Figure 3.2. Reduction of VIPER labeling by pre-treatment of fixed cells with unlabeled CoilR peptide.** U-2 OS cells were transfected to express CoilE-tagged proteins (**A**: mEmerald-CoilE-Actin; **C**: H2B-CoilE-mEmerald; **E**: Mito-CoilE-mEmerald). Cells were fixed, permeabilized, and treated with increasing concentrations of unlabeled CoilR peptide (0, 100, 1000, 10,000, or 100,000 nM). Next, cells were washed, treated with 100 nM CoilR-Cy5, and imaged by confocal FM. Without pre-treatment with

unlabeled CoilR, Cy5 fluorescence was observed and co-localized with mEmerald signal (*Column 1*; **A**, **C**, and **E**). Cy5 labeling was reduced for samples pre-treated with 100 nM unlabeled CoilR (*Column 2*). For cells expressing mEmerald-CoilE-Actin or Mito-CoilE-mEmerald, Cy5 fluorescence became nearly undetectable after pre-treatment with 1000 nm CoilR. Cy5 signal localized to nucleoli was detected for cells pre-treated with ≥1000 nM CoilR, but the signal was reduced and was increasingly difficult to detect. Cells expressing mEmerald-Actin (**B**), H2B-mEmerald (**D**), or Mito-mEmerald (**F**) were treated with 0 or 100,000 nM unlabeled CoilR before treatment with 100 nM CoilR-Cy5. Cy5 fluorescence was not detected for cells expressing these proteins. In merged images, mEmerald is false-colored green, Cy5 is false-colored magenta and Hoechst 33342 (nuclei) is false-colored blue.

We used a competition binding assay to assess VIPER labeling efficiency. Again, we evaluated imaged β-actin, mitochondria, and H2B. Briefly, fixed cells were pre-treated with increasing concentrations of unlabeled CoilR peptide (0, 100, 1000, 10,000, and 100,000 nM). Then cells were treated with 100 nM CoilR-Cy5. Pre-treatment with 100 nM unlabeled CoilR peptide was sufficient to reduce the labeling by CoilR-Cy5 (**Figure 3.2**). Cy5 fluorescence became nearly undetectable after pre-treatment with a 10-fold excess of unlabeled CoilR (1000 nm) for cells expressing mEmerald-CoilE-Actin or Mito-CoilE-mEmerald. Cy5 signal localized to nucleoli was detected for cells pre-treated with ≥1000 nM CoilR, but the signal was reduced and became increasingly difficult to detect. H2B localizes to a small, sub-nuclear volume, a feature that would make a low amount of bound CoilR-Cy5 more detectable. Overall, our results indicate that treatment with 100 nM CoilR-Cy5 will be sufficient to label most, but not all, of an abundant CoilE-tagged target protein.

## Imaging transferrin-bound iron uptake using VIPER

Next we assessed VIPER by imaging two components of the iron uptake machinery: transferrin (Tf) and transferrin receptor 1 (TfR1). The TfR1 pathway is one of the best described systems for receptor-mediated endocytosis[52,53,53–55]. Briefly, iron uptake starts outside of cells, where oxidized iron is bound by the soluble Tf protein. After Tf binds to TfR1, the complex internalizes through clathrin-coated vesicles. These endosomes acidify, which potentiates the release of iron from the Tf/TfR1 complex. Reduced iron is transported into the cytosol, where it is used by iron-requiring proteins

or stored within ferritin. Then the apo-Tf/TfR1 complex recycles to the cell surface. The neutral pH of the extracellular environment facilitates release of Tf from TfR1, enabling the process to restart. Iron uptake is fast, with internalization of the Tf/TfR1 complex into early endosomes occurring within a few minutes of Tf binding and recycling of Tf-TfR1 back to the surface occurring in under 20 min[55].

We used confocal FM to observe Tf and TfR1 localization and trafficking in living cells. We generated a vector with the CoilE tag at the extracellular, C-terminal domain of TfR1 (pcDNA3.1_TfR1-CoilE). For comparative analysis, we acquired a vector encoding TfR1 fused at the C-terminal domain to the monomeric red fluorescent protein mCherry (pCDNA3_TfR1-mCherry; Addgene #55144). We used the CHO TRVb cell line for these studies, which does not express TfR1 or the closely-related transferrin receptor 2 (TfR2)[56]. We selected this cell line in order to ensure that all cellular TfR1 would be tagged by either CoilE or mCherry. Transfected cells were cooled to 4 °C to pause endocytosis and treated for 30 min with fluorescent ligand, Tf-AF488. Cells expressing TfR1-CoilE were simultaneously treated with CoilR-Cy5, while cells expressing TfR1-mCherry were not. Cells were washed, returned to 37 °C, and imaged immediately after labeling (0 min) and again at 30 min.

We observed selective CoilR-Cy5 labeling of TfR1-CoilE in living cells (**Figure 3.3**). At both 0 and 30 min, VIPER-tagged TfR1 co-localized with Tf-AF488, which provides strong evidence that tagged TfR1 retains its ligand-binding function. Most of the fluorescent signal from CoilR-Cy5 (receptor) and AF488 (ligand) was restricted to the cell surface at the initial time-point before appearing in bright, fluorescent endosomes at 30 min. After 30 min, some of the cell surface TfR1 no longer co-localized with Tf, consistent with recycling of TfR1-bound apo-Tf to the cell surface and release of Tf into the media. These results demonstrate that VIPER enables observation of receptor-ligand binding interactions, receptor endocytosis, and receptor recycling (indirectly). We found that the CoilR probe peptides were live-cell impermeant. As a result, CoilR-Cy5 labeling was restricted to the cell surface localized TfR1-CoilE, which enabled us to follow the endocytosis of that pool of receptors.

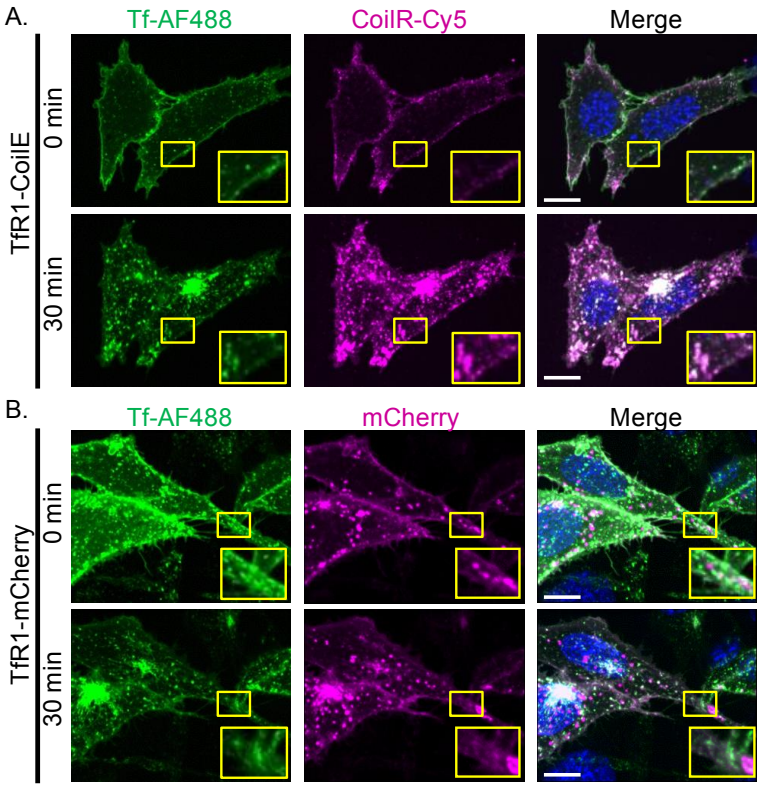


**Figure 3.3. VIPER-tagged transferrin receptor retains transferrin binding and endocytosis.** (**A**) CHO TRVb cells expressing TfR1-CoilE were treated with CoilR-Cy5 and fluorescent ligand (Tf-AF488). In live cells, labeling by both Tf-AF488 and CoilR-Cy5 was localized to the cell surface at 0 min. After 30 min, AF488 and Cy5 signals from the Tf-TfR1 complex were observed together in endocytic vesicles. (**B**) Cells expressing TfR1-mCherry were treated with Tf-AF488. In A and B, yellow boxes delineate the insets, which provide a 2X magnified view. The merged images (right column) include Tf-AF488 (green), the nuclear stain (Hoechst 33342; blue), and either mCherry (red) or CoilR-Cy5 (magenta). Images are single confocal slices (450 nm depth) acquired at 63X (1.4 NA) magnification with fluorescence signal normalized for each channel.

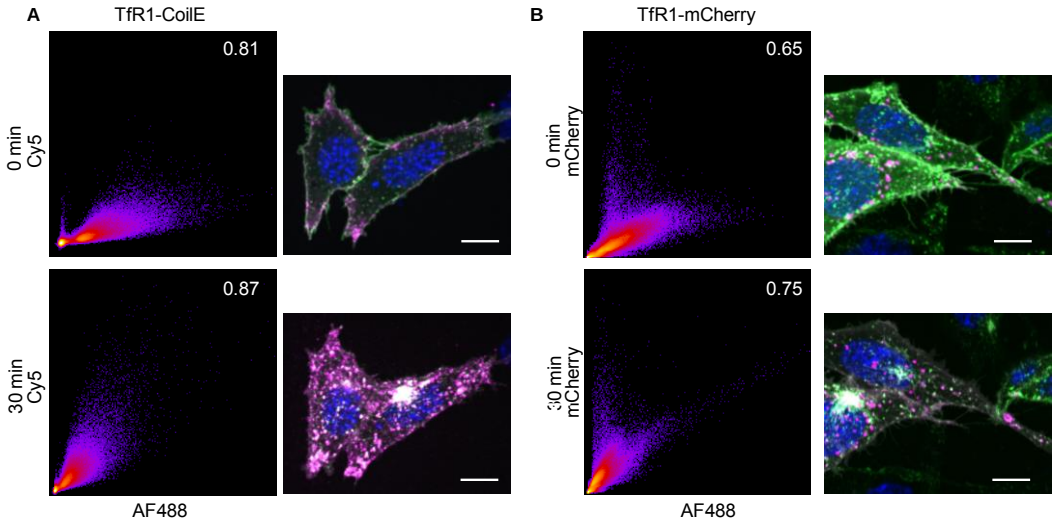


**Figure 3.4. Colocalization analysis of Tf with TfR1.** We generated pixel intensity plots to analyze the colocalization of Tf-AF488 fluorescence with red fluorescence from Cy5-labeling of TfR1-CoilE (**A**) or from TfR1-mCherry (**B**). We analyzed micrographs from **Figure 3.3** for the 0 min (*top*) and 30 min (*bottom*) time points. Plots were generated using Fiji software (Coloc 2 analysis) with Tf-AF488 signal intensity on the horizontal axis and either Cy5 signal intensity (**A**) or mCherry signal intensity (**B**) on the vertical axis. Pearson's correlation values are reported in the upper-right corner of the intensity plot. Micrographs from **Figure 3.3** are provided next to each plot and the scale bars represent 25 μm.

For comparison, the same experiment was performed using cells expressing TfR1-mCherry **(Figure 3.3B**). Again, we observed Tf-AF488 signal primarily at the cell surface (0 min) before it appeared in endosomes (30 min). However, we observed less colocalization of green and red fluorescence because both surface and internal TfR1-mCherry were fluorescent. TfR1-mCherry cells had red fluorescent vesicles at 0 and 30 min that did not contain Tf-AF488 signal. Our observations are supported by analysis of the colocalization of AF488 fluorescence with either Cy5 (TfR1-CoilE) or mCherry (TfR1-mCherry). We found that the Pearson's correlation coefficient of Tf-AF488 with VIPER-labeled receptor (AF488 with Cy5) at both 0 min (81%) and 30 min (87%) was better than that of Tf-AF488 with TfR1-mCherry, which was 65% at 0 min and 75% at 30 min (**Figure 3.4**). The direct comparison of VIPER to mCherry highlights a key feature of the new tag: only VIPER enabled the unambiguous observation of cell-surface receptors being internalized following treatment with fluorescent ligand.

## Time-lapse imaging of iron uptake

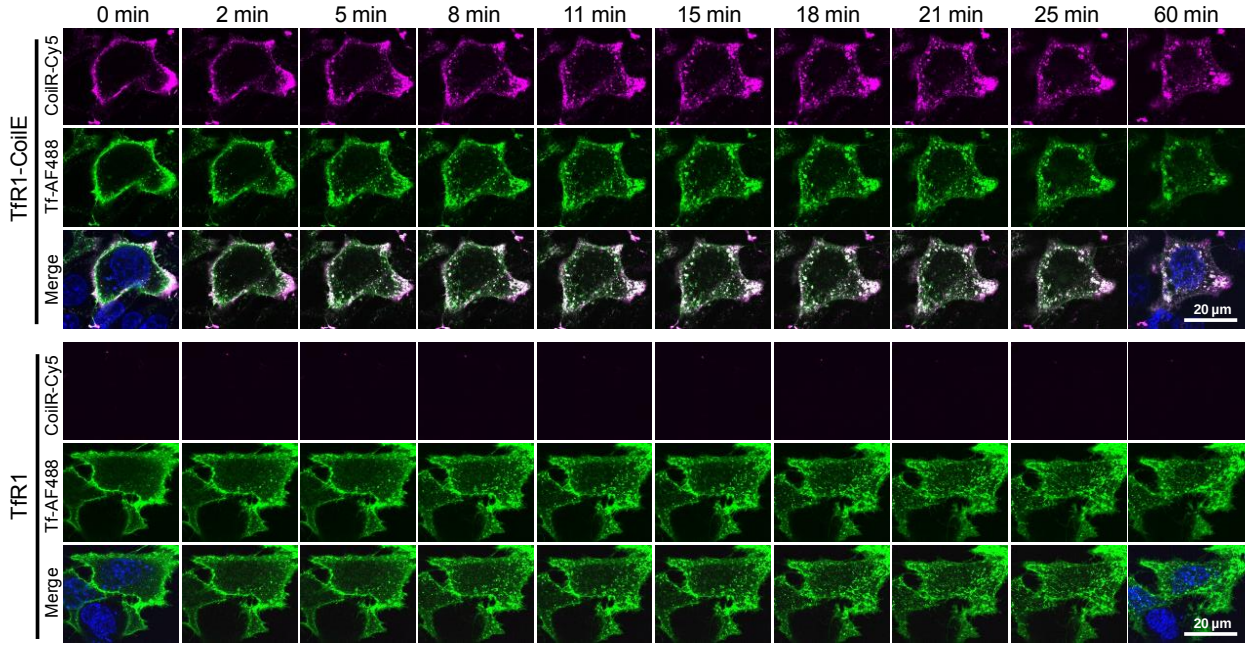


**Figure 3.5. Time-lapse imaging of TfR1 following Tf-AF488 and CoilR-Cy5 treatment.** Live CHO TRVb cells expressing TfR1-CoilE (*top*) or untagged TfR1 (*bottom*) were treated with CoilR-Cy5 and Tf-AF488 and then imaged by confocal fluorescence microscopy. Cells were imaged every 2-3 min for the first 25 min to capture endocytosis of TfR1 and TfR1-CoilE. A final image was taken after 60 min at 37° C. Nuclear stain (Hoechst 33342; blue) was imaged during the first and last capture only to minimize UV-light exposure. Areas where AF488 (green) and Cy5 (magenta) overlap are white in the merge. Images are single confocal slices (450 nm depth) acquired at 63X magnification (1.4 NA). Fluorescence signal was normalized in each channel.

To explore further the co-trafficking of receptor and ligand, we used time-lapse imaging to observe Tf and TfR1 internalization in living cells (Figure 3.5). We transfected CHO TRVb cells with either tagged (TfR1-CoilE) or untagged (TfR1) receptor. Cells were cooled to 4 °C to pause endocytosis and treated with a cold solution of CoilR-Cy5 (500 nM) and Tf-AF488 (50 µg/mL). Cells were washed and returned to 37 °C for imaging. Images were acquired every 2-3 min for 25 min. VIPER labeling was highly specific, with Cy5 signal only observed for cells expressing TfR1-CoilE and not for untagged TfR1. For TfR1-CoilE, both the receptor and ligand were found on the cell surface at 0 min and localized in endosomes within 5 min. We observed colocalization of the Tf-AF488 (green) and VIPER (magenta) signal. We saw

changes in intracellular distribution of TfR1-CoilE between 5 and 25 min, with more Cy5 signal observed in vesicles within the cytoplasm over time. For both TfR1 and TfR1-CoilE, the Tf ligand trafficked into the cell quickly, with few vesicles observed near the cell surface at 5 min, and a greater number of vesicles in the cytoplasm by 15 min.

## Two-color pulse-chase labeling of TfR1

Pulse-chase labeling is an established method for sequentially labeling cells with distinguishable reporters. This method can be used for various imaging applications, including differentiating new from old proteins[34,57] or stimulated from unstimulated receptors[58]. This method relies on fast labeling and live-cell compatibility in order to obtain two-color, time-resolved images of dynamic protein populations. We used VIPER to pulse-label a cell surface population of TfR1 with red-fluorescent Cy5 and then labeled a second population with green fluorescent BODIPY (**Figure 3.6**). Briefly, CHO TRVb cells expressing TfR1-CoilE were cooled to 4 °C and then treated with CoilR-Cy5 to pulse-label receptors on the cell surface. We returned cells to 37 °C and allowed the Cy5-labeled receptors to distribute for 5, 30, or 120 min. Next, cells were treated with ice-cold CoilR-BODIPY to chase-label a second population of receptors. Cells were washed and fixed prior to imaging.

At each time-point, we observed the CoilR-Cy5 labeled TfR1 population (magenta) primarily within vesicles, consistent with rapid endocytosis of TfR1. In contrast, the CoilR-BODIPY labeled TfR1 (green) was primarily localized to the cell surface. A small portion of BODIPY-labeled receptors appeared in fluorescent punctae, consistent with prior reports that some Tf-internalization occurs at 4 °C(55). This experiment was also performed with CHO TRVb expressing untagged TfR1, which verified that CoilR labeling was specific for TfR1-CoilE (**Figure 3.7**). This pulse-chase labeling experiment demonstrates that the VIPER technology can be used to track two distinct populations of receptors over time. Additionally, VIPER labeling was rapid, achieving sufficient labeling within 15 min of treatment.

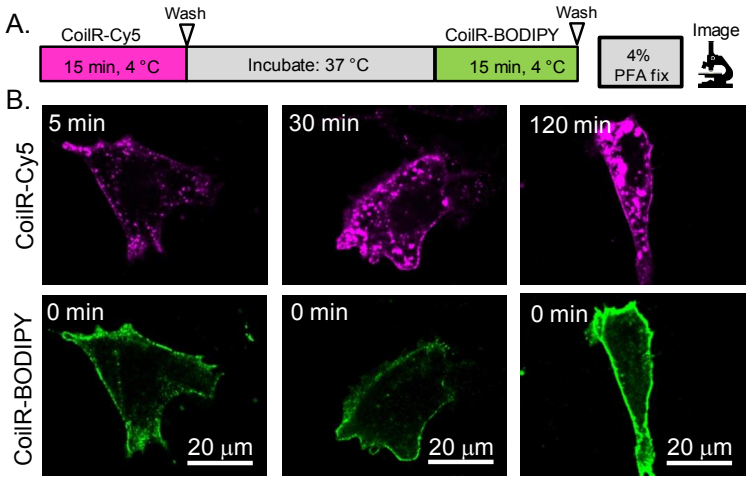


**Figure 3.6. Two-color pulse-chase labeling of TfR1**. (**A**) Schematic of the pulse-chase labeling protocol. (**B**) Cells expressing TfR1-CoilE was pulse-labeled with CoilR-Cy5 (500 nM, 15 min), washed, and returned to 37 °C for 5, 30, or 120 min. TfR1-CoilE was then chase-labeled with CoilR-BODIPY (500 nM, 15 min), fixed, and imaged to detect both Cy5-labeled receptor (magenta) and BODIPY-labeled receptor (green). Nuclear stain (Hoechst 33342) is blue and scale bars represent 20 μm. Images are single confocal slices (450 nm depth) acquired at 63X magnification (1.4 NA) with fluorescence signal normalized for each channel.

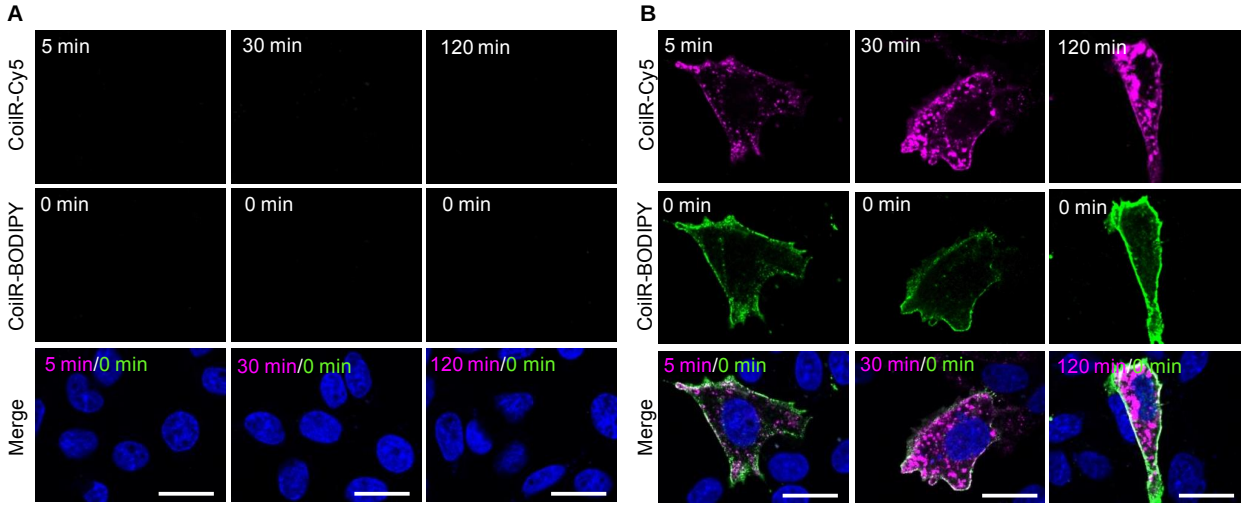


**Figure 3.7. Two-color pulse-chase labeling of untagged TfR1 compared to TfR1-CoilE.** Cells expressing TfR1 (**A**) or TfR1-CoilE (**B**) were pulse-labeled with CoilR-Cy5 (500 nM, 15 min), washed, and returned to 37 °C for 5, 30, or 120 min. Cells were chase-labeled by treatment with CoilR-BODIPY (500 nM, 15 min), fixed, and imaged to detect both Cy5 (magenta) and BODIPY (green) signal. Nuclear stain (Hoechst 33342) is blue and scale bars represent 20 μm. Images are single confocal slices (450 nm depth) acquired at 63X magnification (1.4 NA) with fluorescence signal normalized in each channel. There was no Cy5 or BODIPY fluorescence observed for untagged TfR1-expressing cells treated with CoilR-Cy5 and CoilR-BODIPY. The micrographs in **B** are reproduced from **Figure 3.6**.

## VIPER is a new technology for multi-scale microscopy

A new technology is required for specific and selective tagging of proteins for multi-scale microscopy. For many studies, FM has insufficient resolution to observe the sub-cellular structures or multi-protein complexes under evaluation. In such situations, EM is used for high-resolution imaging of nanoscale features, such as membrane-bound organelles or receptor distribution. Ideally, there would be versatile methods for labeling and observing proteins by both FM and EM.

The instrumentation for multi-scale microscopy is now available. In the current work, we used a commercial CLEM instrument, the FEI Corrsight, which enables biological samples to be pre-screened by FM before processing for EM[59]. This system uses a custom slide holder with slides that have a mapped grid visible by FM and EM. This enables individual cells to be selected, tracked, and correlated using FEI's MAPS software. Furthermore, chemical reporters are commercially available for multi-scale microscopy. Qdots are dual-reporter nanoparticles, providing a label that is brightly fluorescent and electron dense[60]. This endows Qdots with two essential features for multi-scale microscopy.

The VIPER tag can be used to deliver bright organic fluorophores or Qdots. We sought to determine if this unique feature of VIP tags could be used for multi-scale microscopy. For these studies, live CHO TRVb cells were treated with both Tf-AF488 and biotinylated CoilR (CoilR-biotin), which we detected post-fixation using streptavidin-Qdot655. We imaged cells first by confocal FM and then by scanning EM (SEM) (**Figure 3.8**). Fluorescence micrographs allowed us to identify transfected cells, which bound Tf-AF488 (**Figures 3.8A, 3.8B**). We used MAPS software to register the coordinates of fluorescent cells relative to the slide so that we could re-locate the same cells for SEM imaging. The fluorescence micrographs additionally confirmed the specificity of VIPER labeling. We observed bright Qdot655 fluorescence associated with cells expressing TfR1-CoilE (Figure 6A), but not for cells expressing untagged receptor (**Figure 3.8B**).

After acquiring two-color fluorescence micrographs, samples were dehydrated and carbon-coated for imaging by SEM. Micrographs were acquired on an FEI Helios Nanolab 660, which provided a topographical view of the cells pre-selected by FM. At

65,000X magnification, Qdots were observed as white spheres on a gray background by backscatter electron imaging (see inset, **Figure 3.8C**, for a magnified view). Micrographs revealed dense Qdot655 labeling for cells expressing TfR1-CoilE (**Figure 3.8C**). The Qdot labeling enabled by VIPER appeared to be highly specific, with almost no non-specific association with cell surfaces (**Figure 3.8D**).

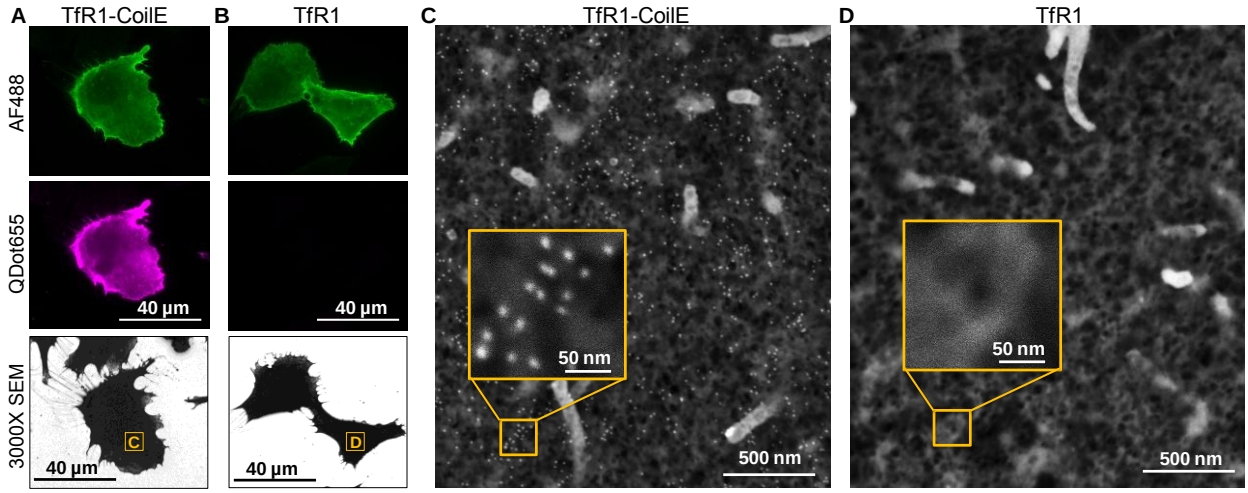


**Figure 3.8. Imaging TfR1 by multi-scale microscopy.** CHO TRVb cells were transfected and then treated with CoilR-biotin and Tf-AF488. After fixation, cells were treated with streptavidin-Qdot655 to detect biotinylated (VIPER-tagged) receptors. (**A**) Fluorescence micrographs of cells expressing TfR1-CoilE. Transfected cells were identified based on binding to Tf-AF488 (green) and labeling by Qdot655 (magenta). (**B**) Fluorescence micrographs of cells expressing untagged TfR1, identified by binding to Tf-AF488. The FEI Corrsight's MAPS software was used to select cells for high-resolution SEM. We selected Region C (in **A**) and Region D (in **B**) for SEM imaging. Samples were processed by chemical dehydration, carbon coated, and imaged at 65,000X magnification. High-resolution SEM micrographs of cells expressing TfR1-CoilE (**C**) showed selective Qdot labeling, while labeling was not observed on cells expressing untagged TfR1 (**D**). The insets provide a magnified view of the boxed region.

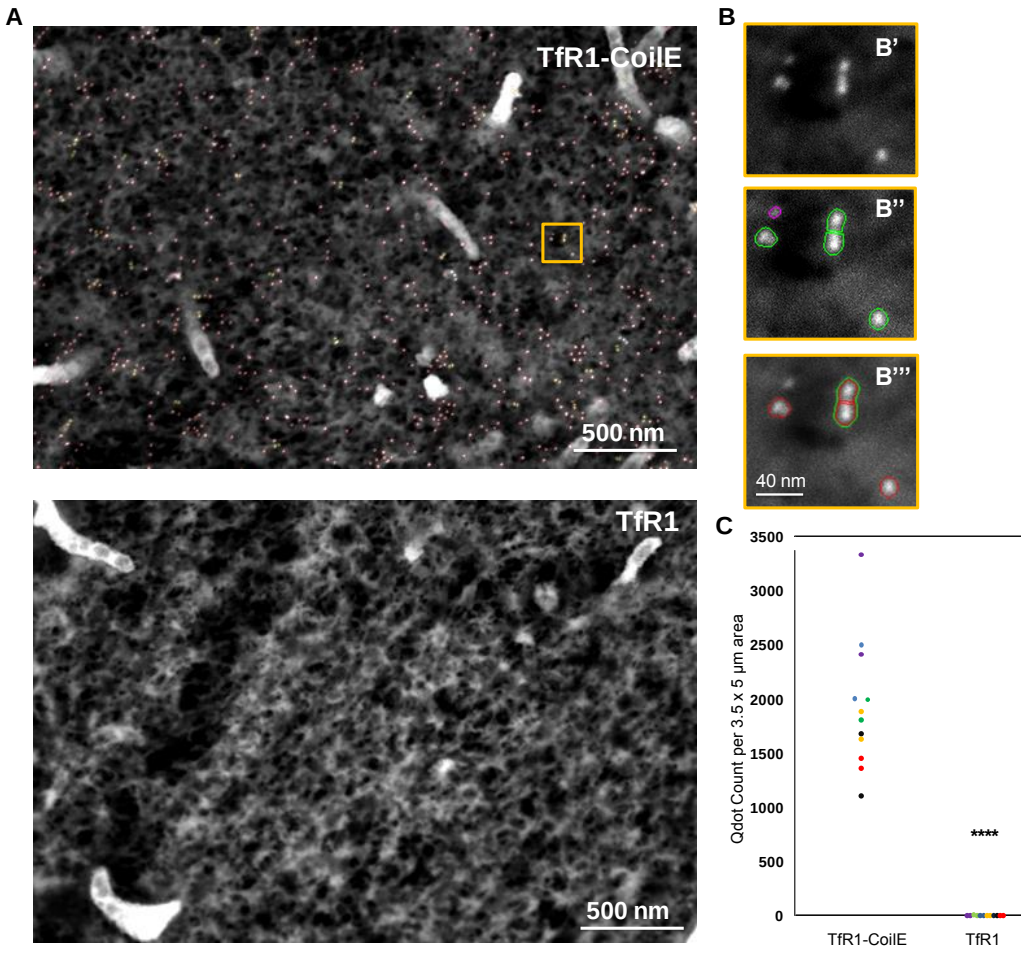


**Figure 3.9. Computer-assisted counting of Qdot655-labeled TfR1 in SEM micrographs**. (**A**) Micrographs were acquired at 65,000X magnification with back scatter electron capture of the cell surface. The field of view shown is 1.75 x 2.5 µm. CHO TRVb cells were transfected with TfR1-CoilE (*top*) or untagged TfR1 (*bottom*) and treated with CoilR-biotin and streptavidin-Qdot655. The counting mask overlay appears as a red outline, with clusters additionally outlined in green. The yellow box defines the inset shown in **B**. (**B**) Magnified view and segmentation analysis of the region designated in **A**. **B'** is the magnified view of the unprocessed image. **B''** shows the top-hat, initial particle detection (green outline) and Watershed separation of contiguous particles. Non-Qdot particles were filtered out (magenta outline) based on size. **B'''** shows the final mask with counted particles outlined in red and clusters (≥2 particles) outlined in green. **C.** Scatter plot of total counted Qdot655 particles per field of view (3.5 x 5 µm) for TfR1 and TfR1-CoilE. We analyzed 2 non-overlapping images per cell and a total of 6 cells per conditions (i.e., TfR1-CoilE and untagged TfR1). See **Table 3.1** for a summary of the data obtained from SEM image analysis. Same-colored data points in **C** and **Table 3.1** correspond to data obtained from the same cell. The difference in Qdot counts for TfR1 versus TfR1-CoilE was statistically significant (**** = $p < 0.0001$).

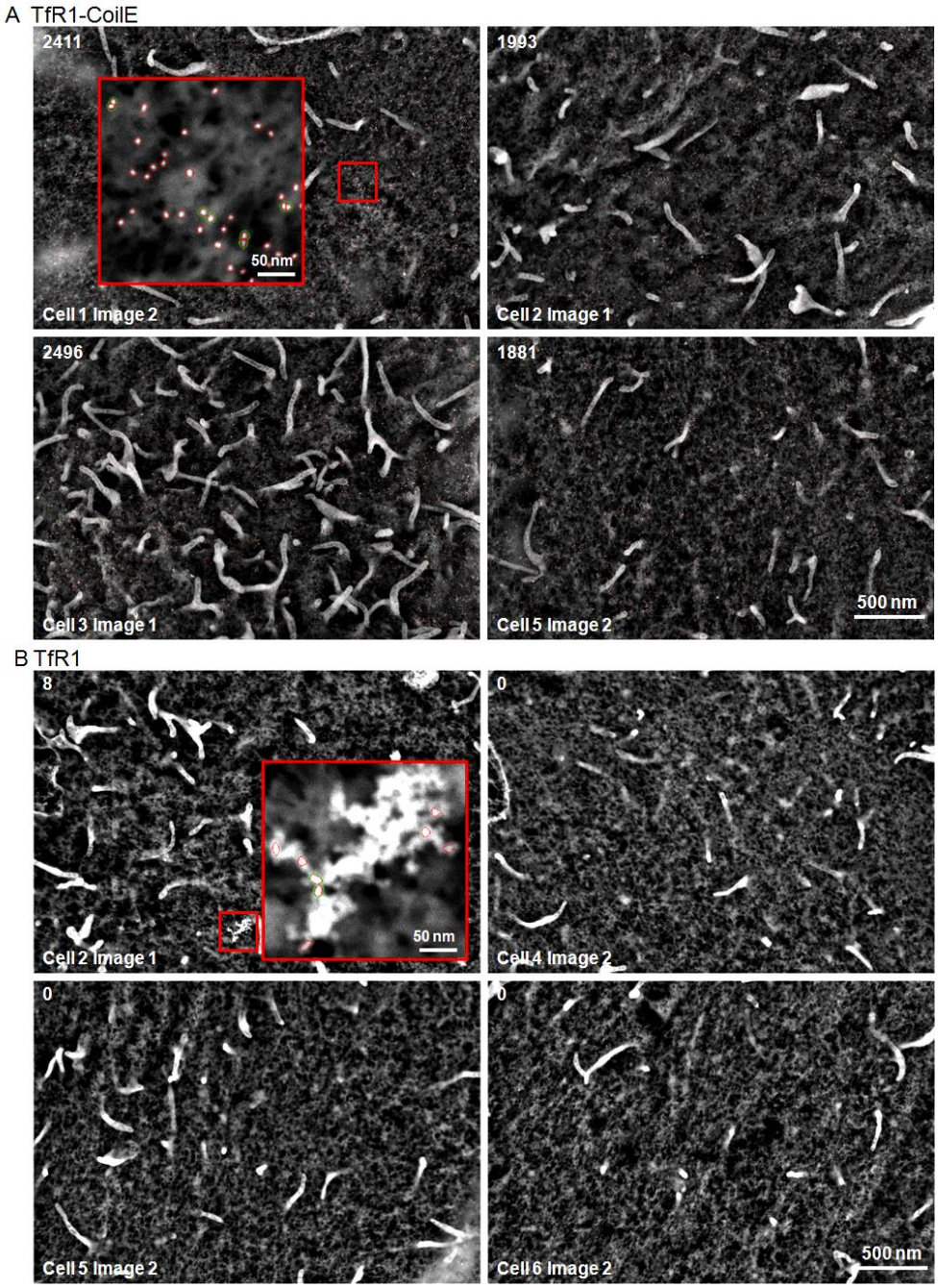


**Figure 3.10. Representative SEM micrographs of CHO TRVb cells expressing TfR1-CoilE (A) or untagged TfR1 (B).** Cells were treated with CoilR-biotin and streptavidin-Qdot655, as described in the SI Methods. The counting mask overlay appears as a red outline, with clusters additionally outlined in green. Images shown are the full field of view from a 65,000X magnification capture (3.5 x 5 μm). Micrograph names correspond to names provided in **Table 3.1** (e.g., Cell X Image Y) and the total Qdot count for each image is reported in the upper left corner. A magnified inset (red box) is provided with the upper left micrograph of **A** and **B** to highlight an area of the cell with particles segmented as Qdots.

Other EM tags use DAB precipitation to generate contrast[30–36], but the reaction product can be difficult to control. In contrast, Qdot-based target detection enables the relative amount of protein present to be quantified because labeling is stoichiometric. To demonstrate this feature, we algorithmically segmented and counted the number of Qdot655 particles per field-of-view (3.5 x 5.0 μm) in SEM micrographs of cells expressing TfR1-CoilE or untagged TfR1. We captured two fields of view per cell and six cells per condition. **Figures 3.9** and **3.10** provide representative micrographs with particle segmentation. In VIPER-labeled cells, we identified single Qdots, dimers, and multimers, but found that most Qdots were distributed as monomers. We determined that there were 110 ± 34 particles/μm2 in cells expressing TfR1-CoilE. The density of particles on the cell surface ranged from 63 to 190 particles/μm2, and we attribute this variation to receptor expression differences between transiently-transfected cells. For cells expressing untagged TfR1, we observed an average of 0 particles/μm2. Our CLEM study shows that VIPER is a new type of EM tag that enables high-fidelity labeling of cell receptors with Qdots. We anticipate that the ability to identify a protein's sub-cellular localization and relative abundance will be useful for various applications in cell biology.

## Comparison of VIPER with immunolabeling for CLEM

We sought to compare indirect immunolabeling with VIPER. Immunolabeling is widely used for labeling and imaging target proteins by FM, EM, and CLEM. Typically, proteins are treated with a primary antibody generated against the protein target and a secondary antibody delivering an electron-dense reporter (e.g., colloidal gold or a Qdot)(36). We selected three commercial antibodies against the extracellular domain of TfR1(8D3[61], Ab1086[62], and Ab216665). Each primary antibody was detected by an anti-host secondary antibody conjugated to Qdot655. We used Qdot655, instead of colloidal gold, to enable a direct comparison with our VIPER Qdot labeling.

For these studies, we used CHO TRVb cells transfected with TfR1-CoilE and treated live with Tf-AF488. We selected transfected cells to image based on an approximate match among samples in green fluorescence. Fixed cells were then either VIPER labeled or immunolabeled. For two of the antibodies, Ab1086 and Ab216665,

we were unable to identify conditions for labeling the receptor—a common problem encountered by researchers using commercial antibodies. We saw no evidence of TfR1-CoilE labeling using either of those antibodies by FM or EM (**Figure 3.11**).

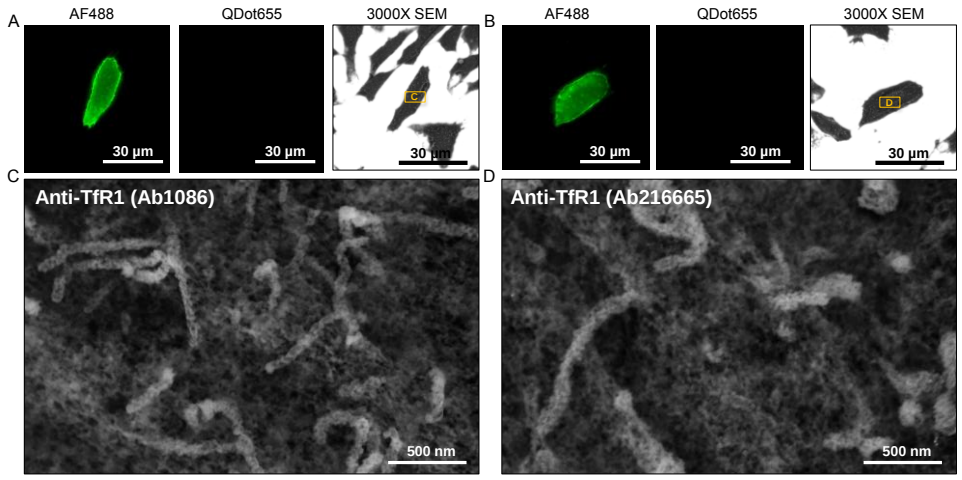


**Figure 3.11. Target labeling and CLEM imaging of TfR1-Coil by anti-TfR1 antibodies Ab1086 and Ab216665.** CHO TRVb cells were transfected with TfR1-CoilE and treated live with 100 nM Tf-AF488**.** After fixation, cells were treated with a primary antibody against TfR1: Ab1086 (**A, C**) or Ab216665 (**B, D**). Cells were treated with the appropriate secondary antibody conjugated to Qdot655. Fluorescence micrographs of cells treated with Ab1086 (**A**) and Ab2166665 (**B**) were acquired, mapped, and imaged by high-resolution SEM. Transfected cells were identified by Tf-AF488 fluorescence, and Qdot fluorescence was not detected for either antibody. We selected region C (in **A**) and region D (in **B**) for SEM imaging at 100,000X magnification. Less than 20 particles were detected on cell surfaces treated with Ab1086 or Ab216665. See **Figure 3.14** and **Table 3.4** for particle counting data.

However, we observed selective labeling of TfR1 using the monoclonal antibody 8D3 detected by a goat anti-rat IgG antibody conjugated to Qdot655 (**Figure 3.12**). Qualitatively, the immunolabeling with 8D3 looked similar to labeling obtained using VIPER (i.e., treatment of fixed cells with CoilR-biotin and streptavidin Qdot-655). However, quantitative analysis of six images per condition (n = 3 cells) enabled us to count 463.9 ± 97 Qdots/µm2 for samples immunolabeled with 8D3 and 269.8 ± 85 Qdots/µm2 for VIPER-labeled cells (**Table 3.7**). Immunolabeling with 8D3 could be more efficient than VIPER labeling. However, it is also possible that indirect detection of the receptor resulted in multiple secondary antibodies bound to a single 8D3 primary.

We next evaluated a widely-used antibody against the cytosolic domain of TfR1(H68.4[63]). Cells had to be permeabilized post-fixation in order to detect TfR1 with H68.4. Permeabilization with Triton X-100 caused damage to the cell membrane that was observable by EM (**Figure 3.12F**). Moreover, loss of Tf-AF488 fluorescence occurred during permeabilization, presumably due to loss of Tf. With H68.4, we observed 182.3 ± 63 Qdots/μm2, substantially less than observed with 8D3 or VIPER. We also compared VIPER-labeling of TfR1 to immunolabeling of Tf. We used a rabbit polyclonal antibody against Tf (Ab84211). Labeling with Ab84211 (90.6 ± 19 Qdots/μm2) was inefficient compared to VIPER, 8D3, or H68.4. Overall, VIPER labeling surpassed immunolabeling for three out of four antibodies evaluated.

Biotinylated Tf enabled us to do an additional comparison with VIPER. TfR1 is a homodimeric receptor that binds two iron-loaded Tf. Complete labeling with CoilR-biotin would place two CoilR-biotin peptides on each receptor complex. Analogously, 100% efficient ligand-binding would place two biotinylated Tf on the receptor complex. Therefore, direct detection of the Tf ligand using streptavidin-Qdot655 should be comparable to direct detection of CoilR-labeled TfR1 using streptavidin-Qdot655. To test this hypothesis, we treated live cells with either CoilR-biotin or biotinylated Tf (**Figure 3.13**). VIPER-labeled cells were additionally treated with Tf-AF488. After fixation, cells were treated with streptavidin-Qdot655. Fluorescent micrographs and high-resolution SEM micrographs are provided in Figure S8, and we observed selective Qdot655 labeling for both samples. In this direct comparison we observed 210.1 ± 71 Qdots/μm2 for VIPER and 257.7 ± 65 Qdots/μm2 for Tf (**Table 3.9**), a difference that is not statistically significant ($p = 0.126$).

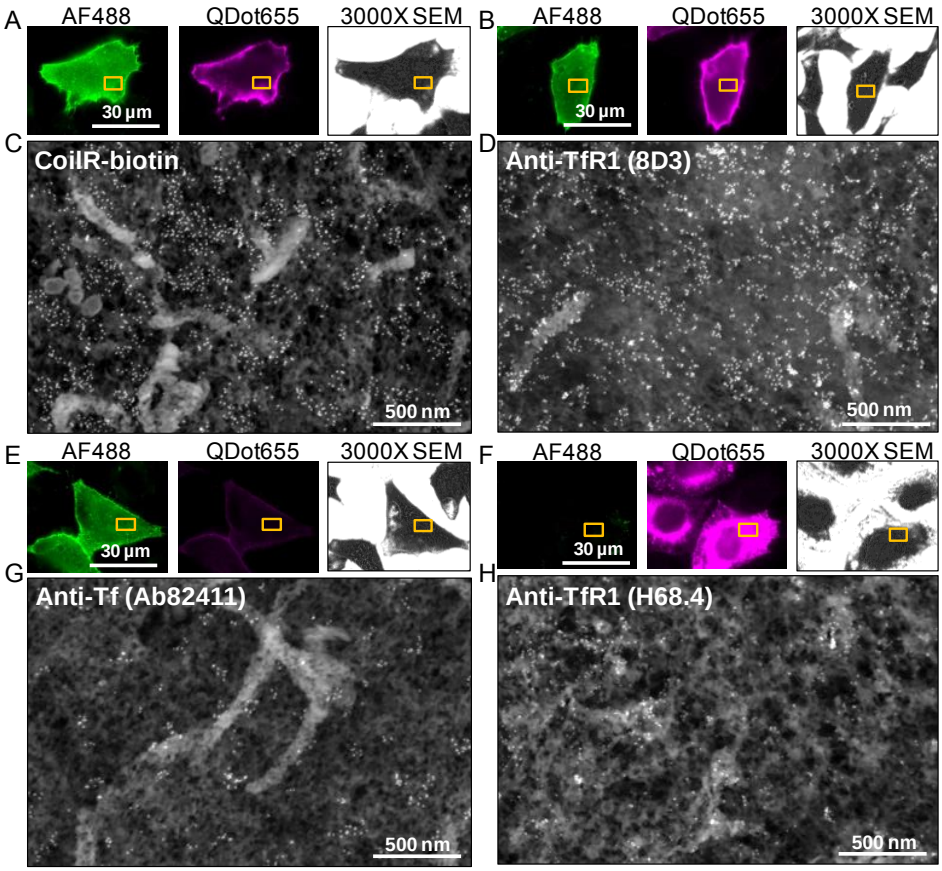


**Figure 3.12. Target labeling and CLEM imaging by VIPER or immunolabeling.** CHO TRVb cells expressing TfR1-CoilE were identified by binding to fluorescent Tf-AF488. For VIPER labeling, fixed cells were treated with CoilR-biotin and streptavidin-Qdot655 (**A**). For immunolabeling, cells were treated with a primary antibody against Tf (Ab82411; **E**) or TfR1 [8D3 (**B**) or H68.4 (**F**)]. Primary antibodies were detected using secondary antibodies conjugated to Qdot655. Fluorescence micrographs of cells labeled with VIPER (**A**), 8D3 (**B**), Ab82411 (**E**), and H68.4 (**F**) were acquired and mapped for high-resolution SEM. After processing, we selected region C (in **A**), region D (in **B**), region G (in **E**), and region H (in **F**) for SEM imaging at 100,000X magnification. The high resolution view shows Qdot labeling of the cell surface for all four treatment conditions. Particle counting and analysis for each condition is provided in **Table S7**. The anti-Tf antibody (Ab82411) labeling was low, with dim Qdot fluorescence, although Qdot signal was visible in an auto-scaled image (*inset*, middle panel of **E**). For H68.4, detergent treatment caused membrane extraction, as observed by SEM, and the Tf-AF488 signal was reduced. The inset in the left panel of **F** is an autoscaled image of the Tf-AF488 fluorescence.

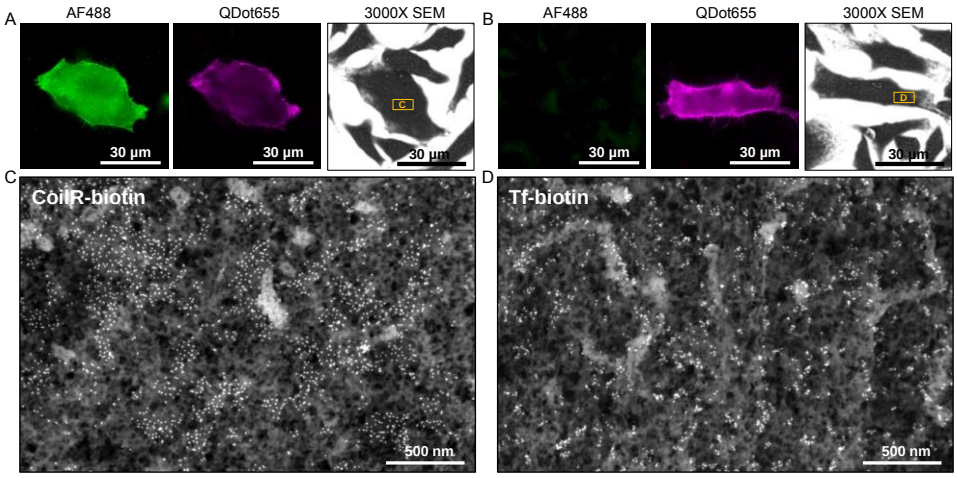


**Figure 3.13. Qdot detection of VIPER compared to Qdot detection of Tf ligand.** CHO TRVb cells were transfected with TfR1-CoilE and treated live with 100 nM CoilR-biotin and 100 nM Tf-AF488 (**A**) or with 100 nM Tf-biotin only (**B**)**.** After fixation, cells were treated with streptavidin-Qdot655 to detect biotinylated TfR1 receptors (**A**, **C**) or biotinylated Tf (**B**, **D**). Cells expressing TfR1-Coil were identified by Tf-AF488 (green) and Qdot655 (magenta) labeling (**A**) or by Qdot655 labeling (**B**). MAPS software was used to select cells for high-resolution SEM. We selected *Region C* (in **A**) and *Region D* (in **B**) for SEM imaging. Samples were processed by chemical dehydration, carbon coated, and imaged at 100,000X magnification. High-resolution SEM micrographs of cells expressing TfR1-CoilE (**C**) showed selective Qdot labeling of the TfR1 receptor. SEM micrographs of cells expressing TfR1-CoilE treated with biotinylated Tf (**D**) showed selective Qdot labeling of the ligand. See **Figure S9A** and **Table S2** for particle counting data.

To summarize, our comparative analyses demonstrate that VIPER labeling is a selective and versatile alternative to commonly used methods for imaging proteins EM or CLEM.

## Conclusion

VIP tags are a new addition to the microscopy toolkit, joining immunolabeling, fluorescent proteins, and other genetically-encoded tags. VIPER is a small tag, adding a peptide of less than 6 kDa to the target protein. We provide evidence that VIPER has high specificity for labeling various sub-cellular targets, including the cytoskeleton, mitochondria, and the nucleus. Once a protein has been modified to include the CoilE tag, it can be labeled with various reporter chemistries either pre- or post-fixation. We demonstrated the range of reporters by labeling a transmembrane receptor, TfR1-CoilE,

with CoilR-BODIPY, CoilR-Cy5, and CoilR-biotin. There are dozens of reactive fluorophores and fluorescent sensors that could be site-specifically conjugated to CoilR, providing many other options for imaging applications.

VIPER is compatible with live-cell, dynamic imaging. We tagged TfR1 with CoilE in order to image iron uptake in cells. VIPER did not appear to affect protein localization, function (e.g., ligand binding), or trafficking. Importantly, VIPER enabled receptor populations to be dynamically observed and spatio-temporally resolved. For example, we treated cells for only 15 min with CoilR probe peptides to observe TfR1 trafficking (see **Figure 3.6**). We did not evaluate shorter CoilR labeling times, but we believe that faster labeling is feasible.

We developed VIPER as a new technology for multi-scale microscopy. We imaged TfR1 using Qdot655, which was detected by FM and SEM. We visualized and quantified VIPER-tagged TfR1 on the surface of cells at high magnification. The CLEM studies presented here demonstrate that VIPER labeling offers a good alternative to immunolabeling. We evaluated four anti-TfR1 antibodies in direct comparison with VIPER. While two selectively labeled TfR1 with CLEM-compatible Qdot655, the H68.4 labeling required processing that compromised the cell membrane.

We anticipate that the EM-compatibility of VIPER will be particularly useful for exploring the sub-cellular localization and assembly of cellular proteins. In separate work, we have detected biotinylated receptors with other reporters, including streptavidin-gold. Alternatively, CoilR could be direct-conjugated to Nanogold for EM or bi-functionalized with a fluorophore plus Nanogold for CLEM[64]. In the future, we plan to explore these options with the goal of using multi-color imaging to study multi-protein assemblies.

VIPER's compatibility with various electron dense reporters creates a flexibility unmatched by the DAB-based tags. However, it is important to emphasize that VIPER does not replace or supersede all other genetically-encoded tags. Rather VIP tags augment other labeling methods, such as immunolabeling or fluorescent proteins, to enable researchers to tag and track multiple distinct targets at once. We anticipate that this enhanced microscopy toolkit will facilitate the generation of more detailed and informative maps of cellular proteins.

## Acknowledgements

This research was supported by generous funding from the OHSU Knight Cancer Institute and the National Institutes of Health (R01 GM122854). J.K.D. received funding from the Oregon chapter of the Achievement Rewards for College Scientists (ARCS) Foundation. We are grateful to Michael Davidson (Florida State University) for depositing his fluorescent protein collection, a valuable community resource, into Addgene. We are grateful to our colleagues at OHSU for their advice and support on this project, particularly Dr. Joe Gray, Dr. James Korkola, Dr. Daniel Zuckerman, Dr. Danielle Jorgens, Paul Marchando, Katie Tallman, and Mandy Meuleners. We also thank Dr. Stefanie Kaech Petrie and Dr. Crystal Chaw of the OHSU Advanced Light Microscopy Core. EM was performed at the Multiscale Microscopy Core. Dr. Timothy McGraw (Cornell University) generously provided the CHO TRVb cell line.

## Materials and Methods

### Chemicals

Unless otherwise noted, all chemicals were purchased from Sigma-Aldrich, ThermoFisher Scientific, or Lumiprobe and used as received. Anhydrous ethanol (Decon Labs; Cat.# 2716) and hexamethyl-disilazane (HMDS; Electron Microscopy Sciences; Cat.# 16700) were used to dehydrate samples for SEM.

### Summary of genetic constructs

A summary of all genetic constructs used in the current work, including peptide and protein sequences, is provided in **Table 3.5**. Bacterial strains and plasmids are summarized in **Table 3.6**. Oligonucleotides were purchased from Integrated DNA Technologies (IDT; **Table 3.7**).

### Mammalian cell culture and maintenance

Chinese Hamster Ovary (CHO) TRVb cells were generously provided by Prof. Timothy E. McGraw (Cornell University, New York). These cells do not express functional transferrin receptor 1 (TfR1) or transferrin receptor 2 (TfR2)[56]. CHO TRVb cells were maintained in Ham's F12 media (Gibco) with 5% fetal bovine serum (FBS) in 10 cm polystyrene dishes. Cells were grown at 37 ºC in a humidified incubator with 5% $CO_2$. Cells were passaged when they reached 80-90% confluency. Cells were detached with 0.25% trypsin/1 mM EDTA (TRED) and seeded at a 1:10 dilution (2 x$10^6$ cells/dish).

U-2 OS cells were purchased from ATCC (Cat. #HTB-96). Cells were maintained in Dulbecco's Modified Eagle Media (DMEM; Gibco) with 10% FBS in 10 cm polystyrene dishes. Cells were grown at 37 ºC in a humidified incubator with 5% $CO_2$. Cells were passaged when they reached 80-90% confluency. They were detached with TRED and seeded at a 1:10 dilution ($10^6$ cells/dish).

### Transfection of plasmid DNA in CHO TRVb or U-2 OS cells

All imaging experiments were conducted in transiently transfected cell lines. For transfections, 5 x $10^4$ cells were seeded into each well of an 8-well chambered slide

(Cellvis) and grown overnight to 70-90% confluency. Transfection was performed using Lipofectamine 2000 (ThermoFisher Scientific) following the manufacturer's instructions. For each well, the transfection mixture contained 500 ng plasmid DNA and 1 µg Lipofectamine 2000 in 400 µL Opti-MEM. After 2 h, the transfection media was removed and replaced with fresh media with serum for recovery. Cells were imaged approximately 24 h after transfection.

**Genetic construction of pET28b(+)_CoilR and pET28b(+)_CoilE**

Genes were synthesized using gene assembly PCR, as described previously[65]. Oligonucleotides were designed using DNAworks(2)(http://helixweb.nih.gov/dnaworks/). Restriction enzyme cut sites *Nco*I and *Hind*III were included in the primers to allow for compatible insertion of *coilR* or *coilE* into the pET28b(+) vector backbone. The *coilE* gene was assembled using primers CoilE-1, CoilE-2, CoilE-3, CoilE-4, CoilE-5 and CoilE-6 (see **Table 3.7** for oligonucleotide sequences). The *coilR* gene was derived from the c*oilR-Lys56* gene, which was assembled using primers CoilR-1, CoilR-2, CoilR-3, CoilR-4, CoilR-5, and CoilR-6.

The amplified *coilR-Lys56* PCR gene product and purified pET28b(+) plasmid (Novagen) were doubly-digested with *Nco*I (NEB) and *Hind*III (NEB), ligated into the digested pET28b(+) plasmid using T4 DNA ligase (NEB), and transformed into chemically-competent *E. coli* cells (DH5$\alpha$; ThermoFisher Scientific). Transformed *E. coli* cells were grown and propagated on LB agar plates supplemented with kanamycin (50 µg/mL). Recombinant colonies were screened with colony PCR and plasmids from positive hits were submitted for sequencing analysis. The pET28b(+)_CoilR-Lys56 plasmid was altered by site-directed mutagenesis to introduce a cysteine at position 56 (Lys56Cys). This generated the pET28b(+)_CoilR plasmid, which was used to express thiol-containing CoilR probe peptides, as described below.

An analogous approach was used to insert the *coilE* gene into pET28b(+) to generate pET28b(+)_CoilE.

**Genetic construction of mEmerald constructs**

Three mEmerald constructs were obtained from Addgene (Michael Davidson's Collection): mEmerald-Actin-C18 (Addgene #53978), Mito-7-mEmerald (Addgene #54160), and H2B-6-mEmerald (Addgene #54111). The parent plasmid for these constructs is mEmerald-C1 (Addgene #53975), which has multiple cloning sites and includes a CMV promoter and neomycin/kanamycin resistance. mEmerald-C1 is adapted from the discontinued Clontech vector pEGFP-C1, with mutations introduced to convert EGFP into mEmerald (mEmerald = EGFP + L64L [silent C192T transition], S72A, N149K, M153T, I167T, A206K). The sequence information for these vectors is on the Addgene website (www.addgene.org).

The mEmerald-Actin-C18 vector was digested with *Bgl*II (NEB). Vectors Mito-7-mEmerald and H2B-6-mEmerald were both digested with *Age*I (NEB). Digested vectors were then purified from a 0.8% low-melting point agarose gel using the Zymoclean Gel DNA Recovery Kit (Zymo). The *coilE* gene was introduced intragenically, between the mEmerald and the target protein using a restriction site (*Bgl*I or *Age*I) located in the middle of the linker (Gly-Gly-Gly-Gly-Pro-Val-Ala-Thr) designed by the Davidson lab (**Table 3.5**). In-Fusion primers were designed following the protocol provided in the In-Fusion HD Cloning Kit user manual (Takara Clontech). Primer sequences for the In-Fusion cloning are provided in **Table 3.7**. For insertion into mEmerald-Actin-C18, the *coilE* gene was amplified with the CoilE *Bgl*I Actin F and CoilE *Bgl*I Actin R primers. For insertion into Mito-7-mEmerald, *coilE* was amplified with the CoilE *Age*I Mito F and CoilE *Age*I Mito R primers. For insertion into H2B-6-mEmerald, *coilE* was amplified with the CoilE-*Age*I H2B F and CoilE-*Age*I H2B R primers. After PCR, the products were analyzed on a 2% agarose gel in TAE. One unit of *Dpn*I (NEB) was added to each PCR reaction to digest pET28b(+)_CoilE and then PCR products were purified via spin column (Takara Clontech).

In-Fusion HD reactions were set up with ~100 ng of linearized vector and 200 ng InFusion PCR product following manufacturer's protocol (In-Fusion HD, Takara Clontech). The reactions were incubated at 50 ºC for 15 min followed by transformation into *E. coli* (Stellar) competent cells (Takara Clontech). Cells were grown and propagated on LB agar plates supplemented with kanamycin (50 µg/mL). Recombinant

colonies were screened and the sequences from positive hits were confirmed via Sanger sequencing.

**Genetic construction of pcDNA3.1_TfR1-CoilE from pcDNA3.1_TfR1**

The pcDNA3.1_TfR1 vector, which encodes murine TfR1, was previously described(3). CoilE-tagged TfR1 was constructed by Gibson assembly. To make pcDNA3.1_TfR1-CoilE, the *coilE* gene was inserted at the C-terminal end of the *tfr1* gene. The *tfr1* stop codon was moved to the end of the *coilE* gene and a sequence encoding a Gly-Ser-Gly-Ser-Gly-Ser-Thr-Gly linker was added between the two genes. Novel *Age*I cut sites were inserted flanking the *coilE* gene on both ends.

Primers for generating Gibson assembly fragments were designed using the NEBuilder® Assembly tool (http://nebuilder.neb.com/) (**Table 3.7**). Gibson assembly fragment 1 was generated by PCR using primers TfR1-CoilE 1 F and TfR1-CoilE 1 R with the vector pcDNA3.1_TfR1 as the template. Gibson assembly fragment 2 was PCR generated using primers TfR1-CoilE 2 F and TfR1-CoilE 2 R and pET28B(+)_CoilE as the template. Gibson assembly fragment 3 was generated using PCR using primers TfR1-CoilE 3 F and TfR1-CoilE 3 R and pcDNA3.1_TfR1 as the template. All PCRs yielded a single product and were purified via PCR and Gel Clean Up Kit (Takara Clontech). The pcDNA3.1_TfR1 vector was digested with *Sma*I and *BstE*II (NEB) and the vector backbone was gel-purified using a 0.6% agarose gel. The vector backbone and all inserts were combined (molar ratio of 1:5 vector-to-insert) and ligated using the Gibson Assembly Mastermix (NEB). The reaction was incubated at 50 ºC for 1 h, transformed to TOP10 *E. coli*, and plated on LB agar plates supplemented with ampicillin (100 µg/mL). Vector-transformed colonies were identified using colony PCR and positive clones were confirmed by Sanger sequencing.

**Expression and purification of CoilR**

We used the pET28b(+)_CoilR plasmid transformed into *E. coli* BL21(DE3) cells (ThermoFisher) to express the CoilR probe peptide. A starter culture was used to inoculate a 1 L flask of LB media with kanamycin (50 µg/mL). When the $OD_{600}$ reached

0.8, we induced expression of CoilR by adding 0.5 mM IPTG for 1 h at 37 ºC. Cells were pelleted by centrifugation and frozen at -20 ºC until purification.

The CoilR peptide was purified under denaturing conditions. Cells were thawed on ice and re-suspended in denaturing lysis buffer (20 mM sodium phosphate, 500 mM NaCl, 8 M urea, 1 mM DTT, pH 7.5). Re-suspended cells were sonicated on ice with a 0.5-inch horn for 8 min with 30 sec on-off intervals (Branson A-450; duty cycle 80% and output control: 8). The lysate was clarified by centrifugation and then incubated with 1 mL of Ni-NTA resin (QIAGEN; resin pre-equilibrated with denaturing lysis buffer) for 1 h at 4 ºC. The resin was then loaded into an Econo-Pac® Chromatography Column (Bio-Rad) and washed with 10 mL denaturing lysis buffer containing 20 mM imidazole and 10 mL lysis buffer containing 50 mM imidazole. The $His_6$-tagged CoilR was eluted from the resin with 20 mL lysis buffer containing 500 mM imidazole. Fractions containing CoilR were combined, concentrated, and buffer exchanged into a low imidazole buffer (20 mM sodium phosphate, 500 mM NaCl, 8 M urea, 10 mM imidazole, 1 mM DTT, pH 7.5) using Amicon Ultra centrifugal filters (3kDa MWCO, Millipore).

The peptides were further purified on a HisTrap FF 1 mL column (GE Healthcare) via FPLC (GE Äkta Purifier). The peptides were eluted with a linear gradient of 20 mM to 500 mM imidazole in lysis buffer over 20 column volumes. Fractions (1 mL) were collected and analyzed by SDS-PAGE. Fractions containing purified peptides were combined, concentrated, and buffer exchanged into 1x TBS/Urea (50 mM Tris pH 8, 150 mM NaCl, 6 M urea) using 3000 kDa Amicon Ultra centrifugal filters. Peptide purity was monitored by SDS-PAGE. Purified peptide solutions were quantified using the Pierce bicinchoninic acid (BCA) assay kit (ThermoFisher) following the manufacturer's instructions. Peptides were stored frozen (-20 °C) in 10% glycerol.

**SDS-PAGE analysis**

Protein samples were analyzed by SDS-PAGE using Criterion XT gels (BioRad). Samples were combined with SDS-PAGE loading dye (50 mM Tris pH 6.9, 100 mM TCEP, 2% SDS, 0.1% Ponceau Red, 10% glycerol) and boiled (5-10 min). Samples were centrifuged briefly before loading and then resolved by SDS-PAGE. Gels

were stained with Coomassie Brilliant Blue and de-stained before imaging on a flat-bed scanner (Canon LiDE220).

**Generation of CoilR-BODIPY and CoilR-Cy5 dye-labeled peptides**

Purified CoilR peptide, containing a single reactive cysteine residue, was buffer-exchanged into Maleimide Labeling Buffer (MLB: 20 mM Tris pH 7.2, 150 mM NaCl, 8 M urea) using Amicon Ultra centrifugal filters (3kDa MWCO, Millipore). MLB was de-gassed under vacuum with stirring immediately before use. CoilR peptide (30 nmol, from 2 mg/mL stock) was reduced in TCEP (30-fold molar excess) in de-gassed MLB (200 µL) for 30 min at 37 ºC.

Reactive maleimide dyes were purchased from Lumiprobe, and stock solutions were prepared in anhydrous DMSO (Sigma-Aldrich). The maleimide dye (40 µL of 100 mM BODIPY or 50 mM Cy5) was added to the reduced CoilR peptide in MLB and incubated on a rotisserie inverter at 4 ºC overnight, protected from light. To make CoilR-BODIPY, the peptide was reacted with a 133-fold molar excess of BODIPY-maleimide (Lumiprobe, #21480). Some of the BODIPY-maleimide precipitated upon addition to the peptide in MLB. To make CoilR-Cy5, the peptide was reacted with a 67-fold molar excess of Sulfo-Cy5-maleimide (Lumiprobe, #23380).

After the reaction, excess fluorophore was removed by centrifugation (Amicon Ultra 3 kDa MWCO) and exchanged into Ni-NTA binding buffer (8M urea, 100 mM $NaH_2PO_4$, 10 mM Tris, 10 mM imidazole, pH = 8.0). Labeled peptide was bound to Ni-NTA resin (Qiagen), washed, and eluted with pH 4.5 elution buffer (8M urea, 100 mM $NaH_2PO_4$, 10 mM Tris, 10 mM imidazole, pH = 4.5). Fractions containing CoilR were combined, concentrated (Amicon Ultra 3kDa MWCO), and buffer-exchanged into MLB, yielding a clear-orange (CoilR-BODIPY) or clear-dark-blue (CoilR-Cy5) solution. Final peptide concentration was determined using the Pierce BCA assay kit (ThermoFisher Scientific) following the manufacturer's instructions. Dye labeling efficiency was estimated using Lumiprobe's suggested protocol. Briefly, we measured absorbance of the labeled peptide at 280 nm and at the excitation maximum of the dye (503 for BODIPY or 646 nm for Sulfo-Cy5) in MLB in a 1-cm quartz cuvette. Labeling efficiency was calculated using the equation:

$$\frac{mol\ dye}{mol\ protein} = \frac{A_{dye}}{\varepsilon_{dye} \times \frac{A_{280} - \left(A_{dye} \times CF\right)}{\varepsilon_{peptide}}}$$

In this equation, $A_{dye}$ is the absorbance of the labeled peptide at 503 nm (BODIPY) or 646 nm (Sulfo-Cy5), $\varepsilon_{dye}$ is the molar extinction coefficient of the dye, $A_{280}$ is the absorbance of the labeled peptide at 280 nm, *CF* is the dye absorbance correction factor at 280 nm, and $\varepsilon_{peptide}$ is the molar extinction coefficient of the peptide at 280 nm (2980 $L \cdot mol^{-1} \cdot cm^{-1}$; calculated using ExPasy, https://web.expasy.org/protparam). See **Table 3.8** for fluorophore values provided by Lumiprobe. Using this equation, we estimated that the CoilR-BODIPY was 30% labeled and the CoilR-Cy5 peptide was 90% labeled. The peptides were diluted to 100 µM in MLB with 10% glycerol and stored at -20 ºC, protected from light.

**Generation of biotinylated probe peptide: CoilR-biotin**

Purified CoilR peptide was buffer-exchanged into de-gassed MLB using Amicon Ultra centrifugal filters (3kDa MWCO, Millipore). CoilR peptide (100 nmol) was reduced with TCEP (1 µmol, 10-fold excess) for 30 min at 37 ºC. The reduced peptide solution was combined with 2 mg (35-fold excess) of EZ-Link-PEG2-biotin (ThermoFisher #21901BID). The reaction mixture (1 mL total volume) was incubated on a rotisserie inverter at 4 ºC overnight. After the reaction, excess biotin was removed by centrifugation (Amicon Ultra, 3 kDa MWCO) by washing exhaustively. The biotinylated peptide was purified by affinity column chromatography. CoilR-biotin was exchanged into 10 mL TBS (20 mM Tris, 150 mM NaCl pH 8.0) before purification of CoilR-biotin on Pierce monomeric avidin agarose resin (ThermoFisher Scientific; Pierce #20228) following the manufacturer's protocol. Fractions were analyzed by SDS-PAGE and anti-biotin Western blot. Fractions containing CoilR-biotin were combined and concentrated by centrifugation (Amicon Ultra 3 kDa MWCO). Final protein concentration was determined by the Pierce BCA assay kit (ThermoFisher Scientific). CoilR-biotin stocks were stored with 10% glycerol at -20 °C.

**Preparation of samples for FM:**

***A. Organelle imaging of VIPER-tagged proteins***

U-2 OS cells expressing mEmerald-actin, mEmerald-CoilE-actin, H2B-mEmerald, H2B-CoilE-mEmerald, Mito-mEmerald, or Mito-CoilE-mEmerald were washed twice with PBS and fixed with 4% paraformaldehyde (PFA) in PBS (pH 7.4) for 15 min at room temperature. Cells were subsequently washed twice with PBS and permeabilized with 0.1% Triton X-100 (10 min). Cells were washed twice to remove detergent. Cells were blocked with 10% FBS, 5% sucrose, 2% BSA (Fraction V) in PBS ("Blocking Solution") for 30 min. Cells were then treated with 100 nM CoilR-Cy5 in Blocking Solution (15 min, room temperature). Cells were washed and then imaged using a Zeiss LSM880 Airyscan line-scanning confocal microscope. This experiment was repeated multiple times, and **Figure 3.1** shows representative images.

***B. Competition binding assay with unlabeled CoilR peptide***

U-2 OS cells expressing mEmerald-actin, mEmerald-CoilE-actin, H2B-mEmerald, H2B-CoilE-mEmerald, Mito-mEmerald, or Mito-CoilE-mEmerald were washed twice with PBS and fixed with 4% PFA in PBS (pH 7.4) for 15 min at room temperature. Cells were subsequently washed twice with PBS and permeabilized with 0.1% Triton X-100 (10 min). Cells were washed twice to remove detergent. Cells were blocked with Blocking Solution for 30 min at room temperature.

Fixed cells expressing CoilE-tagged proteins were treated with increasing concentrations of unlabeled CoilR peptide (0, 100, 1000, 10,000, and 100,000 nM) in Blocking Solution (30 min, room temperature). Cells expressing untagged protein were treated with 0 nM or 100,000 nM unlabeled CoilR peptide. Cells were washed twice and then treated with 100 nM CoilR-Cy5 (30 min, room temperature). Cells were washed three times. Nuclei were stained with 10 µg/mL Hoechst 33342 (10 min) and then washed twice. Cells were imaged using a Zeiss Yokogawa spinning disk confocal microscope. The brightness and contrast (B/C) were optimized for all samples using the images for 0 nM CoilR treated samples during image processing. This experiment was repeated twice, and **Figure 3.2** shows representative images.

***C. Live cell imaging comparison of TfR1-CoilE and TfR1-mCherry***

CHO TRVb cells expressing TfR1-CoilE or TfR1-mCherry were incubated with 10 µg/mL Hoechst 33342 in F12 media supplemented with 10% FBS and 6% BSA for 30 min at 37 ºC. Cells were cooled on ice to pause endocytosis and then incubated with Tf-AF488 (50 µg/mL) in ice-cold F12 with 5% FBS. TfR1-CoilE cells were additionally treated with CoilR-Cy5 (100 nM). After 30 min, cells were washed three times with ice-cold PBS. Cold PBS with 20 mM HEPES was added to cells prior to fluorescence imaging. The Zeiss Yokogawa spinning disk confocal microscope was housed in an incubation chamber (37 ºC) and cells were imaged at 0 and 30 min. Time point captures were focused and acquired manually without the use of microscope automation. This experiment was performed multiple times and **Figure 3.3** shows representative images.

***D. Time-lapse imaging of TfR1-CoilE labeled with CoilR-Cy5 and Tf-AF488***

CHO TRVb cells expressing TfR1 or TfR1-CoilE were incubated with 10 µg/mL Hoechst 33342 in F12 media supplemented with 10% FBS and 6% BSA for 30 min at 37 ºC. Cells were cooled on ice to pause endocytosis and then incubated with CoilR-Cy5 (500 nM) and Tf-AF488 (50 µg/mL) in ice-cold F12 with 5% FBS (no BSA). After 30 min, cells were washed three times with ice-cold PBS. Cold PBS with 20 mM HEPES was added to cells prior to fluorescence imaging. The Zeiss LSM880 Airyscan line-scanning confocal microscope was housed in an incubation chamber and cells were imaged at 37 ºC over the course of 1 h. Time point captures were focused and acquired manually without the use of microscope automation due to drift in image focus over time. Images of AF488 and Cy5 were acquired every 2-4 min for 25 min and a final capture was taken at 60 min. The nuclear stain, Hoechst 33342, was imaged at the 0, 25, and 60 min. This experiment was performed three times and **Figure 3.5** shows representative images.

***E. Pulse-chase labeling of distinct populations of TfR1-CoilE using CoilR probe peptides***

CHO TRVb cells expressing TfR1 or TfR1-CoilE were incubated with 10 µg/mL Hoechst 33342 in F12 media supplemented with 10% FBS and 6% BSA for 30 min at

37 ºC. Cells were cooled on ice to pause endocytosis and then “pulse” labeled with CoilR-Cy5 (500 nM, 15 min) in ice-cold F12 supplemented with 5% FBS. Cells were washed, returned to media, and incubated at 37 ºC for 5, 30, or 120 min. Cells were returned to 4 °C for the “chase” labeling with CoilR-BODIPY (500 nM, 15 min). Cells were washed, fixed with 4% PFA, and imaged on a Zeiss Yokogawa spinning disk confocal microscope. This experiment was performed twice and **Figures 3.6** and **3.7** show representative images.

**Line-scanning confocal imaging**

Micrographs for **Figures 3.1** and **3.5** were acquired on a Zeiss LSM 880 confocal microscope (OHSU Advanced Light Microscopy Core). We used a 63X/1.4 NA oil immersion objective lens and the Zeiss Airy detector. Images were acquired with 2X zoom scanning, resulting in 128X total magnification. Hoechst 33342 was imaged using 405 nm excitation and a 450/50 nm emission filter. AF488 was imaged using 488 nm excitation and a 525/50 nm emission filter. Cy5 was imaged using 633 nm excitation and a 670/30 emission filter. In each experiment, images were acquired as single confocal slices (450 nm depth) with identical acquisition settings optimized for each channel. The Airyscan detector is a 32-channel GaAsp array that uses the additional channels to collect out of focus light for each capture. This additional data was then used to deconvolve the image using the ZEN 2.0 software package (Zeiss).

**Spinning disk confocal imaging**

Micrographs for **Figures 3.2, 3.3**, **3.4, 3.6, and 3.7** were acquired on a Zeiss Yokogawa CSU-X1 spinning disk confocal microscope (OHSU Advanced Light Microscopy Core). We used a 63X/1.4 NA oil immersion objective lens. Hoechst 33342 was imaged using 405 nm excitation and a 450/50 nm emission filter. AF488 or mEmerald were imaged using 488 nm excitation and a 525/50 nm emission filter. TfR1-mCherry was imaged using 534 nm excitation and a 562/45 nm emission filter. Cy5 was imaged using 633 nm excitation and a 670/30 emission filter. In each experiment, the images were captured as single confocal slices (450 nm depth) with identical acquisition settings optimized for each channel.

**Image processing: fluorescence micrographs**

Image processing and analysis was carried out using Fiji Software (Version 2.0.0-rc-46). The brightness and contrast (B/C) were optimized and the same settings were applied for each channel across all samples within an experiment. For example, all images of Tf-AF488's green fluorescence in **Figure 3.5** were set to the same B/C settings (150 to 3,000). Images were sometimes manually cropped to enlarge or highlight a particular feature. Images were false-colored using standard lookup tables: mEmerald (green); AF488 (green); BODIPY (green); mCherry (magenta); Cy5 (magenta); Hoechst 33342 (blue). Colocalization analysis and channel intensity plots for **Figure 3.4** were generated using the Coloc 2 plugin in Fiji (Analyze > Colocalization > Coloc 2). Pearson's correlation values were calculated without thresholding or use of a region of interest.

**Preparation and imaging of samples for multi-scale microscopy:**

***A. Plating and transfection of CHO TRVb for CLEM***

CHO TRVb cells were plated ($10^6$ cells/well) and grown to 90% confluence on indium tin oxide (ITO)-coated coverslips (2SPI Cat#06486-AB) in 6-well dishes. Cells were transfected with 2 µg of pcDNA3.1_TfR1 or pcDNA3.1_TfR1-CoilE and 4 µg of Lipofectamine 2000 in 3 mL Opti-MEM. After 2 h, cells were returned to serum-containing media. After 24 h, cells were labeled and processed for CLEM imaging.

***B. Imaging TfR1 and TfR1-CoilE by CLEM***

CHO TRVb cells were blocked with 10% FBS with 6% BSA in F12 (30 min, 37 ºC). Cells were labeled cold with CoilR-biotin (100 nM) and Tf-A488 (50 µg/mL) in F12 with 5% FBS (30 min, 4 ºC). Cells were washed with cold PBS and fixed in cold 4% PFA (20 min). Cells were washed and then blocked with 10% FBS with 6% BSA in PBS (1 h, room temperature). Cells were subsequently labeled with 10 nM streptavidin-Qdot655 (ThermoFisher Scientific #Q10121MP) in PBS with 6% BSA (1 h, room temperature). Cells were washed with PBS before fluorescence imaging. Cells were mapped using the FEI Corrsight MAPS software.

This experiment was performed three times and **Figure 3.8** shows representative images. Additional images are provided in **Figures 3.9** and **3.10**

***C. Comparison of VIPER with immunolabeling for CLEM***

We evaluated four anti-TfR1 antibodies: 8D3 (Novus Biologicals), Ab1086 (Abcam), Ab216665 (Abcam), and H68.4 (ThermoFisher Scientific). We evaluated one anti-Tf antibody: Ab82411 (Abcam). A summary of the primary and secondary antibodies used for this study are summarized in **Table 3.9**.

All antibodies were evaluated first by FM. We applied each primary antibody to transfected cells live or post-fixation. Secondary Qdot655 conjugates were applied to cells after fixation and samples were evaluated for Qdot fluorescence. Primary and secondary antibodies were used at the dilution recommended by the manufacturer for immunofluorescence. Antibodies were tested against both TfR1 and TfR1-CoilE; no differences in immunolabeling were observed. We found that Ab1086 and Ab216665 were unable to label TfR1 or TfR1-CoilE (**Figure 3.11**). We verified that each secondary antibody was specific for the corresponding primary antibody (e.g., with a no primary control).

For CLEM imaging, transfected CHO TRVb cells were treated with 100 nM Tf-AF488 (30 min at 4 °C). Cells were then washed and fixed with 4% PFA (15 min, 4 °C). For H68.4 immunolabeling, cells were permeabilized with 0.1% Triton-X-100 (10 min, room temperature) and then washed with PBS to remove detergent. Samples were blocked in 1% BSA/PBS (30 min, room temperature). For immunolabeling, primary antibodies were diluted 1:100 (10 µg/mL) in 1% BSA/PBS and applied to cells (1h, room temperature). Cells were washed and treated with the appropriate Qdot655-conjugated secondary antibody diluted 1:200 (5 nM) for 1 h at room temperature and then washed. For VIPER labeling, cells were treated with 100 nM CoilR-biotin (1 h, room temperature), washed, and then treated with 10 nM streptavidin-Qdot655 (1 h, room temperature), and washed. Cells were imaged by FM to detect Tf-AF488 and Qdot655 fluorescence.

This CLEM experiment was performed three times and **Figures 3.11**, **3.12**, **3.15**, and **3.16** show representative images.

### *D. Qdot detection of VIPER compared to Qdot detection of Tf ligand*

We used CLEM to directly compare streptavidin-Qdot655 detection of biotinylated TfR1 versus biotinylated Tf. CHO TRVb cells transfected with TfR1-CoilE were blocked with 10% FBS with 6% BSA in F12 (30 min, 37 ºC). Cells were treated with either CoilR-biotin (100 nM) or 100 nM Tf-biotin (ThermoFisher Scientific #T23363, Lot# 1853655). This lot of Tf-biotin was reported to have an average of 5 biotins/ligand, with a range of 2-5. Both biotinylated ligands were added in F12 media for 30 min at 4 °C. Cells treated with CoilR-biotin were also treated with Tf-AF488 (100 nM) as a counterstain for TfR1. Cells were then washed, fixed with 4% PFA (15 min, 4 °C), and blocked with 6% BSA, 10% serum in PBS (1 h, room temperature). Cells were then treated with 10 nM streptavidin-Qdot655 (ThermoFisher Scientific #Q10121MP; Lot# 1843526) in 6% BSA in PBS (1 h, room temperature). Cells were washed with PBS and imaged by FM to detect Tf-AF488 and/or Qdot655 fluorescence.

This experiment was performed three times and **Figures 3.13** and **3.17** show representative images.

### *E. FEI Corrsight FM*

ITO coverslips were imaged on an FEI Corrsight spinning disk confocal fluorescence microscope. Fiducial markers were added to each ITO-coverslip using a diamond scribe. Then coverslips were mounted on a custom-machined aluminum slide, which prevented disruption of the cells during wet imaging and allowed coverslips to be removed from the metal slide after acquisition. First, the slide was imaged using a 5X/0.25 N.A. objective lens with transmitted light to capture fiducial markers. Then fluorescence micrographs were acquired using a 63X/1.4 N.A. objective lens. Individual cells were imaged for green fluorescence (Tf-AF488) and Qdot655 fluorescence. Transfected cells within each sample were selected for imaging based on Tf-AF488 fluorescence. We attempted to select cells that exhibited similar levels of AF488 fluorescence in order to normalize for cell to cell variations in TfR1 or TfR1-CoilE expression. When Tf-AF488 fluorescence could not be compared (such as loss of fluorescence due to detergent treatment), cells were selected based on average Qdot655 signal on the coverslip. AF488 signal was detected using 488 nm excitation

and a 525/50 nm filter to collect the emitted light. Then, Qdot655 signal was detected using 405 nm excitation and a 690/650 filter to collect the emitted light. Fluorescent cells were mapped using FEI's MAPS software for subsequent imaging via SEM.

### *F. CLEM processing of ITO coverslips*

The FEI's MAPS software enables the same cell to be imaged by FM and SEM. After FM imaging, coverslips were returned to PBS and prepared for SEM. Coverslips were rinsed with deionized water and then dehydrated using 5 min washes with an ethanol gradient: 25%, 50%, 75%, 90%, and 100% (twice). Slides for **Figures 3.8, 3.9, and 3.10** were then chemically dehydrated using 5 min washes of 50%, 75% and 100% (twice) hexamethyl-disilazane (HMDS) in ethanol and then left to fully dry in a fume hood. In contrast, samples for **Figures 3.11-3.13**, and **3.15-3.17** were first dehydrated with an ethanol gradient and then critical point dried using a Leica EM CPD300 critical point dryer. Coverslips were glued to SEM mount pins using conductive silver paint (Pelco Cat#16035). Samples were dried overnight inside a desiccator and flash-coated with 10 nm of carbon using a Leica ACE600 sputter/coater machine.

### *G. FEI Helios Nanolab 660 FIB SEM*

SEM images were acquired on a FEI Helios Nanolab 660 DualBeam. The instrument was set to acquire at 3 kV accelerating voltage and beam current of 0.2 nA. Back scattered electron (BSE) images were acquired via a dedicated BSE detector. MAPS software allowed previously-selected cells to be re-located. Briefly, a three point alignment on the engraved fiduciary pattern was used to globally align the SEM image to the previously captured light image of the ITO slide. Cells could be located using MAPS after global alignment. Cells were imaged at 65,000X magnification (**Figures 3.8-3.10**) or 100,000X magnification (**Figure 3.11-3.13, and 3.15-3.17**). We imaged 2 non-overlapping fields-of-view per cell and six cells (**Figures 3.8-3.10**) or three cells (**Figure 3.11-3.13 and 3.15-3.17)** per condition.

The SEM micrographs display the surface of cells. At high magnification, the cell surface appears dark gray and textured, with cell features such as protrusions or ruffles appearing lighter gray or white due to their closer proximity to the BSE detector. For an

example of a cell with many raised features, see **Figure 3.10A**: Cell 3 Image 1 (*lower left panel*). In contrast, recessed areas of the cell surface appear darker gray. The ITO coverslip appears white in BSE mode, and areas where the cell is thin often appear lighter gray due to signal from the coverslip penetrating through the cell. For an example of a thin cell feature, see **Figure 3.15B:** Cell 3 Image 2 (*lowest right panel*).

**Quantitative image analysis of Qdot labeling in SEM images**

For computer-assisted counting of SEM images, images were acquired at high magnification (65,000X or 100,000X) for optimal particle detection and segmentation. To detect and count particles, segmentation was implemented in MATLAB with a two-step procedure. First, we detected bright objects of interest in a dark background using morphological top-hat filtering(66). This method computes the morphological opening of the image and then subtracts the result from the original image to enhance the original image. Second, simple intensity thresholding (i.e., Otsu's method(67)) was applied to segment the objects followed by applying a Gaussian blur(68) to the improved image. Finally, segmentation was validated by visual assessment to refine parameters and exclude objects falsely annotated. False-annotations were rare, but typically resulted from unspecific intensity background, intensity variations, background artifacts, or errors in segmentation overlooked by the automated procedure described above. A representative Qdot655 image, with segmentation applied, is provided in **Figure 3.9B.**

To separate multiply-clustered objects within SEM images, we differentiated the object's foreground and background. However, to successfully segment the locally clustered or overlapping particles, we performed marker-controlled watershed segmentation(69). We computed the watershed transform of the distance transform of good foreground markers from the segmented mask and looked for the watershed ridge lines of the result. Then, we counted the segmented single particles with results provided in **Tables 3.1-3.4**.

**Statistical analysis of Qdot655 particle counts**

Scatter plots of counted Qdots are provided in **Figures 3.9** and **3.14**. Statistical analysis was done in Graphpad Prism (Version 6.02). Raw counts for each labeling

method were selected for Welch's t-test analysis. For determining statistical significance, labeling methods (*i.e.* Tf-biotin, 8D3, etc.) were compared against VIPER using an unpaired, two-tail t-test. We assumed a Gaussian distribution and unequal variances. Significance values were reported in the figure captions. VIPER (live-labeling protocol) was compared with Tf-biotin. VIPER (fixed-labeling protocol) was compared to 8D3, Ab82411, H68.4, Ab1086, and Ab216665.

## Supplementary Tables and Figures

### Table 3.1: Quantification of Qdots in SEM images comparing TfR1-CoilE and TfR1[‡]

| | Micrograph | count/μm$^2$ | total count[§] | monomer | dimer | ≥ 3 |
|---|---|---|---|---|---|---|
| TfR1-CoilE | Cell 1 Image 1 | 190.3 | 3331 | 2841 | 187 | 37 |
| | Cell 1 Image 2 | 137.8 | 2411 | 2196 | 92 | 10 |
| | Cell 2 Image 1 | 113.9 | 1993 | 1827 | 72 | 6 |
| | Cell 2 Image 2 | 103 | 1803 | 1627 | 82 | 4 |
| | Cell 3 Image 1 | 142.6 | 2496 | 2181 | 133 | 14 |
| | Cell 3 Image 2 | 114.3 | 2000 | 1747 | 106 | 13 |
| | Cell 4 Image 1 | 63.1 | 1104 | 1032 | 30 | 4 |
| | Cell 4 Image 2 | 95.9 | 1679 | 1607 | 30 | 4 |
| | Cell 5 Image 1 | 93.1 | 1629 | 1487 | 62 | 6 |
| | Cell 5 Image 2 | 107.5 | 1881 | 1735 | 70 | 2 |
| | Cell 6 Image 1 | 77.6 | 1358 | 1228 | 55 | 6 |
| | Cell 6 Image 2 | 82.8 | 1449 | 1300 | 64 | 7 |
| | **AVERAGE** | 110±34 | 1928±598 | 1734±493 | 82±44 | 9±9 |
| TfR1 | Cell 1 Image 1 | 0 | 0 | 0 | 0 | 0 |
| | Cell 1 Image 2 | 0 | 0 | 0 | 0 | 0 |
| | Cell 2 Image 1 | 0.5 | 8 | 6 | 1 | 0 |
| | Cell 2 Image 2 | 0.1 | 1 | 1 | 0 | 0 |
| | Cell 3 Image 1 | 0 | 0 | 0 | 0 | 0 |
| | Cell 3 Image 2 | 0 | 0 | 0 | 0 | 0 |
| | Cell 4 Image 1 | 0.1 | 1 | 1 | 0 | 0 |
| | Cell 4 Image 2 | 0 | 0 | 0 | 0 | 0 |
| | Cell 5 Image 1 | 0 | 0 | 0 | 0 | 0 |
| | Cell 5 Image 2 | 0 | 0 | 0 | 0 | 0 |
| | Cell 6 Image 1 | 0 | 0 | 0 | 0 | 0 |
| | Cell 6 Image 2 | 0 | 0 | 0 | 0 | 0 |
| | **AVERAGE** | 0±0 | 1±2 | 1±2 | 0±0 | 0±0 |

[‡] *Entries are color-coded to match points shown in* ***Figure S5C****.*

[§] *Welch's t-test = 11.16, p value <0.0001*

**Table 3.2: Quantification of Qdots in SEM images comparing VIPER-biotin and Tf-biotin**

| | Micrograph | count/μm$^2$ | total count | monomer | dimer | ≥ 3 |
|---|---|---|---|---|---|---|
| VIPER-biotin | **Cell 1 Image 1** | 142.7 | 1712 | 1337 | 146 | 25 |
| | **Cell 1 Image 2** | 249.8 | 2997 | 2169 | 297 | 70 |
| | **Cell 2 Image 1** | 241.2 | 2894 | 2000 | 304 | 86 |
| | **Cell 2 Image 2** | 317.5 | 3810 | 2469 | 468 | 118 |
| | **Cell 3 Image 1** | 144.3 | 1732 | 1393 | 128 | 26 |
| | **Cell 3 Image 2** | 164.9 | 1979 | 1435 | 188 | 49 |
| | **AVERAGE** | **210 ± 71** | **2521 ± 848** | **1800 ± 477** | **255 ± 128** | **62 ± 36** |
| Tf-Biotin | **Cell 1 Image 1** | 299.4 | 3593 | 1238 | 447 | 359 |
| | **Cell 1 Image 2** | 280.2 | 3362 | 1249 | 395 | 342 |
| | **Cell 2 Image 1** | 215.0 | 2580 | 1177 | 317 | 216 |
| | **Cell 2 Image 2** | 214.5 | 2574 | 1140 | 313 | 216 |
| | **Cell 3 Image 1** | 354.7 | 4256 | 1672 | 505 | 409 |
| | **Cell 3 Image 2** | 182.1 | 2185 | 892 | 244 | 214 |
| | **AVERAGE** | **258 ± 65** | **3092 ± 779** | **1228 ± 253** | **370 ± 97** | **293 ± 88** |

**Table 3.3: Quantification of Qdots in SEM images: VIPER versus immunolabeling**

| | Micrograph | count/μm$^2$ | total count | monomer | dimer | ≥ 3 |
|---|---|---|---|---|---|---|
| **VIPER** | **Cell 1 Image 1** | 312.2 | 3746 | 2148 | 429 | 200 |
| | **Cell 1 Image 2** | 331.5 | 3978 | 2331 | 462 | 192 |
| | **Cell 2 Image 1** | 261.1 | 3133 | 1587 | 398 | 196 |
| | **Cell 2 Image 2** | 104.6 | 1255 | 840 | 130 | 40 |
| | **Cell 3 Image 1** | 320.2 | 3842 | 2363 | 452 | 165 |
| | **Cell 3 Image 2** | 288.9 | 3467 | 2056 | 430 | 156 |
| | **AVERAGE** | **270 ± 85** | **3237 ± 1016** | **1888 ± 584** | **384 ± 126** | **158 ± 61** |
| **Anti-TfR1 (8D3)** | **Cell 1 Image 1** | 440.4 | 5285 | 2294 | 595 | 457 |
| | **Cell 1 Image 2** | 389.0 | 4668 | 1861 | 504 | 452 |
| | **Cell 2 Image 1** | 653.5 | 7842 | 2734 | 833 | 802 |
| | **Cell 2 Image 2** | 457.8 | 5493 | 2357 | 633 | 462 |
| | **Cell 3 Image 1** | 393.9 | 4727 | 1782 | 540 | 453 |
| | **Cell 3 Image 2** | 448.8 | 5385 | 1952 | 646 | 515 |
| | **AVERAGE** | **464 ± 97** | **5567 ± 1167** | **2163 ± 364** | **625 ± 115** | **524 ± 139** |
| **Anti- Tf (Ab82411)** | **Cell 1 Image 1** | 106.7 | 1280 | 857 | 148 | 36 |
| | **Cell 1 Image 2** | 107.5 | 1290 | 810 | 156 | 47 |
| | **Cell 2 Image 1** | 95.6 | 1147 | 607 | 138 | 73 |
| | **Cell 2 Image 2** | 99.3 | 1191 | 669 | 153 | 59 |
| | **Cell 3 Image 1** | 62.7 | 752 | 467 | 89 | 32 |
| | **Cell 3 Image 2** | 71.6 | 859 | 492 | 102 | 42 |
| | **AVERAGE** | **91 ± 19** | **1087 ± 227** | **650 ± 161** | **131 ± 28** | **48 ± 15** |
| **Anti-TfR1 (H68.4)** | **Cell 1 Image 1** | 69.6 | 835 | 530 | 86 | 34 |
| | **Cell 1 Image 2** | 181.8 | 2182 | 1149 | 232 | 146 |
| | **Cell 2 Image 1** | 198.0 | 2376 | 1392 | 265 | 120 |
| | **Cell 2 Image 2** | 165.0 | 1980 | 1164 | 213 | 106 |
| | **Cell 3 Image 1** | 238.8 | 2866 | 1484 | 301 | 204 |
| | **Cell 3 Image 2** | 240.4 | 2885 | 1492 | 324 | 196 |
| | **AVERAGE** | **182 ± 63** | **2187 ± 756** | **1202 ± 362** | **237 ± 85** | **134 ± 63** |

**Table 3.4: Quantification of Qdots in SEM images: Immunolabeling with Ab1086 and Ab216665**

| | Micrograph | count/$\mu m^2$ | total count | monomer | dimer | ≥ 3 |
|---|---|---|---|---|---|---|
| **Ab1086** | **Cell 1 Image 1** | 0.0 | 0 | 0 | 0 | 0 |
| | **Cell 1 Image 2** | 0.1 | 1 | 1 | 0 | 0 |
| | **Cell 2 Image 1** | 0.0 | 0 | 0 | 0 | 0 |
| | **Cell 2 Image 2** | 0.0 | 0 | 0 | 0 | 0 |
| | **Cell 3 Image 1** | 0.0 | 0 | 0 | 0 | 0 |
| | **Cell 3 Image 2** | 0.2 | 2 | 2 | 0 | 0 |
| | **AVERAGE** | **0±0** | **1±1** | **1±1** | **0±0** | **0±0** |
| **Ab216665** | **Cell 1 Image 1** | 0.4 | 5 | 5 | 0 | 0 |
| | **Cell 1 Image 2** | 1.6 | 19 | 15 | 2 | 0 |
| | **Cell 2 Image 1** | 0.5 | 6 | 6 | 0 | 0.5 |
| | **Cell 2 Image 2** | 0.0 | 0 | 0 | 0 | 0.0 |
| | **Cell 3 Image 1** | 0.3 | 4 | 4 | 0 | 0 |
| | **Cell 3 Image 2** | 0.4 | 5 | 5 | 0 | 0 |
| | **AVERAGE** | **1±1** | **7±6** | **6±5** | **0±1** | **0±0** |

## Table 3.5. Summary of genetic constructs

| Protein Name | **Sequence** (1-letter amino acid code)<br>Sequence annotation key: **Coil tag**; linker; mEmerald; mCherry | Molecular Weight (Daltons)‡ | pI‡ | Vector name |
|---|---|---|---|---|
| CoilR | MGGS**LEIRAAFLRQRNTALRTEVAELEQEVQRLENEVSQYETRYGPL**GGG<br>AAALGCLAAALEHHHHHH | 7,502.35 | 6.00 | pET28b(+)<br>_CoilR |
| CoilR-Lys56 | MGGS**LEIRAAFLRQRNTALRTEVAELEQEVQRLENEVSQYETRYGPL**GGG<br>AAALGKLAAALEHHHHHH | 7,527.38 | 6.27 | pET28b(+)<br>_CoilR-<br>Lys56 |
| CoilE | MGGS**LEIEAAFLERENTALETRVAELRQRVQRLRNRVSQYRTRYGPL**GGG<br>CLEHHHHH | 6,737.56 | 9.29 | pET28b(+)<br>_CoilE |
| Transferrin receptor 1 (TfR1) | MMDQARSAFSNLFGGEPLSYTRFSLARQVDGDNSHVEMKLAADEEENADN<br>NMKASVRKPKRFNGRLCFAAIALVIFFLIGFMSGYLGYCKRVEQKEECVK<br>LAETEETDKSETMETEDVPTSSRLYWADLKTLLSEKLNSIEFADTIKQLS<br>QNTYTPREAGSQKDESLAYYIENQFHEFKFSKVWRDEHYVKIQVKSSIGQ<br>NMVTIVQSNGNLDPVESPEGYVAFSKPTEVSGKLVHANFGTKKDFEELSY<br>SVNGSLVIVRAGEITFAEKVANAQSFNAIGVLIYMDKNKFPVVEADLALF<br>GHAHLGTGDPYTPGFPSFNHTQFPPSQSSGLPNIPVQTISRAAAEKLFGK<br>MEGSCPARWNIDSSCKLELSQNQNVKLIVKNVLKERRILNIFGVIKGYEE<br>PDRYVVVGAQRDALGAGVAAKSSVGTGLLLKLAQVFSDMISKDGFRPSRS<br>IIFASWTAGDFGAVGATEWLEGYLSSLHLKAFTYINLDKVVLGTSNFKVS<br>ASPLLYTLMGKIMQDVKHPVDGKSLYRDSNWISKVEKLSFDNAAYPFLAY<br>SGIPAVSFCFCEDADYPYLGTRLDTYEALTQKVPQLNQMVRTAAEVAGQL<br>IIKLTHDVELNLDYEMYNSKLLSFMKDLNQFKTDIRDMGLSLQWLYSARG<br>DYFRATSRLTTDFHNAEKTNRFVMREINDRIMKVEYHFLSPYVSPRESPF<br>RHIFWGSGSHTLSALVENLKLRQKNITAFNETLFRNQLALATWTIQGVAN<br>ALSGDIWNIDNEF | 85,731.40 | 6.13 | pcDNA3.1<br>_TfR1 |
| TfR1-CoilE | MMDQARSAFSNLFGGEPLSYTRFSLARQVDGDNSHVEMKLAADEEENADN<br>NMKASVRKPKRFNGRLCFAAIALVIFFLIGFMSGYLGYCKRVEQKEECVK<br>LAETEETDKSETMETEDVPTSSRLYWADLKTLLSEKLNSIEFADTIKQLS<br>QNTYTPREAGSQKDESLAYYIENQFHEFKFSKVWRDEHYVKIQVKSSIGQ<br>NMVTIVQSNGNLDPVESPEGYVAFSKPTEVSGKLVHANFGTKKDFEELSY<br>SVNGSLVIVRAGEITFAEKVANAQSFNAIGVLIYMDKNKFPVVEADLALF<br>GHAHLGTGDPYTPGFPSFNHTQFPPSQSSGLPNIPVQTISRAAAEKLFGK<br>MEGSCPARWNIDSSCKLELSQNQNVKLIVKNVLKERRILNIFGVIKGYEE<br>PDRYVVVGAQRDALGAGVAAKSSVGTGLLLKLAQVFSDMISKDGFRPSRS<br>IIFASWTAGDFGAVGATEWLEGYLSSLHLKAFTYINLDKVVLGTSNFKVS<br>ASPLLYTLMGKIMQDVKHPVDGKSLYRDSNWISKVEKLSFDNAAYPFLAY<br>SGIPAVSFCFCEDADYPYLGTRLDTYEALTQKVPQLNQMVRTAAEVAGQL<br>IIKLTHDVELNLDYEMYNSKLLSFMKDLNQFKTDIRDMGLSLQWLYSARG<br>DYFRATSRLTTDFHNAEKTNRFVMREINDRIMKVEYHFLSPYVSPRESPF<br>RHIFWGSGSHTLSALVENLKLRQKNITAFNETLFRNQLALATWTIQGVAN<br>ALSGDIWNIDNEFGSGSGSTG**MLEIEAAFLERENTALETRVAELRQRVQR<br>LRNRVSQYRTRYGPL**GGGCLETG | 92,312.77 | 6.34 | pcDNA3.1<br>_TfR1-<br>CoilE |
| TfR1-mCherry | MMDQARSAFSNLFGGEPLSYTRFSLARQVDGDNSHVEMKLAVDEEENADN<br>NTKANVTKPKRCSGSICYGTIAVIVFFLIGFMIGYLGYCKGVEPKTECER<br>LAGTESPVREEPGEDFPAARRLYWDDLKRKLSEKLDSTDFTSTIKLLNEN<br>SYVPREAGSQKDENLALYVENQFREFKLSKVWRDQHFVKIQVKDSAQNSV<br>IIVDKNGRLVYLVENPGGYVAYSKAATVTGKLVHANFGTKKDFEDLYTPV<br>NGSIVIVRAGKITFAEKVANAESLNAIGVLIYMDQTKFPIVNAELSFFGH<br>AHLGTGDPYTPGFPSFNHTQFPPSRSSGLPNIPVQTISRAAAEKLFGNME<br>GDCPSDWKTDSTCRMVTSESKNVKLTVSNVLKEIKILNIFGVIKGFVEPD<br>HYVVVGAQRDAWGPGAAKSGVGTALLLKLAQMFSDMVLKDGFQPSRSIIF<br>ASWSAGDFGSVGATEWLEGYLSSLHLKAFTYINLDKAVLGTSNFKVSASP<br>LLYTLIEKTMQNVKHPVTGQFLYQDSNWASKVEKLTLDNAAFPFLAYSGI<br>PAVSFCFCEDTDYPYLGTTMDTYKELIERIPELNKVARAAAEVAGQFVIK<br>LTHDVELNLDYERYNSQLLSFVRDLNQYRADIKEMGLSLQWLYSARGDFF<br>RATSRLTTDFGNAEKTDRFVMKKLNDRVMRVEYHFLSPYVSPKESPFRHV<br>FWGSGSHTLPALLENLKLRKQNNGAFNETLFRNQLALATWTIQGAANALS<br>GDVWDIDNEFSEFGSTGSTGSTGADPPVATMVSKGEEDNMAIIKEFMRFK<br>VHMEGSVNGHEFEIEGEGEGRPYEGTQTAKLKVTKGGPLPFAWDILSPQF<br>MYGSKAYVKHPADIPDYLKLSFPEGFKWERVMNFEDGGVVTVTQDSSLQD | 113,413.42 | 5.87 | mCherry-<br>TFR-20<br>Addgene:<br>55144 |

| | | | | |
|---|---|---|---|---|
| | GEFIYKVKLRGTNFPSDGPVMQKKTMGWEASSERMYPEDGALKGEIKQRL<br>KLKDGGHYDAEVKTTYKAKKPVQLPGAYNVNIKLDITSHNEDYTIVEQYE<br>RAEGRHSTGGMDELYK | | | |
| mEmerald-actin | MVSKGEELFTGVVPILVELDGDVNGHKFSVSGEGEGDATYGKLTLKFICT<br>TGKLPVPWPTLVTTLTYGVQCFARYPDHMKQHDFFKSAMPEGYVQERTIF<br>FKDDGNYKTRAEVKFEGDTLVNRIELKGIDFKEDGNILGHKLEYNYNSHK<br>VYITADKQKNGIKVNFKTRHNIEDGSVQLADHYQQNTPIGDGPVLLPDNH<br>YLSTQSKLSKDPNEKRDHMVLLEFVTAAGITLGMDELYKSGLRSGSGGGS<br>ASGGSGSDDDIAALVVDNGSGMCKAGFAGDDAPRAVFPSIVGRPRHQGVM<br>VGMGQKDSYVGDEAQSKRGILTLKYPIEHGIVTNWDDMEKIWHHTFYNEL<br>RVAPEEHPVLLTEAPLNPKANREKMTQIMFETFNTPAMYVAIQAVLSLYA<br>SGRTTGIVMDSGDGVTHTVPIYEGYALPHAILRLDLAGRDLTDYLMKILT<br>ERGYSFTTTAEREIVRDIKEKLCYVALDFEQEMATAASSSSLEKSYELPD<br>GQVITIGNERFRCPEALFQPSFLGMESCGIHETTFNSIMKCDVDIRKDLY<br>ANTVLSGGTTMYPGIADRMQKEITALAPSTMKIKIIAPPERKYSVWIGGS<br>ILASLSTFQQMWISKQEYDESGPSIVHRKCF | 69,948.42 | 5.58 | mEmerald-actin-C18 Addgene: 53978 |
| mEmerald-CoilE-actin | MVSKGEELFTGVVPILVELDGDVNGHKFSVSGEGEGDATYGKLTLKFICT<br>TGKLPVPWPTLVTTLTYGVQCFARYPDHMKQHDFFKSAMPEGYVQERTIF<br>FKDDGNYKTRAEVKFEGDTLVNRIELKGIDFKEDGNILGHKLEYNYNSHK<br>VYITADKQKNGIKVNFKTRHNIEDGSVQLADHYQQNTPIGDGPVLLPDNH<br>YLSTQSKLSKDPNEKRDHMVLLEFVTAAGITLGMDELYKSGLRSM**LEIEA<br>AFLERENTALETRVAELRQRVQRLRNRVSQYRTRYGPL**GGGRSGSGGGSA<br>SGGSGSDDDIAALVVDNGSGMCKAGFAGDDAPRAVFPSIVGRPRHQGVMV<br>GMGQKDSYVGDEAQSKRGILTLKYPIEHGIVTNWDDMEKIWHHTFYNELR<br>VAPEEHPVLLTEAPLNPKANREKMTQIMFETFNTPAMYVAIQAVLSLYAS<br>GRTTGIVMDSGDGVTHTVPIYEGYALPHAILRLDLAGRDLTDYLMKILTE<br>RGYSFTTTAEREIVRDIKEKLCYVALDFEQEMATAASSSSLEKSYELPDG<br>QVITIGNERFRCPEALFQPSFLGMESCGIHETTFNSIMKCDVDIRKDLYA<br>NTVLSGGTTMYPGIADRMQKEITALAPSTMKIKIIAPPERKYSVWIGGSI<br>LASLSTFQQMWISKQEYDESGPSIVHRKCF | 75,678.93 | 5.83 | mEmerald-CoilE-actin-C18 |
| H2B-mEmerald | MPEPAKSAPAPKKGSKKAVTKAQKKGGKKRKRSRKESYSIYVYKVLKQVH<br>PDTGISSKAMGIMNSFVNDIFERIAGEASRLAHYNKRSTITSREIQTAVR<br>LLLPGELAKHAVSEGTKAITKYTSAKDPPVATMVSKGEELFTGVVPILVE<br>LDGDVNGHKFSVSGEGEGDATYGKLTLKFICTTGKLPVPWPTLVTTLTYG<br>VQCFARYPDHMKQHDFFKSAMPEGYVQERTIFFKDDGNYKTRAEVKFEGD<br>TLVNRIELKGIDFKEDGNILGHKLEYNYNSHKVYITADKQKNGIKVNFKT<br>RHNIEDGSVQLADHYQQNTPIGDGPVLLPDNHYLSTQSALSKDPNEKRDH<br>MVLLEFVTAAGITLGMDELYK | 41,320.19 | 9.26 | H2B-6-mEmerald Addgene: 54111 |
| H2B-CoilE-mEmerald | MPEPAKSAPAPKKGSKKAVTKAQKKGGKKRKRSRKESYSIYVYKVLKQVH<br>PDTGISSKAMGIMNSFVNDIFERIAGEASRLAHYNKRSTITSREIQTAVR<br>LLLPGELAKHAVSEGTKAITKYTSAK*DPPVM***LEIEAAFLERENTALETRV<br>AELRQRVQRLRNRVSQYRTRYGPL**GGGGPVATMVSKGEELFTGVVPILVE<br>LDGDVNGHKFSVSGEGEGDATYGKLTLKFICTTGKLPVPWPTLVTTLTYG<br>VQCFARYPDHMKQHDFFKSAMPEGYVQERTIFFKDDGNYKTRAEVKFEGD<br>TLVNRIELKGIDFKEDGNILGHKLEYNYNSHKVYITADKQKNGIKVNFKT<br>RHNIEDGSVQLADHYQQNTPIGDGPVLLPDNHYLSTQSALSKDPNEKRDH<br>MVLLEFVTAAGITLGMDELYK | 47,060.74 | 9.39 | H2B-6-CoilE-mEmerald |
| Mito-mEmerald | MSVLTPLLLRGLTGSARRLPVPRAKIHSLGDPPVATMVSKGEELFTGVVP<br>ILVELDGDVNGHKFSVSGEGEGDATYGKLTLKFICTTGKLPVPWPTLVTT<br>LTYGVQCFARYPDHMKQHDFFKSAMPEGYVQERTIFFKDDGNYKTRAEVK<br>FEGDTLVNRIELKGIDFKEDGNILGHKLEYNYNSHKVYITADKQKNGIKV<br>NFKTRHNIEDGSVQLADHYQQNTPIGDGPVLLPDNHYLSTQSKLSKDPNE<br>KRDHMVLLEFVTAAGITLGMDELYK | 30,728.05 | 6.56 | Mito-7-mEmerald Addgene: 54160 |
| Mito-CoilE-mEmerald | MSVLTPLLLRGLTGSARRLPVPRAKIHSLG*DPPVM***LEIEAAFLERENTAL<br>ETRVAELRQRVQRLRNRVSQYRTRYGPL**GGGGPVATMVSKGEELFTGVVP<br>ILVELDGDVNGHKFSVSGEGEGDATYGKLTLKFICTTGKLPVPWPTLVTT<br>LTYGVQCFARYPDHMKQHDFFKSAMPEGYVQERTIFFKDDGNYKTRAEVK<br>FEGDTLVNRIELKGIDFKEDGNILGHKLEYNYNSHKVYITADKQKNGIKV<br>NFKTRHNIEDGSVQLADHYQQNTPIGDGPVLLPDNHYLSTQSKLSKDPNE<br>KRDHMVLLEFVTAAGITLGMDELYK | 36,468.60 | 7.77 | Mito-7-CoilE-mEmerald |

‡*Calculated by ExPasy Protparam, https://web.expasy.org/protparam*

**Table 3.6. Bacterial strains and plasmids**

| | Characteristics | Source |
|---|---|---|
| *E. coli* strains | | |
| TOP10 | F– mcrA Δ(mrr-hsdRMS-mcrBC) Φ80lacZΔM15 ΔlacX74 recA1 araD139 Δ(ara leu) 7697 galU galK rpsL (StrR) endA1 nupG | ThermoFisher Scientific |
| BL21(DE3) | fhuA2 [lon] ompT gal (λ DE3) [dcm] ΔhsdS<br>λ DE3 = λ sBamHIo ΔEcoRI-B int::(lacI::PlacUV5::T7 gene1) i21 Δnin5 | ThermoFisher Scientific |
| Plasmids | | |
| pET28b(+) | T7 promoter, His-tag coding sequence, MCS, *lacI* coding sequence, (KanR) | Novagen |
| pcDNA3.1 | CMV promoter, MCS, BGH polyadenylation signal, SV40 origin, (AmpR), (NeoR) | Invitrogen |
| Mito-7-mEmerald | CMV promoter, COX8A, mEmerald (C terminal on backbone) (KanR, NeoR) | Addgene: 54160 |
| H2B-6-mEmerald | CMV promoter, HIST1H2BJ, mEmerald (C terminal on backbone) (KanR, NeoR) | Addgene: 54111 |
| mEmerald-Actin-C18 | CMV promoter, ACTB, mEmerald (C terminal on backbone) (KanR, NeoR) | Addgene: 53978 |

**Table 3.7. Oligonucleotide sequences**

| **Primer Name** | **Sequence** (restriction sites underlined) |
|---|---|
| CoilR-1 (*Nco*I) | GATATACCATGGGCGGCAGCCTGGAAATTGAAGCGGCGTTT |
| CoilR-2 | TCCAGCGCGGTATTTTCACGTTCCAGAAACGCCGCTTCAATTTCC |
| CoilR-3 | GTGAAAATACCGCGCTGGAAACCCGTGTGGCGGAACTGCGTCAGC |
| CoilR-4 | GCTCACACGATTACGCAGACGCTGCACACGCTGACGCAGTTCCGC |
| CoilR-5 | TCTGCGTAATCGTGTGAGCCAGTATCGTACCCGTTATGGCCCGTT |
| CoilR-6 (*Hind*III) | GCAAGCTTGCCCAGCGCAGCAGCCCCTCCGCCTAACGGGCCATAACGGGT |
| CoilE-1 (*Nco*I) | GATATACCATGGGCGGCAGCCTGGAAATTGAAGCGGCGTTT |
| CoilE-2 | TCCAGCGCGGTATTTTCACGTTCCAGAAACGCCGCTTCAATTTCC |
| CoilE-3 | GTGAAAATACCGCGCTGGAAACCCGTGTGGCGGAACTGCGTCAGC |
| CoilE-4 | GCTCACACGATTACGCAGACGCTGCACACGCTGACGCAGTTCCGC |
| CoilE-5 | TCTGCGTAATCGTGTGAGCCAGTATCGTACCCGTTATGGCCCGTT |
| CoilE-6 (*Hind*III) | GCAAGCTTGCCCAGCGCAGCAGCCCCTCCGCCTAACGGGCCATAACGGGT |
| TfR1-CoilE 1 F | AAAGCAGCATTGGTCAAAACATGGTGACCATAGTGCAGTCAAATGGTAAC |
| TfR1-CoilE 1 R | TACCAAACTCATTGTCAATATTCCAAATGTC |
| TfR1-CoilE 2 F | TATTGACAATGAGTTTGGTAGCGGCAGC |
| TfR1-CoilE 2 R | CATGTTACATTTAACCGGTCTCGAGACAG |
| TfR1-CoilE 3 F | GACCGGTTAAATGTAACATGCATAATTAAATAAGAG |
| TfR1-CoilE 3 R | AAATGGATATACAAGCTCCCGGGAGCTTTTTGCAAAAGCCTAG |
| CoilE *Bgl*I Actin F | GTCCGGACTCAGATCTATGCTGGAAATTGAAGCGGCGT |
| CoilE *Bgl*I Actin R | CACCGCTGCCAGATCTGCCGCCACCCAGCGGGCCATAA |
| CoilE *Age*I H2B F | CTAAGGATCCACCGGTAATGCTGGAAATTGAAGCGGCG |
| CoilE *Age*I H2B R | CATGGTGGCGACCGGTCCGCCGCCACCCAGCGGGCC |
| CoilE *Age*I Mito F | TGGGGGATCCACCGGTAATGCTGGAAATTGAAGCGGCG |
| CoilE *Age*I Mito R | CATGGTGGCGACCGGTCCGCCGCCACCCAGCGGGCC |

**Table 3.8. Properties of Sulfo-Cyanine5 maleimide and BODIPY-FL maleimide[‡]**

| **Fluorophore** | **Vendor** | **Excitation maximum** | **Emission maximum** | **Quantum Yield** | **$\varepsilon_{dve}$ ($L \cdot mol^{-1} \cdot cm^{-1}$)** | **$CF_{280}$** |
|---|---|---|---|---|---|---|
| **Sulfo-Cyanine5 Maleimide** | Lumiprobe | 646 nm | 662 nm | 0.28 | 271,000 | 0.04 |
| **BODIPY-FL Maleimide** | Lumiprobe | 503 nm | 509 nm | 0.97 | 80,000 | 0.027 |

[‡]*Values provided on the Lumiprobe website: www.lumiprobe.com.*

**Table 3.9. Summary of primary and secondary antibodies used for immunolabeling.**

| Primary Antibody (1:100 dilution) | Protein Target | Commercial Source (Catalog #) | Lot # | Secondary Antibody (1:200 dilution) | Commercial Source (Catalog.#) | Lot # |
|---|---|---|---|---|---|---|
| **8D3** | TfR1 (extracellular) | Novus Biologicals (#NB100-64979) | 1607 | F(ab')2-Goat anti-Rat IgG (H+L) Secondary Antibody, Qdot 655 | Thermofisher Scientific (#Q-11621MP) | 1863945 |
| **H68.4** | TfR1 (cytoplasmic) | ThermoFisher Scientific (#13-6800) | RB232679 | F(ab')2-Goat anti-Mouse IgG (H+L) Secondary Antibody, Qdot 655 | Thermofisher Scientific ( #Q-11021MP) | 1863429 |
| **Ab82411** | Tf | Abcam (#ab82411) | GR3207592-3 | F(ab')2-Goat anti-Rabbit IgG (H+L) Secondary Antibody, Qdot 655 | Thermofisher Scientific (#Q-11421MP) | 1996360 |
| **Ab1086** | TfR1 (extracellular) | Abcam (#ab1086) | GR3211582-6 | F(ab')2-Goat anti-Mouse IgG (H+L) Secondary Antibody, Qdot 655 | Thermofisher Scientific (#Q-11021MP) | 1863429 |
| **Ab216665** | TfR1 (extracellular) | Abcam (#ab216665) | GR3192662-5 | F(ab')2-Goat anti-Rabbit IgG (H+L) Secondary Antibody, Qdot 655 | Thermofisher Scientific (#Q-11421MP) | 1996360 |

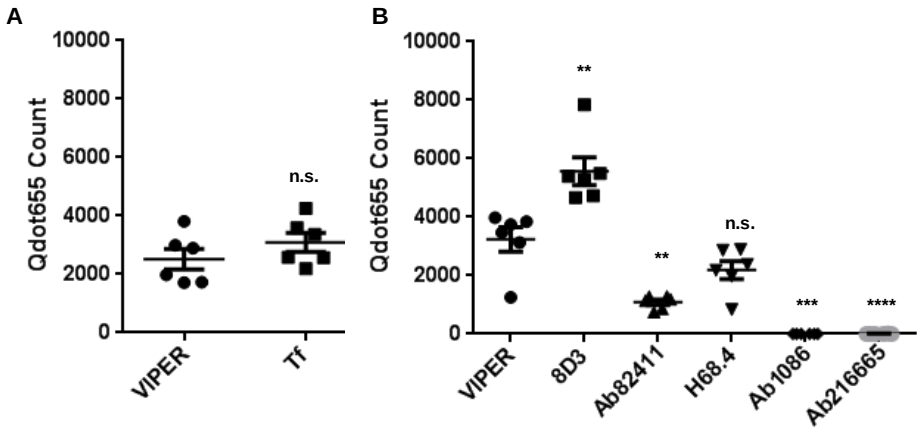


**Figure 3.14. Scatter plot of total Qdot particles counted per field-of-view (4.15 µm x 2.75 µm) for SEM micrographs of cells. A.** Total Qdot particles counted for cells treated with CoilR-biotin versus cells treated with Tf-biotin. Both biotinylated ligands were detected by streptavidin-Qdot655. Data were analyzed using a Welch's t-test and were not statistically significant (n.s.; $p > 0.05$). **B.** Total Qdot particles counted for cells treated with VIPER or immunolabeled. Data were analyzed using a Welch's t-test comparing counts for VIPER versus counts for each antibody. In **B**, n.s. = not significant ($p > 0.05$); ** = $p < 0.01$; *** = $p < 0.001$; and **** = $p < 0.0001$). Raw images with counting masks are provided in **Figures 3.15-3.17**. Raw data counts are provided in **Tables 3.2-3.4**.

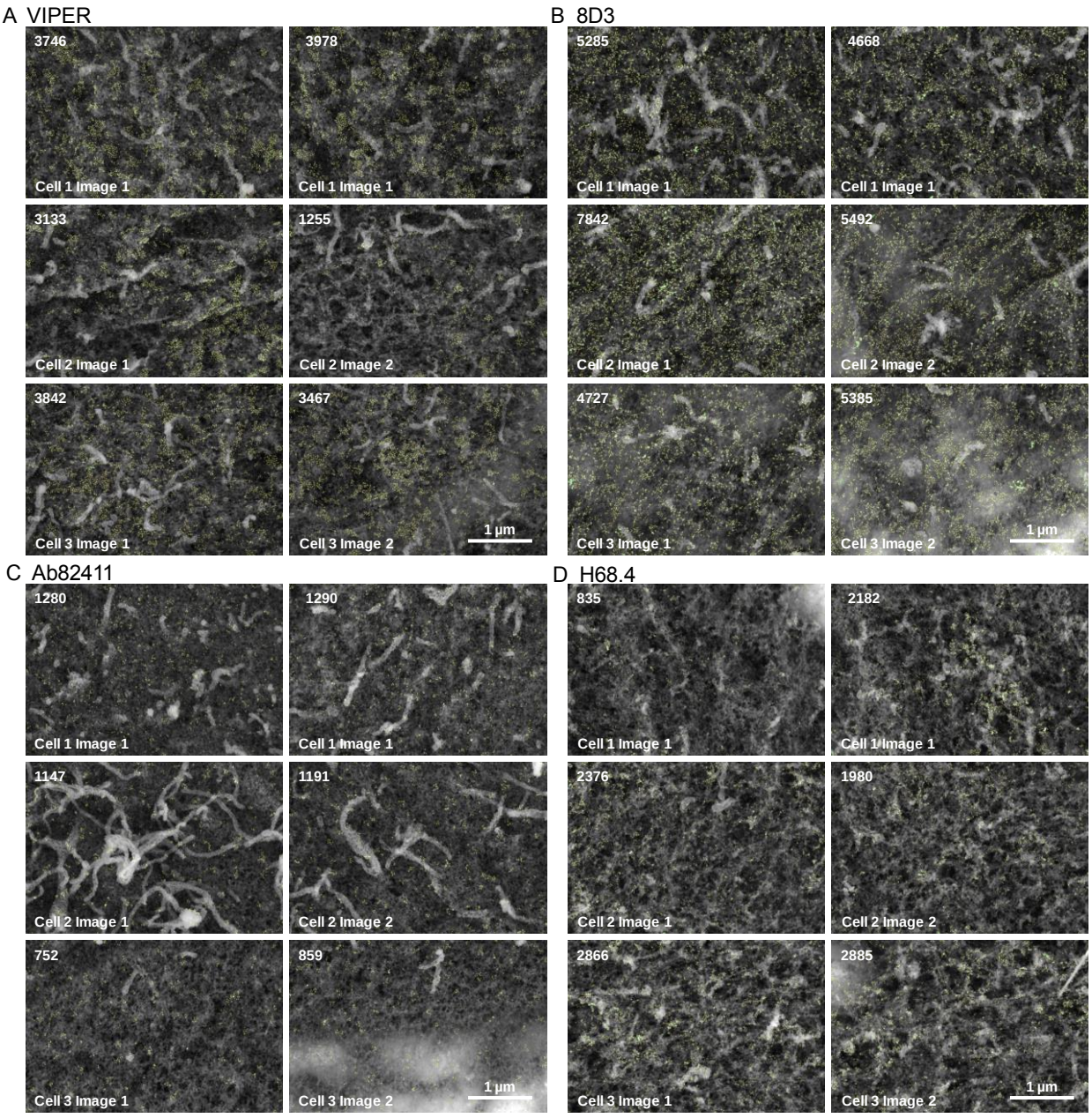


**Figure 3.15. SEM micrographs of CHO TRVb cells expressing TfR1-CoilE labeled with VIPER (A), 8D3 (B), Ab82411 (C), or H68.4 (D). A.** Fixed cells were treated with CoilR-biotin and streptavidin-Qdot655. **B-D.** Fixed cells were treated with the indicated primary antibody and a secondary antibody conjugated to Qdot655. In the micrographs, the counting mask overlay appears as a red outline, with clusters additionally outlined in green. Images shown are the full field of view from a 100,000X magnification capture (4.15 x 2.75 µm). Micrograph names correspond to names provided in **Table 3.3** (e.g., Cell X Image Y) and the total Qdot count for each image is reported in the upper left corner of each micrograph.

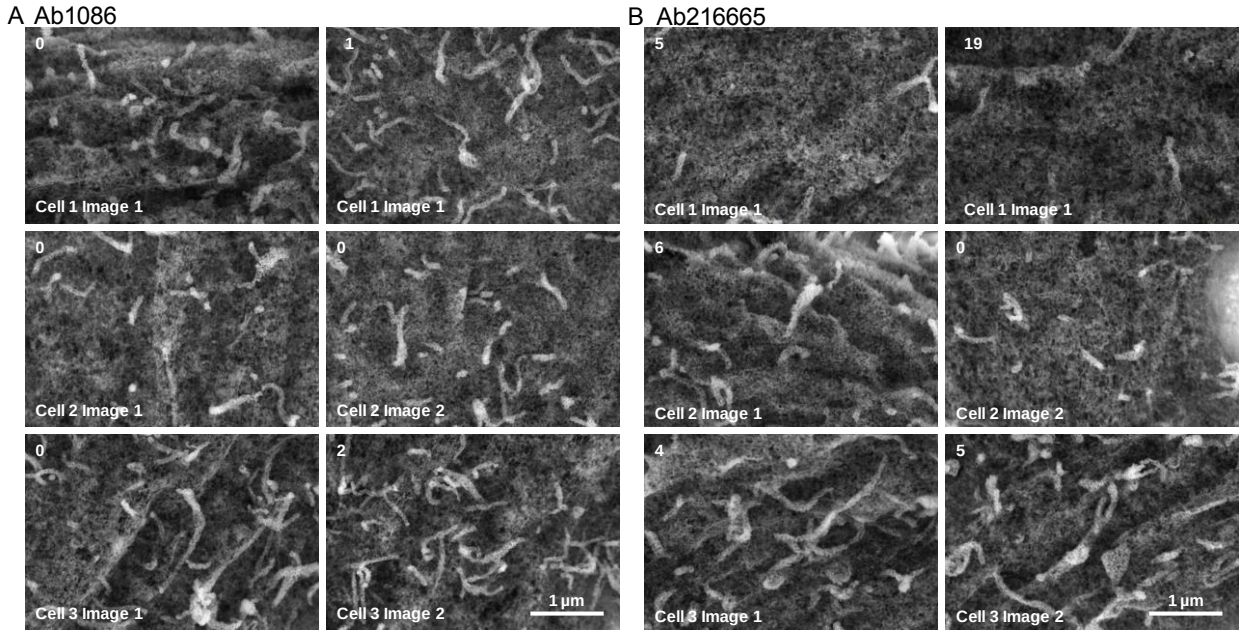


**Figure 3.16. SEM micrographs of CHO TRVb cells expressing TfR1-CoilE labeled with Ab1086 (A) or Ab216665 (B).** Fixed cells were treated with an anti-TfR1 antibody, either Ab1086 (A) or Ab216665 (B), and a secondary antibody conjugated to Qdot655. Neither of these primary antibodies labeled TfR1. In the micrographs, the counting mask overlay appears as a red outline, with clusters additionally outlined in green. Images shown are the full field of view from a 100,000X magnification capture (4.15 x 2.75 µm). Micrograph names correspond to names provided in **Table 3.4** (e.g., Cell X Image Y) and the total Qdot count for each image is reported in the upper left corner of each micrograph.

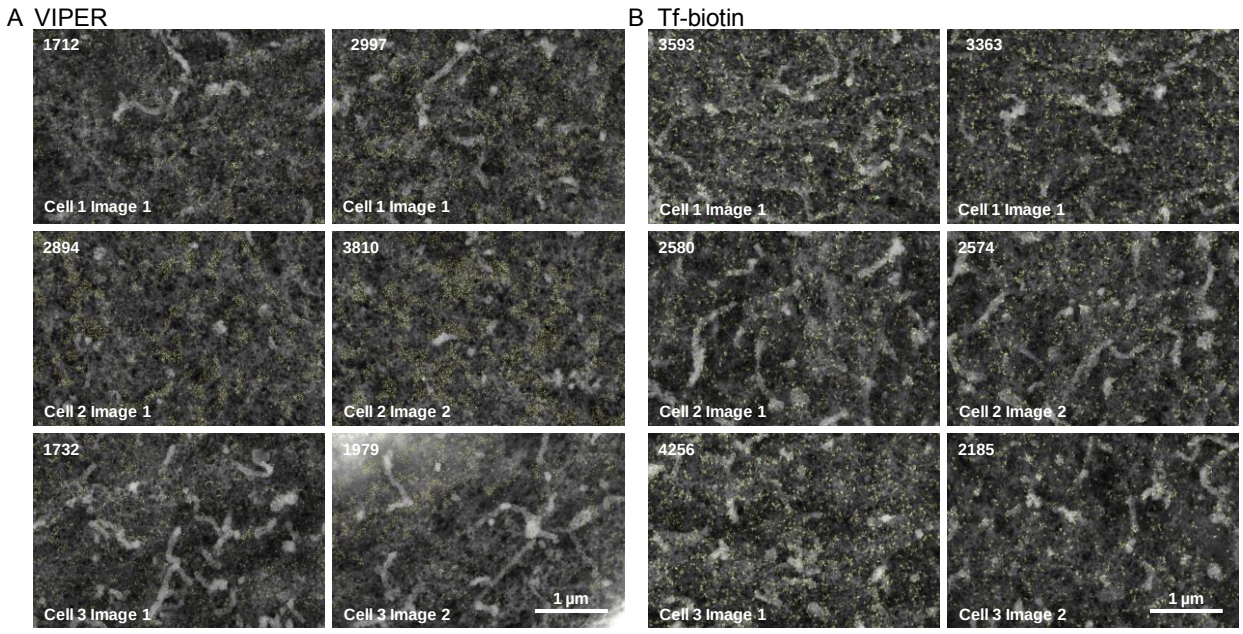


**Figure 3.17. SEM micrographs of CHO TRVb cells expressing TfR1-CoilE labeled with VIPER (A) or Tf-biotin (B).** Live cells were treated with CoilR-biotin (**A**) or Tf-biotin (**B**), fixed, and then treated with streptavidin-Qdot655. In the micrographs, the counting mask overlay appears as a red outline, with clusters additionally outlined in green. Images shown are the full field of view from a 100,000X magnification capture (4.15 x 2.75 µm). Micrograph names correspond to names provided **Table 3.2** (e.g., Cell X Image Y) and the total Qdot count for each image is reported in the upper left corner.

## Works Cited


1. Liu, Z., Lavis, L. D. & Betzig, E. Imaging live-cell dynamics and structure at the single-molecule level. *Mol. Cell* **58**, 644–659 (2015).
2. Huang, L., Pike, D., Sleat, D. E., Nanda, V. & Lobel, P. Potential Pitfalls and Solutions for Use of Fluorescent Fusion Proteins to Study the Lysosome. *PLOS ONE* **9**, e88893 (2014).
3. von Diezmann, A., Shechtman, Y. & Moerner, W. E. Three-Dimensional Localization of Single Molecules for Super-Resolution Imaging and Single-Particle Tracking. *Chem. Rev.* **117**, 7244–7275 (2017).
4. Thompson, A. D., Bewersdorf, J., Toomre, D. & Schepartz, A. HIDE Probes: A New Toolkit for Visualizing Organelle Dynamics, Longer and at Super-Resolution. *Biochemistry* **56**, 5194–5201 (2017).
5. Valm, A. M. *et al.* Applying systems-level spectral imaging and analysis to reveal the organelle interactome. *Nature* **546**, 162–167 (2017).
6. Nixon-Abell, J. *et al.* Increased spatiotemporal resolution reveals highly dynamic dense tubular matrices in the peripheral ER. *Science* **354**, aaf3928 (2016).
7. Hildebrand, D. G. C. *et al.* Whole-brain serial-section electron microscopy in larval zebrafish. *Nature* **545**, 345–349 (2017).
8. Ou, H. D. *et al.* ChromEMT: Visualizing 3D chromatin structure and compaction in interphase and mitotic cells. *Science* **357**, (2017).
9. Sochacki, K. A., Dickey, A. M., Strub, M.-P. & Taraska, J. W. Endocytic proteins are partitioned at the edge of the clathrin lattice in mammalian cells. *Nat. Cell Biol.* **19**, 352–361 (2017).
10. Schnell, U., Dijk, F., Sjollema, K. A. & Giepmans, B. N. G. Immunolabeling artifacts and the need for live-cell imaging. *Nat. Methods* **9**, 152–158 (2012).
11. Griffiths, G. & Lucocq, J. M. Antibodies for immunolabeling by light and electron microscopy: not for the faint hearted. *Histochem. Cell Biol.* **142**, 347–360 (2014).
12. Griffiths, G. & Hoppeler, H. Quantitation in immunocytochemistry: correlation of immunogold labeling to absolute number of membrane antigens. *J. Histochem. Cytochem. Off. J. Histochem. Soc.* **34**, 1389–1398 (1986).
13. Berglund, L. *et al.* A genecentric Human Protein Atlas for expression profiles based on antibodies. *Mol. Cell. Proteomics MCP* **7**, 2019–2027 (2008).
14. Bradbury, A. & Plückthun, A. Reproducibility: Standardize antibodies used in research. *Nat. News* **518**, 27 (2015).
15. Sengupta, P., van Engelenburg, S. B. & Lippincott-Schwartz, J. Superresolution Imaging of Biological Systems Using Photoactivated Localization Microscopy. *Chem. Rev.* **114**, 3189–3202 (2014).
16. Brock, R., Hamelers, I. H. & Jovin, T. M. Comparison of fixation protocols for adherent cultured cells applied to a GFP fusion protein of the epidermal growth factor receptor. *Cytometry* **35**, 353–362 (1999).
17. Costantini, L. M. & Snapp, E. L. Fluorescent proteins in cellular organelles: serious pitfalls and some solutions. *DNA Cell Biol.* **32**, 622–627 (2013).
18. Day, R. N. & Davidson, M. W. The fluorescent protein palette: tools for cellular imaging. *Chem. Soc. Rev.* **38**, 2887–2921 (2009).
19. Gautier, A. *et al.* An engineered protein tag for multiprotein labeling in living cells. *Chem. Biol.* **15**, 128–136 (2008).

20. Keppler, A. *et al.* A general method for the covalent labeling of fusion proteins with small molecules in vivo. *Nat. Biotechnol.* **21**, 86–89 (2003).
21. Los, G. V. *et al.* HaloTag: A Novel Protein Labeling Technology for Cell Imaging and Protein Analysis. *ACS Chem. Biol.* **3**, 373–382 (2008).
22. Miller, L. W., Cai, Y., Sheetz, M. P. & Cornish, V. W. In vivo protein labeling with trimethoprim conjugates: a flexible chemical tag. *Nat. Methods* **2**, 255–257 (2005).
23. Szent-Gyorgyi, C. *et al.* Fluorogen-activating single-chain antibodies for imaging cell surface proteins. *Nat. Biotechnol.* **26**, 235–240 (2008).
24. Wang, J., Yu, Y. & Xia, J. Short Peptide Tag for Covalent Protein Labeling Based on Coiled Coils. *Bioconjug. Chem.* **25**, 178–187 (2014).
25. Morphew, M. k. *et al.* Metallothionein as a clonable tag for protein localization by electron microscopy of cells. *J. Microsc.* **260**, 20–29 (2015).
26. Diestra, E., Fontana, J., Guichard, P., Marco, S. & Risco, C. Visualization of proteins in intact cells with a clonable tag for electron microscopy. *J. Struct. Biol.* **165**, 157–168 (2009).
27. Mercogliano, C. P. & DeRosier, D. J. Concatenated metallothionein as a clonable gold label for electron microscopy. *J. Struct. Biol.* **160**, 70–82 (2007).
28. Risco, C. *et al.* Specific, sensitive, high-resolution detection of protein molecules in eukaryotic cells using metal-tagging transmission electron microscopy. *Struct. Lond. Engl. 1993* **20**, 759–766 (2012).
29. Clarke, N. I. & Royle, S. J. FerriTag is a new genetically-encoded inducible tag for correlative light-electron microscopy. *Nat. Commun.* **9**, 2604 (2018).
30. Lam, S. S. *et al.* Directed evolution of APEX2 for electron microscopy and proximity labeling. *Nat. Methods* **12**, 51–54 (2015).
31. Martell, J. D. *et al.* Engineered ascorbate peroxidase as a genetically encoded reporter for electron microscopy. *Nat. Biotechnol.* **30**, 1143–1148 (2012).
32. Shu, X. *et al.* A Genetically Encoded Tag for Correlated Light and Electron Microscopy of Intact Cells, Tissues, and Organisms. *PLoS Biol.* **9**, e1001041 (2011).
33. Sosinsky, G. E., Giepmans, B. N. G., Deerinck, T. J., Gaietta, G. M. & Ellisman, M. H. Markers for correlated light and electron microscopy. *Methods Cell Biol.* **79**, 575–591 (2007).
34. Gaietta, G. *et al.* Multicolor and electron microscopic imaging of connexin trafficking. *Science* **296**, 503–507 (2002).
35. Kuipers, J. *et al.* FLIPPER, a combinatorial probe for correlated live imaging and electron microscopy, allows identification and quantitative analysis of various cells and organelles. *Cell Tissue Res.* **360**, 61–70 (2015).
36. Liss, V., Barlag, B., Nietschke, M. & Hensel, M. Self-labelling enzymes as universal tags for fluorescence microscopy, super-resolution microscopy and electron microscopy. *Sci. Rep.* **5**, 17740 (2015).
37. Zane, H. K., Doh, J. K., Enns, C. A. & Beatty, K. E. Versatile interacting peptide (VIP) tags for labeling proteins with bright chemical reporters. *ChemBioChem* (2017) doi:10.1002/cbic.201600627.
38. Rodriguez, E. A. *et al.* A far-red fluorescent protein evolved from a cyanobacterial phycobiliprotein. *Nat. Methods* **13**, 763–769 (2016).
39. Shcherbakova, D. M. & Verkhusha, V. V. Near-infrared fluorescent proteins for multicolor in vivo imaging. *Nat. Methods* **10**, 751–754 (2013).

40. Robson Marsden, H. & Kros, A. Self-Assembly of Coiled Coils in Synthetic Biology: Inspiration and Progress. *Angew. Chem. Int. Ed.* **49**, 2988–3005 (2010).
41. Apostolovic, B., Danial, M. & Klok, H.-A. Coiled coils: attractive protein folding motifs for the fabrication of self-assembled, responsive and bioactive materials. *Chem. Soc. Rev.* **39**, 3541–3575 (2010).
42. Moll, J. R., Ruvinov, S. B., Pastan, I. & Vinson, C. Designed heterodimerizing leucine zippers with a ranger of pIs and stabilities up to 10−15 M. *Protein Sci. Publ. Protein Soc.* **10**, 649–655 (2001).
43. Woolfson, D. N. The design of coiled-coil structures and assemblies. *Adv. Protein Chem.* **70**, 79–112 (2005).
44. Reinke, A. W., Grant, R. A. & Keating, A. E. A Synthetic Coiled-Coil Interactome Provides Heterospecific Modules for Molecular Engineering. *J. Am. Chem. Soc.* **132**, 6025–6031 (2010).
45. Bromley, E. H. C., Sessions, R. B., Thomson, A. R. & Woolfson, D. N. Designed α-Helical Tectons for Constructing Multicomponent Synthetic Biological Systems. *J. Am. Chem. Soc.* **131**, 928–930 (2009).
46. Thomas, F., Boyle, A. L., Burton, A. J. & Woolfson, D. N. A Set of de Novo Designed Parallel Heterodimeric Coiled Coils with Quantified Dissociation Constants in the Micromolar to Sub-nanomolar Regime. *J. Am. Chem. Soc.* **135**, 5161–5166 (2013).
47. Yano, Y. *et al.* Coiled-Coil Tag−Probe System for Quick Labeling of Membrane Receptors in Living Cells. *ACS Chem. Biol.* **3**, 341–345 (2008).
48. O'Shea, E. K., Lumb, K. J. & Kim, P. S. Peptide 'Velcro': design of a heterodimeric coiled coil. *Curr. Biol. CB* **3**, 658–667 (1993).
49. Aronsson, C. *et al.* Self-sorting heterodimeric coiled coil peptides with defined and tuneable self-assembly properties. *Sci. Rep.* **5**, (2015).
50. Thompson, K. E., Bashor, C. J., Lim, W. A. & Keating, A. E. SYNZIP Protein Interaction Toolbox: *in Vitro* and *in Vivo* Specifications of Heterospecific Coiled-Coil Interaction Domains. *ACS Synth. Biol.* **1**, 118–129 (2012).
51. Hermanson, G. T. *Bioconjugate techniques*. (Academic Press, 1996).
52. Mayle, K. M., Le, A. M. & Kamei, D. T. The Intracellular Trafficking Pathway of Transferrin. *Biochim. Biophys. Acta* **1820**, 264–281 (2012).
53. Zhao, N. & Enns, C. A. Iron Transport Machinery of Human Cells: Players and Their Interactions. *Curr. Top. Membr.* **69**, 67–93 (2012).
54. Enns, C. A., Larrick, J. W., Suomalainen, H., Schroder, J. & Sussman, H. H. Co-migration and internalization of transferrin and its receptor on K562 cells. *J. Cell Biol.* **97**, 579–585 (1983).
55. Ciechanover, A., Schwartz, A. L., Dautry-Varsat, A. & Lodish, H. F. Kinetics of internalization and recycling of transferrin and the transferrin receptor in a human hepatoma cell line. Effect of lysosomotropic agents. *J. Biol. Chem.* **258**, 9681–9689 (1983).
56. McGraw, T. E., Greenfield, L. & Maxfield, F. R. Functional expression of the human transferrin receptor cDNA in Chinese hamster ovary cells deficient in endogenous transferrin receptor. *J. Cell Biol.* **105**, 207–214 (1987).
57. Beatty, K. E. & Tirrell, D. A. Two-Color Labeling of Temporally Defined Protein Populations in Mammalian Cells. *Bioorg. Med. Chem. Lett.* **18**, 5995–5999 (2008).

58. Lotze, J. *et al.* Time-Resolved Tracking of Separately Internalized Neuropeptide Y2 Receptors by Two-Color Pulse-Chase. *ACS Chem. Biol.* (2017) doi:10.1021/acschembio.7b00999.
59. López, C. S. *et al.* A fully integrated, three-dimensional fluorescence to electron microscopy correlative workflow. *Methods Cell Biol.* **140**, 149–164 (2017).
60. Giepmans, B. N. G., Deerinck, T. J., Smarr, B. L., Jones, Y. Z. & Ellisman, M. H. Correlated light and electron microscopic imaging of multiple endogenous proteins using Quantum dots. *Nat. Methods* **2**, 743–749 (2005).
61. Kissel, K. *et al.* Immunohistochemical localization of the murine transferrin receptor (TfR) on blood-tissue barriers using a novel anti-TfR monoclonal antibody. *Histochem. Cell Biol.* **110**, 63–72 (1998).
62. Ta, H. *et al.* Mapping molecules in scanning far-field fluorescence nanoscopy. *Nat. Commun.* **6**, 7977 (2015).
63. Thul, P. J. *et al.* A subcellular map of the human proteome. *Science* eaal3321 (2017) doi:10.1126/science.aal3321.
64. Takizawa, T., Powell, R. D., Hainfeld, J. F. & Robinson, J. M. FluoroNanogold: an important probe for correlative microscopy. *J. Chem. Biol.* **8**, 129–142 (2015).
65. Hoover, D. M. & Lubkowski, J. DNAWorks: an automated method for designing oligonucleotides for PCR-based gene synthesis. *Nucleic Acids Res.* **30**, e43 (2002).
66. Jianzhuang L et al. (1991) in Circuits and Systems. Conference Proceedings, China., 1991 International Conference on 325-327.
67. Waltz FM, Miller JW (1998) in Machine Vision Systems for Inspection and Metrology VII, Vol. 3521 334-342 (International Society for Optics and Photonics).
68. Parvati K et al. (2008) Image segmentation using gray-scale morphology and marker-controlled watershed transformation. *Discrete Dyn Nature Soc.* 2008.
69. Roerdink JB, Meijster A (2000) The watershed transform: Definitions, algorithms and parallelization strategies. *Fund inform.* 41, 187-228.

# Chapter 4: MiniVIPER is a peptide tag for imaging and translocating proteins in cells

**Julia K. Doh***, Savannah J. Tobin*, Kimberly E. Beatty

**authors contributed equally to the work*

*This work is adapted from a manuscript submitted for publication in April 2020. It has been adapted for this dissertation. My co-author, Savannah Tobin, and I collaborated closely to complete and execute the project. This included generating genetic constructs, probes, collecting and analyzing the data and authoring the manuscript.*

## Abstract

Microscopy allows researchers to interrogate reporter-labeled proteins within a cellular context. To deliver protein-specific contrast, we developed a new class of genetically-encoded peptide tags called Versatile Interacting Peptide (VIP) tags. VIP tags deliver a reporter to a target protein via the formation of a heterodimer between the peptide tag and an exogenously added probe peptide. Two such VIP tags are VIP Y/Z and VIPER. We report herein a new VIP tag named MiniVIPER, which is comprised of a MiniE and MiniR heterodimer. We first demonstrated the selectivity of MiniVIPER by labeling three cellular targets: transferrin receptor 1 (TfR1), histone protein H2B, and the mitochondrial protein TOMM20. We showed that either MiniE or MiniR could serve as the genetically-encoded tag. Next, we demonstrated MiniVIPER's versatility by generating five spectrally-distinct probe peptides to label tagged TfR1. Lastly, we demonstrated two new applications for VIP tags. First, we used MiniVIPER in combination with VIPER to selectively label two different proteins in a single cell (e.g., TfR1 with H2B or TOMM20). Second, we used MiniVIPER to translocate a fluorescent protein to the nucleus through in situ dimerization of mCherry with H2B-mEmerald. In summary, MiniVIPER is a new addition to the growing repertoire of VIP tags that now enable multi-target imaging and artificial dimerization.

## Introduction

Fluorescence microscopy (FM) is a valuable resource for studying protein functions and interactions within a native cellular environment. Multicolor FM observations of proteins or sub-cellular structures are enabled by small molecule stains, immunolabeling, and genetically-encoded tags[1–3]. In particular, genetically-encoded tags are useful for making observations in fixed or living cells. In this category, fluorescent protein tags (e.g., green fluorescent protein, GFP) are ubiquitous in FM imaging. However, fluorescent proteins have disadvantages, including their large (~30 kDa) size. Some variants oligomerize at high concentrations, which can alter the function of the protein under study[4]. Additionally, the fluorescent protein chromophore has limitations on its spectral properties, including the brightness, photostability, and Stokes shift. This last issue was addressed by newer protein tags, such as the SNAP-Tag[5] and HaloTag[6], which form a covalent bond with a fluorescent ligand that can be synthesized with optimal fluorescent properties[7]. However, these tags are still large: the SNAP-Tag is 22 kDa[5] and the HaloTag is 33 kDa[6].

An ideal genetically-encoded tag would be designed to minimize size while retaining labeling specificity. The smallest peptide tag is the tetracysteine tag, comprised of a six amino acid motif (Cys-Cys-Pro-Gly-Cys-Cys) that binds a fluorogenic bi-arsenical reporter[8,9]. However, this tag can cross-react with endogenous cysteine-rich proteins and the reporter is toxic. A few other approaches modify peptide sequences post-translationally via an enzyme, such as biotin ligase[10] or lipoic acid ligase[11].

A separate class of genetically-encoded peptide tag labels target proteins using heterodimeric coiled-coils[12]. For these tags, the protein of interest is fused to a short (3 to 6 kDa)[12] peptide that forms a tight heterodimer with a fluorophore-conjugated peptide[12]. This approach was first used in 2009 by Yano and coworkers to image membrane receptors[13]. Coiled-coil peptides have since been used to deliver fluorogenic probes[14–16], mediate proximity-induced reactions[16–20], localize proteins[21], or regulate transcription[21].

Our contribution to this area was the development of Versatile Interacting Peptide (VIP) tags. VIP tags enable specific protein labeling in live and fixed cells. VIP Y/Z,

consisting of a CoilY and CoilZ dimer, was the first VIP tag published for selectively labeling protein targets in cell lysates and on living cells[22]. We then developed a tag named VIPER, comprised of a heterodimer between a CoilE tag (5.2 kDa) and a CoilR probe peptide. We demonstrated that VIPER is a useful tag for correlative light and electron microscopy and for quantifying cell receptors in micrographs[23].

In the current work, we designed a modified version of VIPER that retains protein labeling specificity in a smaller overall size. We named this tag MiniVIPER, and it is comprised of a heterodimeric coiled-coil between two peptides: MiniE and MiniR. Both peptides are small (4.3 kDa) and either one can serve as the genetic tag. We showed that MiniVIPER enables the selective protein labeling of cellular targets. We illustrated the versatility of MiniVIPER by imaging a cell receptor using five spectrally-distinct fluorophores spanning green to far-red emission. We then demonstrated that this tag enables two useful applications. First, we expressed two VIP-tagged proteins within a single cell and demonstrated the selective labeling of both protein targets. Second, we used MiniVIPER to translocate a protein to the nucleus.

## Design of MiniVIPER

VIP tags are comprised of alpha helical coiled-coils, with each coil consisting of heptad repeats denoted *abcdefg*. The *a* and *d* residues form a hydrophobic core between the two coils, while charged residues at the *e* and *g* positions form salt bridges. We designed MiniVIPER by removing the last (fifth) heptad of the previously published VIPER tag[23]. Additionally, we made a few other modifications (**Figure 4.1**). First, we improved the charge balance by making a *g*-position mutation in MiniE (Arg32Glu) and MiniR (Glu32Arg). All other charged residues were retained at the *e* and *g* positions to discourage the formation of homodimers. An alanine in the fifth position on MiniR was changed to a valine (Ala5Val) to strengthen binding[24]. Overall, MiniVIPER has eight salt-bridges, an Asn-Asn match in the second heptad, and a hydrophobic interface, all features that promote parallel heterodimer formation[25–27].

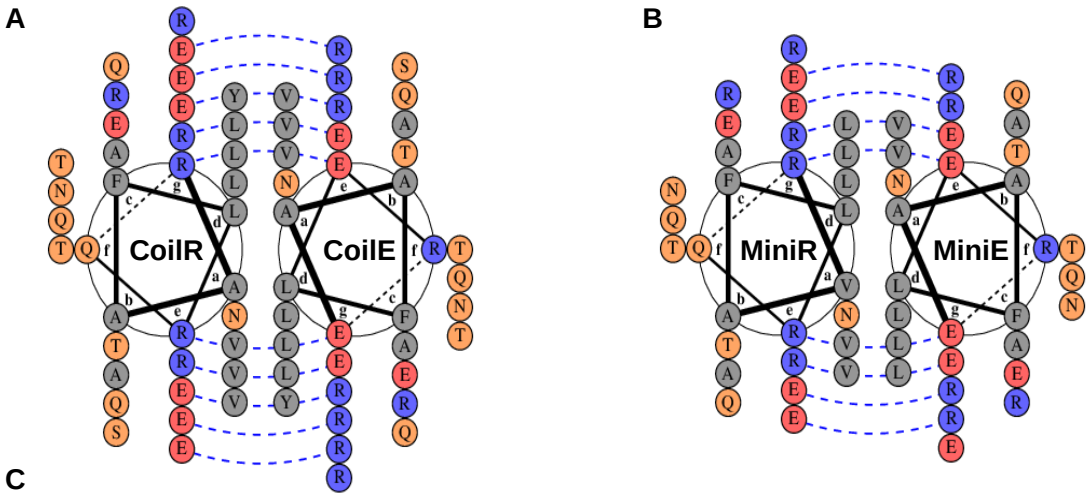


C

| Name | **Peptide Sequence** (1-letter amino acid code)<br>*defg abcdefg abcdefg abcdefg abcdefg abcdefg* | MW (kDa) |
|---|---|---|
| CoilE tag | --**LEIE AAFLERE NTALETR VAELRQR VQRLRNR VSQYRTR** YGPL-- | 5.20 |
| CoilR probe | MGGS **LEIR AAFLRQR NTALRTE VAELEQE VQRLENE VSQYETR** YGPL GGGAAALGCLAAA LEHHHHHH | 7.50 |
| MiniE tag | --**LEIE AAFLERE NTALETR VAELRQR VQRLRNE** YGPL-- | 4.28 |
| MiniE probe | MGSS **LEIE AAFLERE NTALETR VAELRQR VQRLRNE** YGPL GGGAAA WGLCYPWVYG LEHHHHHH | 7.32 |
| MiniR tag | --**LEIR VAFLRQR NTALRTE VAELEQE VQRLENR** YGPL-- | 4.31 |
| MiniR probe | MGSS **LEIR VAFLRQR NTALRTE VAELEQE VQRLENR** YGPL GGGAAA WGLCYPWVYG LEHHHHHH | 7.35 |

**Figure 4.1. Sequence comparison of VIPER and MiniVIPER.** Helical wheel diagrams of (**A**) VIPER and (**B**) MiniVIPER were generated using DrawCoil 1.0 (https://grigoryanlab.org/drawcoil/). Charged residues are colored red or blue, with salt bridges indicated by a dashed line. Polar residues are orange and hydrophobic residues are gray. (**C**) Sequences of VIP tags and probes, with coil-forming amino acids in bold.

## Production of the MiniE and MiniR probe peptides

Probe peptides have a C-terminal histidine tag, $(His)_6$, for purification by immobilized metal affinity chromatography (IMAC)[28]. The probe peptides additionally include a flexible linker, $(Gly)_3$-$(Ala)_3$[29], followed by the sequence Trp-Gly-Leu-Cys-Tyr-Pro-Trp-Val-Tyr-Gly, which enhanced the properties of the probe peptides in three ways. First, the addition of aromatic residues increased the extinction coefficient by over 10-fold, improving the accuracy of quantification by absorbance measurements. Second, inclusion of a dibenzocyclooctyne (DBCO) tag (Leu-Cys-Tyr-Pro-Trp-Val-Tyr) enabled site-specific thiol-maleimide or thiol-yne[30] conjugation reactions at the Cys residue. Third, we found that adding this sequence increased the yield of recombinant peptide expressed in BL21-DE3 cells.

We used standard methods to express and purify the probe peptides: MiniE probe and MiniR probe (**Figure 4.1C**), as described in the Supporting Information. We modified MiniE with a TAMRA-cyclooctyne via thiol-yne conjugation and obtained MiniE-TAMRA (16% labeled). The remaining probe peptides were made via thiol-maleimide chemistry[31]: MiniE-Cy5 (59%), MiniE-biotin (100%), MiniE-Cy3 (52%), MiniE-OregonGreen (OG) 488 (64%), MiniR-Cy5 (29%) and MiniR-biotin (100%). CoilR and CoilY peptides were made as previously described: CoilR-Cy5 (90%)[23], CoilR-AF488 (45%)[28], CoilY-Cy5 (50%)[22], and CoilY-biotin[22].

## Observation of MiniVIPER-labeled proteins in cells

In initial experiments, we confirmed that MiniVIPER enabled selective protein labeling in cells (**Figure 4.2**). First, we imaged transferrin receptor 1 (TfR1) by FM. We selected TfR1 because it has well-characterized membrane localization, transferrin binding, and rapid internalization via clathrin-mediated endocytosis[32,33]. We transfected Chinese hamster ovary (CHO) TRVb ($\Delta$TfR1 $\Delta$TfR2) cells[34] to express untagged (TfR1) or tagged (TfR1-MiniR or TfR1-MiniE) receptors. Live cells were cooled to halt endocytosis and then treated with probe peptide and fluorescent transferrin-AF488 (Tf-AF488) to counter-stain the receptor. Cells were fixed before imaging by confocal FM **(Figure 4.2B)**. Micrographs showed selective labeling of TfR1-MiniR with MiniE-Cy5. We observed Cy5 signal at the cell surface that co-localized with Tf-AF488 signal. The absence of MiniE-Cy5 labeling in cells expressing untagged TfR1 confirmed the specificity of labeling. We found that either MiniR or MiniE could serve as the genetically-encoded tag. TfR1-MiniE was labeled with MiniR-Cy5 and receptor-ligand co-localization was observed by confocal FM. Comparable Tf-AF488 labeling between untagged and tagged TfR1 suggested that the introduction of the tags did not change ligand binding.

Next, we imaged two sub-cellular structures: the nucleus and mitochondria (**Figure 4.2C-4.2D**). We imaged tagged and untagged histone 2B-mEmerald (H2B-mEmerald) and translocase of outer mitochondrial membrane 20-mCherry (TOMM20-mCherry) in transfected human osteosarcoma (U-2 OS) cells. Cells were fixed and permeabilized before treatment with Cy5-conjugated probe peptides. MiniVIPER

labeling was specific and Cy5 fluorescence was observed only in cells expressing tagged targets. For VIP-tagged proteins, we observed co-localization of Cy5 signal with the fluorescent protein (e.g., mCherry with Cy5 in the mitochondria or mEmerald with Cy5 in the nucleus). Protein localization and organelle morphology appeared unaltered between MiniVIPER-tagged and untagged proteins.

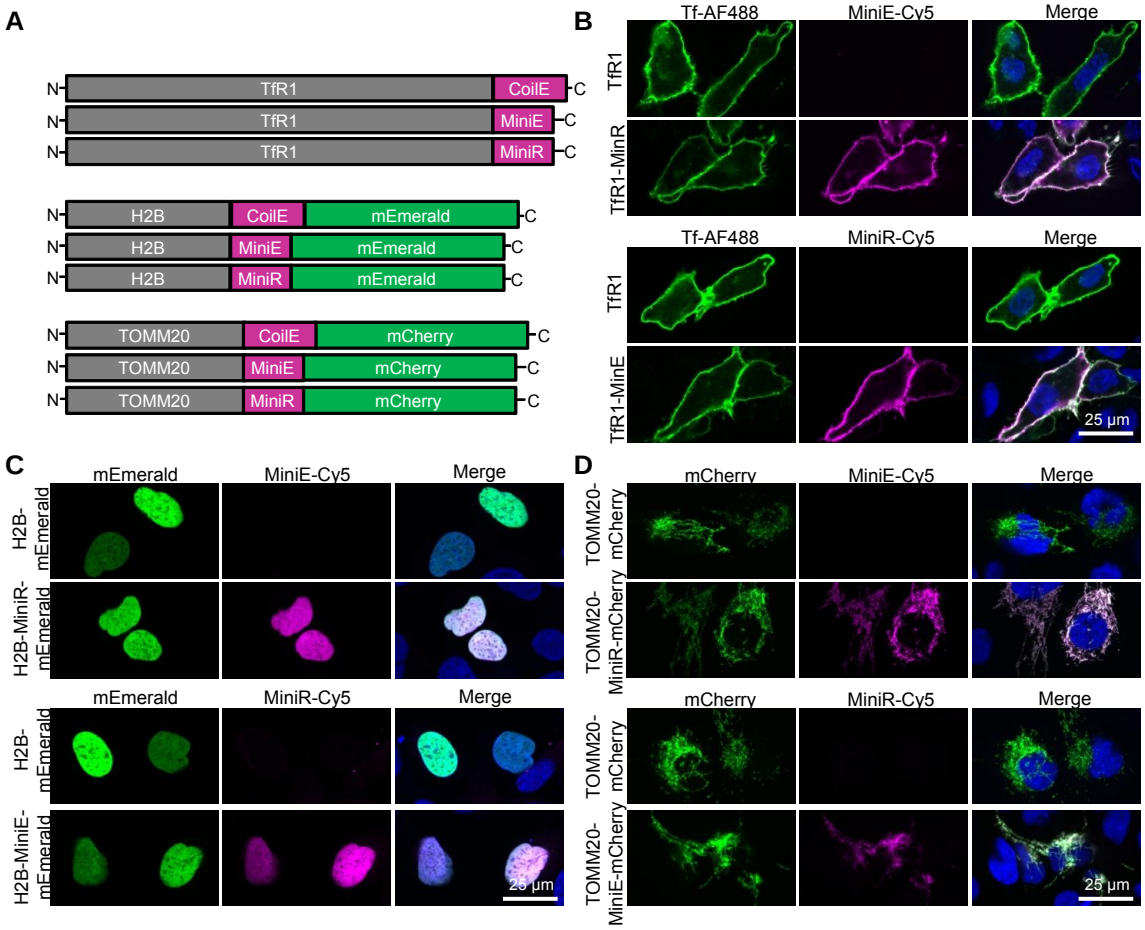


**Figure 4.2. MiniVIPER enabled selective fluorophore labeling of cellular proteins.** (**A**) Representation of the tagged constructs used to label: a cell receptor (TfR1), the nucleus (H2B), and the mitochondria (TOMM20). (**B**) CHO TRVb cells expressing TfR1, TfR1-MiniR, or TfR1-MiniE were treated live on ice with Tf-AF488 and either MiniE-Cy5 (above) or MiniR-Cy5 (below). Cells were fixed before imaging. U-2 OS cells expressing (**C**) H2B-mEmerald, H2B-MiniR-mEmerald, or H2B-MiniE-mEmerald or (**D**) TOMM20-mCherry, TOMM20-MiniR-mCherry, or TOMM20-MiniE-mCherry were treated post-fixation with MiniE-Cy5 (above) or MiniR-Cy5 (below). AF488, mEmerald, and mCherry signal is false colored green. Cy5 signal is false colored magenta. Nuclear stain (blue) is provided in the channel merge and magenta-green overlap appears white. Protein sequences are provided in **Table 4.1**.

## Assessment of VIPER and MiniVIPER cross-reactivity

VIPER and MiniVIPER share four out of five heptad sequences (see **Figure 4.1**), and we anticipated that we might detect cross-reactivity between them. We collected fluorescent micrographs to evaluate pair-wise combinations of the tags (CoilE, MiniE, and MiniR) with Cy5-labeled probe peptides (CoilR-Cy5, MiniR-Cy5, and MiniE-Cy5). As expected from their sequences, we observed labeling of the CoilE tag with both CoilR-Cy5 and MiniR-Cy5 (**Figure 4.3**). Similarly, the MiniE tag was labeled by both "R" probe peptides. Homodimers (e.g., MiniR-MiniR or MiniE-MiniE) were not observed, including for the CoilE tag with MiniE-Cy5. In other words, target protein labeling was only observed for E-R pairs, not for E-E or R-R pairs. Based on these results, we conclude that both CoilE and MiniE dimerize with both CoilR and MiniR.

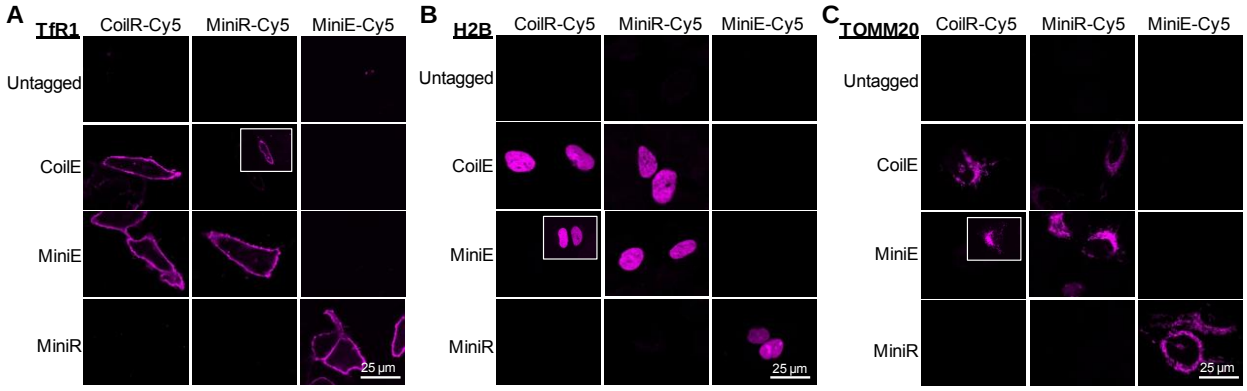


**Figure 4.3. MiniVIPER and VIPER cross-react predictably to form heterodimers.** Cells were transfected to express untagged or tagged TfR1 (**A**), H2B-mEmerald (**B**), or TOMM20-mCherry (**C**). The peptide tag is indicated to the left of the micrographs. Cells were treated live (**A**) or post-fixation (**B/C**) with CoilR-Cy5, MiniR-Cy5, or MiniE-Cy5, as indicated at the top of each column. Micrographs for each target protein were acquired and processed with identical settings to enable direct comparison between pairs. For a few pairs, Cy5 signal was above background, but had to be auto-scaled to observe (see insets). The complete datasets can be found in **Figure 4.4-4.6.**

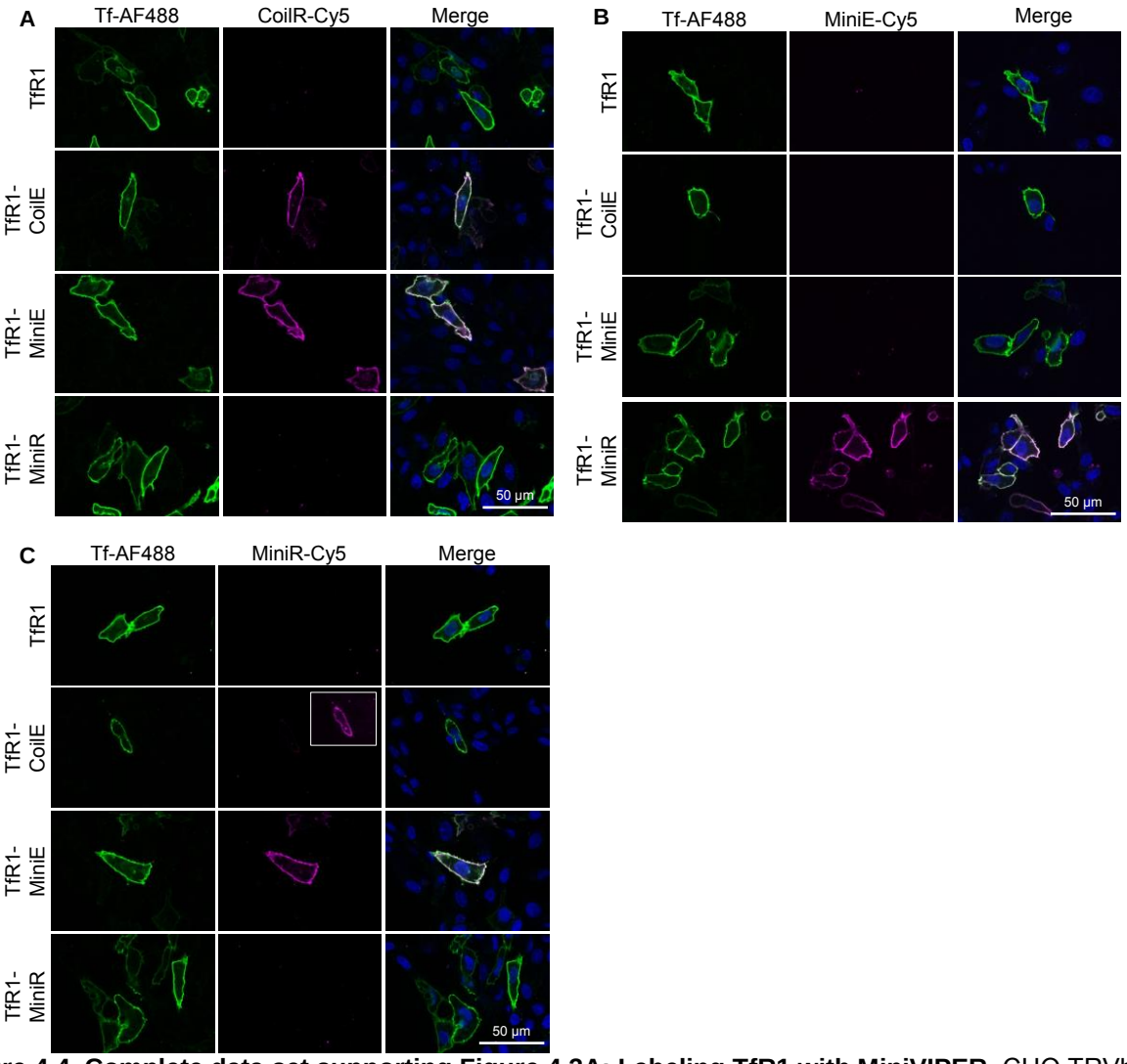


**Figure 4.4. Complete data set supporting Figure 4.3A: Labeling TfR1 with MiniVIPER.** CHO TRVb cells transfected with TfR1, TfR1-CoilE, TfR1-MiniE, or TfR1-MiniR were treated live with Tf-AF488 and (**A**) CoilR-Cy5, (**B**) MiniE-Cy5, or (**C**) MiniR-Cy5. All cells were labeled cold to restrict endocytosis. AF488 is false colored green. Cy5 is false colored magenta. Nuclear stain (blue) is provided in the channel merge and magenta-green overlap appears white. Cells were imaged at 63X magnification as single confocal slices (~0.5 µm). Images treated with the same probe peptide are displayed using the same brightness and contrast settings. An auto-scaled inset is provided in panels where selective VIP labeling occurred, but required different brightness/contrast settings.

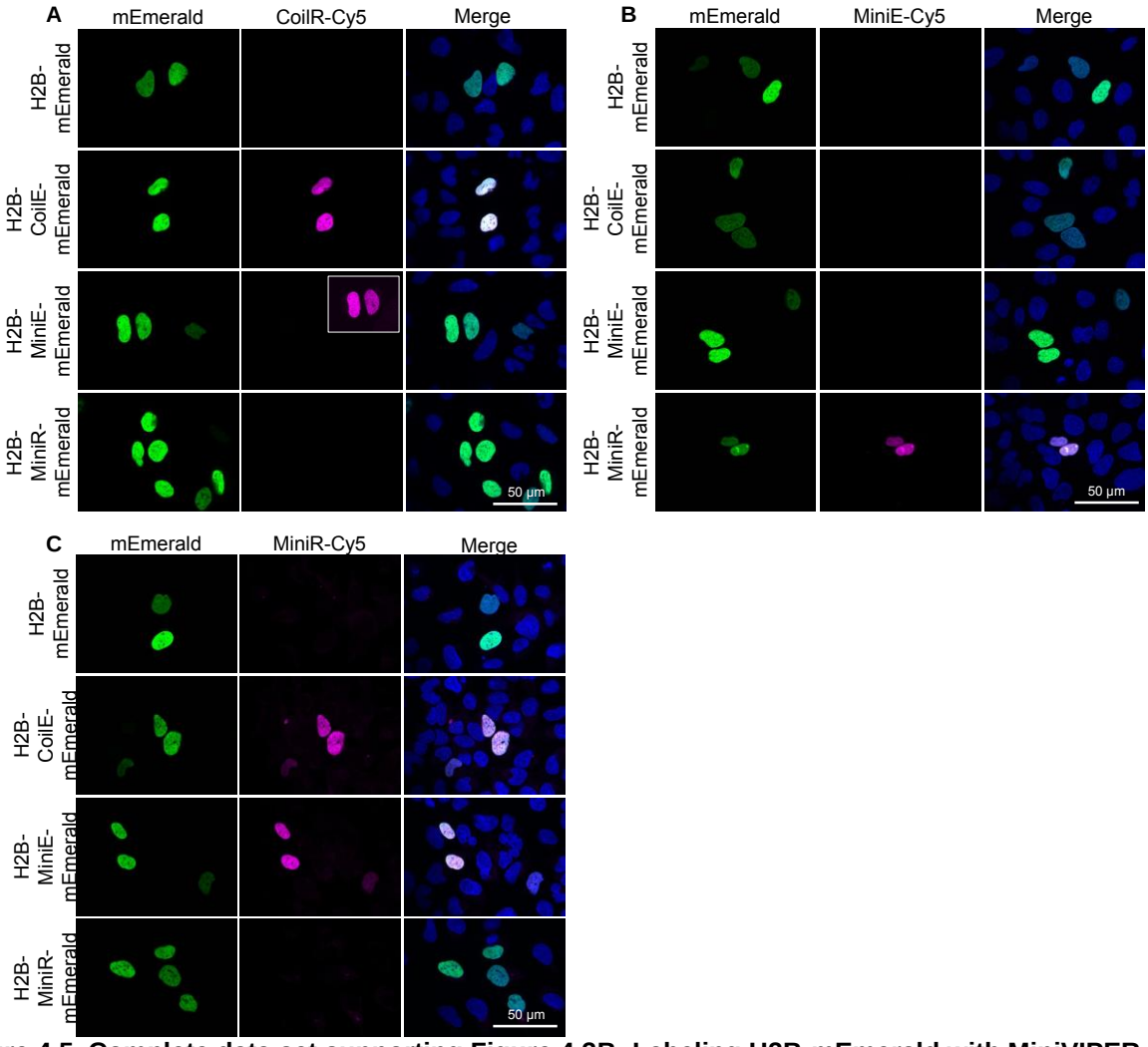


**Figure 4.5. Complete data set supporting Figure 4.3B: Labeling H2B-mEmerald with MiniVIPER.** U-2 OS cells transfected with H2B-mEmerald, H2B-CoilE-mEmerald, H2B-MiniE-mEmerald, or H2B-MiniR-mEmerald were treated post-fixation with (**A**) CoilR-Cy5, (**B**) MiniE-Cy5, or (**C**) MiniR-Cy5. mEmerald is false colored green. Cy5 is false colored magenta. Nuclear stain (blue) is provided in the channel merge and magenta-green overlap appears white. Cells were imaged at 63X magnification as single confocal slices (~0.5 µm). Images treated with the same probe peptide are displayed using the same brightness and contrast settings. An auto-scaled inset is provided in panels where selective VIP labeling occurred, but required different brightness/contrast settings.

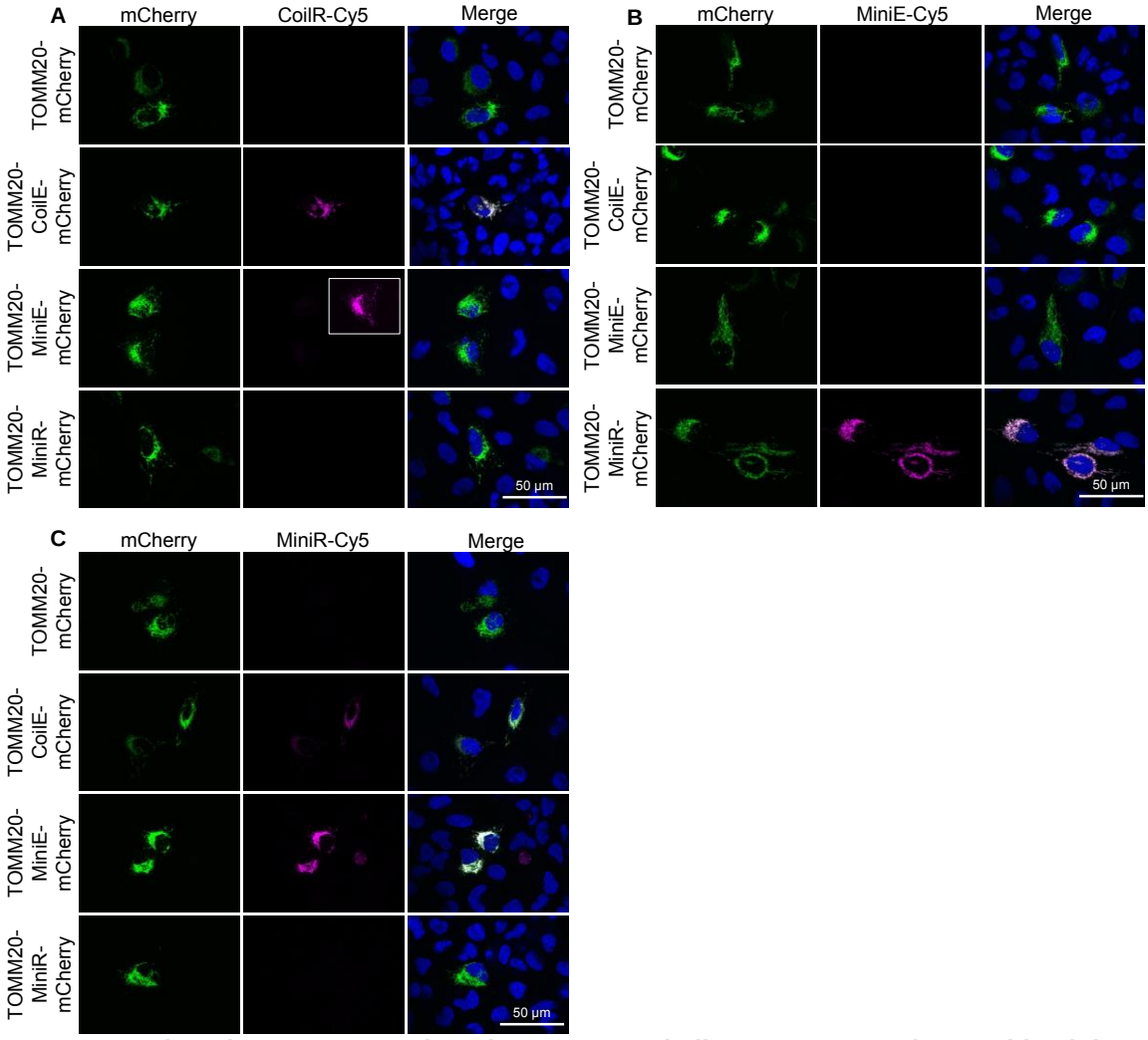


**Figure 4.6. Complete data set supporting Figure 4.3C: Labeling TOMM20-mCherry with MiniVIPER.** U-2 OS cells transfected with TOMM20-mCherry, TOMM20-CoilE-mCherry, TOMM20-MiniE-mCherry, or TOMM20-MiniR-mCherry were treated post fixation with (**A**) CoilR-Cy5, (**B**) MiniE-Cy5, or (**C**) MiniR-Cy5. mCherry is false colored green. Cy5 is false colored magenta. Nuclear stain (blue) is provided in the channel merge and magenta-green overlap appears white. Cells were imaged at 63X magnification as single confocal slices (~0.5 µm). Images treated with the same probe peptide are displayed using the same brightness and contrast settings. An auto-scaled inset is provided in panels where selective VIP labeling occurred, but required different brightness/contrast settings.

## MiniVIPER: One tag, five fluorophores

VIP tags confer a practical advantage for imaging applications in that the peptide tag can be detected with various spectrally-distinct reporter peptides. We demonstrated this feature in cells expressing TfR1-MiniR and labeled with one of five MiniE probe

peptides (**Figure 4.7**). Micrographs showed that TfR1-MiniR could be specifically labeled with spectrally-distinct fluorophores with green to far-red emission. Among these, Cy5 is a preferred fluorophore for super-resolution microscopy[35]. Qdot655 is bright, fluorescent, and photostable, making it ideal for single-particle tracking or detecting low-abundance targets. Additionally, Qdots have an electron dense core for imaging by correlative light and electron microscopy[36,37]. Peptides were attached to commercial fluorophores using either thiol-maleimide chemistry or thiol-yne chemistry, as described above. Other colors should be readily accessible for multi-color imaging applications.

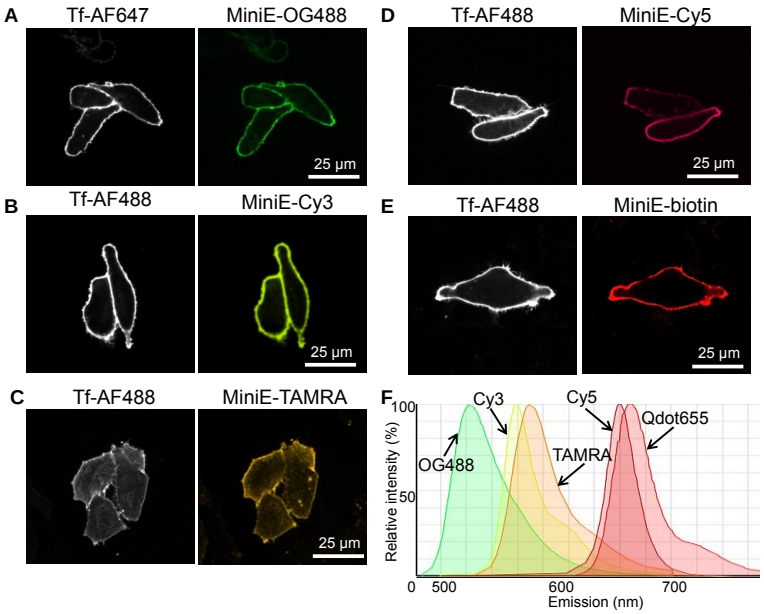


**Figure 4.7. A VIP-tagged protein can be labeled with a variety of fluorophores.** CHO TRVb cells expressing TfR1-MiniR were treated with fluorescent transferrin and one of five probe peptides, as indicated. (**A**) MiniE-OG488 (ex: 501 nm, em: 526 nm, QY: 0.92). (**B**) MiniE-Cy3 (ex: 548 nm, em: 563 nm, QY: 0.14). (**C**) MiniE-TAMRA (ex: 552 nm, em: 571 nm, QY: 0.41). (**D**) MiniE-Cy5 (ex: 646 nm, em: 662 nm; QY 0.18). (**E**) MiniE-biotin and streptavidin-Qdot655 (ex: 405 nm, em: 655 nm; QY 1.0). (**F**) The predicted emission spectra for the indicated fluorophores were generated using SpectraViewer (www.thermofisher.com).

## Combining VIP tags to image two distinct cellular targets

Many new discoveries in cell biology have been enabled by imaging proteins using genetically-encoded tags. Most of these studies rely on spectrally-distinct probes to label more than one target[1], which enables proteins to be examined relative to each

other and in relationship to their environment. In prior work, we demonstrated that VIP tags could be imaged alongside other targets labeled with small molecule stains (e.g., Hoechst), fluorescent ligands (e.g., transferrin), fluorescent proteins, or antibodies[22,23].

In the current work, we demonstrated that VIP tags can be combined to label two distinct protein targets in one cell. First, we used MiniVIPER with VIPER to label two targets: TfR1-MiniR with H2B-CoilE. In co-transfected CHO TRVb cells, we labeled TfR1-MiniR live (with MiniE-Cy5 and Tf-Cy3), fixed cells, and then treated with CoilR-AF488 to label H2B-CoilE in the nucleus. In cells co-expressing both targets, we observed selective MiniVIPER labeling at the cell surface and VIPER labeling in the nucleus, as anticipated (**Figure 4.8A**). We considered the possibility that TfR1-MiniR could heterodimerize with H2B-CoilE, but found no evidence of TfR1 in the nucleus by MiniVIPER labeling or by immunolabeling (**Figure 4.9**). These experiments demonstrate that the MiniR tag and the CoilE tag can be used together to detect two targets in one cell.

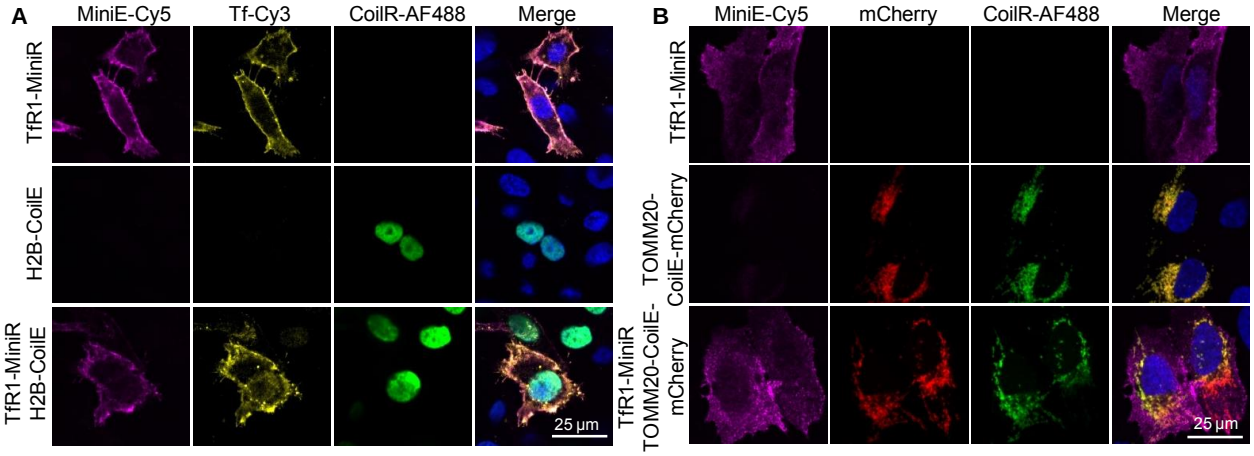


**Figure 4.8. VIP tags can be combined to image two targets simultaneously.** (**A**) CHO TRVb cells were treated with MiniE-Cy5 and Tf-Cy3 (top), CoilR-AF488 (middle), or MiniE-Cy5, Tf-Cy3, and CoilR-AF488 (bottom). (**B**) U-2 OS cells were treated with MiniE-Cy5 (top), CoilR-AF488 (middle) or both MiniE-Cy5 and CoilR-AF488 (bottom). Micrographs were false-colored (Cy5 = magenta, Cy3 = yellow, AF488 = green, mCherry = red, Hoechst 33342 = blue).

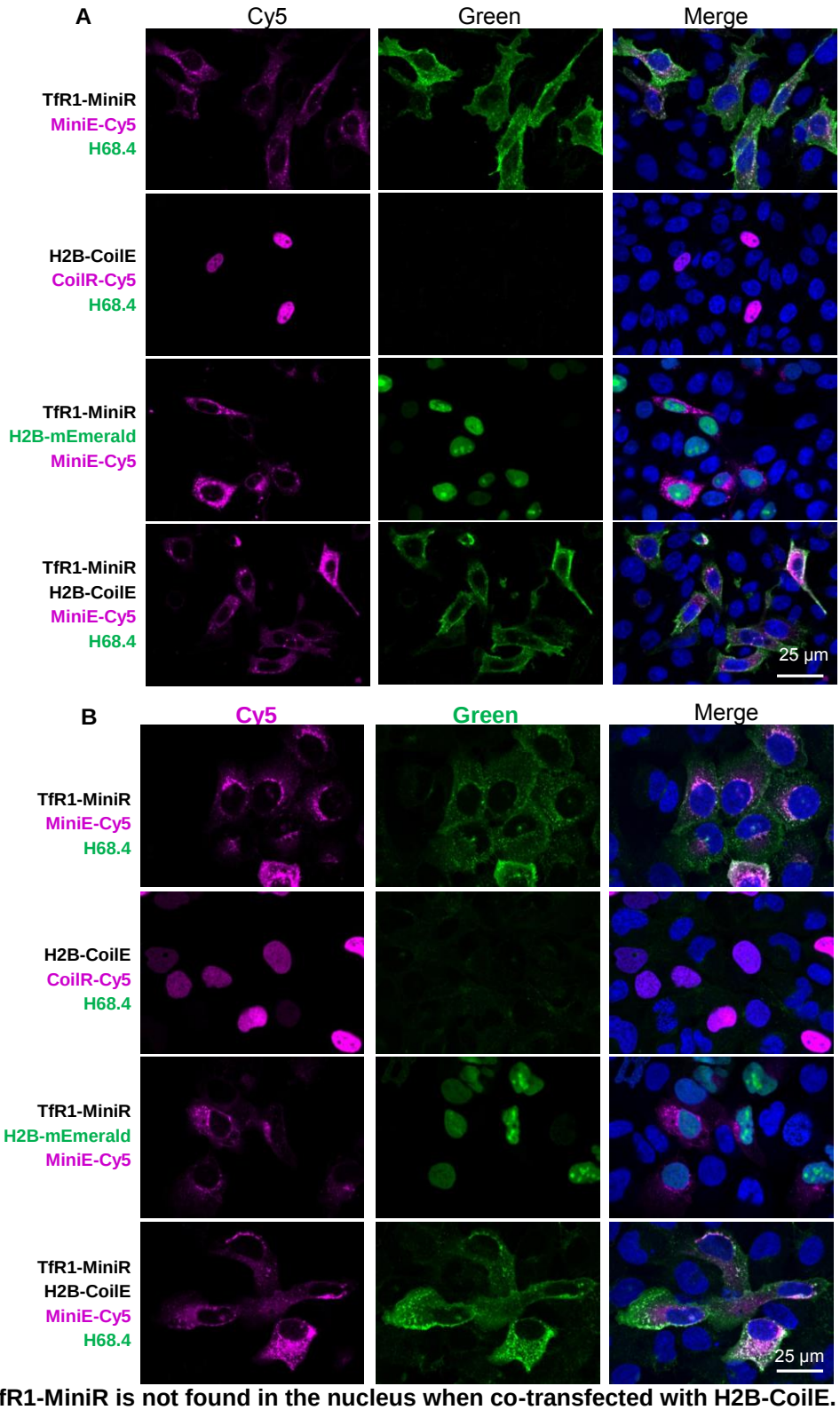


**Figure 4.9. TfR1-MiniR is not found in the nucleus when co-transfected with H2B-CoilE.** (**A**) CHO TRVb or (**B**) U-2 OS cells transfected with either TfR1-MiniR, H2B-CoilE, TfR1-MiniR with H2B-mEmerald or TfR1-MiniR with H2B-CoilE were fixed and permeabilized before labeling with either [Probe Peptide]-

Cy5 or H68.4 (anti-TfR1). Well treatments are listed in the vertical column, with the transfected constructs are indicated black font, [Probe Peptide]-Cy5 treatment are magenta font, and H68.4 antibody treatment or H2B-mEmerald are green font. Cy5 is false colored magenta. AF488 and mEmerald are false colored green. Hoechst 33342 (nuclei) is false colored blue. Cells were imaged at 63X magnification as single confocal slices (~0.5 μm).

Next, we imaged TfR1-MiniR with TOMM20-CoilE-mCherry in U-2 OS cells. Co-transfected cells were labeled live with MiniE-Cy5, fixed, and then treated with CoilR-AF488. In cells expressing both tagged proteins, we observed VIPER labeling (CoilR-AF488 signal) localized to the mitochondria and co-localized with mCherry (**Figure 4.8B)**. In the same cells, MiniVIPER labeling (MiniE-Cy5 signal) was observed at the cell surface and in endosomes, consistent with TfR1 labeling. These results further establish that MiniVIPER and VIPER can be used together to label two distinct targets.

Additionally, we assessed (mini)VIPER compatibility with VIP Y/Z, a previously published VIP tag[22]. We imaged cells expressing proteins labeled with VIP Y/Z along with proteins labeled with MiniVIPER or VIPER. Again, we observed selective labeling of each protein target (**Figure 4.10**).

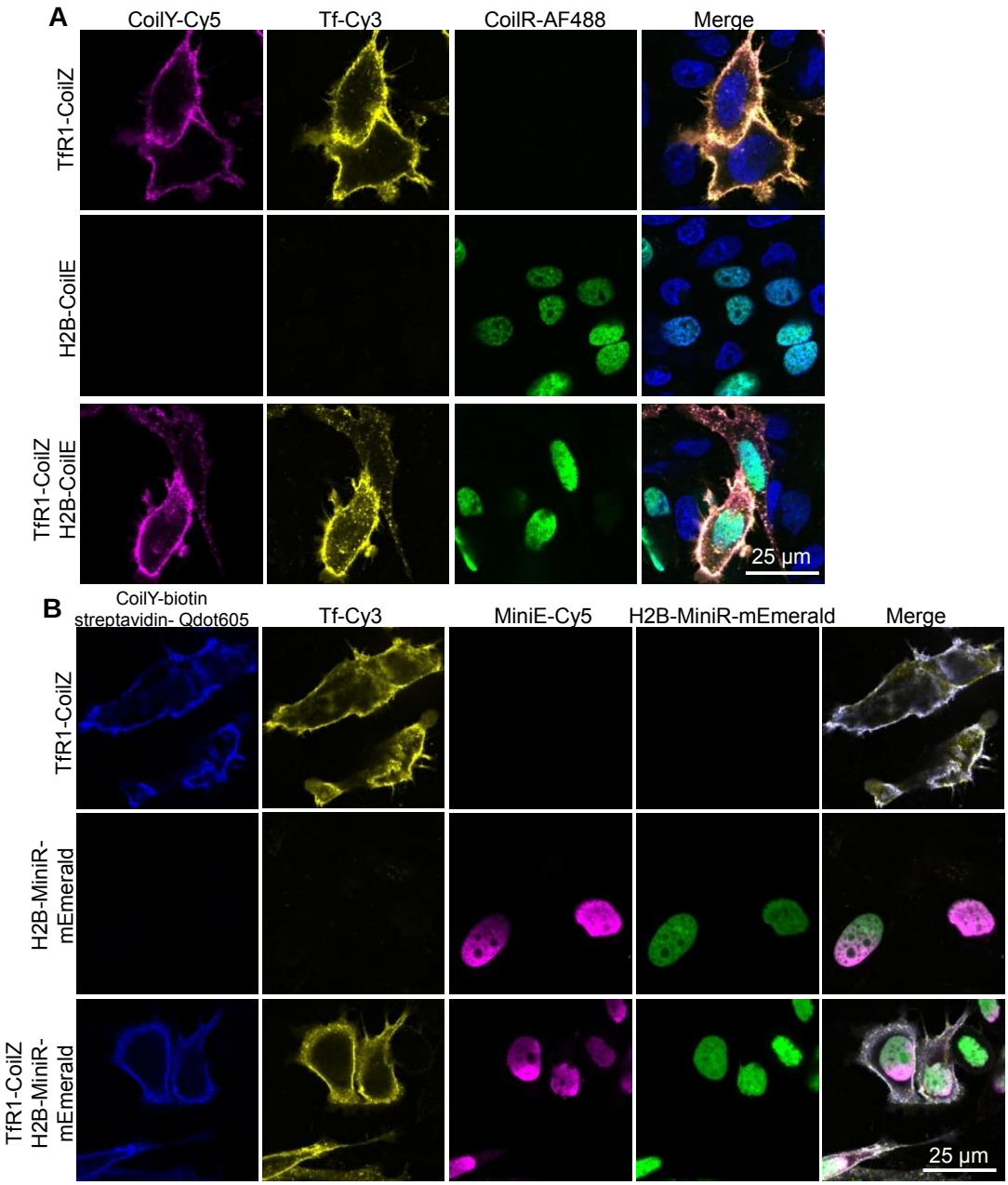


**Figure 4.10. Combining VIP Y/Z with VIPER (A) or MiniVIPER (B) to image two targets simultaneously.** (**A**) CHO TRVb cells transfected with TfR1-CoilZ, H2B-CoilE or both were treated live with CoilY-Cy5 and Tf-Cy3 (top), post-fixation with CoilR-AF488 (middle), or both (bottom). (**B**) CHO TRVb cells transfected with TfR1-CoilZ, H2B-MiniR-mEmerald or both were treated live with Tf-Cy3 and CoilY-biotin (detected post-fixation by streptavidin-Qdot605) (top), post-fixation with MiniE-Cy5 (middle), or both (bottom). All cells were labeled cold to restrict TfR1 endocytosis during live-cell labeling. Cy5 is false colored magenta, Cy3 is false colored yellow, AF488 and mEmerald are false colored green, Qdot605 and Hoechst 33342 are false colored blue. Cells were imaged at 63X magnification as single confocal slices (~0.5 µm).

## VIP-mediated translocation of proteins

The activities of many cellular proteins are controlled by localization, protein-protein interactions, and the movement of a protein between sub-cellular locations (i.e., translocation). Chemically-induced dimerization (CID) systems are often used to study these processes inside cells[38–40]. Another method, bi-molecular fluorescence complementation, uses split fluorescent proteins to detect protein-protein interactions[41]. A third approach detects a translocated protein through binding (e.g., via a coiled-coil dimer) between the target protein and a fluorescent protein[21,42].

Compared to other systems, the benefits of using VIP tags for protein translocation include their small size, directable orientation, stability, and independence of exogenous reagents. With that in mind, we sought to demonstrate that MiniVIPER could be used to translocate proteins in cells. First, cells were transfected to express soluble MiniR-mCherry in the cytosol plus an untagged H2B-mEmerald. We observed red fluorescence throughout the interior of cells, while green fluorescence was only observed in the nuclei (**Figure 4.11A**; top row). Next, cells were transfected to express both MiniR-mCherry and H2B-MiniE-mEmerald, which have both peptides needed to form a MiniVIPER heterodimer. We observed a remarkable difference. Upon expression of the MiniE-tagged protein, red fluorescence was observed solely in the nucleus and it co-localized with the green fluorescent signal (**Figure 4.11A**; bottom row). This indicated to us that the formation of the MiniR-MiniE dimer resulted in the translocation of mCherry to the nucleus. Analogous experiments confirmed that the opposite orientation (e.g., using MiniE-mCherry with H2B-miniR-mEmerald) or VIPER also enabled VIP-mediated protein translocation in living cells (**Figure 4.11B-C**). Next, we quantified these VIP-mediated interactions using Förster resonance energy transfer (FRET) imaging. Green and red fluorescent proteins are established donor-acceptor FRET pairs, although the FRET efficiency is typically low (4-29%)[43,44]. In our model system, described above, we anticipated that mEmerald and mCherry would be close enough (<10 nm) after VIP-mediated dimerization to be detectable by FRET.

We opted to use acceptor photobleaching (AP)-FRET, which measures the increase in donor fluorescence after acceptor photobleaching. The advantage of using AP-FRET is that the FRET efficiency can be determined directly without external

controls[45]. Using a Zeiss LSM880 system, mEmerald fluorescence in the nucleus was measured before and after mCherry photobleaching. We observed FRET efficiencies ranging from 9-13% for cells with VIP-induced mEmerald-mCherry dimers in the nucleus (**Figure 4.11D**). By comparison, when H2B-mEmerald (no VIP tag) was co-expressed in cells with tagged mCherry, the FRET efficiency ranged from -0.9±0.5% to 3.0±1.5%. Negative FRET is attributable to noise from the detectors and background fluorescence from the sample[46].

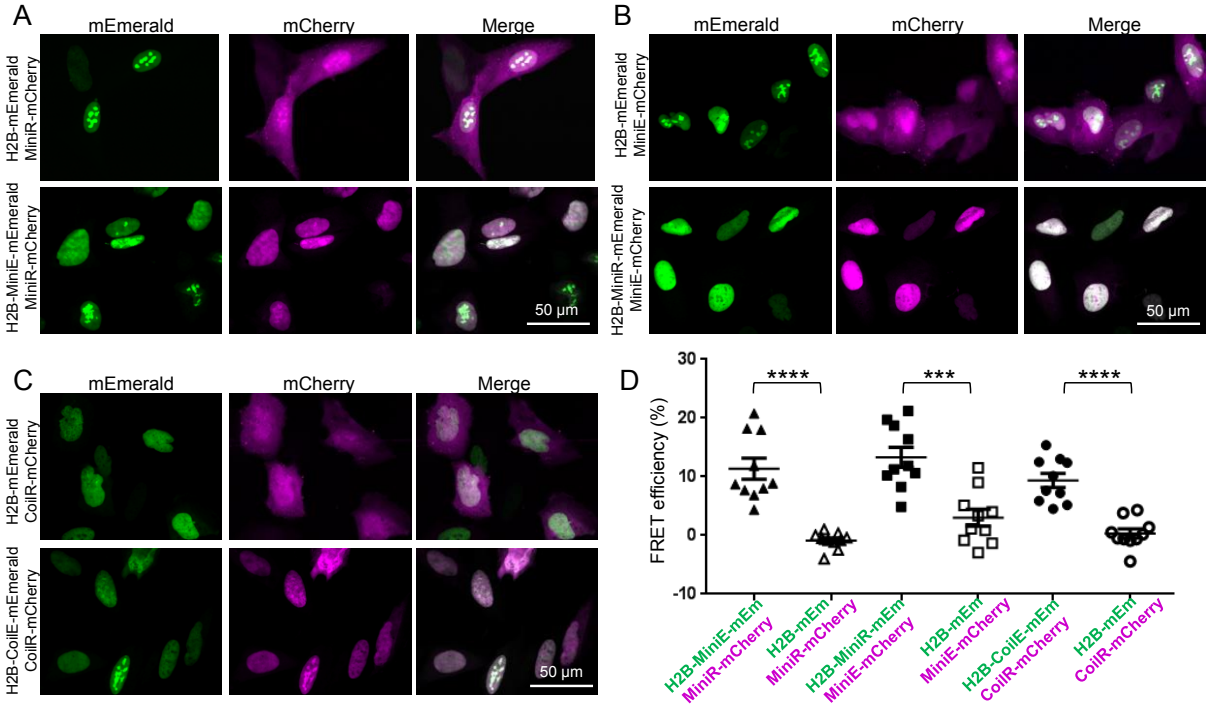


**Figure 4.11. Translocation of mCherry to the nucleus using VIP-mediated protein dimerization.** (A) Cells expressing H2B-mEmerald and MiniR-mCherry (top row) or H2B-MiniE-mEmerald and MiniR-mCherry (bottom row). In the latter condition, formation of the MiniVIPER dimer translocated mCherry to the nucleus, with green-magenta co-localization apparent in white. (B) Cells expressing H2B-mEmerald and MiniE-mCherry (top row) or H2B-MiniR-mEmerald and MiniE-mCherry (bottom row). (C) VIPER-mediated translocation of CoilR-mCherry to the nucleus in the presence of H2B-CoilE-mEmerald. (D) FRET efficiency for cells expressing tagged mCherry with untagged (open symbols) or Coil-tagged (closed symbols) H2B-mEmerald (mEm). FRET efficiency was measured in 10 nuclei per condition (see Table 4.7) and error bars represent the standard error of the mean (*** = $p < 0.001$; **** = $p < 0.0001$).

In summary, we have shown that VIP tags can be used to dimerize two proteins together and that this interaction can be measured using AP-FRET. Overall, these studies demonstrate that VIP tags are effective tools for translocating proteins inside cells.

## Conclusion

In the current work, we introduced MiniVIPER as a small and specific genetically-encoded peptide tag compatible with multiple imaging applications. MiniVIPER enabled fluorescent detection of receptors (TfR1) on live cells or histones (H2B-mEmerald) and mitochondria (TOMM20-mCherry) in fixed cells. Labeling was target-specific and VIP tagging did not interfere with protein localization. At just 4.3 kDa, both the MiniE and the MiniR tags are far smaller than fluorescent proteins and most other tags. Another distinguishing feature is that VIP tags can be detected with a variety of spectrally-distinct probe peptides, as shown in **Figure 4.7**.

We demonstrated two new applications for VIP tags. First, we established the generality of using a combination of two VIP tags for multi-color imaging. We used FM to observe MiniVIPER-labeled TfR1 with either VIPER-labeled H2B or VIPER-labeled TOMM20-mCherry. Furthermore, we demonstrated that the VIP Y/Z tag can be observed together with either VIPER or MiniVIPER. We have not yet combined all three VIP tags together, but that is a logical next step.

In a second application, we used VIP tags to alter the sub-cellular localization of a target protein. Specifically, we used MiniVIPER to translocate cytosolically-expressed mCherry to the nucleus. Interactions were quantified using AP-FRET, which confirmed that VIP-mediated dimerization brought the two target proteins into close proximity.

The versatility of VIP tags makes them amenable to different applications with thoughtful experimental design. While there are other tools for fluorescent protein labeling, multi-target imaging, and artificial dimerization, VIP tags are unique in their ability to enable all of these applications. We believe that this makes VIP tags a beneficial addition to the cell biologist's toolbox.

## Acknowledgements

We are grateful to our colleagues at Oregon Health & Science University for their advice, particularly S. Kaech Petrie and C. Chaw of the Advanced Light Microscopy Core and C. Schultz and A. Thomas for advice on FRET measurements. We thank P. Marchando and M. Naganbabu for aiding in plasmid construction, and W. Yao for assisting with probe peptide production. We thank the late M. Davidson (Florida State University) for constructs from his fluorescent protein collection. This research was supported by generous funding from Oregon Health & Science University and the National Institutes of Health (Grant R01 GM122854). J.K.D. was supported by the Achievement Rewards for College Scientists Foundation Oregon Chapter.

## Materials and Methods

### Chemicals

All chemicals were purchased from Sigma-Aldrich, ThermoFisher Scientific, Lumiprobe, or Click Chemistry Tools. Chemicals were used as received unless otherwise noted.

### Genetic constructs

A description of constructs used in the current work, including peptide and protein sequences, is provided in **Table 4.1**. Oligonucleotides purchased from Integrated DNA Technologies (IDT) are summarized in **Table 4.2**. Bacterial strains and plasmids are in **Table 4.3**.

*A. Genetic construction of pET28b(+)_MiniE and pET28b(+)_MiniR*

The *miniE* and *miniR* genes were synthesized using gene assembly polymerase chain reaction (PCR) as described[23]. Oligonucleotides were designed using DNAworks[47] (*https://hpcwebapps.cit.nih.gov/dnaworks/*), and included NcoI and XhoI restriction enzyme sites for insertion of assembled genes into the pET28b(+) vector backbone (Novagen). See **Table 4.2** for primers used to assemble pET28b(+)_MiniE, and pET28b(+)_MiniR.

Briefly, the genes were assembled and amplified by PCR, analyzed on a 2% agarose gel, and purified using a Nucleospin Gel and PCR Clean-Up kit (Takara). The pET28b(+) plasmid was then doubly digested with NcoI (New England Biolabs; NEB) and XhoI (NEB), dephosphorylated with calf intestinal phosphatase (CIP; NEB), and gel-purified. The vector and gene products (pET28b+ with *miniR* or *miniE*) were ligated using T4 DNA ligase (NEB) and transformed into chemically-competent *E.coli* cells (TOP10; ThermoFisher). Transformed *E. coli* were plated on LB agar plates supplemented with kanamycin (50µg/mL). Colonies were screened by PCR for inserts and positive clones were confirmed by Sanger sequencing.

Other peptide-encoding constructs were made as described: pET28b(+)_CoilR[23], pET28b(+)_CoilE[23], pET28b(+)_CoilY[22], and pET28b(+)_CoilZ[22].

*B. Genetic construction of VIP-tagged fluorescent protein constructs*

The mCherry and mEmerald constructs were obtained from Addgene and included: TOMM20-mCherry-N-10 (Addgene #55146), H2B-6-mEmerald (Addgene #54111), and mCherry2-N1 (Addgene#54517). The VIP-tagged variants of those fluorescent protein constructs were generated by Gibson Assembly[48]. Primers were designed using the NEBuilder® Assembly Tool (*http://nebuilder.neb.com/*) and are provided in **Table 4.2**. Briefly, primers flanking the *miniE*, *miniR,* or *coilE,* gene were used to PCR amplify the tag sequence plus Gibson Assembly overhangs with homology to the recipient vector. All PCR products were purified via a Nucleospin Gel and PCR Clean-Up kit (Takara) prior to assembly. Vectors were restriction digested at the location of tag insertion with BamHI (NEB) and similarly gel purified. The digested vector backbone and VIP gene insert were combined (molar ratio 1:5; vector-to-insert) and ligated using Gibson Assembly Mastermix (NEB) following the manufacturer's instructions. Reactions were transformed into TOP10 *E. coli*, and plated on LB agar plates supplemented with kanamycin (50 µg/mL). Colonies were screened by PCR for inserts and positive clones were confirmed by Sanger sequencing.

In the construction of H2B-CoilE, H2B-6-mEmerald (Addgene #54111) was digested with AgeI (NEB) and NotI (NEB) to remove the portion encoding mEmerald. Then the *coilE* gene was introduced via Gibson Assembly.

*C. Genetic construction of vectors encoding TfR1*

The pcDNA3.1_TfR1 vector, which encodes murine TfR1, was previously described[49]. The pcDNA3.1_TfR1-CoilE vector, encoding TfR1-CoilE was previously described[23].

The pcDNA3.1_TfR1-MiniE, pcDNA3.1_TfR1-MiniR and pcDNA3.1_TfR1-CoilZ constructs were generated using Gibson Assembly. The *miniR, miniE* and *coilZ* gene inserts were constructed by PCR amplification using primers with Gibson Assembly overhangs homologous to the recipient TfR1 vector. See **Table 4.2** for primers used to construct the gene inserts. All PCR products were purified prior to assembly as described above (*Section B*).

The pcDNA3.1_TfR1 vector was restriction digested with AgeI (NEB) at the location of tag insertion and gel purified. The digested vector backbone and VIP gene insert were combined (molar ratio 1:5; vector-to-insert) and ligated using Gibson Assembly Mastermix (NEB) following the manufacturer's instructions. Reactions were transformed into TOP10 *E. coli*, and plated on LB agar plates supplemented with ampicillin (100 µg/mL). Colonies were screened by PCR for inserts and positive clones were confirmed by Sanger sequencing.

**Expression and purification of MiniE and MiniR**

A detailed step-by-step protocol for making probe peptides was described in Doh *et al. Bio-Protocol* 2019[28].

The pET28b(+)_MiniE plasmid was transformed into *E.coli* BL21(DE3) cells (ThermoFisher) to express MiniE probe peptide. A starter culture was used to inoculate a 1L flask of 2xYT media with kanamycin (50 µg/mL) at 37 °C. When the $OD_{600}$ reached 1.0, the expression of MiniE was induced by adding 0.25 mM IPTG (Goldbio) and peptide was expressed for 4 h at 30 °C. Cells were pelleted by centrifugation and frozen at -20 °C until purification.

MiniE peptide was purified under denaturing conditions. Cells were thawed on ice and resuspended in Denaturing Lysis Buffer (100 mM $NaH_2PO_4$, 10 mM Tris, 6 M urea, 20 mM imidazole, 1 mM PMSF, pH 8). Resuspended cells were sonicated on ice with a 0.5-inch horn for 8 cycles of 30 sec on, 1 min off intervals (Branson A-450; duty 40% and output control: 4). The lysate was clarified by centrifugation, and then incubated (1 h at 4 °C) with pre-equilibrated Ni-NTA resin (Qiagen); 4 mL of slurry per gram of bacterial pellet (wet weight). The resin was then loaded onto an Econo-Pac® Chromatography Column (Bio-Rad) and washed with 5 column volumes (CV) of Denaturing Lysis Buffer. Next, 20 CV of Wash Buffer (100 mM $NaH_2PO_4$, 10 mM Tris, 6 M urea, pH 6.4) was used to remove non-specifically bound proteins. The $His_6$-tagged MiniE peptide was eluted from the resin with 8 CV of Elution Buffer (100 mM $NaH_2PO_4$, 10 mM Tris, 6 M urea, pH 4.5). All fractions from the peptide purification were analyzed by SDS-PAGE and eluted fractions containing MiniE were combined and concentrated using a molecular weight cut off (MWCO) centrifugal filter (3 kDa MWCO, Millipore).

Purified peptide solutions were quantified using Beer's law ($A = \varepsilon \ell c$) by measuring the absorbance 280 nm in a 1-cm quartz cuvette via an Infinite M200 Pro plate reader (Tecan). In this equation, $A$ is absorbance, $\varepsilon$ is the molar extinction coefficient, $\ell$ is the path length and $c$ is the concentration. The extinction coefficients for each peptide can be found in **Table 4.4**. Peptides were stored frozen (-20 °C) in 100 mM NaH2PO4, 10 mM Tris, 2 M urea, and 10% glycerol.

An analogous approach was used to express (from pET28b(+)_MiniR), purify, and quantify MiniR probe peptide.

**SDS-PAGE analysis**

Protein expression and purification were analyzed by SDS-PAGE using 12% Bis-Tris Criterion XT gels (BioRad). Samples were combined with SDS-PAGE loading dye (50 mM Tris pH 6.9, 100mM TCEP, 2% SDS, 0.1% Ponceau Red, 10% glycerol) and boiled (5-10 min). Samples were centrifuged briefly before loading, and then resolved by SDS-PAGE. When applicable, gels were imaged on an Amersham Typhoon 5 multimodal scanner (GE) for fluorescence analysis. Gels were stained with Coomassie Brilliant Blue and de-stained before imaging on a flat-bed scanner (Canon LiDE220).

**Generation of probe peptides**

A summary of the reactive fluorophores used to make probe peptides is included in **Table 4.5**. A summary of probe peptides used in the current work can be found in **Table 4.6**.

*A. Generation of fluorophore-labeled probe peptides by thiol-maleimide chemistry*

Fluorophore-labeled MiniE probe peptides were generated by solid state labeling[31]. Purified MiniE, containing a single reactive cysteine residue, was dye-labeled with Sulfo-Cyanine5 (Cy5) maleimide (Lumiprobe), Sulfo-Cyanine3 (Cy3) maleimide (Lumiprobe), or Oregon Green 488 (OG488) maleimide (ThermoFisher); see **Table 4.5**. Reactive maleimide dyes were prepared in anhydrous DMSO (Sigma-Aldrich). For each reaction, 100 nmol of MiniE was reduced for 30 min with 10 mM DTT at 4 °C on a rotisserie. Ammonium sulfate was added to 75% saturation with 20 mM

DTT to precipitate the reduced peptide for 2 h at 4 °C on a rotisserie. Precipitated peptide was pelleted and washed three times with 1 mL of Labeling Buffer (125 mM $NaH_2PO_4$, 200 mM NaCl, 1.2 mM EDTA, 4.6 M ammonium Sulfate, pH 7.5) before resuspension in 200 µL of Labeling Buffer. Next, the reactive fluorophore was added (10-fold molar excess for Sulfo-Cy5 maleimide and 40-fold molar excess for Sulfo-Cy3 maleimide and Oregon Green 488 maleimide) with TCEP (10-fold molar excess). MiniE was reacted with the dyes at 4°C on a rotisserie overnight, protected from light.

The next day, excess fluorophore was removed by Ni-NTA purification. Dye-labeled peptide was diluted in 50 mL of Ni-NTA Binding Buffer (100 mM $NaH_2PO_4$, 10 mM Tris, 6 M urea, pH 8) and bound to 1 mL of pre-equilibrated Ni-NTA resin for 1 h at 4 °C on a rotisserie. Dilution of the peptide solution was required to reduce the concentration of EDTA for compatibility with the Ni-NTA resin. The resin was loaded onto an Econo-Pac® Chromatography Column (BioRad) and washed with 20 CV of Wash Buffer (100 mM $NaH_2PO_4$, 10 mM Tris, 6 M urea, pH 6.4) until the washes appeared colorless. Peptide was eluted in 8 CV of Elution Buffer (100 mM $NaH_2PO_4$, 10 mM Tris, 6 M urea, pH 4.5). All fractions from the dye labeling and purification were analyzed by SDS-PAGE and imaged on an Amersham Typhoon 5 to detect fluorescent peptides. Eluted fractions containing dye-labeled MiniE were combined and concentrated using 3 kDa MWCO filtration, resulting in an orange (MiniE-OG488), dark blue (MiniE-Cy5), or dark-pink (MiniE-Cy3) solution. Peptides were stored frozen (-20 °C) in 20 mM Tris pH 7.4, 150 mM NaCl, 2 M urea, 10% glycerol.

Final peptide concentrations were determined by Beer's law. Absorbance 280 nm measurements were taken in a 1-cm quartz cuvette using an Infinite M200 Pro plate reader. Dye labeling efficiency was estimated using Thermofisher's protocol (*http://tools.thermofisher.com/content/sfs/brochures/TR0031-Calc-FP-ratios.pdf*). Briefly, we measured the peptide's absorbance at 280 nm and at the excitation maximum of the dye in a 1-cm quartz cuvette. Labeling efficiency was calculated using the equation:

$$\frac{mol\ dye}{mol\ protein} = \frac{A_{dye}}{\varepsilon_{dye} \times \frac{A_{280} - (A_{dye} \times CF)}{\varepsilon_{peptide}}}$$

In this equation, $A_{dye}$ is the absorbance of the labeled peptide at the dye excitation maximum, $\varepsilon_{dye}$ is the molar extinction coefficient of the dye, $A_{280}$ is the absorbance of the labeled peptide at 280 nm, *CF* is the dye absorbance correction factor at 280 nm, and $\varepsilon_{peptide}$ is the molar extinction coefficient of the peptide at 280 nm. See **Table 4.5** for properties of the reactive fluorophores used. Using this equation, we estimated that MiniE-Cy5 was 59% ± 1% labeled, MiniE-Cy3 was 52% ± 2% labeled, and MiniE-OG 488 was 64% ± 2% labeled. The peptides were stored in 10% glycerol at -20 °C, protected from light.

MiniR was analogously labeled with Sulfo-Cy5 maleimide (Lumiprobe) to make MiniR-Cy5 (29% ± 2% labeled). CoilR-Cy5[23], CoilR-AF488[28], and CoilY-Cy5[22] probe peptides were previously described.

*B. Generation of MiniE-TAMRA using thiol-yne "click chemistry"*

We generated MiniE-TAMRA using a modified protocol published by Pentelute and coworkers[30]. Purified MiniE was buffer exchanged into Click Buffer (200 mM sodium phosphate pH 8.0, 2 mM DTT, 5% DMSO, 1 M urea) using a molecular weight cut off filter (MWCO, 3 kDa). We included 1 M Urea in the reaction buffer to ensure that the peptide remained in solution. Following buffer exchange, 50 nmol of peptide was reacted with 200 nmol (4-fold molar excess) DBCO-TAMRA (Click Chemistry Tools) for 3.5 hours at 37 °C. Excess fluorophore was removed by 3 kDa MWCO filtration (Millipore). Next, dye-labeled peptide was diluted in 15 mL of Click Binding Buffer (0.2 mM sodium phosphate pH 8.0 and 1 M urea) and bound to 0.5 mL of pre-equilibrated Ni-NTA resin for 1 h at 4 °C on a rotisserie. The resin was loaded onto an Econo-Pac® Chromatography Column (Bio-Rad), washed with 50 mL of Click Binding Buffer and eluted in 5 mL of Click Binding Buffer with 500 mM imidazole. All fractions from the dye labeling and purification were analyzed by SDS-PAGE and imaged on an Amersham Typhoon to analyze fluorescence. Eluted fractions containing MiniE-TAMRA were combined and concentrated using MWCO (3 kDa) filtration and exchanged into TBS-Urea (0.5 M urea, 300 mM NaCl, 50 mM Tris, pH 8). Labeling efficiency was calculated using the equation above. We estimated that MiniE-TAMRA was 16% ± 0% labeled.

*C. Generation of biotinylated probe peptides*

Purified MiniE was biotinylated with EZ-Link Maleimide-PEG2-Biotin (ThermoFisher) by solid state labeling, using the previously described method[28]. EZ-Link Maleimide-PEG2-Biotin (100-fold molar excess) and TCEP (10-fold molar excess) was added to 100 nmol of peptide. Excess biotin was removed by Ni-NTA purification, and all eluted fractions were combined and buffer exchanged into TBS-0.5 M urea (0.5 M urea, 300 mM NaCl, 50 mM Tris, pH 8). The biotinylated peptide was then purified by Pierce Monomeric Avidin Agarose (ThermoFisher) according to the manufacturer's instructions. Fractions were analyzed by SDS-PAGE and anti-biotin Western blot. Elutions containing MiniE-biotin were combined, concentrated, and buffer exchanged into TBS-6 M urea (6M urea, 300 mM NaCl, 50 mM Tris pH 8) by 3 kDa MWCO filtration (Millipore). Final protein concentration was determined by absorbance, and was assumed to be 100% biotinylated. Biotinylated peptide was stored in 10% glycerol at -20 °C.

MiniR was biotinylated using the same protocol and assumed to be 100% biotinylated after purification on avidin resin. CoilY-Biotin was made as previously described[22].

**Mammalian cell culture and maintenance**

Chinese Hamster Ovary (CHO) TRVb (ΔTfR1 ΔTfR2) cells were generously provided by Prof. Timothy E. McGraw (Cornell University, New York). These cells do not express functional transferrin receptor 1 (TfR1) or transferrin receptor 2 (TfR2)[34]. CHO TRVb cells were maintained in Ham's F12 media (Gibco) supplemented with 5% fetal bovine serum (FBS) in 10 cm polystyrene dishes. Cells were grown in a humidified incubator at 37 °C with 5% $CO_2$ and passaged when they reached 80-90% confluency. Cells were detached with 0.25% trypsin/1 mM EDTA (TRED) and seeded at a 1:10 dilution (2 x $10^6$ cells/dish).

U-2 OS cells were purchased from ATCC (Cat #HTB-96). Cells were maintained in McCoy's 5A media (HyClone) with 10% FBS in 10 cm polystyrene dishes. Cells were grown in a humidified incubator at 37 °C with 5% $CO_2$ and passaged when they reached

80-90% confluency. They were detached with TRED and seeded at a 1:10 dilution (2 x $10^6$ cells/dish).

**Transfection of vector DNA into CHO TRVb or U-2 OS cells**

All imaging experiments were conducted in transiently transfected cell lines. For fluorescence imaging, 5 x $10^4$ cells were seeded into each well of an 8-well chambered slide (Cellvis; Cat. No. C8-1.5H-N) and grown overnight to 70-90% confluency. Transfection was performed using Lipofectamine 2000 (ThermoFisher) following the manufacturer's instructions. All constructs used for transfections can be found in **Table 4.1**. For TfR1-tagged constructs, the transfection mixture in each well contained 500 ng vector DNA and 1 µg Lipofectamine 2000 (DNA:Lipofectamine ratio 1:2) in 250 µL of Opti-MEM. For fluorescent protein-tagged constructs (e.g., TOMM20-mCherry or H2B-mEmerald), the transfection mixture in each well contained 100 ng vector DNA and 200 ng Lipofectamine 2000 (DNA:Lipofectamine ratio 1:2) in 250 µL of Opti-MEM. After 3-4 h, the transfection media was removed and replaced with fresh media with FBS for recovery. Cells were imaged approximately 24 h after transfection.

Vectors were co-transfected for either labeling two targets or for VIP-mediated artificial dimerization. For these experiments, the selected vectors were combined to form transfection mixtures in each well containing 500 ng of total vector DNA. The DNA mixture was combined with 1 µg Lipofectamine 2000 in 250 µL of Opti-MEM (DNA:Lipofectamine ratio 1:2). Proportions of DNA were modulated depending on the construct to reduce over-expression. We used a 4:1 ratio of TfR1:H2B, a 4:1 ratio of TfR1:TOMM20 and a 1:1 ratio for H2B:mCherry. After 4 h, the transfection media was removed and replaced with fresh media with FBS and cells were imaged approximately 24 h after transfection.

**Preparation of samples for fluorescence imaging**

A detailed step-by-step protocol for fluorescence imaging was described in *Doh et al. Bio-Protocol* 2019[50].

*A. Labeling intracellular VIP-tagged proteins in fixed cells*

U2-OS cells transfected with untagged or VIP-tagged H2B-mEmerald or TOMM20-mCherry were washed twice with Dulbecco's phosphate-buffered saline (DPBS pH 7.4) and fixed with 4% paraformaldehyde (PFA) in DPBS for 15 min at room temperature. Cells were subsequently washed twice with DPBS and permeabilized with 0.1% Triton X-100 in DPBS for 10 min. Cells were washed twice with DPBS to remove detergent and blocked for 30 min in Blocking Solution (10% FBS, 5% sucrose, 2% BSA (Fraction V) in DPBS). Cells were treated with 100 nM probe peptide in Blocking Solution for 30 min at room temperature, covered from light. Cells were washed twice with DPBS and nuclei were stained with 10 µg/mL Hoechst 33342 (Invitrogen, 10 min). Cells were washed twice and then imaged. Micrographs were processed and analyzed in ImageJ (*see below*).

*B. Labeling VIP-tagged TfR1 on live cells*

Transfected CHO TRVb cells were blocked with 10% FBS, 6% BSA in Ham's F12 media for 30 min at 37 °C in a humidified incubator with 5% CO2. Cells were cooled to 4 °C to pause endocytosis, then incubated (30 min) with a cold mixture of 50 µg/mL Tf-AF488 (ThermoFisher) and 100 nM probe peptide in F12 media (no FBS). Cells were washed three times with cold DPBS and then fixed with 4% PFA for 15 min at 4 °C. Cells were washed twice with DPBS, nuclei were stained with 10 µg/mL Hoechst 33342 (10 min), and washed twice more with DPBS before imaging. Micrographs were processed and analyzed in ImageJ (see below).

*C. Labeling of receptors with biotinylated peptides and streptavidin Qdots*

A modified procedure "B" was used for labeling receptors with quantum dots (Qdots). For cells labeled with biotinylated probe peptide, the nuclear stain was omitted. After VIP labeling and fixation, cells were blocked for 1 h in 10% FBS, 6% BSA in DPBS protected from light. Cells were then incubated with 10 nM Qdot 655 streptavidin conjugate (Invitrogen) in 6% BSA in DPBS for 1 h, covered from light. Cells were washed twice with DPBS and imaged as described below. Micrographs were processed and analyzed in ImageJ (*see below*)**.**

*D. Labeling of two targets using MiniVIPER, VIPER and VIP Y/Z*

CHO TRVb cells were co-transfected with TfR1-MiniR and either H2B-CoilE or TOMM20-CoilE-mCherry. Cells were blocked with 10% FBS, 6% BSA in F12 for 30 min at 37 °C in a humidified incubator with 5% CO2. Cells were cooled to 4 °C to pause endocytosis, then incubated (30 min) with cold 100 nM MiniE-Cy5 in F12 media (no FBS). For cells expressing both TfR1-MiniR with H2B-CoilE, fluorescent ligand (50 µg/mL Tf-Cy3) was also added during this incubation period. Cells were washed three times with DPBS and then fixed with 4% PFA in DPBS for 15 min at 4 °C. Cells were washed three times with DPBS and incubated in Blocking Solution for 30 min at room temperature, covered from light. Cells were labeled with 100 nM CoilR-AF488 in Blocking Solution for 1 h, covered from light. Cells were washed three times with DPBS, nuclei were stained with 10 µg/mL Hoechst 33342 (10 min), and washed thrice before imaging. Micrographs were processed and analyzed in ImageJ (*see below*).

An analogous approach was used for labeling cells co-transfected with: i) TfR1-CoilZ and H2B-CoilE; ii) TfR1-CoilZ and H2B-MiniR-mEmerald. For imaging TfR1-CoilZ and H2B-CoilE, cells were labeled live with 100 nM CoilY-Cy5 and 50 µg/mL Tf-Cy3, then labeled post-fixation with 100 nM CoilR-AF488. For imaging TfR1-CoilZ and H2B-MiniR-mEmerald, cells were labeled live with 100 nM CoilY-biotin and 50 µg/mL Tf-Cy3, then labeled post-fixation with 100 nM MiniE-Cy5 and 10 nM streptavidin-Qdot605. Micrographs were processed and analyzed in ImageJ (see below).

*E. Assessing TfR1 localization by immunolabeling*

When combining VIP tags to image TfR1 and H2B, the TfR1 was labeled live on the cell surface (**Figure 4.8** in main article). The intracellular population of TfR1 needed to be assessed to ensure that VIP-tagged TfR1 and H2B did not inappropriately dimerize when co-transfected for multi-target microscopy experiments. We used immunolabeling to detect TfR1 in the plasma membrane and intracellular populations of the receptor. Briefly, CHO TRVb or U-2 OS cells transfected with TfR1-MiniR and H2B-CoilE were fixed with 4% PFA in DPBS for 15 min at room temperature. Cells were subsequently washed twice with DPBS and permeabilized with 0.1% Triton X-100 in DPBS for 10 min. Cells were washed twice with DPBS to remove detergent and blocked

for 30 min in Blocking Solution. Cells were treated with 100 nM MiniE-Cy5 and/or 10 µg/mL H68.4 (anti-TfR1; ThermoFisher) in Blocking Solution for 1 h at room temperature. Cells were washed twice with DPBS, and H68.4 was detected with 10 µg/mL anti-mouse-AF488 (ThermoFisher) in Blocking Solution for 1 h at room temperature. Nuclei were stained with 10 µg/mL Hoechst 33342 (10 min). Cells were washed twice more, and then imaged using a Zeiss Yokogawa spinning disk confocal microscope. Immunolabeling of TfR1 demonstrated that TfR1 and H2B did not co-localize. Furthermore, TfR1 was not observed in the nucleus.

*F. Protein Translocation using MiniVIPER*

For imaging artificial dimerization and translocation, cells were co-transfected with H2B-mEmerald and mCherry vectors as described above. VIP-tagged mCherry was co-transfected with untagged H2B-mEmerald or VIP-tagged H2B-mEmerald (e.g. MiniE-mCherry and H2B-MiniR-mCherry). The following day, transfected cells were fixed with 4% PFA in DPBS for 15 min at room temperature. Cells were washed twice with DPBS and nuclei were stained with 10 µg/mL Hoechst 33342 (10 min).

Cells were washed twice more, and then imaged using a Zeiss Yokogawa spinning disk confocal microscope for qualitative assessment of mCherry localization.

**Fluorescence Microscopy and Image Analysis**

Cells were imaged on a Zeiss Yokogawa spinning disk confocal microscope. For **Figures 4.2-4.10** a 64X (N.A. 1.4) objective lens was used. For the micrographs in **Figure 4.11** in the main article, a 40X (NA 0.9) objective lens was used. When imaging samples within the same experiment, the same acquisition settings (e.g., laser intensity and exposure time) were used for all samples. The following excitation (ex) laser lines and emission filters (em) were used for the indicated fluorophores:

Hoechst 33342 – ex: 405 nm; em: 405/50 nm
mEmerald, AF488, OG488 – ex: 488 nm; em: 525/50 nm
TAMRA, Cy3, mCherry – ex: 561 nm; em: 629/62 nm
Cy5 – ex: 638 nm; em: 690/50 nm

Qdot655 – ex:405 nm; em: 690/50 nm

Images were adjusted and false-colored for publication using ImageJ. The brightness and contrast were normalized for all samples treated with the same fluorophore within an experiment. The ImageJ 'Channels' tool was used to false color individual channels and to create a multicolored merge image. Scale bars were added in ImageJ. Micrographs were cropped to enable larger views of relevant cells. Figures were prepared in Microsoft PowerPoint.

**Acceptor Photobleaching FRET**

Acceptor photobleaching FRET was used to measure VIP dimerization. FRET measurements were acquired on a Zeiss LSM880 line-scanning confocal microscope with a 63X (1.40 NA) oil immersion objective lens with ZEN Black software. In brief, a region-of-interest (ROI) was drawn in the nucleus (25 x 25 pixels) of cells expressing H2B-[VIP Tag]-mEmerald and [VIP Tag]-mCherry. ROIs were drawn on areas of uniform fluorescence (i.e. not on nucleoli).

First, the ROI was imaged for both red and green fluorescence. Spectroscopic filtering (through the use of a diffraction grating) was used to minimize the cross-talk between the mEmerald and mCherry channels. mEmerald was imaged using 488 nm excitation and 495-571 nm emission range. mCherry was imaged using 561 nm excitation and 575-678 nm emission range.

Next, each ROI was treated with high intensity red laser light to bleach the mCherry fluorophore and to eliminate FRET.

Lastly, each ROI was imaged again for red and green fluorescence. The red fluorescence measurement served to ensure that the ROI no longer was red fluorescent after photobleaching. The green fluorescence was measured with the expectation that if FRET was lost (via acceptor photobleaching), then the green fluorescence signal would increase.

To summarize the workflow, a time series was programmed and each ROI was:

- Imaged 3 times (mEmerald and mCherry excitation and emission settings).

- Photo-bleached with 5 intervals of 561 nm laser (100% power). Pixel dwell time (how long each pixel was exposed) for the laser was 42.27 µsec. This step bleached mCherry signal, thus eliminating FRET.
- Imaged 3 times after photo-bleaching (mEmerald and mCherry excitation and emission settings).

ZEN Black software calculated the mean fluorescence intensity for each ROI before and after bleaching and outputted a table of average pixel fluorescence intensity. FRET efficiency was calculated by subtracting the ROI's mean mEmerald fluorescence before bleaching ($mEm_{before}$) from the mean mEmerald fluorescence after ($mEm_{after}$) bleaching, and dividing the difference by $mEm_{before}$ and multiplying by 100[45], using this equation:

$$FRET\ efficiency\ = \frac{mEm_{after} - mEm_{before}}{mEm_{before}} x\ 100$$

A summary of FRET efficiency data is provided in **Table 4.7**.

# Supplementary Tables

## Table 4.1. Summary of genetic constructs.

| Protein Name | **Sequence** (1-letter amino acid code)<br>Sequence annotation key: **Coil tag**; linker; mEmerald; mCherry | Size (Daltons) | pI | Vector Name |
|---|---|---|---|---|
| **CoilY** | MGSS**NTVKELKNYIQELEERNAELKNLKEHLKFAKAELEFELAAHKFE**GGGAAAC LGKLAAALEHHHHHH | 7826.85 | 6.43 | pET28b(+) _CoilY |
| **CoilE** | MGGS**LEIEAAFLERENTALETRVAELRQRVQRLRNRVSQYRTRYGPL**GGGCLEHH HHH | 6737.56 | 9.29 | pET28b(+) _CoilE |
| **CoilR** | MGGS**LEIRAAFLRQRNTALRTEVAELEQEVQRLENEVSQYETRYGPL**GGGAAALG CLAAALEHHHHHH | 7502.35 | 6.00 | pET28b(+) _CoilR |
| **MiniE** | MGSS**LEIEAAFLERENTALETRVAELRQRVQRLRNEYGPL**GGGAAAWGLCYPWVY GLEHHHHHH | 7322.19 | 6.27 | pET28b(+) _MiniE |
| **MiniR** | MGSS**LEIRVAFLRQRNTALRTEVAELEQEVQRLENRYGPL**GGGAAAWGLCYPWVY GLEHHHHHH | 7349.26 | 6.57 | pET28b(+) _MiniR |
| **Transferrin Receptor 1 (TfR1)** | MMDQARSAFSNLFGGEPLSYTRFSLARQVDGDNSHVEMKLAADEEENADNNMKAS VRKPKRFNGRLCFAAIALVIFFLIGFMSGYLGYCKRVEQKEECVKLAETEETDKS ETMETEDVPTSSRLYWADLKTLLSEKLNSIEFADTIKQLSQNTYTPREAGSQKDE SLAYYIENQFHEFKFSKVWRDEHYVKIQVKSSIGQNMVTIVQSNGNLDPVESPEG YVAFSKPTEVSGKLVHANFGTKKDFEELSYSVNGSLVIVRAGEITFAEKVANAQS FNAIGVLIYMDKNKFPVVEADLALFGHAHLGTGDPYTPGFPSFNHTQFPPSQSSG LPNIPVQTISRAAAEKLFGKMEGSCPARWNIDSSCKLELSQNQNVKLIVKNVLKE RRILNIFGVIKGYEEPDRYVVVGAQRDALGAGVAAKSSVGTGLLLKLAQVFSDMI SKDGFRPSRSIIFASWTAGDFGAVGATEWLEGYLSSLHLKAFTYINLDKVVLGTS NFKVSASPLLYTLMGKIMQDVKHPVDGKSLYRDSNWISKVEKLSFDNAAYPFLAY SGIPAVSFCFCEDADYPYLGTRLDTYEALTQKVPQLNQMVRTAAEVAGQLIIKLT HDVELNLDYEMYNSKLLSFMKDLNQFKTDIRDMGLSLQWLYSARGDYFRATSRLT TDFHNAEKTNRFVMREINDRIMKVEYHFLSPYVSPRESPFRHIFWGSGSHTLSAL VENLKLRQKNITAFNETLFRNQLALATWTIQGVANALSGDIWNIDNEF | 85731.40 | 6.13 | pcDNA3.1_ TfR1 |
| **TfR1-CoilZ** | MDQARSAFSNLFGGEPLSYTRFSLARQVDGDNSHVEMKLAADEEENADNNMKASV RKPKRFNGRLCFAAIALVIFFLIGFMSGYLGYCKRVEQKEECVKLAETEETDKSE TMETEDVPTSSRLYWADLKTLLSEKLNSIEFADTIKQLSQNTYTPREAGSQKDES LAYYIENQFHEFKFSKVWRDEHYVKIQVKSSIGQNMVTIVQSNGNLDPVESPEGY VAFSKPTEVSGKLVHANFGTKKDFEELSYSVNGSLVIVRAGEITFAEKVANAQSF NAIGVLIYMDKNKFPVVEADLALFGHAHLGTGDPYTPGFPSFNHTQFPPSQSSGL PNIPVQTISRAAAEKLFGKMEGSCPARWNIDSSCKLELSQNQNVKLIVKNVLKER RILNIFGVIKGYEEPDRYVVVGAQRDALGAGVAAKSSVGTGLLLKLAQVFSDMIS KDGFRPSRSIIFASWTAGDFGAVGATEWLEGYLSSLHLKAFTYINLDKVVLGTSN FKVSASPLLYTLMGKIMQDVKHPVDGKSLYRDSNWISKVEKLSFDNAAYPFLAYS GIPAVSFCFCEDADYPYLGTRLDTYEALTQKVPQLNQMVRTAAEVAGQLIIKLTH DVELNLDYEMYNSKLLSFMKDLNQFKTDIRDMGLSLQWLYSARGDYFRATSRLTT DFHNAEKTNRFVMREINDRIMKVEYHFLSPYVSPRESPFRHIFWGSGSHTLSALV ENLKLRQKNITAFNETLFRNQLALATWTIQGVANALSGDIWNIDNEFGSGSGSTG **QKVAQLKNRVAYKLKENAKLENIVARLENDNANLEKDIANLEKDIANLERDVAR**TG | 92534.95 | 6.24 | pcDNA3.1_ TfR1-CoilZ |
| **TfR1-CoilE** | MMDQARSAFSNLFGGEPLSYTRFSLARQVDGDNSHVEMKLAADEEENADNNMKAS VRKPKRFNGRLCFAAIALVIFFLIGFMSGYLGYCKRVEQKEECVKLAETEETDKS ETMETEDVPTSSRLYWADLKTLLSEKLNSIEFADTIKQLSQNTYTPREAGSQKDE SLAYYIENQFHEFKFSKVWRDEHYVKIQVKSSIGQNMVTIVQSNGNLDPVESPEG YVAFSKPTEVSGKLVHANFGTKKDFEELSYSVNGSLVIVRAGEITFAEKVANAQS FNAIGVLIYMDKNKFPVVEADLALFGHAHLGTGDPYTPGFPSFNHTQFPPSQSSG LPNIPVQTISRAAAEKLFGKMEGSCPARWNIDSSCKLELSQNQNVKLIVKNVLKE RRILNIFGVIKGYEEPDRYVVVGAQRDALGAGVAAKSSVGTGLLLKLAQVFSDMI SKDGFRPSRSIIFASWTAGDFGAVGATEWLEGYLSSLHLKAFTYINLDKVVLGTS NFKVSASPLLYTLMGKIMQDVKHPVDGKSLYRDSNWISKVEKLSFDNAAYPFLAY SGIPAVSFCFCEDADYPYLGTRLDTYEALTQKVPQLNQMVRTAAEVAGQLIIKLT HDVELNLDYEMYNSKLLSFMKDLNQFKTDIRDMGLSLQWLYSARGDYFRATSRLT TDFHNAEKTNRFVMREINDRIMKVEYHFLSPYVSPRESPFRHIFWGSGSHTLSAL VENLKLRQKNITAFNETLFRNQLALATWTIQGVANALSGDIWNIDNEFGSGSGST GM**LEIEAAFLERENTALETRVAELRQRVQRLRNRVSQYRTRYGPL**GGGCLETG | 92312.77 | 6.34 | pcDNA3.1_ TfR1-CoilE |
| **TfR1-MiniE** | MMDQARSAFSNLFGGEPLSYTRFSLARQVDGDNSHVEMKLAADEEENADNNMKAS VRKPKRFNGRLCFAAIALVIFFLIGFMSGYLGYCKRVEQKEECVKLAETEETDKS ETMETEDVPTSSRLYWADLKTLLSEKLNSIEFADTIKQLSQNTYTPREAGSQKDE SLAYYIENQFHEFKFSKVWRDEHYVKIQVKSSIGQNMVTIVQSNGNLDPVESPEG YVAFSKPTEVSGKLVHANFGTKKDFEELSYSVNGSLVIVRAGEITFAEKVANAQS FNAIGVLIYMDKNKFPVVEADLALFGHAHLGTGDPYTPGFPSFNHTQFPPSQSSG | 91049.28 | 6.06 | pcDNA3.1_ TfR1-MiniE |

| | | | | |
|---|---|---|---|---|
| | LPNIPVQTISRAAAEKLFGKMEGSCPARWNIDSSCKLELSQNQNVKLIVKNVLKE<br>RRILNIFGVIKGYEEPDRYVVVGAQRDALGAGVAAKSSVGTGLLLKLAQVFSDMI<br>SKDGFRPSRSIIFASWTAGDFGAVGATEWLEGYLSSLHLKAFTYINLDKVVLGTS<br>NFKVSASPLLYTLMGKIMQDVKHPVDGKSLYRDSNWISKVEKLSFDNAAYPFLAY<br>SGIPAVSFCFCEDADYPYLGTRLDTYEALTQKVPQLNQMVRTAAEVAGQLIIKLT<br>HDVELNLDYEMYNSKLLSFMKDLNQFKTDIRDMGLSLQWLYSARGDYFRATSRLT<br>TDFHNAEKTNRFVMREINDRIMKVEYHFLSPYVSPRESPFRHIFWGSGSHTLSAL<br>VENLKLRQKNITAFNETLFRNQLALATWTIQGVANALSGDIWNIDNEFGSGSGST<br>GM**LEIEAAFLERENTALETRVAELRQRVQRLRNEYGPL**GGGTG | | | |
| **TfR1-MiniR** | MMDQARSAFSNLFGGEPLSYTRFSLARQVDGDNSHVEMKLAADEEENADNNMKAS<br>VRKPKRFNGRLCFAAIALVIFFLIGFMSGYLGYCKRVEQKEECVKLAETEETDKS<br>ETMETEDVPTSSRLYWADLKTLLSEKLNSIEFADTIKQLSQNTYTPREAGSQKDE<br>SLAYYIENQFHEFKFSKVWRDEHYVKIQVKSSIGQNMVTIVQSNGNLDPVESPEG<br>YVAFSKPTEVSGKLVHANFGTKKDFEELSYSVNGSLVIVRAGEITFAEKVANAQS<br>FNAIGVLIYMDKNKFPVVEADLALFGHAHLGTGDPYTPGFPSFNHTQFPPSQSSG<br>LPNIPVQTISRAAAEKLFGKMEGSCPARWNIDSSCKLELSQNQNVKLIVKNVLKE<br>RRILNIFGVIKGYEEPDRYVVVGAQRDALGAGVAAKSSVGTGLLLKLAQVFSDMI<br>SKDGFRPSRSIIFASWTAGDFGAVGATEWLEGYLSSLHLKAFTYINLDKVVLGTS<br>NFKVSASPLLYTLMGKIMQDVKHPVDGKSLYRDSNWISKVEKLSFDNAAYPFLAY<br>SGIPAVSFCFCEDADYPYLGTRLDTYEALTQKVPQLNQMVRTAAEVAGQLIIKLT<br>HDVELNLDYEMYNSKLLSFMKDLNQFKTDIRDMGLSLQWLYSARGDYFRATSRLT<br>TDFHNAEKTNRFVMREINDRIMKVEYHFLSPYVSPRESPFRHIFWGSGSHTLSAL<br>VENLKLRQKNITAFNETLFRNQLALATWTIQGVANALSGDIWNIDNEFGSGSGST<br>GMGSS**LEIRVAFLRQRNTALRTEVAELEQEVQRLENRYGPL**TG | 91136.41 | 6.14 | pcDNA3.1_<br>TfR1-MiniR |
| **H2B-mEmerald** | MPEPAKSAPAPKKGSKKAVTKAQKKGGKKRKRSRKESYSIYVYKVLKQVHPDTGI<br>SSKAMGIMNSFVNDIFERIAGEASRLAHYNKRSTITSREIQTAVRLLLPGELAKH<br>AVSEGTKAITKYTSAKDPPVATMVSKGEELFTGVVPILVELDGDVNGHKFSVSGE<br>GEGDATYGKLTLKFICTTGKLPVPWPTLVTTLTYGVQCFARYPDHMKQHDFFKSA<br>MPEGYVQERTIFFKDDGNYKTRAEVKFEGDTLVNRIELKGIDFKEDGNILGHKLE<br>YNYNSHKVYITADKQKNGIKVNFKTRHNIEDGSVQLADHYQQNTPIGDGPVLLPD<br>NHYLSTQSALSKDPNEKRDHMVLLEFVTAAGITLGMDELYK | 41320.19 | 9.26 | H2B-6-<br>mEmerald<br>Addgene:<br>54111 |
| **H2B-CoilE** | MPEPAKSAPAPKKGSKKAVTKAQKKGGKKRKRSRKESYSIYVYKVLKQVHPDTGI<br>SSKAMGIMNSFVNDIFERIAGEASRLAHYNKRSTITSREIQTAVRLLLPGELAKH<br>AVSEGTKAITKYTSAKDPM**LEIEAAFLERENTALETRVAELRQRVQRLRNRVSQY<br>RTRYGPL** | 19388.45 | 10.4<br>2 | H2B-6-<br>CoilE |
| **H2B-CoilE-mEmerald** | MPEPAKSAPAPKKGSKKAVTKAQKKGGKKRKRSRKESYSIYVYKVLKQVHPDTGI<br>SSKAMGIMNSFVNDIFERIAGEASRLAHYNKRSTITSREIQTAVRLLLPGELAKH<br>AVSEGTKAITKYTSAKDPPVM**LEIEAAFLERENTALETRVAELRQRVQRLRNRVS<br>QYRTRYGPL**GGGGPVATMVSKGEELFTGVVPILVELDGDVNGHKFSVSGEGEGDA<br>TYGKLTLKFICTTGKLPVPWPTLVTTLTYGVQCFARYPDHMKQHDFFKSAMPEGY<br>VQERTIFFKDDGNYKTRAEVKFEGDTLVNRIELKGIDFKEDGNILGHKLEYNYNS<br>HKVYITADKQKNGIKVNFKTRHNIEDGSVQLADHYQQNTPIGDGPVLLPDNHYLS<br>TQSALSKDPNEKRDHMVLLEFVTAAGITLGMDELYK | 47060.74 | 9.39 | H2B-6-<br>CoilE-<br>mEmerald |
| **H2B-MiniE-mEmerald** | MPEPAKSAPAPKKGSKKAVTKAQKKGGKKRKRSRKESYSIYVYKVLKQVHPDTGI<br>SSKAMGIMNSFVNDIFERIAGEASRLAHYNKRSTITSREIQTAVRLLLPGELAKH<br>AVSEGTKAITKYTSAKDPM**LEIEAAFLERENTALETRVAELRQRVQRLRNEYGPL**<br>PVATMVSKGEELFTGVVPILVELDGDVNGHKFSVSGEGEGDATYGKLTLKFICTT<br>GKLPVPWPTLVTTLTYGVQCFARYPDHMKQHDFFKSAMPEGYVQERTIFFKDDGN<br>YKTRAEVKFEGDTLVNRIELKGIDFKEDGNILGHKLEYNYNSHKVYITADKQKNG<br>IKVNFKTRHNIEDGSVQLADHYQQNTPIGDGPVLLPDNHYLSTQSKLSKDPNEKR<br>DHMVLLEFVTAAGITLGMDELYK | 45775.31 | 9.24 | H2B-6-<br>MiniE-<br>mEmerald |
| **H2B-MiniR-mEmerald** | MPEPAKSAPAPKKGSKKAVTKAQKKGGKKRKRSRKESYSIYVYKVLKQVHPDTGI<br>SSKAMGIMNSFVNDIFERIAGEASRLAHYNKRSTITSREIQTAVRLLLPGELAKH<br>AVSEGTKAITKYTSAKDPM**LEIRVAFLRQRNTALRTEVAELEQEVQRLENRYGPL**<br>PVATMVSKGEELFTGVVPILVELDGDVNGHKFSVSGEGEGDATYGKLTLKFICTT<br>GKLPVPWPTLVTTLTYGVQCFARYPDHMKQHDFFKSAMPEGYVQERTIFFKDDGN<br>YKTRAEVKFEGDTLVNRIELKGIDFKEDGNILGHKLEYNYNSHKVYITADKQKNG<br>IKVNFKTRHNIEDGSVQLADHYQQNTPIGDGPVLLPDNHYLSTQSKLSKDPNEKR<br>DHMVLLEFVTAAGITLGMDELYK | 45802.38 | 9.29 | H2B-6-<br>MiniR-<br>mEmerald |
| **TOMM20-mCherry** | MVGRNSAIAAGVCGALFIGYCIYFDRKRRSDPNFKNRLRERRKKQKLAKERAGLS<br>KLPDLKDAEAVQKFFLEEIQLGEELLAQGEYEKGVDHLTNAIAVCGQPQQLLQVL<br>QQTLPPPVFQMLLTKLPTISQRIVSAQSLAEDDVEGGSGDPPVATMVSKGEEDNM<br>AIIKEFMRFKVHMEGSVNGHEFEIEGEGEGRPYEGTQTAKLKVTKGGPLPFAWDI<br>LSPQFMYGSKAYVKHPADIPDYLKLSFPEGFKWERVMNFEDGGVVTVTQDSSLQD<br>GEFIYKVKLRGTNFPSDGPVMQKKTMGWEASSERMYPEDGALKGEIKQRLKLKDG<br>GHYDAEVKTTYKAKKPVQLPGAYNVNIKLDITSHNEDYTIVEQYERAEGRHSTGG<br>MDELYK | 43840.92 | 6.08 | TOMM20-<br>mCherry-<br>N-10<br>Addgene:<br>55146 |
| **TOMM20-CoilE-** | MVGRNSAIAAGVCGALFIGYCIYFDRKRRSDPNFKNRLRERRKKQKLAKERAGLS<br>KLPDLKDAEAVQKFFLEEIQLGEELLAQGEYEKGVDHLTNAIAVCGQPQQLLQVL | 49157.01 | 6.71 | TOMM20-<br>CoilE- |

| | | | | |
|---|---|---|---|---|
| **mCherry** | QQTLPPPVFQMLLTKLPTISQRIVSAQSLAEDDVEGGSGM**LEIEAAFLERENTAL ETRVAELRQRVQRLRNRVSQYRTRYGPL**DPPVATMVSKGEEDNMAIIKEFMRFKV HMEGSVNGHEFEIEGEGEGRPYEGTQTAKLKVTKGGPLPFAWDILSPQFMYGSKA YVKHPADIPDYLKLSFPEGFKWERVMNFEDGGVVTVTQDSSLQDGEFIYKVKLRG TNFPSDGPVMQKKTMGWEASSERMYPEDGALKGEIKQRLKLKDGGHYDAEVKTTY KAKKPVQLPGAYNVNIKLDITSHNEDYTIVEQYERAEGRHSTGGMDELYK | | | mCherry |
| **TOMM20-MiniE-mCherry** | MVGRNSAIAAGVCGALFIGYCIYFDRKRRSDPNFKNRLRERRKKQKLAKERAGLS KLPDLKDAEAVQKFFLEEIQLGEELLAQGEYEKGVDHLTNAIAVCGQPQQLLQVL QQTLPPPVFQMLLTKLPTISQRIVSAQSLAEDDVEGGSGM**LEIEAAFLERENTAL ETRVAELRQRVQRLRNEYGPL**DPPVATMVSKGEEDNMAIIKEFMRFKVHMEGSVN GHEFEIEGEGEGRPYEGTQTAKLKVTKGGPLPFAWDILSPQFMYGSKAYVKHPAD IPDYLKLSFPEGFKWERVMNFEDGGVVTVTQDSSLQDGEFIYKVKLRGTNFPSDG PVMQKKTMGWEASSERMYPEDGALKGEIKQRLKLKDGGHYDAEVKTTYKAKKPVQ LPGAYNVNIKLDITSHNEDYTIVEQYERAEGRHSTGGMDELYK | 48238.94 | 5.96 | TOMM20-MiniE-mCherry |
| **TOMM20-MiniR-mCherry** | MVGRNSAIAAGVCGALFIGYCIYFDRKRRSDPNFKNRLRERRKKQKLAKERAGLS KLPDLKDAEAVQKFFLEEIQLGEELLAQGEYEKGVDHLTNAIAVCGQPQQLLQVL QQTLPPPVFQMLLTKLPTISQRIVSAQSLAEDDVEGGSGM**LEIRVAFLRQRNTAL RTEVAELEQEVQRLENRYGPL**DPPVATMVSKGEEDNMAIIKEFMRFKVHMEGSVN GHEFEIEGEGEGRPYEGTQTAKLKVTKGGPLPFAWDILSPQFMYGSKAYVKHPAD IPDYLKLSFPEGFKWERVMNFEDGGVVTVTQDSSLQDGEFIYKVKLRGTNFPSDG PVMQKKTMGWEASSERMYPEDGALKGEIKQRLKLKDGGHYDAEVKTTYKAKKPVQ LPGAYNVNIKLDITSHNEDYTIVEQYERAEGRHSTGGMDELYK | 48266.01 | 6.10 | TOMM20-MiniR-mCherry |
| **mCherry** | MVSKGEEDNMAIIKEFMRFKVHMEGSVNGHEFEIEGEGEGRPYEGTQTAKLKVTK GGPLPFAWDILSPQFMYGSKAYVKHPADIPDYLKLSFPEGFNWERVMNFEDGGVV TVTQDSSLQDGEFIYKVKLRGTNFPSDGPVMQCRTMGWEASTERMYPEDGALKGE IKQRLKLKDGGHYDAEVKTTYKAKKPVQLPGAYNVDIKLDILSHNEDYTIVEQYE RAEGRHSTGGMDELYK | 26738.16 | 5.27 | mCherry2-N1 Addgene:54517 |
| **CoilR-mCherry** | **MGGSLEIRAAFLRQRNTALRTEVAELEQEVQRLENEVSQYETRYGPL**DPPVATMV SKGEEDNMAIIKEFMRFKVHMEGSVNGHEFEIEGEGEGRPYEGTQTAKLKVTKGG PLPFAWDILSPQFMYGSKAYVKHPADIPDYLKLSFPEGFNWERVMNFEDGGVVTV TQDSSLQDGEFIYKVKLRGTNFPSDGPVMQCRTMGWEASTERMYPEDGALKGEIK QRLKLKDGGHYDAEVKTTYKAKKPVQLPGAYNVDIKLDILSHNEDYTIVEQYERA EGRHSTGGMDELYK | 32753.87 | 5.13 | CoilR-mCherry2-N1 |
| **MiniE-mCherry** | **MLEIEAAFLERENTALETRVAELRQRVQRLRNEYGPL**DPPVATMVSKGEEDNMAI IKEFMRFKVHMEGSVNGHEFEIEGEGEGRPYEGTQTAKLKVTKGGPLPFAWDILS PQFMYGSKAYVKHPADIPDYLKLSFPEGFNWERVMNFEDGGVVTVTQDSSLQDGE FIYKVKLRGTNFPSDGPVMQCRTMGWEASTERMYPEDGALKGEIKQRLKLKDGGH YDAEVKTTYKAKKPVQLPGAYNVDIKLDILSHNEDYTIVEQYERAEGRHSTGGMD ELYK | 31716.82 | 5.19 | MiniE-mCherry2-N1 |
| **MiniR-mCherry** | **MLEIRVAFLRQRNTALRTEVAELEQEVQRLENRYGPL**DPPVATMVSKGEEDNMAI IKEFMRFKVHMEGSVNGHEFEIEGEGEGRPYEGTQTAKLKVTKGGPLPFAWDILS PQFMYGSKAYVKHPADIPDYLKLSFPEGFNWERVMNFEDGGVVTVTQDSSLQDGE FIYKVKLRGTNFPSDGPVMQCRTMGWEASTERMYPEDGALKGEIKQRLKLKDGGH YDAEVKTTYKAKKPVQLPGAYNVDIKLDILSHNEDYTIVEQYERAEGRHSTGGMD ELYK | 31743.89 | 5.26 | MiniR-mCherry2-N1 |

## Table 4.2. Oligonucleotide sequences

| Primer Name | Sequence<br>Sequence annotation key: restriction enzyme cut site |
|---|---|
| CoilE-1 (NcoI) | GATATACCATGGGCGGCAGCCTGGAAATTGAAGCGGCGTTT |
| CoilE-2 | TCCAGCGCGGTATTTTCACGTTCCAGAAACGCCGCTTCAATTTCC |
| CoilE-3 | GTGAAAATACCGCGCTGGAAACCCGTGTGGCGGAACTGCGTCAGC |
| CoilE-4 | GCTCACACGATTACGCAGACGCTGCACACGCTGACGCAGTTCCGC |
| CoilE-5 | TCTGCGTAATCGTGTGAGCCAGTATCGTACCCGTTATGGCCCGTT |
| CoilE-6 (HindIII) | GCAAGCTTGCCCAGCGCAGCAGCCCCTCCGCCTAACGGGCCATAACGGGT |
| CoilR-1 (NcoI) | GATATACCATGGGCGGCAGCCTGGAAATTGAAGCGGCGTTT |
| CoilR-2 | TCCAGCGCGGTATTTTCACGTTCCAGAAACGCCGCTTCAATTTCC |
| CoilR-3 | GTGAAAATACCGCGCTGGAAACCCGTGTGGCGGAACTGCGTCAGC |
| CoilR-4 | GCTCACACGATTACGCAGACGCTGCACACGCTGACGCAGTTCCGC |
| CoilR-5 | TCTGCGTAATCGTGTGAGCCAGTATCGTACCCGTTATGGCCCGTT |
| CoilR-6 (HindIII) | GCAAGCTTGCCCAGCGCAGCAGCCCCTCCGCCTAACGGGCCATAACGGGT |
| 1F_MiniE (NcoI) | GGTACCATGGGTTCTTCTCTGGAAATCGAAGCG |
| 2R_MiniE | GTGTTTTCACGTTCCAGGAACGCCGCTTCGATTTCCAGAG |
| 3F_MiniE | GTTCCTGGAACGTGAAAACACCGCGCTCGAAACCCGTGTT |
| 4R_MiniE | TGAACACGCTGACGCAGTTCCGCAACACGGGTTTCGAGCG |
| 5F_MiniE | CTGCGTCAGCGTGTTCAGCGTCTGCGTAACGAATACGGTC |
| 6R_MiniE | AGCCGCACCACCACCCAGCGGACCGTATTCGTTACGCAGA |
| 7F_MiniE | GGTGGTGGTGCGGCTGCATGGGGTCTGTGCTACCCGTGGG |
| 8R_MiniE (XhoI) | GTGCTCGAGACCGTAAACCCACGGGTAGCACAGA |
| 1F_MiniR (NcoI) | GCGCCATGGGTTCTTCTCTCGAAATCCGTGTTGCGT |
| 2R_MiniR | CGGTGTTACGCTGACGCAGGAACGCAACACGGATTTCGAG |
| 3F_MiniR | GCGTCAGCGTAACACCGCGCTGCGTACCGAAGTTGCGGAA |
| 4R_MiniR | GACGCTGAACTTCCTGTTCCAGTTCCGCAACTTCGGTACG |
| 5F_MiniR | GGAACAGGAAGTTCAGCGTCTGGAAAACCGTTACGGTCCG |
| 6R_MiniR | TGCCGCAGCACCACCACCCAGCGGACCGTAACGGTTTTCC |
| 7F_MiniR | GGTGGTGCTGCGGCATGGGGTCTGTGCTACCCGTGGGTTT |
| 8R_MiniR (XhoI) | GCGCTCGAGACCGTAAACCCACGGGTAGCACAG |
| TfR1-CoilE 1 F | AAAGCAGCATTGGTCAAAACATGGTGACCATAGTGCAGTCAAATGGTAAC |
| TfR1-CoilE 1 R | TACCAAACTCATTGTCAATATTCCAAATGTC |
| TfR1-CoilE 2 F | TATTGACAATGAGTTTGGTAGCGGCAGC |
| TfR1-CoilE 2 R | CATGTTACATTTAACCGGTCTCGAGACAG |
| TfR1-CoilE 3 F | GACCGGTTAAATGTAACATGCATAATTAAATAAGAG |
| TfR1-CoilE 3 R | AAATGGATATACAAGCTCCCGGGAGCTTTTTGCAAAAGCCTAG |
| TfR1-MiniR F | GCGGCAGCGGTAGCACCGGTATGGGTTCTTCTCTCGAAATCCG |
| TfR1-MiniR R | CATGTTACATTTAACCGGTCAGCGGACCGTAACGGTTTTC |
| TfR1_MiniE_1 | TTGACAATGAGTTTGGTAGCG |
| TfR1_MiniE_2 | AGGCGGCCTCGATCTCCAGCATACCGGTGCTACCGCTGCCGCTACCAAACTCATTGTCAA |
| TfR1_MiniE_3 | GAGATCGAGGCCGCCTTCCTCGAGAGGGAGAACACCGCCCTGGAGACCAGGGTGGCCGAG |

| | |
|---|---|
| TfR1_MiniE_4 | AGAGGGCCGTACTCGTTCCTCAGCCTCTGCACCCTCTGCCTCAGCTCGGCCACCCTGGTC |
| TfR1_MiniE_5 | GAACGAGTACGGCCCTCTGGGAGGCGGAACCGGTTAAATGTAACATGCATAATTAAATAA |
| TfR1_MiniE_6 | CTGCTCTTATTTAATTATGCATGTTACATTTAACCG |
| TfR1-CoilZ F | TGGTAGCGGCAGCGGTAGCACCGGTCAGAAAGTGGCGC |
| TfR1-CoilZ R | TGCATGTTACATTTAACCGGTACGCGCCACGTCACGTTC |
| TOMM20-CoilE-mCh F | GAAGGCGGTAGCGGGATGCTGGAAATTGAAGCGGC |
| TOMM20-CoilE-mCh R | GGCGACCGGTGGATCCAGCGGGCCATAACGGGT |
| TOMM20-MiniR-mCh F | AGATGATGTGGAAGGCGGTAGCGGGATGCTCGAAATCCGTGTTGC |
| TOMM20-MiniR-mCh R | TCACCATGGTGGCGACCGGTGGATCCAGCGGACCGTAACGGTTTTC |
| TOMM20-MiniE-mCh F | AGATGATGTGGAAGGCGGTAGCGGGATGCTGGAGATCGAGGCCGCCTTC |
| TOMM20-MiniE-mCh R | TCACCATGGTGGCGACCGGTGGATCCAGAGGGCCGTACTCGTTCCTCAG |
| H2B-CoilE F | CAGCGCTAAGGATCCAATGCTGGAAATTGAAGCG |
| H2B-CoilE R | TTATGATCTAGAGTCGCTTACAGCGGGCCATAACG |
| H2B-CoilE-mEm F | CTAAGGATCCACCGGTAATGCTGGAAATTGAAGCGGCG |
| H2B-CoilE-mEm R | CATGGTGGCGACCGGTCCGCCGCCACCCAGCGGGCC |
| H2B-MiniE-mEm F | CAGCGCTAAGGATCCAATGCTGGAGATCGAGGCC |
| H2B-MiniE-mEm R | CATGGTGGCGACCGGCAGAGGGCCGTACTCGTTC |
| H2B-MiniR-mEm F | CAGCGCTAAGGATCCAATGCTCGAAATCCGTGTTGC |
| H2B-MiniR-mEm R | CATGGTGGCGACCGGCAGCGGACCGTAACGGTTTTC |
| MiniR-mCherry F | CGACGGTACCGCGGGCCCGGATGCTCGAAATCCGTGTTGC |
| MiniR-mCherry R | ATGGTGGCGACCGGTGGATCCAGCGGACCGTAACGGTTTTC |
| MiniE-mCherry F | GTACCGCGGGCCCGGATGCTGGAGATCGAGGCC |
| MiniE-mCherry R | GGCGACCGGTGGATCCAGAGGGCCGTACTCGTTC |
| CoilR-mCherry F | CGACGGTACCGCGGGCCCGGATGGGCGGCAGCCTTGAAATTC |
| CoilR-mCherry R | ATGGTGGCGACCGGTGGATCCAGCGGGCCATAACGGGTTTCA |

## Table 4.3. Bacterial strains and plasmids

| *E.coli* strains | Characteristics | Source |
|---|---|---|
| TOP10 | F- mcrA Δ( mrr-hsdRMS-mcrBC) Φ80lacZΔM15 Δ lacX74 recA1 araD139 Δ( araleu)7697 galU galK rpsL (StrR) endA1 nupG | ThermoFisher Scientific |
| BL21(DE3) | fhuA2 [lon] ompT gal (λ DE3) [dcm] ΔhsdS λ DE3 = λ sBamHIo ΔEcoRI-B int::(lacI::PlacUV5::T7 gene1) i21 Δnin5 | ThermoFisher Scientific |
| Plasmids | | |
| pET28b(+) | T7 promoter, His-tag coding sequence, MCS, *lacI* coding sequence, (KanR) | Novagen |
| pcDNA3.1 | CMV promoter, MCS, BGH polyadenylation signal, SV40 origin, (AmpR), (KanR) | Invitrogen |
| mCherry-TOMM20-N-10 | CMV promoter, TOMM20, mCherry (C terminal on backbone), (KanR, NeoR) | Addgene: 55146 |
| H2B-6-mEmerald | CMV promoter, HIST1H2BJ, mEmerald (C terminal on backbone), (KanR,NeoR) | Addgene: 54111 |
| mCherry2-N1 | CMV promoter, mCherry, (KanR,NeoR) | Addgene: 54517 |

## Table 4.4. Peptide Properties

| VIP | Sequence | Size (Daltons) | pI | $\varepsilon^{\dagger}$ ($M^{-1}$ $cm^{-1}$) |
|---|---|---|---|---|
| **CoilE tag** | **LEIE AAFLERE NTALETR VAELRQR VQRLRNR VSQYRTR YGPL** | 5202.85 | 10.78 | 2560 |
| **CoilR probe** | MGGS **LEIR AAFLRQR NTALRTE VAELEQE VQRLENE VSQYETR YGPL** GGGAAALGCLAAALE*HHHHHH* | 7502.27 | 6.07 | 2560 |
| **MiniE tag** | **LEIE AAFLERE NTALETR VAELRQR VQRLRNE YGPL** | 4284.79 | 4.93 | 1280 |
| **MiniE probe** | MGSS **LEIE AAFLERE NTALETR VAELRQR VQRLRNE YGPL** GGGAAAWGLCYPWVYGLE*HHHHHH* | 7322.19 | 6.27 | 15470 |
| **MiniR tag** | **LEIR VAFLRQR NTALRTE VAELEQE VQRLENR YGPL** | 4311.91 | 6.38 | 1490 |
| **MiniR probe** | MGSS **LEIR VAFLRQR NTALRTE VAELEQE VQRLENR YGPL** GGGAAAWGLCYPWVYGLE*HHHHHH* | 7349.18 | 6.73 | 15220 |

*† Molar extinction coefficients at 280 nm were calculated using ExPasy (https://web.expasy.org/protparam).*

## Table 4.5. Properties of fluorophores used to label peptides

| Fluorophore | Vendor | Excitation Maximum | Emission Maximum | Quantum Yield (QY) | $\varepsilon_{dye}$ ($M^{-1}$•$cm^{-1}$) | $CF_{280}$ |
|---|---|---|---|---|---|---|
| **Oregon Green 488 Maleimide** | ThermoFisher Scientific | 501 nm | 526 nm | 0.92 (pH 9.0)[51] | 79,000 | 0.12 |
| **Sulfo-Cyanine3 Maleimide** | Lumiprobe | 548 nm | 563 nm | 0.14 (pH 7.0)[52] | 162,000 | 0.06 |
| **TAMRA-DBCO** | Click Chemistry Tools | 552 nm | 571 nm | 0.41 (pH 7.4)[53] | 92,000 | 0.2 |
| **Sulfo-Cyanine5 Maleimide** | Lumiprobe | 646 nm | 662 nm | 0.18 (pH 7.0)[52] | 271,000 | 0.04 |

*Excitation and emission values provided on the Lumiprobe, ThermoFisher or Click Chemistry Tools websites: www.lumiprobe.com, https://www.thermofisher.com/us/en/home.html, https://clickchemistrytools.com/.*

## Table 4.6. Summary of probe peptides

| VIP | Percent labeled | Labeling Reaction | Source |
|---|---|---|---|
| **MiniR-Cy5** | 29%±2% | Solid state maleimide-thiol conjugation | Current work. |
| **MiniR-biotin** | 100% | Solid state maleimide-thiol conjugation | Current work. |
| **MiniE-Cy5** | 59%±1% | Solid state maleimide-thiol conjugation | Current work. |
| **MiniE-OG488** | 64%±2% | Solid state maleimide-thiol conjugation | Current work. |
| **MiniE-TAMRA** | 16%+0% | In-solution thiol-yne reaction | Current work. |
| **MiniE-Cy3** | 52%+2% | Solid state maleimide-thiol labeling | Current work. |
| **MiniE-biotin** | 100% | Solid state maleimide-thiol labeling | Current work. |
| **CoilR-Cy5** | 90% | In-solution maleimide-thiol conjugation | Ref. 1 |
| **CoilR-AF488** | 45% | In-solution maleimide-thiol conjugation | Ref. 6 |
| **CoilY-Cy5** | 50% | In-solution maleimide-thiol conjugation | Ref. 3 |
| **CoilY-biotin** | N/A | In-solution maleimide-thiol conjugation | Ref. 3 |

## Table 4.7. FRET efficiency in nuclei of fixed cells

| H2B-CoilE-mEm CoilR-mCherry | H2B-MiniE-mEm MiniR-mCherry | H2B-MiniR-mEm MiniE-mCherry | H2B-mEm CoilR-mCherry | H2B-mEm MiniR-mCherry | H2B-mEm MiniE-mCherry |
|---|---|---|---|---|---|
| **FRET efficiency (%)** | | | | | |
| 7.6 | 8.7 | 11.9 | -0.9 | -0.5 | 5.1 |
| 5.9 | 20.8 | 10.6 | 4.3 | -1.1 | -1.3 |
| 15.4 | 6.9 | 10.2 | 1.4 | 0.4 | 11.5 |
| 12.4 | 4.4 | 8.3 | -0.6 | -0.4 | 3.4 |
| 12.5 | 7.7 | 4.9 | 0.5 | -0.8 | -0.8 |
| 5.2 | 8.0 | 11.3 | -0.6 | 0.0 | 0.9 |
| 4.5 | 8.9 | 21.2 | -4.4 | -2.5 | 1.1 |
| 7.2 | 18.2 | 18.7 | 3.8 | -0.8 | 9.0 |
| 10.1 | 11.9 | 19.7 | -0.5 | 1.0 | 4.0 |
| 13.0 | 18.0 | 16.4 | 0.2 | -4.0 | -2.9 |
| **Average (%)** | | | | | |
| 9.4 | 11.4 | 13.3 | 0.3 | -0.9 | 3.0 |
| **Standard Error of the Mean (%)** | | | | | |
| 1.2 | 1.8 | 1.7 | 0.8 | 0.5 | 1.5 |

## Works Cited


1. Giepmans, B. N. G., Adams, S. R., Ellisman, M. H. & Tsien, R. Y. The Fluorescent Toolbox for Assessing Protein Location and Function. *Science* **312**, 217–224 (2006).
2. Crivat, G. & Taraska, J. W. Imaging proteins inside cells with fluorescent tags. *Trends Biotechnol.* **30**, 8–16 (2012).
3. Vandemoortele, G., Eyckerman, S. & Gevaert, K. Pick a Tag and Explore the Functions of Your Pet Protein. *Trends Biotechnol.* (2019) doi:10.1016/j.tibtech.2019.03.016.
4. Costantini, L. M. & Snapp, E. L. Fluorescent proteins in cellular organelles: serious pitfalls and some solutions. *DNA Cell Biol.* **32**, 622–627 (2013).
5. Keppler, A. *et al.* A general method for the covalent labeling of fusion proteins with small molecules in vivo. *Nat. Biotechnol.* **21**, 86–89 (2003).
6. Los, G. V. *et al.* HaloTag: A Novel Protein Labeling Technology for Cell Imaging and Protein Analysis. *ACS Chem. Biol.* **3**, 373–382 (2008).
7. Lavis, L. D. Teaching Old Dyes New Tricks: Biological Probes Built from Fluoresceins and Rhodamines. *Annu. Rev. Biochem.* **86**, 825–843 (2017).
8. Griffin, B. A., Adams, S. R. & Tsien, R. Y. Specific Covalent Labeling of Recombinant Protein Molecules Inside Live Cells. *Science* **281**, 269–272 (1998).
9. Adams, S. R. *et al.* New Biarsenical Ligands and Tetracysteine Motifs for Protein Labeling in Vitro and in Vivo: Synthesis and Biological Applications. *J. Am. Chem. Soc.* **124**, 6063–6076 (2002).
10. Howarth, M., Takao, K., Hayashi, Y. & Ting, A. Y. Targeting quantum dots to surface proteins in living cells with biotin ligase. *Proc. Natl. Acad. Sci. U. S. A.* **102**, 7583–7588 (2005).
11. Fernández-Suárez, M. *et al.* Re-directing lipoic acid ligase for cell surface protein labeling with small-molecule probes. *Nat. Biotechnol.* **25**, 1483–1487 (2007).
12. Yano, Y. & Matsuzaki, K. Live-cell imaging of membrane proteins by a coiled-coil labeling method—Principles and applications. *Biochim. Biophys. Acta BBA - Biomembr.* **1861**, 1011–1017 (2019).
13. Yano, Y. & Matsuzaki, K. Tag–probe labeling methods for live-cell imaging of membrane proteins. *Biochim. Biophys. Acta BBA - Biomembr.* **1788**, 2124–2131 (2009).
14. Tsutsumi, H. *et al.* Fluorogenically active leucine zipper peptides as tag-probe pairs for protein imaging in living cells. *Angew. Chem. Int. Ed Engl.* **48**, 9164–9166 (2009).
15. Tsutsumi, H., Abe, S., Mino, T., Nomura, W. & Tamamura, H. Intense blue fluorescence in a leucine zipper assembly. *Chembiochem Eur. J. Chem. Biol.* **12**, 691–694 (2011).
16. Nomura, W. *et al.* Development of crosslink-type tag-probe pairs for fluorescent imaging of proteins. *Biopolymers* **94**, 843–852 (2010).
17. Wang, J., Yu, Y. & Xia, J. Short Peptide Tag for Covalent Protein Labeling Based on Coiled Coils. *Bioconjug. Chem.* **25**, 178–187 (2014).
18. Reinhardt, U. *et al.* Peptide-Templated Acyl Transfer: A Chemical Method for the Labeling of Membrane Proteins on Live Cells. *Angew. Chem. Int. Ed.* **53**, 10237–10241 (2014).

19. Reinhardt, U., Lotze, J., Mörl, K., Beck-Sickinger, A. G. & Seitz, O. Rapid Covalent Fluorescence Labeling of Membrane Proteins on Live Cells via Coiled-Coil Templated Acyl Transfer. *Bioconjug. Chem.* **26**, 2106–2117 (2015).
20. Lotze, J. *et al.* Time-Resolved Tracking of Separately Internalized Neuropeptide Y2 Receptors by Two-Color Pulse-Chase. *ACS Chem. Biol.* (2017) doi:10.1021/acschembio.7b00999.
21. Lebar, T., Lainšček, D., Merljak, E., Aupič, J. & Jerala, R. A tunable orthogonal coiled-coil interaction toolbox for engineering mammalian cells. *Nat. Chem. Biol.* 1–7 (2020) doi:10.1038/s41589-019-0443-y.
22. Zane, H. K., Doh, J. K., Enns, C. A. & Beatty, K. E. Versatile interacting peptide (VIP) tags for labeling proteins with bright chemical reporters. *ChemBioChem* (2017) doi:10.1002/cbic.201600627.
23. Doh, J. K. *et al.* VIPER is a genetically encoded peptide tag for fluorescence and electron microscopy. *Proc. Natl. Acad. Sci.* 201808626 (2018) doi:10.1073/pnas.1808626115.
24. Acharya, A., Ruvinov, S. B., Gal, J., Moll, J. R. & Vinson, C. A Heterodimerizing Leucine Zipper Coiled Coil System for Examining the Specificity of a Position Interactions: Amino Acids I, V, L, N, A, and K. *Biochemistry* **41**, 14122–14131 (2002).
25. Zeng, X., Herndon, A. M. & Hu, J. C. Buried asparagines determine the dimerization specificities of leucine zipper mutants. *Proc. Natl. Acad. Sci. U. S. A.* **94**, 3673–3678 (1997).
26. Gonzalez, L., Woolfson, D. N. & Alber, T. Buried polar residues and structural specificity in the GCN4 leucine zipper. *Nat. Struct. Biol.* **3**, 1011–1018 (1996).
27. Mason, J. M. & Arndt, K. M. Coiled coil domains: stability, specificity, and biological implications. *Chembiochem Eur. J. Chem. Biol.* **5**, 170–176 (2004).
28. Doh, J., Tobin, S. & Beatty, K. Generation of CoilR Probe Peptides for VIPER-labeling of Cellular Proteins. *BIO-Protoc.* **9**, (2019).
29. George, R. A. & Heringa, J. An analysis of protein domain linkers: their classification and role in protein folding. *Protein Eng.* **15**, 871–879 (2002).
30. Zhang, C., Dai, P., Vinogradov, A. A., Gates, Z. P. & Pentelute, B. L. Site-Selective Cysteine-Cyclooctyne Conjugation. *Angew. Chem. Int. Ed Engl.* **57**, 6459–6463 (2018).
31. Kim, Y. *et al.* Efficient Site-Specific Labeling of Proteins via Cysteines. *Bioconjug. Chem.* **19**, 786–791 (2008).
32. Mayle, K. M., Le, A. M. & Kamei, D. T. The Intracellular Trafficking Pathway of Transferrin. *Biochim. Biophys. Acta* **1820**, 264–281 (2012).
33. Zhao, N. & Enns, C. A. Iron Transport Machinery of Human Cells: Players and Their Interactions. *Curr. Top. Membr.* **69**, 67–93 (2012).
34. McGraw, T. E., Greenfield, L. & Maxfield, F. R. Functional expression of the human transferrin receptor cDNA in Chinese hamster ovary cells deficient in endogenous transferrin receptor. *J. Cell Biol.* **105**, 207–214 (1987).
35. Dempsey, G. T., Vaughan, J. C., Chen, K. H., Bates, M. & Zhuang, X. Evaluation of fluorophores for optimal performance in localization-based super-resolution imaging. *Nat. Methods* **8**, 1027–1036 (2011).

36. Chang, Y.-P., Pinaud, F., Antelman, J. & Weiss, S. Tracking bio-molecules in live cells using quantum dots. *J. Biophotonics* **1**, 287–298 (2008).
37. Vu, T. Q., Lam, W. Y., Hatch, E. W. & Lidke, D. S. Quantum dots for quantitative imaging: from single molecules to tissue. *Cell Tissue Res.* **360**, 71–86 (2015).
38. Spencer, D. M., Wandless, T. J., Schreiber, S. L. & Crabtree, G. R. Controlling signal transduction with synthetic ligands. *Science* **262**, 1019–1024 (1993).
39. Fegan, A., White, B., Carlson, J. C. T. & Wagner, C. R. Chemically controlled protein assembly: techniques and applications. *Chem. Rev.* **110**, 3315–3336 (2010).
40. Rutkowska, A. & Schultz, C. Protein Tango: The Toolbox to Capture Interacting Partners. *Angew. Chem. Int. Ed.* **51**, 8166–8176 (2012).
41. Bimolecular fluorescence complementation (BiFC) analysis as a probe of protein interactions in living cells. - PubMed - NCBI. https://www.ncbi.nlm.nih.gov/pubmed/18573091.
42. Zhao, N. *et al.* A genetically encoded probe for imaging nascent and mature HA-tagged proteins in vivo. *Nat. Commun.* **10**, 1–16 (2019).
43. McCullock, T. W., MacLean, D. M. & Kammermeier, P. J. Comparing the performance of mScarlet-I, mRuby3, and mCherry as FRET acceptors for mNeonGreen. *PLOS ONE* **15**, e0219886 (2020).
44. Krogt, G. N. M. van der, Ogink, J., Ponsioen, B. & Jalink, K. A Comparison of Donor-Acceptor Pairs for Genetically Encoded FRET Sensors: Application to the Epac cAMP Sensor as an Example. *PLOS ONE* **3**, e1916 (2008).
45. Van Munster, E. B., Kremers, G. J., Adjobo-Hermans, M. J. W. & Gadella, T. W. J. Fluorescence resonance energy transfer (FRET) measurement by gradual acceptor photobleaching. *J. Microsc.* **218**, 253–262 (2005).
46. Berney, C. & Danuser, G. FRET or No FRET: A Quantitative Comparison. *Biophys. J.* **84**, 3992–4010 (2003).
47. Hoover, D. M. & Lubkowski, J. DNAWorks: an automated method for designing oligonucleotides for PCR-based gene synthesis. *Nucleic Acids Res.* **30**, e43 (2002).
48. Gibson, D. G. Enzymatic assembly of overlapping DNA fragments. *Methods Enzymol.* **498**, 349–361 (2011).
49. Williams, A. M. & Enns, C. A. A mutated transferrin receptor lacking asparagine-linked glycosylation sites shows reduced functionality and an association with binding immunoglobulin protein. *J. Biol. Chem.* **266**, 17648–17654 (1991).
50. Doh, J., Enns, C. & Beatty, K. Implementing VIPER for Imaging Cellular Proteins by Fluorescence Microscopy. *BIO-Protoc.* **9**, (2019).
51. Oregon Green 488 carboxylic acid. in *Handbook of Fluorescent Dyes and Probes* 302–303 (John Wiley & Sons, Ltd, 2015). doi:10.1002/9781119007104.ch109.
52. Lavis, L. D. & Raines, R. T. Bright Building Blocks for Chemical Biology. *ACS Chem. Biol.* **9**, 855–866 (2014).
53. Grimm, J. B. *et al.* A general method to improve fluorophores for live-cell and single-molecule microscopy. *Nat. Methods* **12**, 244–250 (2015).

# Chapter 5: Concluding Remarks

## The Development of Versatile Interacting Peptide (VIP) Tags

In this thesis, I have demonstrated that VIP tags are a viable and effective technology for labeling proteins for light and electron microscopy. Each chapter introduced a new VIP tag alongside validation and imaging applications of the technology.

The inception of the project began with VIP Y/Z (CoilY and CoilZ), described in **Chapter 2**[1]. VIP tags were shown to specifically label target proteins in vitro in cell lysates and on the surface of live cells. VIP Y/Z was bi-directional, meaning either CoilY or CoilZ could serve as the probe or the tag. These labeling properties allowed for the labeling of two target proteins in one sample. Cell surface-localized fluorescent proteins were used as model target proteins for validating VIP Y/Z.

In **Chapter 3**, VIPER, a dimer of CoilE and CoilR, was introduced as the next VIP tag[2]. VIPER was used to specifically label organelle protein markers in order to demonstrate sensitive and specific labeling or proteins inside fixed cells. Next, VIPER was used to image transferrin receptor 1 (TfR1) on the surface of live cells, allowing for tracking of receptor internalization or pulse-chase labeling of receptor populations. The most significant application of VIPER was the demonstration that VIP tags are a new class of protein tags for correlative light and electron microscopy (CLEM). For these studies, CoilE-tagged receptor was labeled with a biotinylated CoilR probe peptide. Subsequent treatment with a streptavidin-conjugated electron-dense nanoparticle allowed for CLEM imaging. Additionally, Qdot particles could be counted, enabling a quantitative assessment of receptors on the cell surface. Using the workflow developed for imaging receptors by SEM, VIPER compared favorably to immunolabeling, outcompeting 4 out of 5 of the antibodies tested.

A smaller, more charge-balanced variant of VIPER, MiniVIPER[3], was described in **Chapter 4**. This tag was selective and bi-directional, as either MiniE or MiniR could serve as the peptide tag. MiniVIPER was validated as a specific and selective tag using organelle protein markers for the mitochondria and nuclei. We generated multiple probe peptide reporters for MiniVIPER, allowing the same protein to be labeled with 1 of 5

different spectrally-distinct probe peptides. Two new applications of VIP tags were described in this chapter. In one case, VIP tags could be combined to allow for imaging of two different protein targets inside one cell. In another case, VIP tags could be used to translocate a fluorescent protein (VIP-mCherry) to the nucleus (H2B-VIP-mEmerald) using in situ dimerization mediated by coiled-coil formation.

## The Limitations of VIP tags

Despite the demonstrated efficacy of VIP tags, the protein target labeling efficiency depends upon the quality of the probe peptides. Future work should focus on improving the conjugation efficiency of labeling probe peptides with fluorophores, through improvements in the reaction or improvements in the isolation of probe peptides. To date, VIP probe peptides are generated by recombinant expression, purification, and in vitro conjugation to reactive fluorophores. This process typically relies on thiol-maleimide chemistry. The ligation efficiency has been highly variable, resulting in probe peptides that were 16-90% labeled with fluorophore. The unlabeled peptide was not separated from the fluorophore-labeled peptide. This means that even with 100% coiled-coil formation on the target protein, the maximum efficiency of VIP labeling would always be equal to the percent conjugation of the fluorophore. In other words, a protein population labeled 100% with a 40% fluorescent-VIP probe would only demonstrate a maximum of 40% target labeling. In the future, the probe peptide quality could be improved a few different ways. For example, the fluorophore conjugation efficiency can be addressed by optimizing the reaction conditions for thiol-maleimide labeling. Alternative ligation chemistry should be considered (i.e., alkyne-azide click chemistry[4,5]). Another strategy is to separate labeled and unlabeled probe peptide during the purification, which would be possible using size-exclusion chromatography[6].

There is another limitation of coiled-coil peptide tags: the probe peptide is cell-membrane impermeable unless modified with a cell-penetrating motif. As a result, the live cell applications with VIP tags detailed in this thesis have been limited to studying proteins on the cell surface. This feature can be beneficial for studying receptors, but excludes dynamic studies of proteins inside living cells. However, we have overcome this issue. In 2019, my collaboration with the Reich group (UC Santa Barbara)

successfully delivered CoilR probe peptide into living cells using hollow-gold nanoshells (HGNs)[7]. The HGNs were functionalized with cell penetrating peptides and CoilR probe peptide. Once the HGNs were inside the cell the cargo was released with 2-photon excitation. This method was used to track and label the mitochondria and histone H2B in living cells.

## Limitations of genetically-modified cell lines

All of the work presented in this thesis relied on transfected or transduced cells that were over-expressing VIP-tagged constructs. Over-expression has a number of drawbacks, including protein misfolding and mislocalization, disturbing cellular function or poorly representing the native levels (and thus behavior) of the protein of study. These are issues encountered in my own work, particularly when using fluorescent protein fusions. I also observed large variations in expression levels from cell to cell. I overcame this issue whenever possible by selectively imaging cells that had similar levels of protein expression between tagged and untagged protein targets.

In future VIP technology applications, such as studying novel cell biology, the tagged protein's expression levels should be controlled so that they represent endogenous expression levels of the target protein. This can be achieved with inducible promoters, isolation of a stable, clonal cell line, or, better yet, integration of the VIP tag sequence at the endogenous locus of the target in the genome. A knock-in of the VIP tag at the endogenous location is the most desirable as even a clone with "perfect" levels of expression does not have control over where the gene is integrated nor will it be controlled by the endogenous promotor of the protein of interest.

## Future Directions

In the initial inception of VIP tags, we chose tight-binding peptides to ensure the durability and stability of the reporter labeling. VIPER, as an example, was designed from a high affinity coiled-coil pair ($K_D$ = 13 pM[8]) and is thus expected to be irreversible. There are benefits and applications however, to lower affinity peptides. The first example would be cyclic fluorescence[9,10]. Cyclic fluorescence enables imaging of more targets without expanding the number of colors. Two or more targets can be labeled

with the same color through the unbinding of probes after imaging, allowing consecutive rounds of labeling of different targets with the same fluorophore color. Another application is PAINT[11–13] super-resolution imaging, where the stochastic binding and unbinding of fluorescent probes can be used to make targets “blink” for localization microscopy.

The E3-K3 peptide pair, for example, has been documented to be reversible[14,15] with a $K_D$ of 70 nM. New VIP tag sequences could be designed with lower affinities to enable stochastic binding and unbinding. For localization microscopy, a $k_{on}$ of $10^6$ $(Ms)^{-1}$ was suggested[12]. Alternatively, existing dimers, such as VIP Y/Z and VIPER, could be redesigned to reduce their affinity. In the case of redesigning VIP pairs, adding branched or bulky hydrophobic resides in the binding interface (*a* and *d* position of the coiled-coil) or the removal of salt bridges (*g* and *e* position) can lower binding stability [16,17].

In future work, VIP tags could be adjusted to enable the brighter reporter signal. Bright fluorescent signal is needed for long-term imaging applications or for screening and imaging of rare targets[18,19]. This can be done in two ways, addressing either the VIP tag or the probe peptide. First, VIP tags can be encoded as tandem repeats, similar in approach to the SunTag[20], to allow for multiple probe peptides to be added to a target protein. Alternatively, the probe peptide itself could be modified with multiple fluorophores per peptide. Care would be taken to ensure that the fluorophores were not so proximal that they would quench each other, which would result in a loss of fluorescence[21]. Both approaches can be additionally combined for even brighter signal. Overall, brighter probes are a desirable feature of any labeling method due to the benefits they provide to microscopic imaging in overcoming photobleaching or the difficulty of imaging rare targets.

In addition to further development of the VIP technology, future work should focus on the application of VIP tags to learn new, previously inaccessible biology. As an example, I initiated a collaboration with Caroline Enns (OHSU) to study iron sensing using VIP tags. Appendix D details preliminary results showing the use of VIP tags to study and image Hfe and Transferrin receptor 2 (Tfr2). Hfe and Tfr2 are mouse variants of the human proteins, HFE and TfR2.

HFE is a crucial protein in maintaining iron homeostasis, but the molecular mechanism of regulation remains unknown. A model has been proposed where TfR2 is a co-receptor for HFE, and helps HFE sense iron. In this model TfR2 and HFE are expected to bind and traffic into the cell together as a result of iron saturation. As HFE lacks a good antibody, VIP tags open up the opportunity to track HFE in cells, allowing us to prove or disprove this proposed model of iron sensing.

In conclusion, this thesis demonstrated that VIP tags are an effective and specific genetically-encoded peptide tag for fluorescence and electron microscopy. VIP tags enable fixed-cell imaging, live-cell imaging, and the observation of multiple targets simultaneously by multi-color fluorescence imaging. VIP tags also enable protein translocation or the ability to swap reporters with ease. The limitations described above are surmountable in future work. For example, we already demonstrated the intracellular delivery of probe peptides by hollow gold nanoshells allowed VIP tags to be used for imaging proteins inside of live cells. Lastly, some future ideas for the progression of this project include designing lower-affinity VIP tags for reversible binding, increasing the brightness of VIP tags, and using VIP tags in cell biology applications.

## Works Cited


1. Zane, H. K., Doh, J. K., Enns, C. A. & Beatty, K. E. Versatile interacting peptide (VIP) tags for labeling proteins with bright chemical reporters. *ChemBioChem* (2017) doi:10.1002/cbic.201600627.
2. Doh, J. K. *et al.* VIPER is a genetically encoded peptide tag for fluorescence and electron microscopy. *Proc. Natl. Acad. Sci.* 201808626 (2018) doi:10.1073/pnas.1808626115.
3. Doh, J. K., Tobin, S. & Beatty, K. E. MiniVIPER is a peptide tag for imaging and translocating proteins in cells. (2020).
4. Sletten, E. M. & Bertozzi, C. R. Bioorthogonal Chemistry: Fishing for Selectivity in a Sea of Functionality. *Angew. Chem. Int. Ed.* **48**, 6974–6998 (2009).
5. Kolb, H. C., Finn, M. G. & Sharpless, K. B. Click Chemistry: Diverse Chemical Function from a Few Good Reactions. *Angew. Chem. Int. Ed.* **40**, 2004–2021 (2001).
6. Porath, J. & Flodin, P. Gel filtration: a method for desalting and group separation. *Nature* **183**, 1657–1659 (1959).
7. Morgan, E., Doh, J. K., Beatty, K. E. & Reich, N. O. VIPERnano : Improved live cell intracellular protein tracking. *ACS Appl. Mater. Interfaces* (2019) doi:10.1021/acsami.9b12679.
8. Moll, J. R., Ruvinov, S. B., Pastan, I. & Vinson, C. Designed heterodimerizing leucine zippers with a ranger of pIs and stabilities up to 10−15 M. *Protein Sci. Publ. Protein Soc.* **10**, 649–655 (2001).
9. Lin, J.-R., Fallahi-Sichani, M. & Sorger, P. K. Highly multiplexed imaging of single cells using a high-throughput cyclic immunofluorescence method. *Nat. Commun.* **6**, 1–7 (2015).
10. Lin, J.-R., Fallahi-Sichani, M., Chen, J.-Y. & Sorger, P. K. Cyclic Immunofluorescence (CycIF), A Highly Multiplexed Method for Single-cell Imaging. *Curr. Protoc. Chem. Biol.* **8**, 251–264 (2016).
11. Sharonov, A. & Hochstrasser, R. M. Wide-field subdiffraction imaging by accumulated binding of diffusing probes. *Proc. Natl. Acad. Sci. U. S. A.* **103**, 18911–18916 (2006).
12. Nieves, D. J., Gaus, K. & Baker, M. A. B. DNA-Based Super-Resolution Microscopy: DNA-PAINT. *Genes* **9**, (2018).
13. Schnitzbauer, J., Strauss, M. T., Schlichthaerle, T., Schueder, F. & Jungmann, R. Super-resolution microscopy with DNA-PAINT. *Nat. Protoc.* **12**, 1198–1228 (2017).
14. Yano, Y. *et al.* Coiled-Coil Tag−Probe System for Quick Labeling of Membrane Receptors in Living Cells. *ACS Chem. Biol.* **3**, 341–345 (2008).
15. Reinhardt, U. *et al.* Peptide-Templated Acyl Transfer: A Chemical Method for the Labeling of Membrane Proteins on Live Cells. *Angew. Chem. Int. Ed.* **53**, 10237–10241 (2014).
16. Hodges, R. S. De novo design of α-helical proteins: basic research to medical applications. *Biochem. Cell Biol.* **74**, 133–154 (1996).
17. Lupas, A. Coiled coils: new structures and new functions. *Trends Biochem. Sci.* **21**, 375–382 (1996).
18. Sanderson, J. *Understanding Light Microscopy*. (John Wiley & Sons, 2019).
19. Zhang, J., Mehta, S. & Schultz, C. *Optical Probes in Biology*. (CRC Press, 2016).

20. Tanenbaum, M. E., Gilbert, L. A., Qi, L. S., Weissman, J. S. & Vale, R. D. A protein-tagging system for signal amplification in gene expression and fluorescence imaging. *Cell* **159**, 635–646 (2014).
21. Albani, J. R. Chapter 4 - Fluorescence Quenching. in *Structure and Dynamics of Macromolecules: Absorption and Fluorescence Studies* (ed. Albani, J. R.) 141–192 (Elsevier Science, 2004). doi:10.1016/B978-044451449-3/50004-6.

# Appendix A: Generation of CoilR probe peptides for VIPER-labeling of cellular proteins

**Julia K. Doh**, Savannah J. Tobin, and Kimberly E. Beatty

*This work is adapted from a manuscript originally published by Bio-Protocol on November 5, 2019 in volume 9, issue 21. It has been adapted for this dissertation and reprinted with permission. Dr. Beatty, Savannah Tobin, and I developed the methods and authored the protocols in this appendix chapter.*

## Abstract

Versatile Interacting Peptide (**VIP**) tags are a new class of genetically-encoded tag designed for imaging cellular proteins by fluorescence and electron microscopy. In 2018, we reported the VIPER tag[1], which contains two elements: a genetically-encoded peptide tag (i.e., CoilE) and a probe peptide (i.e., CoilR). These two peptides deliver contrast to a protein of interest by forming a specific, high-affinity heterodimer. The probe peptide was designed with a single cysteine residue for site-specific modification via thiol-maleimide chemistry. This feature can be used to attach a variety of biophysical reporters to the peptide, including bright fluorophores for fluorescence microscopy or electron-dense nanoparticles for electron microscopy. In this Bio-Protocol, we describe our methods for expressing and purifying recombinant CoilR. Additionally, we describe protocols for making fluorescent or biotinylated probe peptides for labeling CoilE-tagged cellular proteins.

## Background

Fluorescence microscopy (FM), electron microscopy (EM), and correlative light and EM (CLEM) enable investigations into the multi-protein complexes and macromolecular interactions that mediate normal and disease-associated cellular functions. However, multiscale microscopy is restricted by the shortage of methods for attaching FM-, EM-, and CLEM-compatible reporter chemistries to target proteins. Additionally, there are few methods for protein labeling that facilitate switching between

imaging systems. As a result, most multiscale imaging studies obtain protein-specific contrast with immunolabeling. However, there are known drawbacks to immunolabeling. The large size of antibodies reduces localization precision, and labeling protocols can disrupt cellular ultra-structure[2]. Scarce proteins and rare interactions can elude detection unless immunolabeling is efficient[2-4]. Many antibodies have poor target specificity and cross-reactivity[5-8], which can result in misleading observations.

The central obstacle that has limited progress in multiscale microscopy is the shortage of genetic tags for labeling proteins. Most tags were developed for FM[9], with the most commonly used tags being fluorescent proteins [*e.g.*, GFP[10]][11,12]. By comparison, there are few genetic tags for EM or CLEM[13]. We saw this as an opportunity to create a new class of genetically-encoded peptide tags for multiscale microscopy[1,14]. We named this technology Versatile Interacting Peptide (VIP) tags (**Figure A.1**). VIP tags consist of a heterodimeric coiled-coil between a genetically-encoded peptide tag and a reporter-conjugated peptide ("probe peptide"). Binding is driven by a hydrophobic interface and inter-strand salt bridges between the two coils. Initially we reported VIP Y/Z, which was used to label cellular proteins with fluorophores and Qdots[14]. This pair consists of a heterodimeric CoilY-CoilZ pair with a reported dissociation constant ($K_D$) of less than 15 nM[15]. Either CoilY or CoilZ could serve as the genetically-encoded tag. In 2018, we reported the VIPER tag, which enables high-affinity labeling of proteins for imaging by FM and CLEM[1]. Binding between the CoilE tag and the CoilR probe peptide to form VIPER is specific and nearly irreversible [$K_D$ ~$10^{-11}$ M[16]].

For VIP tags, the versatility is imparted by the customizable probe peptide. After introduction of the CoilE tag onto a target protein, the protein can be labeled with one of many different reporters attached to CoilR (**Figure A.2**). For example, we imaged the transmembrane receptor, TfR1-CoilE, with CoilR-BODIPY, CoilR-Cy5 (see **Figure A.1**), and CoilR-biotin[1]. In other words, the probe peptide can be customized for different studies or imaging systems without changing the genetic tag. This is possible because CoilR encodes a single cysteine residue for site-specific modification via thiol-maleimide chemistry. The CoilR probe peptide can be bioconjugated to a variety of probes,

including fluorophores, small molecules (*e.g.*, biotin), or nanoparticles. Many companies sell thiol-reactive probes, which makes this conjugation reaction accessible to labs without synthetic chemistry expertise. For more information on bioconjugation reactions, we recommend reading Hermanson's *Bioconjugate Techniques*[17].

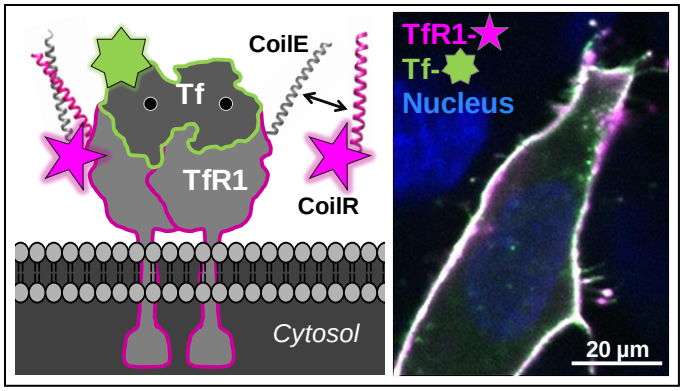


**Figure A.1. Versatile interacting peptide (VIP) tags are a new technology for imaging proteins by FM, EM, or CLEM.** VIPER labeling of transferrin receptor 1 (TfR1) is mediated by heterodimer formation between the CoilE tag and a fluorescent CoilR probe peptide. Fluorescent micrograph: VIPER-tagged TfR1 labeled with CoilR-Cy5 (magenta) and colocalized with fluorescent transferrin (Tf-AF488; green) at the cell surface of transfected CHO TRVb cells (63x magnification). Magenta-green signal overlap appears white and nuclei are blue.

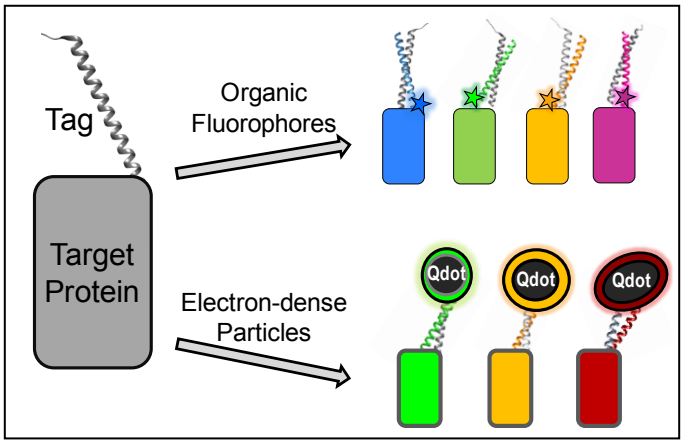


**Figure A.2. VIP tags are a versatile technology for multi-scale microscopy.** After a target protein is tagged, it can be labeled using a variety of probe peptides selected for the particular application.

In this Bio-Protocol, we provide methods for making CoilR probe peptides that can be used for VIPER-labeling of cellular proteins for imaging by FM or EM. The CoilR

peptide and the CoilE tag sequences are provided in **Table A.1**. As described in prior work[1], we used gene assembly PCR to enable the recombinant expression of probe peptides in *E. coli*. The method for peptide expression is described in Procedure A. CoilR was designed to interact with CoilE via an optimized alpha-helical coil-coil, as originally described by Vinson and coworkers[16]. We included a hexahistidine tag at the C-terminus of CoilR for purification by immobilized metal affinity chromatography (IMAC)[18]; this is described in **Procedure B**.

**Table A.1. Sequences of CoilR and CoilE**

| Peptide | **Amino acid sequence** (designated by 1-letter amino acid code)[§]<br>*defg abcdefg abcdefg abcdefg abcdefg abcdefg*[ǂ] | MW (kDa) |
|---|---|---|
| **CoilR** (Probe peptide) | *MGGS* **LEIR AAFLRQR NTALRTE VAELEQE VQRLENE VSQYETR YGPL** *GGGAAALG* **C** *LAAA*LE HHHHHH | 7.5 |
| **CoilE** (Genetic tag) | **LEIE AAFLERE NTALETR VAELRQR VQRLRNR VSQYRTR YGPL** | 5.2 |

[§] *Italics*: Linker sequence; **Bold**: Peptide coil; **C**: Cysteine (conjugation site).

[ǂ] Heptad position. Residues *a* and *d* form a hydrophobic interface, residues at *e* and *g* form interstrand salt bridges.

**Procedures C** and **D** describe thiol-maleimide reactions to label CoilR with a small molecule reporter. In Procedure C, we describe the method that we used to generate probe peptides in our prior work[1]. In Procedure D, we adapted a method described by Weiss and coworkers for solid state-based labeling of peptides[19]. Lastly, we include methods for purifying fluorophore-labeled (**Procedure E**) or biotinylated (**Procedure F**) probe peptide.

## Materials and Reagents

*Note: "*" indicates a brand that is critical to the success of the experiment.*

### Materials

1. Universal pipette tips (USA Scientific TipOne™, catalog numbers: 1112-1770, 1163-1730, and 1121-3812)
2. Microcentrifuge tubes, 1.5 ml (Thermo Scientific, catalog number: 02-682-002)
3. Sterile serological pipettes (Thermo Scientific, catalog number: 13-678-11D + E)
4. Sterile 14 ml culture tubes (Corning, Falcon™, catalog number: 352059)
5. Disposable polystyrene spectrophotometer cuvettes (Thermo Scientific, catalog number: 14-955-127)

6. Conical 50 ml tubes (Thermo Scientific, Nunc™, catalog number: 12-565-270)
7. Chromatography column (Bio-Rad, Econo-Pac™, catalog number: 7321010)
8. Ring stand (Fisher, catalog number: 11-474-207)
9. Adjustable ring stand clamps (United Scientific Supplies, catalog number: CLHD03)
10. Molecular weight cut off (MWCO) 3 kDa filters (Sigma-Aldrich, Amicon Ultra™, catalog number: UFC900324)
11. Quartz 10.00 mm cuvette (Hellma Analytics, Ultra-Micro Cell, catalog number: 105-250-15-40)

**Reagents**

1. pET28b(+)_CoilR [Available by MTA from OHSU or made as published[1]]
2. BL21 (DE3) *E. coli* (New England Biolabs, catalog number: C2527I)
3. SOC outgrowth media (New England Biolabs, provided with catalog number: C2527I)
4. Miller Luria-Bertani (LB) agar (BD Difco™, catalog number: 244520)
5. Miller LB broth (BD Difco™, catalog number: BD 244610)
6. 2X YT (Thermo Scientific, Fisher BioReagents, catalog number: BP9743500)
7. Kanamycin sulfate (Thermo Scientific, Fisher Chemical, catalog number: BP906-5)
8. IPTG (GoldBio, catalog number: I2481C5)
9. *Ni-NTA agarose (Qiagen, catalog number: 30230)
10. *Pierce Monomeric Avidin Agarose (Thermo Scientific Pierce™, catalog number: 20228)
11. Sodium Phosphate Monobasic Anhydrous (Thermo Scientific, Fisher BioReagents™, catalog number: BP329-500)
12. Urea (Thermo Scientific, Fisher BioReagents™, catalog number: U15 3)
13. Tris Base (Thermo Scientific, Fisher BioReagents™, catalog number: BP152 5)
14. Tris HCl (Thermo Scientific, Fisher BioReagents™, catalog number: BP153 1)
15. NaCl (Thermo Scientific, Fisher BioReagents™, catalog number: BP358-1)
16. Glycerol (Thermo Scientific, Fisher BioReagents™, catalog number: BP229-1)

17. Imidazole (ACROS Organics, catalog number: AC39674-1000)
18. Coomassie Brilliant Blue R-250 (Thermo Scientific, catalog number: 20278)
19. Methanol (Thermo Scientific, Fisher Chemical, catalog number: A412)
20. Acetone (Thermo Scientific, Fisher Chemical, catalog number: A18)
21. Nitrogen gas
22. Ammonium sulfate (EMD Millipore, catalog number: AX1385-1)
23. TCEP-HCl (GoldBio, catalog number: TCEP10)
24. Dithiothreitol (DTT) (Thermo Scientific, Molecular Probes™, catalog number: D1532)
25. TC-grade DMSO (Sigma, catalog number: D2650-5X10ML)
26. *Sulfo-Cy5-maleimide (Lumiprobe, catalog number: 23380)
27. *Biotin-PEG2-maleimide (Thermo Scientific, catalog number: 21901BID)
28. D-Biotin (Ark Pharma, catalog number: AK-44010)
29. Pierce BCA assay kit (Thermo Fisher Scientific, catalog number: 23227)
30. 12% Bis-Tris polyacrylamide protein gels (Bio-Rad Criterion™ XT, catalog number: 3450119)
31. MES (Thermo Scientific, Fisher BioReagents™, catalog number: BP300-100)
32. Anti-biotin HRP antibody (Jackson Immunoresearch, catalog number: 200-032-211)
33. Streptavidin-HRP (Thermo Scientific, catalog number: ENN100)

**Equipment**

1. Pipettes (*e.g.*, Rainin Pipet-Lite™ XLS, catalog numbers: 17014407, 17014411, 17014412, and 17014413)
2. Glass 2 L Erlenmeyer flask (Corning, Pyrex™, catalog number: 49802L)
3. Electronic pipettor (Eppendorf Easypet™, catalog number: 4430000018)
4. -20 °C freezer (Thermo Scientific, Revco™, catalog number: 13 990 206)
5. Incubator and shaker (New Brunswick Excella™ E24, catalog number: M1352-0010)
6. Spectrophotometer (Eppendorf, Biophotometer Plus, catalog number: 6132)
7. Rotisserie (Thermo Scientific, catalog number: 400110Q)

8. Sonifier (Branson Ultrasonics™, catalog number: 101063198R)
9. Sonifier 1/8 inch micro-tip (Branson Ultrasonics™, catalog number: 22-309796)
10. Refrigerated centrifuge (Thermo Scientific, Sorvall Legend XTR Centrifuge, catalog number: 75211731)
11. Microcentrifuge (Eppendorf, catalog number: 022620304)
12. Heat block (Fisher, Isotemp™, catalog number: 88-860-022)
13. Electrophoresis cell (Bio-Rad Criterion™, catalog number: 165-6001)
14. Power supply (Bio-Rad PowerPac™ HC, catalog number: 1645052)
15. Plate reader (Tecan Infinite M200 Pro, catalog number: 30050303)
16. (Optional) Fluorescence and western blot imager (i.e., GE Healthcare Amersham™ Typhoon 5 multimode scanner, catalog number: 29187191 or Protein Simple, FluorChem Q)

## Procedures

### A. Expression of recombinant CoilR

CoilR is generated by recombinant expression in *E. coli*. The growth and purification of CoilR follows standard protocols for making and purifying histidine-tagged peptides under inducible expression. For detailed background, protocols, and troubleshooting, we recommend referring to the *Qiaexpressionist* handbook (Qiagen)[20].

1. Obtain or generate a plasmid encoding the CoilR peptide (*i.e.*, pET28b(+)_CoilR)[1].

*Note: The pET28b(+)_CoilR plasmid encodes kanamycin resistance.*

2. Transform the plasmid into *E. coli* BL21 (DE3) competent cells, following NEB's instructions for product C2527.
    a. Plate cells on LB/agar/kanamycin (50 µg/ml) and grow overnight at 37 °C.
    b. Pick single colonies and inoculate 5 ml starter cultures (one colony per 5 ml culture) in LB supplemented with kanamycin (50 µg/ml) in sterile 14 ml culture tubes.
    c. Grow overnight in a shaking incubator (225 rpm, 37 °C). We grow several starter cultures in case of variation in growth is observed (e.g., a culture grows slowly).

3. Use one overnight culture to inoculate (2.5 ml, 1:200 dilution) 500 ml of 2X YT sterile media in a 2 L Erlenmeyer flask supplemented with kanamycin (50 µg/ml). Grow at 225 rpm, 37 °C until the $OD_{600}$ reaches 0.8 to 1.0.
    a. Monitor growth by measuring $OD_{600}$ of the culture in a disposable cuvette on a spectrophotometer.
    b. It will take approximately 2-4 h for the culture to reach this $OD_{600}$.
    c. Prior to induction, take a 1 ml sample of the uninduced culture for peptide expression analysis by SDS-PAGE.
        i. For each sample: Pellet 1 ml of bacterial culture in a microcentrifuge tube (10,000 *x g*, 2 min).
        ii. Resuspend the pellet in Buffer B (Recipe 1). Normalize the sample by adding Buffer B to the pellet. Use the equation: volume = $OD_{600}$ x 100 µl Buffer B.
        iii. Freeze at -20 °C.
4. Lower the temperature of the incubator/shaker to 25 °C and induce peptide expression for 2-4 h by addition of 0.1 mM IPTG.

*Note: The peptide will degrade if the induction is done at 37 °C, reducing the overall yield.*

    a. Monitor expression by taking 1 ml samples every hour during the induction. Normalize as described in **Step A3c**.
5. Harvest cells by centrifugation in a refrigerated centrifuge (5,000 *x g*, 15 min, 4 °C).
    a. Discard the supernatant.
    b. Transfer the pelleted bacteria to a tared 50 ml conical tube to obtain the weight of the wet pellet.
    c. Store the pellet frozen (-20 °C). The pellet can be stored for several months at -20 °C.

*Note: If desired, cell lysis (Step B4) can be performed the same day as the peptide expression. However, we typically freeze the pellet before proceeding to purification the next day.*

6. Analyze peptide expression by SDS-PAGE. See **Figure A.3** for a representative

SDS-PAGE analysis of CoilR expression and purification.

a. Thaw protein samples from time-points collected during induction. Freezing and thawing in the presence of Buffer B will partially lyse the cells.

*Note: If lysis is incomplete, freeze-thaw the samples several times to break open cells.*

b. Pellet insoluble debris (10 min, 10,000 *x g*).
c. Transfer the clarified lysate to a new microcentrifuge tube.
d. Add 5x TCEP-SDS loading dye (Recipe 5). Boil samples for 5 min, pellet by centrifugation, and then load 10-15 µl sample/well onto the protein gel.
e. Analyze peptide expression by SDS-PAGE.
    i. We recommend analyzing on a BioRad Criterion Bis-Tris Gel (12%; 26-well) run in MES running buffer (Recipe 4) at constant voltage (180 V).
    ii. Run until the loading dye reaches the bottom of the gel, approximately 35 min.
    iii. After electrophoresis, stain the protein gel with Coomassie stain (Recipe 6) and then destain (Destain solution, Recipe 7) before imaging.
    iv. CoilR will migrate on the gel as a monomer (7.5 kDa) and a dimer (15 kDa).

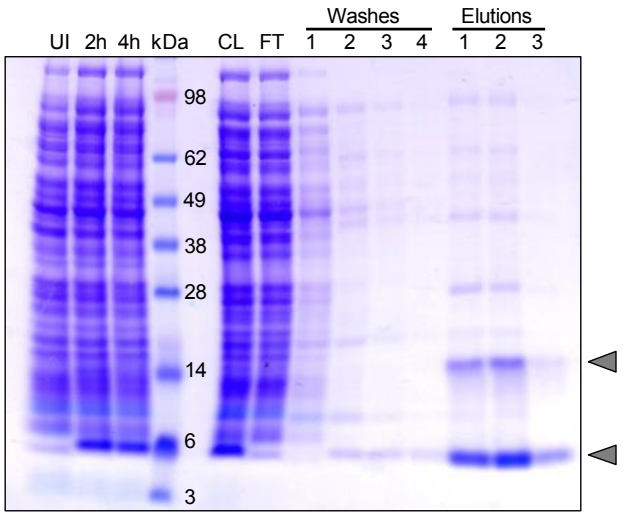


**Figure A.3. Peptide expression in *E. coli* and denaturing purification of CoilR.** Samples were collected from uninduced (UI) and induced (2 h and 4 h) cells, lysed, and resolved by SDS-PAGE. CoilR was purified from clarified lysate by IMAC (i.e., on Ni-NTA resin) under denaturing conditions. CL = clarified lysate; FT = flow-through (unbound fraction). Wash 1: Buffer B (pH 8) with 10 mM imidazole. Washes 2-4: Buffer C (pH 6.8) with 10 mM imidazole. Elutions 1-3: Buffer E (pH 4.3). The CoilR peptide (MW = 7502.35 Da) migrates as a monomer at ~6 kDa and an apparent dimer at ~14 kDa (gray arrowheads).

## B. Purification of recombinant CoilR by IMAC

1. Prior to peptide purification, measure and adjust the pH of all purification buffers.
   a. Buffer B: 8 M Urea, 100 mM $NaH_2PO_4$, 10 mM Tris-Cl, pH 8 (Recipe 1)
   b. Buffer C: 8 M Urea, 100 mM $NaH_2PO_4$, 10 mM Tris-Cl, pH 6.5 (Recipe 2)
   c. Buffer E: 8 M Urea, 100 mM $NaH_2PO_4$, 10 mM Tris-Cl, pH 4.5 (Recipe 3)

*Note: Unless otherwise noted, all steps should be done on ice with pre-chilled buffers.*

2. Thaw the *E. coli* pellet (from **Step A5**) on ice.
3. Resuspend the pellet in Buffer B. Use 5 ml Buffer B per gram of wet weight.
4. Lyse by sonication on ice.
   a. We use a Branson sonifier fitted with a 1/8" Branson microtip to lyse bacteria. We lysed cells at 40% duty cycle, output: 4. The sample was pulsed for 30 sec and then left to rest for 1 min on ice for 8 cycles.
   b. Avoid foaming of the sample, which will cause protein loss.
   c. Alternatively, cells can be lysed by other methods (*e.g.*, freeze-thaw or French press).

5. Clarify the lysate by centrifugation in a refrigerated centrifuge (10,000 *x g*, 30 min, 4 °C).

*Note: Keep a sample of the clarified lysate for analysis by SDS-PAGE.*

6. Incubate the clarified lysate with Ni-NTA agarose resin (Qiagen) for 1 h at 4 °C on a rotisserie.
    a. Buffer B should be supplemented with 10-20 mM imidazole to reduce non-specific protein binding to the resin.
    b. Use 1 ml of resin per 1 gram of pellet (wet weight).
    c. Alternatively, bind at 4 °C overnight.

*Note: If you observe CoilR peptide in the flow through and initial washes then the resin was overloaded. Use more resin in the binding step.*

7. Load the lysate-resin mixture onto a clean, fritted chromatography column.
8. Collect the flow-through. Save a sample for analysis by SDS-PAGE.
9. Wash the resin with 5 column volumes (CV) of Buffer B.
10. Wash the resin with 10-50 CV of Buffer C.
    a. The CoilR peptide will elute at ~pH 6. The wash buffer should be between pH 6.3 – pH 7.0.
    b. Save a sample from each wash step to analyze by SDS-PAGE.
    c. Wash until no further impurities elute.
11. Elute the CoilR peptide in Buffer E. Elute in 5 fractions of 2 CV each.
    a. Most of the peptide will elute in the first 3 elutions.
    b. Elute in additional volume if you detect incomplete elution (see **Figure A.3**).
12. Monitor the purification by SDS-PAGE. Analyze samples from the clarified lysate, flow-through, washes, and elution.
    a. Gel running conditions are the same as from **Step A6d-A6e**.
13. Combine fractions containing the purified peptide based on results from Step B12.
14. Concentrate and exchange the purified CoilR into desired buffer using a 3 kDa MWCO filter.
    a. We recommend exchanging into TBS Urea (Recipe 9) using the MWCO filter. This buffer is compatible with the thiol-maleimide conjugation reaction

(**Procedure C**).

b. Keep the peptide concentration between 0.5 mg/ml and 2 mg/ml to avoid issues with solubility. If a white precipitate is observed in the peptide solution, the peptide is too concentrated.

15. Quantify the peptide concentration using the Pierce BCA assay kit (Thermo Fisher Scientific).
    a. The protein concentration can also be estimated by measuring the absorbance at 280 nm. However, the extinction coefficient of CoilR is low (2,980 $L \cdot mol^{-1} \cdot cm^{-1}$); so the concentration will be more accurate if determined by BCA assay.
    b. Include replicates and dilutions to obtain an accurate concentration.
16. Add 5-10% glycerol to the concentrated peptide, aliquot (200 µl/tube), and freeze (-20 °C). CoilR peptide can be stored frozen for several months.

**C. Generation of CoilR probe peptides by thiol-maleimide conjugation in solution**

VIPER-labeling is specific and efficient in living and fixed cells expressing CoilE-tagged protein. However, the quality of labeling is directly related to the quality of the probe peptide. This is because unlabeled CoilR and labeled CoilR will both dimerize with CoilE-tagged cellular proteins. We recommend using peptides that are > 50% labeled with the reporter chemistry.

We have found that the efficiency of the thiol-maleimide bioconjugation reaction is variable. Therefore we have included two approaches for modifying CoilR: **Procedure C** and **Procedure D**. We have used both successfully to label CoilR with reporters, with the preferred protocol being dependent on the researcher. **Procedure C** describes a conventional thiol-maleimide conjugation reaction in solution; this is the method used to generate probe peptides described in our 2018 publication[1]. This method can be used to attach a fluorescent probe, such as Sulfo-Cyanine5 (Cy5)-maleimide, or to biotinylate CoilR.

1. Prepare buffers, TCEP, and a stock solution of the reactive maleimide. If these stocks are already made, then proceed to **Step C2**.

a. We recommend labeling in TBS Urea (Recipe 9). The reaction should be done in a thiol-free buffer between pH 7 - pH 7.5.
b. Degas the buffer before using. This can be done by bubbling a stream of nitrogen gas through the buffer or by vacuum degassing.
c. Prepare 0.5 M TCEP (Recipe 10).

2. Prepare a concentrated stock solution of the maleimide probe at 20-100 mg/ml in anhydrous DMSO. For Cy5-maleimide or other fluorophores, protect the solution from light.
   a. More concentrated stocks are preferable to limit the amount of DMSO in the reaction.
   b. Stocks can be stored at -20 °C.
   c. The maleimide will hydrolyze in water, so storage in DMSO is recommended.
3. Thaw the purified CoilR peptide on ice. The concentrated peptide stock should be in TBS Urea and degassed by nitrogen.
   a. The reaction will proceed better if the peptide is concentrated. We recommend using a stock that is 2 mg/ml (~270 µM).
   b. A typical labeling reaction will include 50 to 200 nmoles of CoilR peptide.
   c. If the peptide is not in an appropriate buffer, transfer into a different buffer at this point using a 3 kDa MWCO filter and degas before proceeding to **Step C4**.
4. Reduce the peptide by the addition of a 10-fold molar excess of TCEP. Incubate for 30 min at 50 °C.
5. Initiate the conjugation reaction by adding at least 20-fold molar excess of the maleimide probe. Mix well. Incubate for 2 h at room temperature or at 4 °C overnight on a rotisserie.
   a. For fluorophore-labeling, protect the reaction from light.
6. After labeling, add TBS Urea Binding Buffer (Recipe 11) to a total volume of 15 ml.
   a. Save a sample of the crude reaction mixture for analysis by SDS-PAGE.

7. Concentrate and buffer exchange the crude reaction on a 3 kDa MWCO filter to remove unreacted probe. Buffer exchange into TBS Urea Binding Buffer which is compatible with Ni-NTA purification. Save a sample for analysis by SDS-PAGE.
   a. For CoilR-fluorophores, continue the buffer exchange until the filtrate becomes colorless or stops changing color with subsequent buffer exchanges. Then proceed to **Procedure E**.
   b. For biotinylated CoilR, a 40 ml wash is sufficient to remove most of the free biotin moieties. Then proceed to **Procedure F**.

## D. Generation of CoilR probe peptides by thiol-maleimide chemistry using solid state-based labeling (SSL)

In 2008, Weiss and coworkers described a new method for modifying proteins using thiol-maleimide chemistry [21]. In that work, the protein was first precipitated with ammonium sulfate and reduced with DTT before fluorophore conjugation. They named this method solid state-based labeling (SSL). The advantage of this approach is that it is easy to do, efficient (70-90% labeled[21]) and thiol-specific. We currently use both SSL and solution-based labeling to generate probe peptides. **Procedure D** is adapted from Weiss and coworkers published method[21].

1. Prepare SSL Buffer (Recipe 12) and the reducing agents (1M DTT [Recipe 13] and 0.5 M TCEP). If these stocks are already made, then proceed to **Step D2**.
2. Thaw the purified CoilR peptide on ice.
   a. A typical labeling reaction will include 50 to 200 nmoles of CoilR peptide.
   b. The volume should be less than 1 ml, but the peptide will become concentrated by precipitation in Step D4.
3. Reduce the peptide by the addition of 10 mM DTT, from a 1 M stock. Incubate for 30 min at 4 °C on a rotisserie.
4. Precipitate the reduced peptide by slow addition of ammonium sulfate powder to a final concentration of 70-75%.
   a. For an overview of protein precipitation, see the 1998 publication by Wingfield[22].

b. Encor Biotechnology has a useful online tool for calculating the amount of ammonium sulfate to add; see: http://www.encorbio.com/protocols/AM-SO4.htm.
    i. *Example*: For a 500 µl peptide solution at 4 °C, add 0.23 g of ammonium sulfate to get a 70% saturated solution.

5. After a precipitate forms, add 10 mM DTT and reduce for 2 h at 4 °C on a rotisserie.
6. Wash the reduced peptide slurry with ice-cold SSL Buffer to remove DTT.
    a. Pellet the slurry by centrifugation (4 min, 14,000 x g, 4 °C). Discard the supernatant.
    b. Add 1 ml SSL Buffer and invert the sample several times.
    c. Repeat steps **D6a/b** 3-5 times to remove all excess DTT.
    d. After the last centrifugation step, resuspend the pellet in 100 µl SSL Buffer.

*Note: Any residual DTT will react with the maleimide probe so it is critical to wash the peptide pellet several times.*

7. Perform the thiol-maleimide conjugation on reduced peptide in the solid state.
    a. Add 10- to 30-fold molar excess probe to the reduced peptide. Mix by inverting the tube several times.
        i. Use a concentrated stock (20-100 mg/ml) of maleimide probe (e.g., Cy5-maleimide) in anhydrous DMSO.
    b. Mix the reaction on a rotisserie for 15 min at 4 °C.
    c. Add 5- to 10-fold molar excess TCEP. Mix and continue to incubate for 45 min at 4 °C on a rotisserie.
        i. For fluorophore labeling, protect the tube from light.
        ii. Keep the amount of the maleimide higher than the amount of TCEP in the reaction because the maleimide probe can undergo a side-reaction with TCEP[21].
        iii. The reaction can be incubated overnight.
8. After labeling, we recommend washing the reaction mixture with SSL Buffer to remove excess maleimide.

a. Pellet the reaction by centrifugation (4 min, 14,000 x g, 4 °C). Discard the supernatant.
b. Resuspend in SSL Buffer (1 ml).
c. Pellet by centrifugation (4 min, 14,000 x g, 4 °C). Discard the supernatant.

9. Resuspend the pellet from Step 8 in Buffer B.
   a. *Note: High concentrations of EDTA will strip nickel from the Ni-NTA agarose used in **Procedure E**. Add enough Buffer B to ensure that the final concentration of EDTA is less than 1 mM.*
   b. Save a sample of the crude reaction mixture for analysis by SDS-PAGE.
10. Proceed to purification, following **Procedure E** (for fluorescent peptides) or **Procedure F** (for biotinylated peptides).

**E. Purification of CoilR-Fluorophore probe peptide**

This procedure removes excess unreacted free dye from fluorophore-labeled CoilR (*i.e.*, CoilR-Cy5) while also purifying the peptide. This section additionally describes the method used to quantify the fluorophore labeling of the peptide. *Note: Protect the peptide from light and keep the peptide on ice, unless otherwise noted.*

1. Bind the labeled CoilR peptide to Ni-NTA agarose resin for 1 h at 4 °C.
   a. For a typical labeling reaction (50-200 nmol CoilR), we recommend using 0.5 ml Ni-NTA resin and binding in a large volume (20-40 ml) of TBS Urea Binding Buffer.
2. Load the lysate-resin mixture onto a clean, fritted chromatography column.
3. Collect the flow-through and save a sample for analysis by SDS-PAGE.
4. Wash the resin with 20 column volumes (CV) of TBS Urea Binding Buffer.
   a. Continue washing until fractions are colorless.
   b. Save washes for analysis by SDS-PAGE.
5. **Optional step:** Wash the resin with 10 CV of TBS Urea Binding Buffer supplemented with 20% ethanol. The addition of ethanol can help remove free fluorophore.
6. Elute the CoilR peptide with 5-10 CV of TBS Urea Imidazole (Recipe 14).
   a. Fractions should be dark blue for Cy5-labeled peptide.

b. Continue to elute until the fractions are nearly colorless before proceeding to the next step.
c. Alternatively**,** elute in a low pH buffer (*e.g.*, Buffer E).

7. Analyze the purification by SDS-PAGE, following **Steps A6d-A6e**. For a representative analysis see **Figure A.4**.
   a. Analyze the crude reaction, samples from the purification (flow through, washes, elutions), and the concentrated elution.
   b. Image the gel on a fluorescence scanner to detect labeled peptide. A representative 2-color scan acquired using a Protein Simple imaging system is provided in Figure 5A. Alternatively, we recommend imaging on a GE Amersham$^{TM}$ Typhoon multimode scanner using the appropriate detection settings (i.e., Cy5: ex: 635 nm, em: 670/30 nm).
   c. After fluorescence imaging, stain the protein gel with Coomassie stain, destain, and image to detect total protein.
8. Concentrate and buffer exchange the elutions containing labeled peptide into a storage buffer of choice using a 3 kDa MWCO filter.

*Note: We recommend storing the peptide in TBS Urea.*

9. Determine the degree of labeling (moles of fluorophore per mole of protein). We recommend following the protocol published by Thermo Scientific [Tech Tip #31: Calculate dye:protein (F/P) molar ratios] [23].
   a. Determine the amount of fluorophore in the solution by measuring the absorption at the fluorophore's absorbance maximum ($Abs_{max}$) and using the published extinction coefficient ($\varepsilon_{FL}$) (**Table A.2**).
   b. Determine the amount of peptide in the solution by measuring the absorbance at 280 nm.
      i. The fluorophore will also absorb at 280 nm and a correction factor (CF) must be used (*e.g.*, CF for Cy5 = 0.04).
      ii. The extinction coefficient (ε) of the CoilR peptide is 2,980 $L \cdot mol^{-1} \cdot cm^{-1}$ (www.expasy.org).
   c. Calculate the molarity of the peptide and the degree of labeling using the following equations:

$$\text{Protein (M)} = \frac{\text{Abs}_{280} - (\text{Abs}_{max} \times \text{CF})}{\varepsilon_{protein}}$$

$$\text{Degree of labeling} = \frac{\text{Abs}_{max}}{\text{Protein (M)} \times \varepsilon_{Fluor}}$$

d. We offer the following recommendations:
   i. Absorbance readings are only accurate in the linear range of the spectrophotometer (between 0.1 and 1.0).
   ii. We suggest preparing several dilutions of the peptide and replicates to obtain more accurate results.
   iii. We measured absorbance in a quartz cuvette on a Tecan Infinite M200 Pro with a cuvette port.

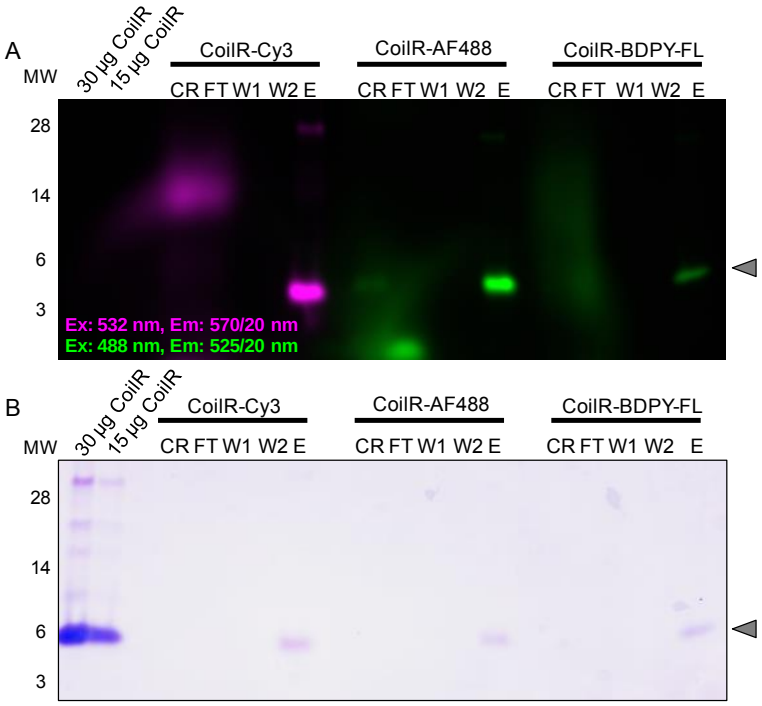


**Figure A.4. Analysis of CoilR probe peptides by SDS-PAGE.** CoilR was labeled with sulfo-Cyanine3 (CoilR-Cy3; 60% labeled), AlexaFluor-488 (CoilR-AF488; 45% labeled), or BODIPY-FL (CoilR-BDPY-FL: 40% labeled). The crude reaction (CR) was purified on Ni-NTA resin to remove free dye. Samples were resolved by SDS-PAGE and the gel was scanned for green (ex: 488 nm, em: 525/50 nm) and red (ex: 532 nm, em: 570/20 nm) fluorescence (A). The same gel was subsequently stained for total protein with Coomassie (B). CR = diluted crude reaction (pre-column), FT = flow-through (unbound protein/fluorophore), W = wash (TBS Urea Binding Buffer), E = elution (TBS Urea Imidazole). Unreacted CoilR peptide (15 and 30 µg) was included for reference and CoilR is indicated by a gray arrowhead.

**Table A.2. Values for quantifying CoilR labeling with Cy5-maleimide‡**

| | $Abs_{max}$ (nm) | ε ($L \cdot mol^{-1} \cdot cm^{-1}$) | $CF_{280}$ |
|---|---|---|---|
| CoilR | 280 | 2,980 | N/A |
| Sulfo-Cyanine5 (Cy5) | 646 | 271,000 | 0.04 |

‡Values provided on the Lumiprobe website: www.lumiprobe.com.

10. Store the fluorophore-labeled peptide in 5-10% glycerol.
    a. Aliquot (100 µl/tube) and freeze (-20 °C). The peptide can be stored (frozen and protected from light) for several months.
    b. Final stocks should be between 1-50 µM for experimental convenience.
    c. To minimize freeze-thaw cycles, a thawed aliquot can be divided into smaller single-use volumes (*e.g.*, 10 µl) and re-frozen.

## F. Purification of biotinylated probe peptide (CoilR-biotin)

This procedure is intended for purifying CoilR peptide that was biotinylated using **Procedure C** or **D**. For an overview of avidin-based affinity chromatography and a troubleshooting guide, refer to the Pierce® Monomeric Avidin Agarose instructions, available online[24]. After purification and elution from the monomeric avidin resin, the CoilR-biotin peptide is assumed to be 100% biotinylated.

1. Prepare the buffers and equilibrate them to room temperature.
    a. TBS: 20 mM Tris, 150 mM NaCl pH 7 (Recipe 8).
    b. Biotin Buffer: 2 mM biotin in DPBS pH 7.4 (Recipe 15).
    c. Regeneration Buffer: 0.1 M glycine, pH 2.8 (Recipe 16).
2. Add the Pierce Monomeric Avidin Agarose to a clean, fritted chromatography column and drain.
    a. For 100 nmoles of CoilR peptide, use 1 ml of resin.
3. Block non-reversible biotin binding sites on the resin:
    a. Wash with 5 column volumes (CV) of TBS.
    b. Wash with 5 CV of Biotin Buffer to block any non-reversible biotin binding sites.

c. Wash with 5 CV of Regeneration Buffer to remove biotin bound to reversible biotin-binding sites on the resin.
d. Wash with 5 CV of TBS to re-equilibrate the column.
e. Plug the column to prevent flow; the resin is now ready to be used.

4. Dilute the biotinylated peptide sample to approximately 5 ml in TBS. Apply to the column.
5. Incubate the sample with the resin for 30 min at room temperature.
6. Unplug the column and collect the flow-through. Save a sample of the flow-through and all subsequent wash and elution steps for analysis by SDS-PAGE.
7. Wash the resin twice with 5 CV of TBS.
8. Elute the biotinylated protein in 5 CV of Biotin Buffer. Collect 1 ml fractions.
9. Elute in 5 CV of Regeneration Buffer. Collect 1 ml fractions. This elution step is included because some peptides do not elute with excess biotin.
10. Regenerate the resin. Wash with 5 CV of Regeneration Buffer.

Collect and analyze to ensure that this wash does not contain biotinylated peptide.

11. Analyze all fractions by SDS-PAGE (see **Step A6d-A6e**).

*Note: In our experience, CoilR-biotin elutes in both the Biotin Buffer and the Regeneration Buffer, with more eluting in the Biotin Buffer.*

12. Analyze all fractions by Western blot (using your preferred method) to detect biotinylated proteins. For example, we detect biotinylated proteins using either an anti-biotin HRP antibody (Jackson Immunoresearch) or using a streptavidin-HRP (Thermo Scientific).
13. Combine fractions containing biotinylated peptide based on the analysis in **Steps F11-F12**.
14. Concentrate and exchange the biotinylated peptide into desired buffer using a 3 kDa MWCO filter.
    a. We recommend exchanging into TBS Urea.
    b. Keep the peptide concentration between 0.5 mg/ml and 2 mg/ml.
15. Quantify the protein yield of the purification using the Pierce BCA assay kit.

a. The crude reaction will contain unmodified and biotinylated peptide. The amount of CoilR-biotin retrieved after monoavidin-based purification is thus expected to be less than the amount of CoilR used in the reaction.
b. The biotinylation (%) of the peptide in the crude reaction mixture can be estimated by dividing the nmoles of CoilR-biotin obtained from the monoavidin purification by the nmoles of CoilR in the labeling reaction.
c. The CoilR-biotin obtained from this procedure is presumed to be 100% biotinylated once it is eluted from the monoavidin column because unreacted peptide (*i.e.*, CoilR) will not bind to the resin.

16. Store the biotin-labeled peptide in 5-10% glycerol.
    d. Aliquot (100 µl/tube) and freeze (-20 °C). The peptide can be stored for several months.
    e. Final stocks should be between 1 µM and 50 µM for experimental convenience.
    f. To minimize freeze-thaw cycles, a thawed aliquot can be divided into smaller single-use volumes (*e.g.*, 10 µl) and re-frozen.

## Recipes

*Notes:*

- *Buffers are made in autoclaved DI water unless otherwise stated.*
- *The pH of Tris buffers change with temperature.*
- *The pH of urea-containing buffers (Buffer B, Buffer C, and Buffer E) should be checked and adjusted immediately prior to use.*
- *The pH of DPBS is 7.0.*

1. Buffer B (Ni-NTA peptide purification)
   8 M Urea
   100 mM $NaH_2PO_4$
   10 mM Tris-Cl pH 8.0
2. Buffer C (Ni-NTA peptide purification)
   8 M Urea

100 mM $NaH_2PO_4$

10 mM Tris-Cl pH 6.5

3. Buffer E (Ni-NTA peptide purification)

    8 M Urea

    100 mM $NaH_2PO_4$

    10 mM Tris-Cl pH 4.5

4. MES running buffer

    50 mM MES

    50 mM Tris pH 7.3

    1 mM EDTA

    0.1% w/v SDS

5. TCEP/SDS Loading Dye (5x)

    300 mM Tris pH 6.8

    50 mM TCEP

    10% w/v SDS

    65% v/v glycerol

    0.025% v/v Ponceau Red

6. Coomassie Stain

    45% v/v methanol

    0.3% w/v Coomassie Brilliant Blue R-250

    10% v/v acetic acid

7. Destain Solution

    20% methanol v/v

    10% acetic acid v/v

8. Tris-Buffered Saline (TBS)

    20 mM Tris pH 7.4

    150 mM NaCl

9. TBS Urea

    20 mM Tris pH 7.4

    150 mM NaCl

    2 M Urea

10. 0.5 M TCEP

    Dissolve the TCEP and then adjust the pH to 7 by the addition of 10 M NaOH.

    Note: Single-use aliquots of TCEP can be stored at -20 °C.

11. TBS Urea Binding Buffer

    20 mM Tris pH 8.0

    150 mM NaCl

    2 M Urea

12. Solid state-based labeling (SSL) Buffer, pH 7.5

    125 mM $NaH_2PO_4$

    200 mM NaCl

    1.25 mM EDTA

    4.6 M Ammonium Sulfate (75% saturated solution)

13. 1 M DTT

    1 M DTT in water

    Note: Single-use aliquots can be prepared and stored at -20 °C.

14. TBS Urea Imidazole

    20 mM Tris pH 7.4

    150 mM NaCl

    2 M Urea

    500 mM imidazole

15. Biotin Buffer

    2 mM biotin in DPBS

16. Regeneration buffer

    0.1 M glycine, pH 2.8

## Sequences

The amino acid sequence of CoilR expressed from pET28b(+)_CoilR is provided in **Table A.1**.

## Acknowledgments

KEB is grateful for support from the OHSU School of Medicine and the National Institutes of Health (R01 GM122854). JKD was partially funded by the Portland Chapter of Achievement Rewards for College Scientists (ARCS). The protocols described herein were originally described in two prior publications[1,14]. We are grateful to our colleagues at OHSU, particularly Drs. Hannah Zane and Jonathan White, for their contributions to the development of the VIP tags.

## Works Cited


1. Doh, J. K.; White, J. D.; Zane, H. K.; Chang, Y. H.; López, C. S.; Enns, C. A.; Beatty, K. E.: VIPER is a genetically encoded peptide tag for fluorescence and electron microscopy. *Proc. Natl. Acad. Sci. U.S.A.* **2018**, *115*, 12961-12966.
2. Schnell, U.; Dijk, F.; Sjollema, K. A.; Giepmans, B. N. G.: Immunolabeling artifacts and the need for live-cell imaging. *Nat. Meth.* **2012**, *9*, 152-158.
3. Griffiths, G.; Lucocq, J. M.: Antibodies for immunolabeling by light and electron microscopy: not for the faint hearted. *Histochem. Cell Biol.* **2014**, *142*, 347-360.
4. Griffiths, G.; Hoppeler, H.: Quantitation in immunocytochemistry: correlation of immunogold labeling to absolute number of membrane antigens. *J Histochem Cytochem* **1986**, *34*, 1389-98.
5. Berglund, L.; Björling, E.; Oksvold, P.; Fagerberg, L.; Asplund, A.; Al-Khalili Szigyarto, C.; Persson, A.; Ottosson, J.; Wernérus, H.; Nilsson, P.; Lundberg, E.; Sivertsson, Å.; Navani, S.; Wester, K.; Kampf, C.; Hober, S.; Pontén, F.; Uhlén, M.: A Genecentric Human Protein Atlas for Expression Profiles Based on Antibodies. *Mol. Cell. Proteomics* **2008**, *7*, 2019-2027.
6. Bradbury, A.; Pluckthun, A.: Reproducibility: Standardize antibodies used in research. *Nature* **2015**, *518*, 27-9.
7. Bordeaux, J.; Welsh, A.; Agarwal, S.; Killiam, E.; Baquero, M.; Hanna, J.; Anagnostou, V.; Rimm, D.: Antibody validation. *Biotechniques* **2010**, *48*, 197-209.
8. Baker, M.: Reproducibility crisis: Blame it on the antibodies. *Nature* **2015**, *521*, 274-6.
9. Liu, Z.; Lavis, Luke D.; Betzig, E.: Imaging Live-Cell Dynamics and Structure at the Single-Molecule Level. *Mol. Cell.* **2015**, *58*, 644-659.
10. Tsien, R. Y.: The green fluorescent protein. *Annu. Rev. Biochem.* **1998**, *67*, 509-544.
11. Rodriguez, E. A.; Campbell, R. E.; Lin, J. Y.; Lin, M. Z.; Miyawaki, A.; Palmer, A. E.; Shu, X.; Zhang, J.; Tsien, R. Y.: The Growing and Glowing Toolbox of Fluorescent and Photoactive Proteins. *Trends Biochem. Sci.* **2017**, *42*, 111-129.
12. Cranfill, P. J.; Sell, B. R.; Baird, M. A.; Allen, J. R.; Lavagnino, Z.; de Gruiter, H. M.; Kremers, G. J.; Davidson, M. W.; Ustione, A.; Piston, D. W.: Quantitative assessment of fluorescent proteins. *Nat Methods* **2016**, *13*, 557-62.
13. Ellisman, M. H.; Deerinck, T. J.; Shu, X.; Sosinsky, G. E.: Chapter 8 - Picking Faces out of a Crowd: Genetic Labels for Identification of Proteins in Correlated Light and Electron Microscopy Imaging. In *Methods in cell biology*; Thomas, M.-R., Paul, V., Eds.; Academic Press, 2012; Vol. 111; pp 139-155.
14. Zane, H. K.; Doh, J. K.; Enns, C. A.; Beatty, K. E.: Versatile interacting peptide (VIP) tags for labeling proteins with bright chemical reporters. *ChemBioChem* **2017**, *18*, 470-474.
15. Reinke, A. W.; Grant, R. A.; Keating, A. E.: A Synthetic Coiled-Coil Interactome Provides Heterospecific Modules for Molecular Engineering. *J. Am. Chem. Soc.* **2010**, *132*, 6025-6031.
16. Moll, J. R.; Ruvinov, S. B.; Pastan, I.; Vinson, C.: Designed heterodimerizing leucine zippers with a range of pIs and stabilities up to $10^{-15}$ M. *Prot. Sci.* **2001**, *10*, 649-655.

17. Hermanson, G. T.: *Bioconjugate Techniques*; 3rd ed.; Academic Press, 2013.
18. Hochuli, E.; Dobeli, H.; Schacher, A.: New metal chelate adsorbent selective for proteins and peptides containing neighbouring histidine residues. *J Chromatogr* **1987**, *411*, 177-84.
19. Kim, Y.; Ho, S. O.; Gassman, N. R.; Korlann, Y.; Landorf, E. V.; Collart, F. R.; Weiss, S.: Efficient site-specific labeling of proteins via cysteines. *Bioconjugate chemistry* **2008**, *19*, 786-91.
20. Morimoto-Tomita, M.; Uchimura, K.; Rosen, S. D.: Novel extracellular sulfatases: Potential roles in cancer. *Trends Glycosci. Glycotechnol.* **2003**, *15*, 159-164.
21. Kim, Y.; Ho, S. O.; Gassman, N. R.; Korlann, Y.; Landorf, E. V.; Collart, F. R.; Weiss, S.: Efficient Site-Specific Labeling of Proteins via Cysteines. *Bioconjugate Chem.* **2008**, *19*, 786-791.
22. Wingfield, P.: Protein Precipitation Using Ammonium Sulfate. *Current Protocols in Protein Science* **1998**, *13*, A.3F.1-A.3F.8.
23. TECH TIP #31 Calculate dye:protein (F/P) molar ratios. Thermo Scientific Inc., 2011.
24. Pierce® Monomeric Avidin Agarose. Thermo Scientific Inc., 2011.

# Appendix B: Implementing VIPER for Imaging Cellular Proteins by Fluorescence Microscopy

**Julia K. Doh**, Caroline A. Enns, and Kimberly E. Beatty

*This work is adapted from a manuscript originally published by Bio-Protocol on November 5, 2019 in volume 9, issue 21. It has been adapted for this dissertation and reprinted with permission.*

## Abstract

Genetically-encoded tags are useful tools for multicolor and multi-scale cellular imaging. Versatile Interacting Peptide (**VIP**) tags, such as VIPER, are new genetically-encoded tags that can be used in various imaging applications. VIP tags consist of a coiled-coil heterodimer, with one peptide serving as the genetic tag and the other ("probe peptide") delivering a reporter compatible with imaging. Heterodimer formation is rapid and specific, allowing proteins to be selectively labeled for live-cell and fixed-cell imaging. In this Bio-Protocol, we include a detailed guide for implementing the VIPER technology for imaging receptors on live cells and intracellular targets in fixed cells.

## Background

Fluorescence microscopy (FM) enables researchers to observe the architecture and assembly of proteins in cells dynamically and in multicolor[1-4]. Fluorescence imaging relies on strategies for labeling target proteins with bright, fluorescent reporter molecules. Labeling can be achieved in a number of ways[5-7], including immunolabeling, fluorescent proteins (e.g., green fluorescent protein)[8,9], chemical stains (e.g., DAPI, MitoTracker, or phalloidin conjugates)[10,11], and self-labeling tags[12-14]. The most useful tags can be used to deliver diverse chemical reporters with optimal properties, such as spectrally-distinct colors, high quantum yield and extinction coefficient ("brightness"), and photostability[15,16]. Tags that can bind to a variety of bright fluorophore ligands include the SNAP tag[17,18], Halo tag[19], TMP tag[20], and FAPs[21]. However, these protein

tags are large (18-33 kDa), which can change protein folding, trafficking, and function[22-25]. A few peptide tags have been described for cell imaging, as exemplified by the tetracysteine tag, but these can have non-specific interactions and limited color choices[26-29].

An alternative approach is to use a peptide tag that forms a heterodimeric coiled-coil with a reporter peptide. This is the approach that we[30,31] and others[32-37] have used to label cellular proteins[38,39]. One advantage of this approach is that the genetic tag is small—just 4 to 7 kDa. A second advantage is that reporter peptide labeling is typically restricted to the cell surface, which is useful for labeling and tracking transmembrane receptors[40] (i.e., in pulse-chase experiments[30,32]). We named our coiled-coil tags Versatile Interacting Peptide (VIP) tags. Our first tag, VIP Y/Z, enabled the selective fluorescent labeling of target proteins in cell lysates and on live cells[31]. Next we described VIPER, which is comprised of a CoilE tag and a CoilR probe peptide. We showed that the probe peptide can be customized to the imaging application by conjugation to one of a number of reactive fluorophores and small molecules (i.e., biotin). VIPER labeled sub-cellular structures in fixed cells and transmembrane receptors on live cells. Proteins could be imaged by FM or correlative light and EM (CLEM)[30].

For any genetic tag, it is important to insert the tag at a location in the amino acid sequence where it will not interfere with the binding interactions, localization, folding, or function of the protein of interest. It is beyond the scope of this paper to dictate the location of the genetic tag for all feasible protein targets. We recommend reading Erik Snapp's paper "Design and Use of Fluorescent Fusion Proteins in Cell Biology" for a discussion on choosing a tag insertion site[41]. For VIP tags, we offer the following suggestions and recommendations for tag placement.

1) For any new fusion protein, we recommend analyzing the localization, trafficking, and function to ensure that the tagged protein retains the same behavior as the untagged protein.
2) Avoid placing the VIP tag in critical locations. In other words, tags should not be placed at catalytic residues, binding interfaces, or sites of post-translational modifications (e.g., glycosylation, phosphorylation, zymogen cleavage, *etc*.).

Furthermore, for secreted proteins, the tag should be placed after the signal peptide to avoid being cleaved.

3) Careful evaluation of the protein crystal structure, when available, can be invaluable in deciding where to place a tag.
4) We recommend including a short linker (3-6 amino acids) between the VIP tag and the target protein[42-45].
5) Practically speaking, we assume that a protein that maintains normal behavior after fusion to a fluorescent protein (e.g., GFP or mCherry) will tolerate a VIP tag at the same position.
6) For live cell labeling, the CoilE tag should be cell-surface accessible. For example, for imaging transferrin receptor 1 (TfR1) we placed the tag on the extracellular, C-terminal domain.
7) For fixed cell labeling, the tag can be placed either at the N- or C-terminus or between two domains (*i.e.*, between mEmerald and actin, as described for our mEmerald-CoilE-actin-C18 construct).

This protocol includes methods for implementing VIPER for imaging cellular proteins by FM. These imaging experiments are performed on transfected mammalian tissue culture cells. In **Procedure A** we provide a transfection protocol for introducing plasmid DNA encoded VIP-tagged constructs into cells. In **Procedure B**, we describe labeling a transmembrane receptor on the surface of living cells. In **Procedure C**, we describe methods for imaging intracellular targets in fixed cells.

## Materials and Reagents

*Note: "*" indicates a brand that is critical to the success of the experiment.*

**Materials**

1. Polystyrene 10 cm tissue culture dish (Thermo Scientific, Nunc™, catalog number: 12565020)
2. Polystyrene 6-well tissue culture plate (Thermo Scientific, BioLite™, catalog number: 12-556-004)
3. 8-well chambered coverglass with #1.5 glass (*i.e.*, Cellvis, catalog number: C8-

1.5H-N or Thermo Scientific, Nunc™ Lab-Tek™, catalog number: 155411)

4. LDPE 500 ml squeeze wash bottle (Thermo Scientific, catalog number: 24010500)
5. Transfer bulb pipette (VWR, catalog number: 16001-182)

**Reagents**

1. U-2 OS cells (ATCC, catalog number: HTB-96)
2. CHO TRVb cells (courtesy of Prof. Timothy McGraw, Cornell University, Ithaca, New York) [46]
3. Ham's F-12 Medium (Life Technologies, Gibco™, catalog number: 11765062)
4. McCoy's 5A Medium (Life Technologies, Gibco™, catalog number: 16600082)
5. Dulbecco's phosphate-buffered saline without calcium or magnesium; DPBS (Gibco™, catalog number: 14190144)
6. Trypsin-EDTA (0.25%) (Life Technologies, Gibco™, catalog number: 25200056)
7. Fetal bovine serum; FBS (GE, Hyclone™, catalog number: SH30910.03)
8. *Lipofectamine™ 2000 (Thermo Scientific, catalog number: 11668019)
9. Opti-MEM (Life Technologies, Gibco™, catalog number: 31985070)
10. Plasmid DNA of VIP-tagged protein (generated by the user)
11. mEmerald-actin-C18 (Addgene, catalog number: 53978)
12. Human transferrin Alexa Fluor™ 488 conjugate; Tf-AF488 (Invitrogen, catalog number: T13342)
13. Hoechst 33342 nucleic acid stain (Invitrogen, catalog number: H1399)
14. Bovine serum albumin (BSA) fraction V (Research Products International, catalog number: A30075100.0)
15. Immersion oil (Carl Zeiss Immersol™ 518 F, catalog number: 4449620000000)
16. Sodium azide (Sigma, catalog number: 71289-5G)
17. Triton X-100 (Sigma Aldrich, catalog number: 93443-100ML)
18. Saponin (MilliporeSigma, catalog number: 558255100GM)

**Equipment**

1. Hemocytometer (Hausser Scientific, catalog number: 1475)

2. Humidified $CO_2$ Incubator (New Brunswick Galaxy 170S, catalog number: C0170S-120-0000)
3. Tissue culture hood (Thermo Scientific 1300 Series A2)
4. Tissue culture inverted light microscope (Carl Zeiss, Zeiss Primovert)
5. Spinning disk confocal fluorescence microscope (Zeiss Yokogawa CSU-X1 on Zeiss AxioObserver)
6. Line scanning (Airyscanning) fluorescence microscope (Zeiss LSM880 on inverted microscope stand)

**Software**

1. Fiji (ImageJ Version 2.0.0-rc-46)[47]

## Procedures

### A. Transfecting cell lines to express a VIPER-tagged protein

VIP tags have been used in a number of cell lines successfully. Receptor imaging using VIPER (**Procedure B**) was done in Chinese hamster ovary (CHO) TRVb cells. CHO TRVb cells do not express TfR1 or transferrin receptor 2[46] which makes it a useful cell line for imaging TfR1-CoilE. Labeling intracellular targets in fixed cells (**Procedure C**) was done in U-2 OS, a human osteosarcoma cell line. We have used VIP tags in other cell lines not discussed in this publication (*e.g.*, HEK293 and AU565).

We recommend optimizing plating density and transfection conditions for each cell line. Refer to ThermoFisher's *Protocol Pub No. MAN0007824 Rev 1.0*[48] for more information on transfection with Lipofectamine 2000. In our procedure, we recommend passaging cells on Day 1, transfecting cells on Day 2, and VIPER labeling cells on Day 3 for imaging (see **Procedures B-C**).

Recommendations for **Procedure A**:

- Use sterile technique and work within a tissue culture (laminar flow) hood when working with live tissue culture cell lines.
- When transfecting cells with a vector encoding a CoilE-tagged protein (e.g., pcDNA3.1_TfR1-CoilE), we also recommend transfecting cells with an

untagged protein to compare labeling specificity (e.g., pcDNA3.1_TfR1). Untransfected cells are also useful controls for labeling specificity.

- The amino acid sequence for TfR1-CoilE and mEmerald-CoilE-actin-C18 can be found in the **Sequences** section below.
- The DNA quality is paramount for high transfection efficiency. Quantify DNA quality by UV spectroscopy and verify that the 260/280 nm ratio falls between 1.8-2.0.
- There are many different methods for introducing genes into cells and we encourage researchers to use methods that have been optimized for their cell lines.

1. **Day 1:** Passage cells and seed into an 8-well chambered coverslip.
   a. Before starting, visually inspect cells on a tissue culture microscope (*e.g.*, by bright field illumination, low magnification) to confirm that cells are adherent, healthy, and 80-90% confluent.
   b. Seed 5 x $10^4$ cells per well (for U-2 OS or CHO TRVb) into Nunc™ Lab-Tek™ 8-well chambered coverslips.
   c. For other cell lines, seed at a density that will result in 80-90% confluency after 24 h.
   d. Do not include antibiotics in the media.
   e. For U-2 OS, grow cells in McCoy's 5A medium supplemented with 10% FBS.
   f. For CHO TRVb cells, grow cells in Ham's F12 medium supplemented with 5% FBS.
2. Incubate cells overnight in a humidified tissue culture incubator (37 °C with 5% $CO_2$).
3. **Day 2:** Prepare the transfection mixture:
   a. Dilute vector DNA into Opti-MEM.
      i. For an 8-well chambered coverslip, use 500 ng DNA per well.
      ii. Keep the volume of DNA to less than 10% of the total volume in the transfection mixture.
   b. Dilute Lipofectamine 2000 into Opti-MEM and incubate for 5 min:

i. For 8-well chambered coverslips, use 1,000 ng Lipofectamine 2000 per well.

c. Combine equal volumes of the Lipofectamine 2000 and DNA solutions and mix by pipetting. The final ratio of DNA to Lipofectamine 2000 will be 1:2. Incubate mixture for at least 30 min at room temperature.

4. Transfect cells:
   a. Aspirate media from cells.
   b. Add Opti-MEM to wells. For 8-well chambered coverslips, use 200 µl per well.
   c. Dilute the transfection mixture into each well (1:5 dilution) by adding 50 µl of the transfection mixture. The total volume of fluid in each well should be 250 µl.
   d. Gently mix the solution by pipetting up and down or by rocking the chambered slide.
   e. Incubate cells in the transfection mixture for 4 h in a tissue culture incubator (37 °C, 5% $CO_2$).
      i. This time frame is recommended for U-2 OS and CHO TRVb cells.
      ii. Monitor cells by viewing on a TC microscope. Cell size and shape should appear unchanged during transfection. If cells contract or detach, then adjust the transfection conditions.
   f. Aspirate to remove the transfection media and wash once with complete media (*e.g.*, media with FBS).
   g. Add complete media and grow in a tissue culture incubator (37 °C, 5% $CO_2$) for at least 24 h. Cells will be ready for use between 24 and 48 h after transfection.

**B. Application: Labeling a transmembrane receptor with VIPER on living cells**

Investigations into cell surface receptors are enabled by VIP tags, which can be used to tag and track receptors in living cells. When imaging live cells, VIPER labeling is restricted to the cell surface because the probe peptide (*e.g.*, CoilR-Cy5) is live cell-impermeant. This feature is an advantage for observing receptor trafficking or population changes in localization over time.

**Procedure B** describes a method for imaging iron uptake in cells. Briefly, iron uptake in the cell is mediated by a transmembrane receptor named transferrin receptor 1 (TfR1). This receptor binds and transports iron-bound transferrin (Tf) into cells through clathrin-mediated endocytosis. We used VIPER to observe this process. Specifically, we describe a method for labeling TfR1-CoilE with red-fluorescent CoilR-Cy5 for imaging by confocal FM. As a counter-stain for the receptor, we also treat cells with fluorescent Tf (i.e., Tf-AF488), which binds to TfR1. The cells are labeled live at 4°C in order to halt the process of endocytosis. The methods described here could be used to image other cell receptors.

Receptor labeling is performed on live cells and TfR1 can be imaged either live or post-fixation. In **Procedure B**, we specify that the cells are fixed prior to imaging. This is done for convenience, and is recommended for users optimizing labeling conditions. Alternatively, as described in our publication, cells can be imaged live (i.e., by time-lapse) to observe receptor trafficking[30].

**Procedure B** commences on *Day 3* with transfected cells in 8-well chambered slides, generated as described in **Procedure A**. We recommend including unlabeled or single-labeled controls for imaging. We also recommend assessing VIP labeling specificity by including an untagged protein control. An example slide layout is provided in **Figure B.1**.

| | | | |
|---|---|---|---|
| pcDNA3.1_TfR1-CoilE<br>**Hoechst** | pcDNA3.1_TfR1-CoilE<br>**100 nM CoilR-Cy5**<br>**50 µg/mL Tf-AF488**<br>**Hoechst** | pcDNA3.1_TfR1-CoilE<br>**100 nM CoilR-Cy5**<br>**Hoechst** | pcDNA3.1_TfR1-CoilE<br>**50 µg/mL Tf-AF488**<br>**Hoechst** |
| pcDNA3.1_TfR1<br>**Hoechst** | pcDNA3.1_TfR1<br>**100 nM CoilR-Cy5**<br>**50 µg/mL Tf-AF488**<br>**Hoechst** | pcDNA3.1_TfR1<br>**100 nM CoilR-Cy5**<br>**Hoechst** | pcDNA3.1_TfR1<br>**50 µg/mL Tf-AF488**<br>**Hoechst** |

**Figure B.1. Layout of an 8-well chambered coverslip for imaging CHO TRVb cells expressing TfR1.** *Top row:* Cells expressing Coil-E tagged receptor (TfR1-CoilE). *Bottom Row:* Cells expressing untagged receptor (TfR1). The first line in each well indicates the vector used in the transfection. The subsequent lines indicate the labeling reagents, which are color-coded based on their fluorescence.

Recommendations for **Procedure B:**

- Preserving cell morphology and health is important for optimal labeling and imaging.
- Never let the cells go dry when processing cells for imaging. The preferred method for removing fluid from 8-well coverslips is to briskly invert the slide in a flicking motion. The surface tension of water will ensure an adequate layer of fluid remains in the well after it has been emptied.
- Reduce cell loss by gently dispensing solutions against the walls of the well. DPBS can be stored in a squeeze wash bottle for convenience when washing.
- Optimize labeling with the probe peptide. VIPER labeling efficiency will depend on the quality of the probe peptide, incubation temperature and time, and the target protein properties (abundance and localization). We have successfully labeled and imaged target proteins with 1 nM to 1 µM probe peptide. Previous experiments featuring competition with unlabeled peptide showed that 100 nM of peptide was enough to label most of an abundant protein target[30].

1. **Day 3:** Visually inspect transfected cells on a tissue culture microscope (*e.g.*, by bright field illumination, low magnification) to confirm that cells are adherent, healthy, and 80-90% confluent.
2. Remove media and add 100 µl of Live Cell Block Solution (Recipe 1) to each well. Return to the tissue culture incubator for 30 min.
   *Note: We include this step to reduce non-specific binding to live-cell surfaces.*
3. While the cells are in Live Cell Block Solution, prepare the labeling solution in pre-chilled Ham's F12 media without serum.
   a. Dilute CoilR probe peptide and 50 µg/ml Tf-AF488 into Ham's F12 media. Prepare at least 100 µl solution per well. We recommend first trying 100 nM CoilR-Cy5.

b. Analogous to a standard immunolabeling optimization, we recommend testing a range of probe peptide concentrations to obtain optimal signal to noise (*e.g.*, 1 nM to 500 nM CoilR-Cy5).
c. Other labeling reagents can be added to the labeling solution at this time, such as ligands, antibodies, or organelle stains.

4. Remove Live Cell Block Solution from each well.
5. Add 100 µl cold labeling solution to each well. Label cells for 30 min at 4 °C, protected from light.
6. Wash each well three times with ice-cold DPBS.
   a. *Optional step:* Add complete Ham's F12 media to each well and incubate the sample at 37 °C for 5 to 30 minutes to enable labeled receptors to traffic (*e.g.*, endocytose).
   b. *Optional step:* For pulse-chase labeling instructions, refer to our prior publication[30].
7. Fix the cells using ice-cold 4% v/v paraformaldehyde (PFA) in DPBS for 15 min at 4 °C.
   a. Prepare the fixative by diluting 20% v/v PFA 5-fold into DPBS. Make fresh fixative for every experiment.
   b. An opened solution of 20% v/v PFA can be stored in a sealed vial for up to 2 weeks.
8. Wash each well twice with DPBS.
9. Optional Step: Immunolabeling can be done at this point in the procedure.
10. Stain the nuclei with Hoechst 33342 (10 µg/ml) in DPBS for 5 min at 37 °C.
11. Wash wells once with DPBS.
12. Add Mounting Medium (Recipe 2) to wells.
13. Image cells by FM. See Doh's Supporting Information for more information on the imaging system and acquisition parameters[30]. The imaging parameters that we used are summarized below:
    a. Image cells using 63x/1.4 NA oil immersion objective lens on a Zeiss Yokogawa CSU-X1 spinning disk confocal microscope.

b. Capture single confocal slices with identical acquisition settings optimized for each channel.
c. Hoechst 33342 was imaged using 405 nm excitation and a 450/50 nm emission filter.
d. AF488 was imaged using 488 nm excitation and a 525/50 nm emission filter.
e. Cy5 was imaged using 633 nm excitation and a 670/30 emission filter.

**C. Application: Labeling an intracellular target with VIPER in cells post-fixation**

In **Procedure C**, we describe methods for imaging intracellular targets in fixed cells using VIPER. VIPER enables selective labeling of cellular proteins associated with organelles in fixed cells, including the cytoskeleton, nucleus, and mitochondria[30]. We used expression vectors that encoded target proteins fused to mEmerald, a green fluorescent protein. Fusion to a fluorescent protein was used to confirm that VIP-tagged proteins localized correctly. For fusion proteins, the CoilE tag was inserted between mEmerald and the target protein (*e.g.*, β-actin or histone H2B). This approach can also be used to label other intracellular targets[30]. Labeling intracellular targets requires that cells be fixed before treatment with a CoilR probe peptide because the peptide does not cross live cell membranes. We provide a different recipe for blocking fixed cells to reduce non-specific labeling. Similar to **Procedure B**, we recommend handling live cells carefully to retain viability and reduce cell loss.

In **Procedure C**, we describe a method for highlighting actin in U-2 OS cells expressing a fusion protein: mEmerald-CoilE-actin-C18. Fixed cells are treated with CoilR-Cy5 probe peptide. This procedure starts with transfected cells in 8-well chambered coverslips on *Day 3*, which can be prepared as described in **Procedure A**. We recommend including unlabeled or single-labeled controls for each fluorophore (*i.e.*, mEmerald, Hoechst, and Cy5) and including an untagged protein control (mEmerald-actin-C18). An example slide layout is provided in **Figure B.2**.

| | | | |
|---|---|---|---|
| mEmerald-CoilE-actin-C18<br>10 nM CoilR-Cy5<br>Hoechst | mEmerald-CoilE-actin-C18<br>100 nM CoilR-Cy5<br>Hoechst | mEmerald-CoilE-actin-C18<br>200 nM CoilR-Cy5<br>Hoechst | mEmerald-CoilE-actin-C18<br>Hoechst |
| mEmerald-actin-C18<br>10 nM CoilR-Cy5<br>Hoechst | mEmerald-actin-C18<br>100 nM CoilR-Cy5<br>Hoechst | mEmerald-actin-C18<br>200 nM CoilR-Cy5<br>Hoechst | mEmerald-actin-C18<br>Hoechst |

**Figure B.2. Layout of an 8-well chambered coverslip for imaging U-2 OS cells expressing either mEmerald-CoilE-actin-C18 (top row) or mEmerald-actin-C18 (bottom row).** The first line in each well indicates the vector used in the transfection. The subsequent lines indicate labeling reagents, which are color-coded based on their fluorescence. In this setup, three probe peptide concentrations (*i.e.*, 10, 100, and 200 nM CoilR-Cy5) are included to enable the identification of the optimal labeling conditions.

1. **Day 3:** Visually inspect each well on a tissue culture microscope to confirm that cells are adherent, healthy, and 80-90% confluent.
2. Remove media and wash each well once with DPBS.
3. Fix cells with 4% v/v PFA in DPBS for 10 min at room temperature.
4. Wash each well twice with DPBS to remove fixative.
5. Permeabilize cells with 0.1% v/v Triton X-100 in DPBS for 10 min at room temperature. Alternatively, cells can be permeabilized with 0.1% w/v saponin in DPBS.
6. Rinse wells twice with DPBS to remove detergent.
7. Remove DPBS and add 100 µl of Fixed Cell Block Solution (Recipe 3) to each well. Incubate for 30 min at room temperature.
8. During the block step, prepare the labeling solution in Fixed Cell Block Solution:
    a. Use 1 to 500 nM CoilR probe peptide (*i.e.*, CoilR-Cy5) in Fixed Cell Block Solution.
    b. We recommend testing a range of probe peptide concentration to obtain an optimal signal to noise ratio.
    c. Prepare 100 µl solution per well. Other labeling reagents can be added to the labeling solution at this time, such as ligands, primary antibodies, or organelle stains.
9. Remove Fixed Cell Block Solution and add the prepared CoilR labeling solution

to each well. Protect the slide from light and incubate for 30 min at room temperature.

10. Wash the wells 3 times with DPBS.
11. Stain the nuclei with Hoechst 33342 (10 µg/ml) in DPBS for 5-10 min at room temperature.
12. Wash wells once with DPBS.
13. Add Mounting Medium to wells.
14. Image cells by FM. **Figure B.3** provides representative micrographs of cells expressing mEmerald-CoilE-actin-C18 or mEmerald-actin-C18. See Doh et al.'s Supporting Information for more information on the imaging system and acquisition parameters [30], which are summarized below:
    a. Image cells using a 63x/1.4 NA oil immersion objective lens on a Zeiss Yokogawa CSU-X1 spinning disk confocal microscope (or similar system).
    b. Capture single confocal slices with identical acquisition settings optimized for each channel.
    c. Hoechst 33342 was imaged using 405 nm excitation and a 450/50 nm emission filter.
    d. mEmerald was imaged using 488 nm excitation and a 525/50 nm emission filter.
    e. Cy5 was imaged using 633 nm excitation and a 670/30 emission filter.

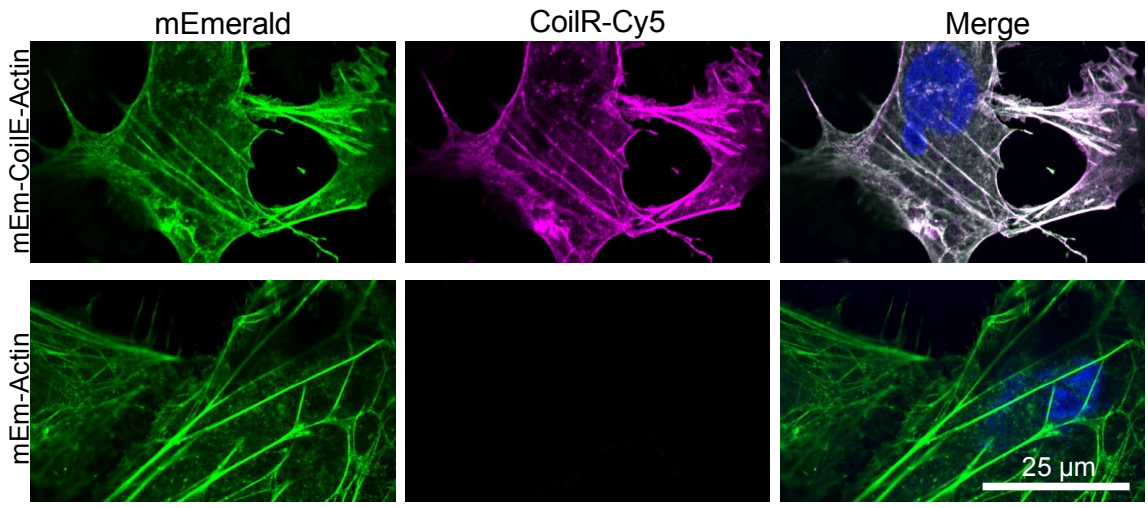


**Figure B.3. Highlighting actin in U-2 OS cells using VIPER.** U-2 OS cells were transfected with vectors encoding mEmerald-CoilE-Actin-C18 (mEm-CoilE-Actin; *top row*) or mEmerald-Actin-C18 (mEm-Actin; *bottom row*), labeled post-fixation by treatment with CoilR-Cy5 (100 nM), and then imaged by confocal FM. CoilR-Cy5 labeling was specific to CoilE-tagged protein, with Cy5 (magenta) and mEmerald (green) fluorescence appearing co-localized (white) in the merged image. Cy5 labeling was not observed in cells expressing mEmerald-actin-C18. The merge includes the nucleus false-colored blue (Hoechst 33342).

## Recipes

*Notes:*

- *Buffers are made in autoclaved DI water unless otherwise stated.*
- *The pH of Tris buffers changes with temperature, and the pH should be measured at room temperature.*
- *The pH of DPBS is 7.0.*

1. Live Cell Block Solution

   10% v/v FBS, 6% w/v BSA, in Ham's F12 media

   *Note: Block solution can be prepared in other media, such as McCoy's 5A*

2. Mounting Medium

   90% v/v glycerol

   10 mM Tris pH 7.0

   0.1% w/v sodium azide

3. Fixed Cell Block Solution

   10% v/v FBS, 5% w/v sucrose, 2% w/v BSA in DPBS

## Sequences

For fusion proteins incorporating VIP tags, we adopted a standardized naming convention. This N-to-C naming convention indicates the position of the tag in the name. For example, a C-terminal fusion of CoilE to Protein X will be named “ProteinX-CoilE” while an N-terminal fusion would be named “CoilE-ProteinX”. An intragenic fusion between two domains, Protein X and Protein Y, would be named “ProteinX-CoilE-ProteinY”.

*The amino acid sequence of CoilR expressed from pET28b(+)_CoilR (7502.35 Da) is:*

MGGS **LEIR AAFLRQR NTALRTE VAELEQE VQRLENE VSQYETR YGPL**GGGAAALGCLAAALE*HHHHHH*

Sequence Key: **CoilR**, conjugation handle, *hexa-histidine tag for purification*

*The pcDNA3.1_TfR1-CoilE vector encodes TfR1 with a C-terminal CoilE tag (TfR1-CoilE). The amino acid sequence is:*

MMDQARSAFSNLFGGEPLSYTRFSLARQVDGDNSHVEMKLAADEEENADNNMKASVRKPKRFNGRLCFAAIALVIFFLIGFMSGYLGYCKRVE
QKEECVKLAETEETDKSETMETEDVPTSSRLYWADLKTLLSEKLNSIEFADTIKQLSQNTYTPREAGSQKDESLAYYIENQFHEFKFSKVWRD
EHYVKIQVKSSIGQNMVTIVQSNGNLDPVESPEGYVAFSKPTEVSGKLVHANFGTKKDFEELSYSVNGSLVIVRAGEITFAEKVANAQSFNAI
GVLIYMDKNKFPVVEADLALFGHAHLGTGDPYTPGFPSFNHTQFPPSQSSGLPNIPVQTISRAAAEKLFGKMEGSCPARWNIDSSCKLELSQN
QNVKLIVKNVLKERRILNIFGVIKGYEEPDRYVVVGAQRDALGAGVAAKSSVGTGLLLKLAQVFSDMISKDGFRPSRSIIFASWTAGDFGAVG
ATEWLEGYLSSLHLKAFTYINLDKVVLGTSNFKVSASPLLYTLMGKIMQDVKHPVDGKSLYRDSNWISKVEKLSFDNAAYPFLAYSGIPAVSF
CFCEDADYPYLGTRLDTYEALTQKVPQLNQMVRTAAEVAGQLIIKLTHDVELNLDYEMYNSKLLSFMKDLNQFKTDIRDMGLSLQWLYSARGD
YFRATSRLTTDFHNAEKTNRFVMREINDRIMKVEYHFLSPYVSPRESPFRHIFWGSGSHTLSALVENLKLRQKNITAFNETLFRNQLALATWT
IQGVANALSGDIWNIDNEF*GSGSGSTGM***LEIEAAFLERENTALETRVAELRQRVQRLRNRVSQYRTRYGPL***GGG***CLETG

Key: **CoilE**, *linker*

*The mEmerald-CoilE-actin-C18 was made by inserting the CoilE sequence into mEmerald-actin-C18 (Addgene, #53978), as described [30]. The amino acid sequence for mEmerald-CoilE-actin-C18 is:*

MVSKGEELFTGVVPILVELDGDVNGHKFSVSGEGEGDATYGKLTLKFICTTGKLPVPWPTLVTTLTYGVQCFARYPDHMKQHDFFKSAMPEGY
VQERTIFFKDDGNYKTRAEVKFEGDTLVNRIELKGIDFKEDGNILGHKLEYNYNSHKVYITADKQKNGIKVNFKTRHNIEDGSVQLADHYQQN
TPIGDGPVLLPDNHYLSTQSKLSKDPNEKRDHMVLLEFVTAAGITLGMDELYK*SGLRSM***LEIEAAFLERENTALETRVAELRQRVQRLRNRVS**
**QYRTRYGPL***GGGRSGSGGGSASGGSGS*DDDIAALVVDNGSGMCKAGFAGDDAPRAVFPSIVGRPRHQGVMVGMGQKDSYVGDEAQSKRGILTL
KYPIEHGIVTNWDDMEKIWHHTFYNELRVAPEEHPVLLTEAPLNPKANREKMTQIMFETFNTPAMYVAIQAVLSLYASGRTTGIVMDSGDGVT
HTVPIYEGYALPHAILRLDLAGRDLTDYLMKILTERGYSFTTTAEREIVRDIKEKLCYVALDFEQEMATAASSSSLEKSYELPDGQVITIGNE
RFRCPEALFQPSFLGMESCGIHETTFNSIMKCDVDIRKDLYANTVLSGGTTMYPGIADRMQKEITALAPSTMKIKIIAPPERKYSVWIGGSIL
ASLSTFQQMWISKQEYDESGPSIVHRKCF

Key: mEmerald, **CoilE**, *linker*

## Acknowledgments

Research for this project was supported by the OHSU School of Medicine and the National Institutes of Health (R01 GM122854). JKD was partially funded by the Portland Chapter of Achievement Rewards for College Scientists (ARCS). The protocols described herein were originally described in Doh, Zane, et al.[30]. Fluorescent organelle constructs (Actin, H2B, and Mito) were acquired from the Michael Davidson Fluorescent Protein library from Addgene. CHO TRVb cells were provided by Prof. Timothy McGraw. We are grateful to our colleagues at OHSU for their contributions to this work, particularly Dr. Hannah Zane and Dr. Jonathan White.

## Works Cited


1. Valm, A. M. *et al.* Applying systems-level spectral imaging and analysis to reveal the organelle interactome. *Nature* **546**, 162-167, doi:10.1038/nature22369 (2017).
2. Liu, T. L. *et al.* Observing the cell in its native state: Imaging subcellular dynamics in multicellular organisms. *Science* **360**, doi:10.1126/science.aaq1392 (2018).
3. Guo, Y. *et al.* Visualizing Intracellular Organelle and Cytoskeletal Interactions at Nanoscale Resolution on Millisecond Timescales. *Cell* **175**, 1430-1442.e1417, doi:https://doi.org/10.1016/j.cell.2018.09.057 (2018).
4. Liu, Z., Lavis, Luke D. & Betzig, E. Imaging Live-Cell Dynamics and Structure at the Single-Molecule Level. *Mol. Cell.* **58**, 644-659, doi:http://dx.doi.org/10.1016/j.molcel.2015.02.033 (2015).
5. Vandemoortele, G., Eyckerman, S. & Gevaert, K. Pick a Tag and Explore the Functions of Your Pet Protein. *Trends Biotechnol*, doi:10.1016/j.tibtech.2019.03.016 (2019).
6. Giepmans, B. N., Adams, S. R., Ellisman, M. H. & Tsien, R. Y. The fluorescent toolbox for assessing protein location and function. *Science* **312**, 217-224, doi:10.1126/science.1124618 (2006).
7. Crivat, G. & Taraska, J. W. Imaging proteins inside cells with fluorescent tags. *Trends Biotechnol* **30**, 8-16, doi:10.1016/j.tibtech.2011.08.002 (2012).
8. Shaner, N. C., Steinbach, P. A. & Tsien, R. Y. A guide to choosing fluorescent proteins. *Nature methods* **2**, 905-909, doi:10.1038/nmeth819 (2005).
9. Snapp, E. L. Fluorescent proteins: a cell biologist's user guide. *Trends Cell Biol* **19**, 649-655, doi:10.1016/j.tcb.2009.08.002 (2009).
10. Cottet-Rousselle, C., Ronot, X., Leverve, X. & Mayol, J.-F. Cytometric assessment of mitochondria using fluorescent probes. *Cytometry Part A* **79A**, 405-425, doi:10.1002/cyto.a.21061 (2011).
11. Bucevičius, J., Lukinavičius, G. & Gerasimaitė, R. The Use of Hoechst Dyes for DNA Staining and Beyond. *Chemosensors* **6**, 18 (2018).
12. Keppler, A. *et al.* A general method for the covalent labeling of fusion proteins with small molecules in vivo. *Nature biotechnology* **21**, 86-89, doi:10.1038/nbt765 (2003).
13. Gautier, A. *et al.* An engineered protein tag for multiprotein labeling in living cells. *Chem Biol* **15**, 128-136, doi:10.1016/j.chembiol.2008.01.007 (2008).
14. Los, G. V. *et al.* HaloTag: a novel protein labeling technology for cell imaging and protein analysis. *ACS Chem Biol* **3**, 373-382, doi:10.1021/cb800025k (2008).
15. Dempsey, G. T., Vaughan, J. C., Chen, K. H., Bates, M. & Zhuang, X. Evaluation of fluorophores for optimal performance in localization-based super-resolution imaging. *Nature methods* **8**, 1027-1036, doi:10.1038/nmeth.1768 (2011).
16. Li, H. & Vaughan, J. C. Switchable Fluorophores for Single-Molecule Localization Microscopy. *Chem Rev* **118**, 9412-9454, doi:10.1021/acs.chemrev.7b00767 (2018).
17. Keppler, A. *et al.* A general method for the covalent labeling of fusion proteins with small molecules in vivo. *Nature Biotech.* **21**, 86-89 (2003).

18. Gautier, A. *et al.* An Engineered Protein Tag for Multiprotein Labeling in Living Cells. *Chem. Biol.* **15**, 128-136, doi:http://dx.doi.org/10.1016/j.chembiol.2008.01.007 (2008).
19. Los, G. V. *et al.* HaloTag: A Novel Protein Labeling Technology for Cell Imaging and Protein Analysis. *ACS Chem. Biol.* **3**, 373-382, doi:10.1021/cb800025k (2008).
20. Miller, L. W., Cai, Y., Sheetz, M. P. & Cornish, V. W. In vivo protein labeling with trimethoprim conjugates: a flexible chemical tag. *Nat. Meth.* **2**, 255-257 (2005).
21. Szent-Gyorgyi, C. *et al.* Fluorogen-activating single-chain antibodies for imaging cell surface proteins. *Nat. Biotech.* **26**, 235-240, doi:http://www.nature.com/nbt/journal/v26/n2/suppinfo/nbt1368_S1.html (2008).
22. Brock, R., Hamelers, I. H. L. & Jovin, T. M. Comparison of fixation protocols for adherent cultured cells applied to a GFP fusion protein of the epidermal growth factor receptor. *Cytometry* **35**, 353-362, doi:10.1002/(SICI)1097-0320(19990401)35:4<353::AID-CYTO8>3.0.CO;2-M (1999).
23. Huang, L., Pike, D., Sleat, D. E., Nanda, V. & Lobel, P. Potential Pitfalls and Solutions for Use of Fluorescent Fusion Proteins to Study the Lysosome. *PLoS ONE* **9**, e88893, doi:10.1371/journal.pone.0088893 (2014).
24. Costantini, L. M. & Snapp, E. L. Fluorescent proteins in cellular organelles: serious pitfalls and some solutions. *DNA and cell biology* **32**, 622-627, doi:10.1089/dna.2013.2172 (2013).
25. Johnson, G. R., Buck, T. E., Sullivan, D. P., Rohde, G. K. & Murphy, R. F. Joint modeling of cell and nuclear shape variation. *Mol Biol Cell* **26**, 4046-4056, doi:10.1091/mbc.E15-06-0370 (2015).
26. Griffin, B. A., Adams, S. R. & Tsien, R. Y. Specific covalent labeling of recombinant protein molecules inside live cells. *Science* **281**, 269-272 (1998).
27. Gaietta, G. *et al.* Multicolor and electron microscopic imaging of connexin trafficking. *Science* **296**, 503-507 (2002).
28. Cohen, J. D., Thompson, S. & Ting, A. Y. Structure-Guided Engineering of a Pacific Blue Fluorophore Ligase for Specific Protein Imaging in Living Cells. *Biochemistry* **50**, 8221-8225, doi:10.1021/bi201037r (2011).
29. Liu, D. S. *et al.* Computational design of a red fluorophore ligase for site-specific protein labeling in living cells. *Proc. Natl. Acad. Sci. U.S.A.* **111**, E4551-E4559, doi:10.1073/pnas.1404736111 (2014).
30. Doh, J. K. *et al.* VIPER is a genetically encoded peptide tag for fluorescence and electron microscopy. *Proc. Natl. Acad. Sci. U.S.A.* **115**, 12961-12966, doi:10.1073/pnas.1808626115 (2018).
31. Zane, H. K., Doh, J. K., Enns, C. A. & Beatty, K. E. Versatile interacting peptide (VIP) tags for labeling proteins with bright chemical reporters. *ChemBioChem* **18**, 470-474 (2017).
32. Lotze, J. *et al.* Time-Resolved Tracking of Separately Internalized Neuropeptide Y2 Receptors by Two-Color Pulse-Chase. *ACS Chem. Biol.*, doi:10.1021/acschembio.7b00999 (2018).
33. Reinhardt, U. *et al.* Peptide-Templated Acyl Transfer: A Chemical Method for the Labeling of Membrane Proteins on Live Cells. *Angew. Chem. Int. Ed.*, 10237-10241, doi:10.1002/anie.201403214 (2014).

34. Reinhardt, U., Lotze, J., Mörl, K., Beck-Sickinger, A. G. & Seitz, O. Rapid Covalent Fluorescence Labeling of Membrane Proteins on Live Cells via Coiled-Coil Templated Acyl Transfer. *Bioconjugate Chemistry* **26**, 2106-2117, doi:10.1021/acs.bioconjchem.5b00387 (2015).
35. Tsutsumi, H. *et al.* Fluorogenically Active Leucine Zipper Peptides as Tag–Probe Pairs for Protein Imaging in Living Cells. *Angew. Chem. Int. Ed.* **48**, 9164-9166, doi:10.1002/anie.200903183 (2009).
36. Nomura, W. *et al.* Development of crosslink-type tag-probe pairs for fluorescent imaging of proteins. *Peptide Science* **94**, 843-852, doi:10.1002/bip.21444 (2010).
37. Tsutsumi , H., Abe , S., Mino , T., Nomura, W. & Tamamura, H. Intense Blue Fluorescence in a Leucine Zipper Assembly. *ChemBioChem* **12**, 691-694, doi:10.1002/cbic.201000692 (2011).
38. Lotze, J., Reinhardt, U., Seitz, O. & Beck-Sickinger, A. G. Peptide-tags for site-specific protein labelling in vitro and in vivo. *Mol Biosyst* **12**, 1731-1745, doi:10.1039/c6mb00023a (2016).
39. Yano, Y. & Matsuzaki, K. Live-cell imaging of membrane proteins by a coiled-coil labeling method—Principles and applications. *Biochimica et Biophysica Acta (BBA) - Biomembranes* **1861**, 1011-1017, doi:https://doi.org/10.1016/j.bbamem.2019.02.009 (2019).
40. Yano, Y. *et al.* Coiled-Coil Tag-Probe System for Quick Labeling of Membrane Receptors in Living Cells. *ACS Chem. Biol.* **3**, 341-345 (2008).
41. Snapp, E. Design and use of fluorescent fusion proteins in cell biology. *Current protocols in cell biology* **Chapter 21**, 21 24 21-21 24 13, doi:10.1002/0471143030.cb2104s27 (2005).
42. Chen, X., Zaro, J. L. & Shen, W.-C. Fusion protein linkers: Property, design and functionality. *Advanced Drug Delivery Reviews* **65**, 1357-1369, doi:https://doi.org/10.1016/j.addr.2012.09.039 (2013).
43. Argos, P. An investigation of oligopeptides linking domains in protein tertiary structures and possible candidates for general gene fusion. *Journal of molecular biology* **211**, 943-958, doi:10.1016/0022-2836(90)90085-Z (1990).
44. George, R. A. & Heringa, J. An analysis of protein domain linkers: their classification and role in protein folding. *Protein engineering* **15**, 871-879 (2002).
45. Crasto, C. J. & Feng, J. A. LINKER: a program to generate linker sequences for fusion proteins. *Protein engineering* **13**, 309-312 (2000).
46. McGraw, T. E., Greenfield, L. & Maxfield, F. R. Functional expression of the human transferrin receptor cDNA in Chinese hamster ovary cells deficient in endogenous transferrin receptor. *J Cell Biol* **105**, 207-214 (1987).
47. Schindelin, J. *et al.* Fiji: an open-source platform for biological-image analysis. *Nat Methods* **9**, 676-682, doi:10.1038/nmeth.2019 (2012).
48. Lipofectamine® 2000 Reagent Protocol 2013. (2013). <tools.thermofisher.com/content/sfs/manuals/Lipofectamine_2000_Reag_protocol.pdf>.

# Appendix C: Protocol for Imaging VIPER-labeled Cellular Proteins by Correlative Light and Electron Microscopy

**Julia K. Doh**, Young Hwan Chang, Caroline A. Enns, Claudia S. López, and Kimberly E. Beatty

*This work is adapted from a manuscript originally published by Bio-Protocol on November 5, 2019 in volume 9, issue 21. It has been adapted for this dissertation and reprinted with permission.*

## Abstract

Advances in fluorescence microscopy (FM), electron microscopy (EM), and correlative light and EM (CLEM) offer unprecedented opportunities for studying diverse proteins and nanostructures involved in fundamental cell biology. It is now possible to visualize and quantify the spatial organization of cellular proteins and other macromolecules by FM, EM, and CLEM. However, tagging and tracking cellular proteins across size scales is restricted by the scarcity of methods for attaching appropriate reporter chemistries to target proteins. Namely, there are few genetic tags compatible with EM. To overcome these issues we developed Versatile Interacting Peptide (VIP) tags, genetically-encoded peptide tags that can be used to image proteins by fluorescence and EM. VIPER, a VIP tag, can be used to label cellular proteins with bright, photo-stable fluorophores for FM or electron-dense nanoparticles for EM. This protocol provides an instructional guide for implementing VIPER for imaging a cell-surface receptor by CLEM.

## Background

Multiple protein targets can be imaged at once by fluorescence microscopy (FM), electron microscopy (EM), or correlative light and EM (CLEM)[1-5]. FM enables multi-color microscopy in both living and fixed cells, and acquiring data can be relatively fast and easy. However, EM offers better resolution for imaging nanoscale features, including cell receptors, membrane boundaries, neuronal connections[6], chromatin organization[7], or the endocytic machinery[8]. We anticipate an increased reliance on multi-color, cross-

platform imaging for investigating proteins associated with normal cell function and human diseases[9-18]. Currently, most high-resolution imaging studies obtain protein-specific contrast with immunolabeling, which has known shortcomings[19-22].

The central obstacle that has limited progress in multi-scale microscopy is the shortage of genetic tags for labeling proteins. There are a number of protein tags available for imaging proteins by FM, including fluorescent proteins and self-labeling enzyme tags[23,24]. However, there are few genetic tags for EM or CLEM[25]. Most EM tags rely on the oxidation of diaminobenzidine (DAB) to form a polymer that is stained with osmium tetroxide to generate contrast. Examples include APEX[26,27], miniSOG[28], the tetracysteine tag[29], and others[30,31]. Among the DAB-reliant EM tags, miniSOG, FLIPPER[30], and the tetracysteine tag are compatible with CLEM. However, DAB staining is finicky, and it can be difficult to localize the stain sufficiently to resolve targets. Further progress in multi-scale microscopy will require new methods for labeling proteins with EM- and CLEM-compatible reporters, such as quantum dots (Qdots)[2] or FluoroNanogold™ particles[32].

We recently described a new class of tags for multiscale microscopy called Versatile Interacting Peptide (**VIP**) tags[33,34]. VIP tags use heterodimerizing coiled-coil peptides to label proteins. One coil is expressed as a fusion to the protein of interest. This coil has a partner, the probe peptide, that is conjugated to a reporter molecule to deliver protein-specific contrast. The probe peptide can be conjugated to a number of reporters, such as fluorophores, small molecules (e.g., biotin), or nanoparticles.

In this Bio-Protocol we outline the use of VIPER to image a transmembrane receptor by CLEM. VIPER is a VIP tag comprised of CoilE tag and CoilR probe peptide. In **Procedure A**, we describe the plating and transfection of cells to express a CoilE-tagged receptor: transferrin receptor 1 (TfR1-CoilE). **Procedure B** describes how to label a cell receptor with CoilR-biotin for subsequent detection with streptavidin-Qdot655. In **Procedure C** we have an illustrated guide on how to mount ITO coverslips to a slide holder for correlative fluorescence imaging. **Procedure D** describes image acquisition with a commercially available CLEM microscope, the FEI CorrSight™. In **Procedures E** and **F** we describe methods for preparing samples for EM. **Procedure G** details the acquisition of SEM micrographs on a Helios Nanolab™ 660 EM. We

additionally developed a quantitative image analysis pipeline for automated image segmentation on high magnification SEM images (see the **Data Analysis** section). This program runs in Matlab and reports the number of nanoparticles within a field of view in SEM micrographs.

## Materials and Reagents

**Note:** *"*" indicates a brand that is critical to the success of the experiment.*

### Materials

1. Aluminum coverslip holder

   **Note:** *We used a custom machined aluminum plate with a hole for a 22 x 22 mm coverslip. This plate is 76 x 26 x 1.5 mm with a 12 mm diameter hole in the center.*
2. *Indium tin-oxide 22 x 22 mm coverslips (2SPI, catalog number: 06486-AB)
3. Tape (Scotch® Magic™ Tape)
4. Desiccator cabinet (Thermo Scientific Nalgene™, catalog number: 53170070)
5. Desiccant (Drierite™, catalog number: D1085)
6. Kimwipes (Kimtech, catalog number: 34120)
7. *Conductive silver paint "Leitsilber" (Ted Pella, catalog number: 16035)
8. *SEM pin stub specimen mount (Ted Pella, catalog number: 16144)
9. *Carbon thread (Leica, catalog number: 16771511116)
10. LDPE 500 ml squeeze wash bottle (Thermo Scientific, catalog number: 24010500)
11. Transfer bulb pipette (VWR, catalog number: 16001-182)

### Reagents

1. CHO TRVb cells (courtesy of Prof. Timothy McGraw, Cornell University, Ithaca, New York) [35]
2. Ham's F-12 Medium (Life Technologies, Gibco™, catalog number: 11765062)
3. Dulbecco's phosphate-buffered saline without calcium or magnesium; DPBS (Gibco™, catalog number: 14190144)
4. Trypsin-EDTA (0.25%) (Life Technologies, Gibco™, catalog number: 25200056)

5. Fetal bovine serum (FBS) (GE, Hyclone™, catalog number: SH30910.03)
6. *Lipofectamine™ 2000 (Thermo Scientific, catalog number: 11668019)
7. Opti-MEM (Life Technologies, Gibco™, catalog number: 31985070)
8. *Streptavidin-Qdot™ 655 conjugate (Invitrogen, catalog number: Q10121MP)
9. Anhydrous ethanol (Decon Labs, catalog number: 2716)
10. 20% v/v paraformaldehyde (PFA) stock (Electron Microscopy Sciences, catalog number: 15713S)

**Equipment**

1. Hemocytometer (Hausser Scientific, catalog number: 1475)
2. Humidified $CO_2$ Incubator (New Brunswick Galaxy 170S, catalog number: C0170S-120-0000)
3. Tissue culture hood (Thermo Scientific 1300 Series A2)
4. Tissue culture inverted light microscope (Carl Zeiss, Zeiss Primovert)
5. Fine point tweezers (Ted Pella Dumostar Biology, catalog number: 525-PS)
6. Diamond-tipped scribe (Ted Pella, catalog number: 54468)
7. Stainless steel crinkle washers (Tousimis Washers, catalog number: 8767-01)
8. Orbital Shaker (Stovall Belly Dancer™, catalog number: BDRAA1158)
9. Spinning disk confocal fluorescence microscope (FEI CorrSight™)
10. 63x objective lens (Carl Zeiss, 1.4 NA Plan-Apochromat M27, catalog number: 420780-9900-000)
11. 5x objective lens (Carl Zeiss, 0.16 NA EC Plan-Neofluar M27, catalog number: 420330-9901-000)
12. Scanning electron microscope (FEI Helios Nanolab™ 660 SEM)
13. Critical point dryer (Leica EM CPD300)
14. High Vacuum Flash Carbon Coating Machine (Leica EM ACE600)

**Software**

1. FEI MAPS (FEI version 2.1.38.1199 and version 3.0)
2. FEI Helios Nanolab™ xT Microscope Control (FEI version 5.5.1 and version 10.1.7)

3. Matlab (Mathworks Software Version R2017b)

## Procedures

### A. Transfecting cell lines to express a VIPER-tagged protein

This protocol describes the transfection of a tissue culture cell line to express a VIPER-tagged transmembrane receptor (i.e., TfR1-CoilE). We used the CHO TRVb cell line because it does not express TfR1 or transferrin receptor 2[35]. After transfection, all TfR1 receptor will encode the C-terminal CoilE tag on the extracellular domain.

We recommend optimizing plating density and transfection conditions for each cell line. Refer to Thermo Fisher's Protocol Pub No. MAN0007824 Rev 1.0[36] for more information on transfection with Lipofectamine 2000. In our protocol, we recommend passaging cells on **Day 1**, transfecting cells on **Day 2**, and VIPER labeling cells on **Day 3** (see Procedure B).

Recommendations for **Protocol A:**

- Use sterile technique and work within a tissue culture (laminar flow) hood when working with live cells.
- When transfecting cells with a vector encoding a CoilE-tagged protein (e.g., pcDNA3.1_TfR1-CoilE), we also recommend transfecting cells with an untagged protein to compare labeling specificity (e.g., pcDNA3.1_TfR1). Untransfected cells also serve as a control for labeling specificity.
- The sequence for TfR1-CoilE can be found in the **Sequences** section.

1. **Day 1:** Passage cells and plate onto indium tin oxide (ITO) coverslips
   a. Before starting, visually inspect cells on a tissue culture microscope to confirm that cells are adherent, healthy, and 80-90% confluent.
   b. Place single 22 x 22 mm ITO coverslips into each well of a sterile 6-well polystyrene tissue culture plate.
      i. The ITO coverslips are provided in a small box with the conductive side oriented face up. Transfer the coverslip to the 6-well plate without flipping the coverslip over. Maintain this orientation during transfection, labeling,

and processing.

ii. Pre-coating coverslips with poly-L-lysine or other cell-surface treatments may be necessary to adhere cells to glass. CHO TRVb cells adhere to glass without additional support.

c. Seed 1 x $10^6$ cells per well (for CHO TRVb). Grow cells in Ham's F12 medium supplemented with 5% FBS. Do not include antibiotics in the media.

i. For other cell lines, seed at a density that will result in 80-90% confluency after 24 h.

2. Incubate cells overnight in a humidified tissue culture incubator (37 °C with 5% $CO_2$).
3. **Day 2:** Prepare the transfection mixture
   a. Dilute vector DNA into Opti-MEM:
      i. For a 6-well plate, use 2 µg DNA in 100 µl of Opti-MEM per well.
      ii. The DNA quality is paramount for a high transfection efficiency. Quantify DNA quality by UV spectroscopy and verify that the 260/280 nm ratio falls between 1.8 and 2.0.
      iii. Keep the volume of DNA to less than 10% of the total volume in the transfection mixture.
   b. Dilute Lipofectamine 2000 into Opti-MEM and incubate for 5 min:
      i. For a 6-well plate, use 4 µg Lipofectamine2000 in 100 µl of Opti-MEM per well.
   c. Combine equal volumes of the Lipofectamine2000 and DNA solutions and mix by pipetting. The final ratio of DNA to Lipofectamine2000 will be 1:2. Incubate mixture for at least 30 min at room temperature.
4. Transfect cells:
   a. Aspirate media from cells.
   b. Add Opti-MEM to wells. For 6-well dishes use 800 µl per well.
   c. Add 200 µl of the transfection mixture to each well (1:5 dilution). The total volume of fluid in each well should be 1 ml.
   d. Gently mix the solution by pipetting up and down or by rocking the plate.
   e. Incubate cells in the transfection mixture for 4 h in a tissue culture incubator

(37 °C, 5% $CO_2$).

i. This time frame is recommended for transfecting CHO TRVb cells.

ii. Monitor cells by viewing on a TC microscope. Cell size and shape should appear unchanged during transfection. If cells contract or detach, then adjust the transfection conditions.

f. Aspirate to remove the transfection media and wash once with complete media (*e.g.*, media with FBS).

g. Add complete media and grow in a tissue culture incubator (37 °C, 5% $CO_2$) for at least 24 h. Cells will be ready for use between 24 and 48 h after transfection.

## B. Labeling VIPER-tagged receptors with Qdots on ITO coverslips

**Protocol B** describes a method for labeling a transmembrane receptor (TfR1-CoilE) with a biotinylated probe peptide (CoilR-biotin). Biotinylated receptor is subsequently detected with a streptavidin-Qdot655 conjugate. The biotinylated receptor could be labeled with other streptavidin conjugates, such as streptavidin-gold. We counter-stained with fluorescent transferrin (Tf-AF488), the ligand of TfR1, to enable the rapid identification of transfected cells. Lastly, live cells were cooled to 4 °C to pause endocytosis during labeling of the cell-surface receptor.

1. **Day 3.** Visually inspect each well on a tissue culture microscope to confirm that transfected cells are adherent, healthy, and 80-90% confluent.
2. Remove media and add 500 µl of Live Cell Block Solution (**Recipe 1**) to each well. Return to the tissue culture incubator for 30 min.
   a. Use a pipette or transfer bulb pipette to aspirate media from wells, taking care to always leave enough media to keep the cells and coverslips hydrated.
3. While the cells are in Live Cell Block Solution, prepare the CoilR labeling solution.
   a. Dilute CoilR-biotin probe peptide and 50 µg/ml Tf-AF488 into pre-chilled Ham's F12 media without serum. Prepare 500 µl of the labeling solution per well.

b. We recommend testing a range of probe peptide concentrations to obtain optimal signal to noise (*e.g.*, 100 nM to 500 nM). For CHO TRVb cells expressing TfR1-CoilE we recommend 100 nM CoilR-biotin in Ham's F12 media.
c. Other labeling reagents can be added at this time.

**Note:** *Qdots have spectral overlap with Hoechst 33342, so we do not use this nuclear stain for these studies.*

4. Remove Block Solution 1 from each well.
5. Add 500 µl of the labeling solution to each well. Label cells for 30 min at 4 °C, protected from light.
   a. Labeling is done at 4 °C in pre-chilled media to restrict endocytosis of VIPER-labeled receptors. Accessibility of the receptors on the cell surface will be especially critical for the subsequent SEM detection of CoilR-biotin with streptavidin-Qdots.
6. Wash each well three times with ice-cold DPBS.
7. Fix the cells using ice-cold 4% v/v PFA in DPBS. Incubate cells in fixative for 15 min at 4 °C.
8. Wash each well twice with DPBS to remove fixative.
9. Block the ITO coverslips with 800 µl Qdot Block Solution (**Recipe 2**) for 1h at room temperature.
10. While cells are in Qdot Block Solution prepare the Qdot labeling solution:
    a. The Qdots are supplied by Invitrogen as a 1 µM stock solution. Before using, centrifuge (17,000 *x g*, 5 min) the streptavidin-Qdot655 conjugate to remove aggregated Qdots from solution.
    b. A range of concentrations should be tested to ensure optimal labeling.
    c. We used 10 nM streptavidin-Qdot655 in Qdot Labeling Solution (**Recipe 3**) for CHO TRVb transfected with TfR1-CoilE.
    d. Prepare 500 µl of labeling solution per well (*e.g.*, 3 ml of solution for 6 samples).
11. Remove Qdot Block Solution from each well.

12. Add 500 µl of the streptavidin-Qdot655 labeling solution to each well and label for 1 h at room temperature. Protect samples from light during this step.
13. After Qdot labeling, wash three times with DPBS.
14. Image and map ITO coverslips by confocal FM (e.g., with an FEI CorrSight™) before processing samples for CLEM (Procedure C and D).

## C. Mounting ITO coverslips for CLEM imaging

This procedure describes the methods for handling ITO coverslips prepared in **Procedure B**. This procedure uses a custom-machined aluminum slide to hold the ITO coverslips during imaging. This slide was created by Ingo Gestmann (FEI). The dimensions of the slide are 76 x 26 x 1.5 mm. The hole is 12 mm in diameter, which is compatible with the 22 x 22 mm ITO coverslips. There are likely commercially-available coverslip holders, but we have not tested any. The custom-machined aluminum slide (**Figure C.1**) has a piece of coverglass glued with epoxy to one side (**Side B**). The other side remains open, with a circular chamber (**Side A**).

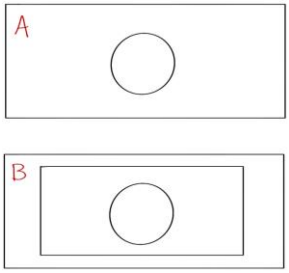


**Figure C.1. Diagram of the aluminum coverslip holder.** Side A shows a circular hole. Side B has a rectangular piece of coverglass glued to cover the circular hole. This set-up allows the user to create an enclosed chamber of buffer by taping an ITO coverslip to side A.

1. Using a diamond-tipped scribe, scratch a small “F” into the center of the ITO coverslip to create a fiducial marker. Make strokes roughly 1 cm in length. A larger fiducial generates better correlation later on during SEM, but it should still be fully visible through the hole in the aluminum slide (see **Figure C.2**). The coverslip can be stabilized during this process by holding it down with fine point tweezers.

a. For multiple samples, use the scribe to make additional marks to enable quick differentiation of your samples. An example scheme would be:
    i. Sample 1: “F” only; no notch
    ii. Sample 2: notch below “F”
    iii. Sample 3: notch above “F”
    iv. Sample 4: notch to the left of “F”
    v. Sample 5: notch to the right of “F”
    vi. Sample 6: notch below and above “F”

**Figure C.2. An “F” carved into the center of a 22 x 22 mm ITO coverslip.** Note the size of the “F” relative to the size of the coverslip.

2. Place the aluminum slide on the laboratory bench with side A facing up.
3. Pipette DPBS into the circular chamber drop-wise until the chamber is full. Add one more drop to create a raised meniscus (**Figure C.3**).

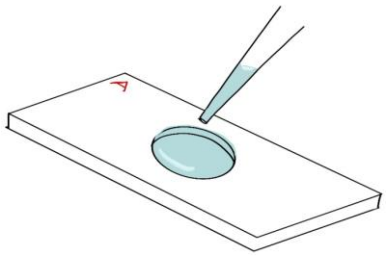

**Figure C.3. The aluminum coverslip holder with the circular chamber filled with buffer.**

4. Remove the labeled ITO coverslip from the 6-well plate using fine point tweezers.
5. Allow the excess DPBS to drip off but do not let the coverslip dry out. The ITO coverslip should be wet for the next step.
6. Position one edge of the wet ITO coverslip against the aluminum coverslip holder with the cells facing down, towards the surface of Side A (**Figure C.4**).

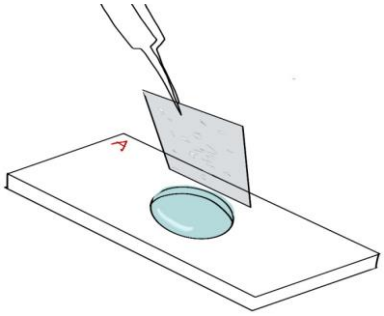

**Figure C.4. Positioning the ITO coverslip on the aluminum coverslip holder.** The side of the ITO coverslip with the adhered cells is positioned facing towards the chamber.

7. Use tweezers to carefully lower the ITO coverslip onto Side A. The ITO coverslip should be floating on a thin layer of fluid (**Figure C.5**). Do this quickly to avoid trapping air in the chamber.
    a. There should be no bubbles in the chamber between the ITO coverslip and the glass on Side B of the slide. Air bubbles will dry out the cells. Small bubbles are permissible if they do not contact the ITO coverslip when the slide is inverted.
    b. If a large air bubble is trapped under the ITO coverslip, use tweezers to lift the ITO coverslip at a shallow angle before dropping the ITO coverslip onto the DPBS again.
    c. The coverslip can also be nudged gently off of the slide with tweezers to free the bubble from the side of the coverslip.
    d. The position of the coverslip can be adjusted at this point as long as it is free-floating.
    e. Make sure you can see the entire fiducial marker (“F”) through the hole of the chamber.

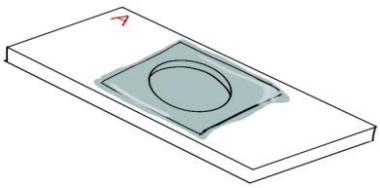

**Figure C.5. The ITO coverslip floating on a thin layer of DPBS over the circular chamber on Side A of the aluminum coverslip holder**

8. Blot excess fluid from the slide. Fold a Kimwipe in half and touch the folded edge to the side of the coverslip to blot excess fluid (**Figure C.6**). Repeat for all four sides until dry. If there is fluid on top of the coverslip you can lay a piece of tissue on top of the coverslip to blot the remainder. Only do this step after blotting the sides.
    a. *This will "seal" the coverslip to the slide. Moving or re-positioning the ITO coverslip at this point could damage the cells.*
    b. *If there is a bubble in the circular chamber or the ITO coverslip is poorly positioned after this step, DPBS can be added gently to the sides of the coverslip. Wait for the DPBS to flow underneath the coverslip and then lift it off the slide.*

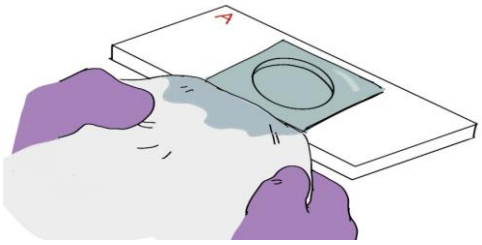

**Figure C.6. Removing excess DPBS from the aluminum coverslip holder by blotting with a Kimwipe.**

9. Tear a strip of clear tape (*e.g.*, 3M Scotch™ tape) in half and secure the coverslip to the slide by taping at the sides. Repeat for all sides (**Figure C.7**).
   **Note:** *Avoid applying an excess of tape because it will need to be removed after fluorescence imaging.*

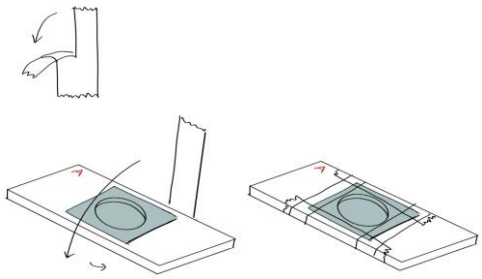

**Figure C.7. Attaching the coverslip to the aluminum coverslip holder using clear tape.**

10. Repeat this procedure for each ITO coverslip.
11. Image the prepared samples on an inverted confocal fluorescence microscope. We imaged an FEI CorrSight™ in the following Procedure D.

**Note:** *We recommend imaging soon after preparing the samples because some evaporation may occur.*

## D. Fluorescence imaging and mapping cells on an FEI CorrSight™ System

This procedure describes using the FEI CorrSight™ imaging system to collect micrographs of labeled cells. Samples prepared in **Procedure A-C** are first imaged by confocal FM to identify fluorescent cells. Confocal FM is used to image VIPER fluorescence (Qdot655) and Tf-AF488 on the cell surface. During FM imaging, the FEI MAPS software enables the user to select and "map" cells for subsequent high-resolution imaging by scanning EM (SEM). **Figure C.8** provides an overview of the FEI MAPS software.

**Note:** *Once the slide is placed on the stage and imaging commences, the slide must remain in place until it is fully mapped. Even small adjustment to the slide placement will shift the slide and make the map inaccurate, which makes it difficult to re-locate cells for SEM imaging.*

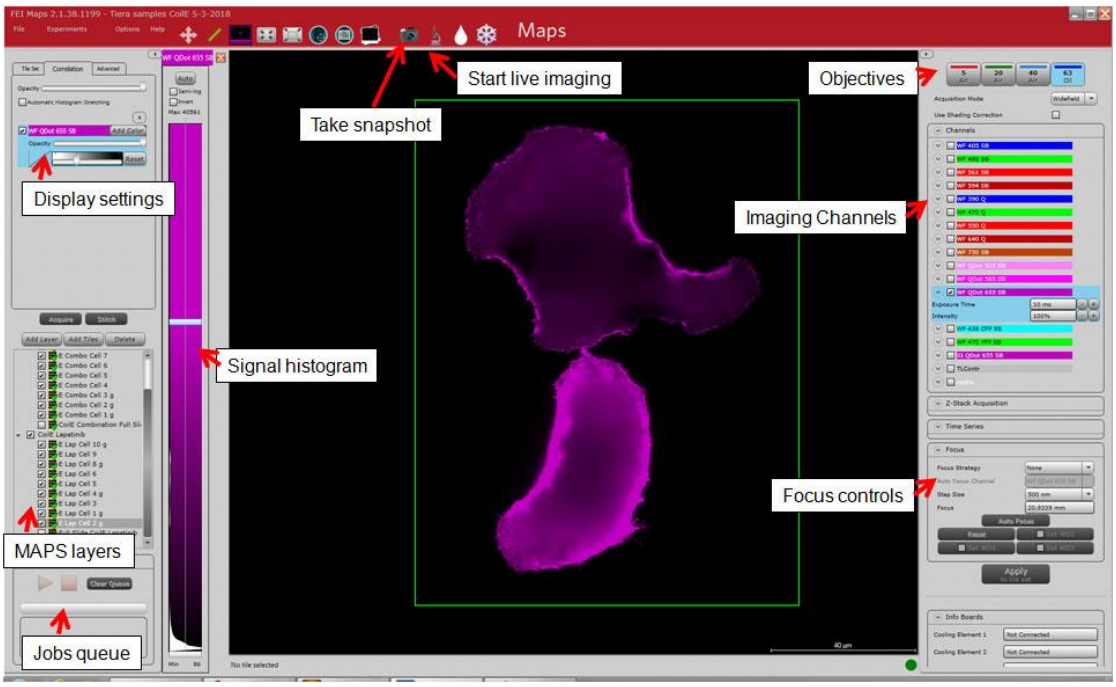


**Figure C.8. Annotated screen capture of the FEI MAPS 2.1.38 software.**

1. Place immersion oil on the 63x objective lens. Then switch to the 5x objective lens. This can be controlled in the panel labeled “Objectives”. Refer to **Figure C.8** for software controls from this point on. Additional information can be found in the FEI CorrSight™ user manual[37].

   **Note:** *This is a critical step. Removing the slide after 5x imaging to load oil on the 63x objective will offset the mapping. This will make re-locating cells difficult by SEM.*
2. Place the aluminum coverslip holder on the microscope stage with the ITO coverslip (Side A) facing downwards towards the objective.
3. Turn off all the fluorescence channels using the panel labeled “Imaging Channels” by unchecking all the boxes in that panel. Image the sample using transmitted light.
   a. In the panel labeled “Imaging Channels,” turn on the “TLControl” (transmitted light) channel by checking its box.
   b. In the panel labeled “Focus Controls,” set the focus to 20 mm.
   c. Start live imaging by clicking the button labeled “Live Imaging”.
   d. Adjust the focus with scroll wheel of the mouse until the cells and the fiducial

marker (“F”) are in focus. You can adjust the step size of the focusing in the panel labeled “Focus controls.”

**Note:** *The focal plane will vary across the coverslip. Therefore, it is important is to keep the fiducial “F” in focus as you move the stage.*

4. Drive the stage to the edge of the circular hole in the aluminum coverslip holder.
   a. To do this, left click on the live image where you want the stage to move.
   b. Once you have located an edge, take a snapshot (**Figure C.9**) by clicking the button labeled “Take snapshot”. The “Take snapshot” function loads the data into an aggregate layer called “PreviewImages” in the layers panel.

      **Note:** *This is not a viable place to store image data. However, these preview snapshots allow you to reference the edges of the circular chamber. These boundaries are needed in order to draw the tile-set that will capture the whole ITO coverslip.*
   c. Continue taking snapshots until you can determine of the boundaries of the circular chamber. This can generally be done with 4 snapshots placed at the top, bottom, left, and right of the circle.

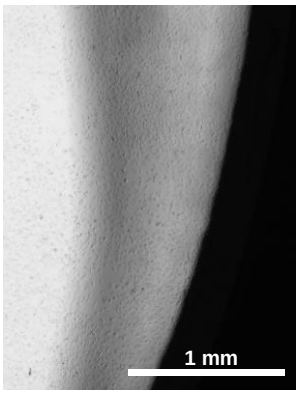


**Figure C.9. A snapshot of the ITO coverslip (light gray) showing the boundary of the circular chamber in the aluminum coverslip holder (black).**

5. Left click and drag over the slide hole (using the snapshots of the hole boundaries to guide you) and right-click “Add tiles here”. This will create a tile array to image the entire slide, capturing the fiducial F.
6. Execute the acquisition in the “Jobs queue” panel to generate a stitched tile

image of the coverslip by transmitted light (**Figure C.10**).

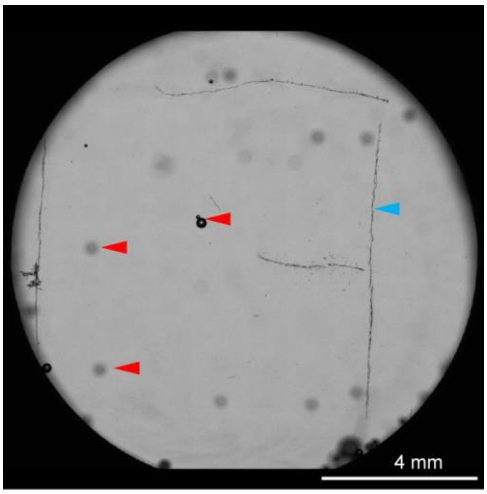


**Figure C.10. A stitched tile image showing the ITO coverslip (light gray) mounted on the aluminum coverslip holder (black).** Note that the entire "F" fiducial, denoted by a blue arrowhead, was captured and in focus. Small air bubbles can also be seen, with a few denoted by a red arrowhead.

7. Prepare to image cells by FM.
    a. Check box on the "WF 488 SB" channel in the "Imaging Channels" panel. This setting excites Tf-AF488 at 488 nm and collects emission through a 525/50 nm filter.
    b. Check box on the "WF Qdot 655 SB" channel. This setting excites Qdot655 at 405 nm and collects emission through a 690/50 nm filter.
    c. You can modify the intensity of each channel in the "Imaging Channels" panel by clicking on the channel name. Leave the intensity at 100% and set the exposure time appropriately by imaging live in these channels.
        i. "Good" acquisition settings generate signal that occupies more than 50% of the dynamic range of the 16-bit detector, without saturated signal in any pixels. This can be observed in the panel labeled "Signal histogram."
    d. The settings may require some adjustment after switching to the 63x objective lens.
8. Cells can now be imaged and mapped at 63x magnification.
    a. During image acquisition use the 5x objective to locate cells by low magnification. Then switch to the 63x objective oil lens to collect high-

resolution images. When a cell is “mapped”, the fluorescence image is acquired and the image is automatically saved with the coordinate location.

b. We recommend selecting cells for imaging based on their Tf-AF488 signal to avoid biasing cell selection towards the brightest Qdot655 signal (*i.e.*, the brightest VIPER-labeled cells).
c. We recommend taking 5x fluorescence images of the slide. These images are helpful for locating the mapped cells by SEM. This is especially true for samples with high cell density, where finding individual cells based on size and shape alone is difficult.
d. Repeated switching between 5x and 63x can create air bubbles in the immersion oil. These do not affect imaging at 63x, but the bubbles will appear in the 5x images.

9. To map cells, locate a desired cell at 63x magnification using the live-imaging function. Left click and drag a single tile over the cell location and right-click “Add tiles here”. This will create a tile to image the cell and register its location.
10. Execute the acquisition in the “Jobs queue panel”.
    **Note:** *The FEI MAPS acquisition software will remember the absolute position of cells imaged at 63x relative to the full size of the coverslip mapped at 5x magnification.*
11. Create a new layer for each cell. You can group samples by creating Layer groups. For each layer, make the names descriptive (*e.g.*, Cell 1 VIPER Qdot slide A). The names will become the folder names where data is stored.
    **Note:** *All of the individual images collected by the FEI MAPS software are automatically named “Tile_000_0001”. Therefore, descriptive layer names are important.*
12. After imaging and mapping, remove the slide from the FEI CorrSight™ microscope.
13. Clean the slide thoroughly with lens paper to remove immersion oil. Then clean with lens paper using 70% ethanol.
14. Remove the tape gently and return the ITO coverslip to DPBS in a 6-well plate for further processing (**Figure C.11**).

a. The ITO coverslip should be oriented with cells facing upwards in the 6-well plate.
b. The tape can be scored with a razor blade to help remove it from the aluminum slide.
c. If the sample is “stuck” on the aluminum slide after tape removal, apply a few drops of DPBS around the edges of the slide and wait for the fluid to move under the coverslip, lifting it from the slide. Forcing the coverslip off with tweezers can break the coverslip or damage the cells by sliding them against the aluminum slide.

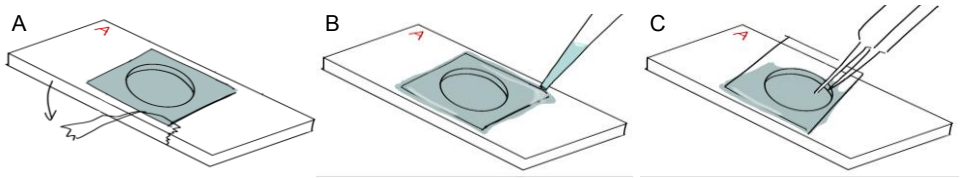


**Figure C.11. Removing the ITO coverslip on the aluminum coverslip holder.** (A) Remove the tape by pulling towards the side, instead of by pulling up, to minimize force applied to coverslip. (B) Add fluid to the edges of the ITO coverslip and wait for it to penetrate underneath the coverslip. (C) Use fine point tweezers to gently lift the coverslip off from the edges.

## E. Processing ITO coverslips for SEM imaging.

This procedure describes the methods used to dehydrate samples for SEM imaging on the Helios Nanolab™ 660. The methods continue from the last step of **Procedure D**, after samples have been imaged by FM and ITO coverslips are placed in a 6-well plate.

1. Prepare solutions of ethanol that will be used to dehydrate samples.
   a. Dilutions should be prepared with anhydrous ethanol and sterile DI water.
   b. Prepare 10-15 ml stocks of: 25%, 50%, 75%, and 90% (v/v) ethanol. Undiluted (“100% ethanol”) will also be used for dehydrating samples.
      **Note:** *For SEM imaging, it is critical to fully remove water from the cells when dehydrating because residual water can cause cell breakage and deformation (**Figure C.12**). Using a fresh bottle of anhydrous ethanol every time minimizes this risk.*

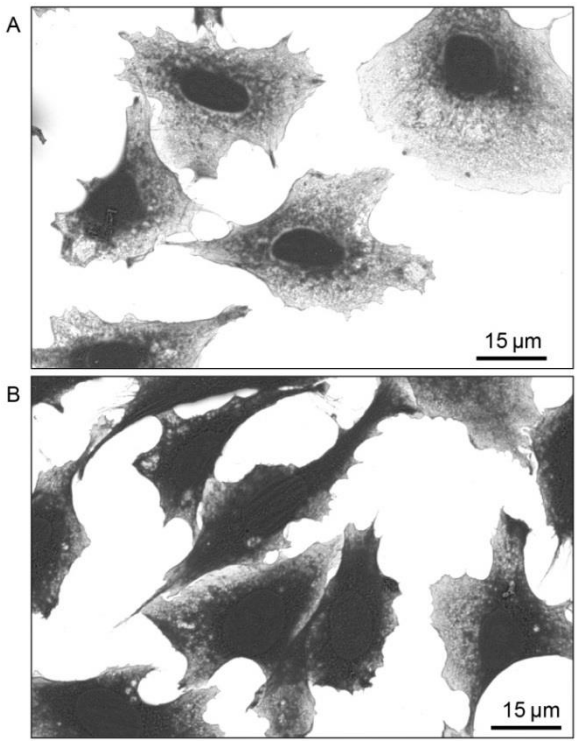


**Figure C.12. Micrographs of dehydrated CHO TRVb cells processed for SEM imaging.** SEM micrographs were acquired in backscattered mode on an FEI Helios Nanolab$^{TM}$ 660 SEM at 3,500x magnification (horizontal field width: 119 µm). The ITO coverslip appears bright white in this acquisition mode. A. Micrographs of damaged cells that were dehydrated with an ethanol gradient prepared using an old bottle of ethanol (opened and reused over several months). Cells are light gray and have a lace-like appearance with pronounced nuclei. The white ITO substrate can be seen from behind cells that are damaged, resulting in cells that are light gray around the nucleus. B. Micrographs of well-preserved cells that were dehydrated with an ethanol gradient prepared using a new bottle of anhydrous ethanol. In contrast to cells in A, these cells are intact, appear dark gray, and are more raised.

2. Withdraw most of the DPBS from the ITO coverslips using a micropipette or transfer pipette. Leave a small layer of fluid over the cells. If the samples dry out in air, the cells may break or appear damaged by SEM. To minimize this risk, never let the ITO coverslips go dry. This is especially important when using high percentages of ethanol, which evaporates quickly.
3. Wash the ITO coverslips with DI water (1.5 ml/well) to remove salts. Wash 5 min at room temperature with gentle agitation.
   **Note:** *Gentle agitation can be achieved by hand or on a rocking stage.*
4. Withdraw most of the water from the wells, again working to ensure that the

coverslips remain wet.

5. Add 25% v/v ethanol (1.5 ml/well) to the slides to start the dehydration gradient. Incubate 5 min at room temperature with gentle agitation.
6. Withdraw most of most of the 25% v/v ethanol from the wells, leaving enough solution so that the slides stay covered.
7. Repeat Steps E5 and E6 with: 50%, 75%, 90%, and 100% ethanol.
   **Note:** *This ethanol step-gradient dehydrates the cells slowly to minimize cell shrinking and structural damage during dehydration.*
8. Incubate coverslips a second time in 100% ethanol to ensure that all water is removed from the samples.
9. Coverslips are now ready to be loaded into the critical point dryer.
10. Use a critical point dryer (Leica EM CPD300) to dehydrate samples.
    a. Open the sample chamber and load the ITO coverslips.
       i. Using fine point tweezers, transfer the first layer of coverslips with the cells facing up.
       ii. ITO coverslips can be stacked on top of each other through the use of stainless steel crinkle washers. Place a washer gently on top of the ITO coverslip, and then add the next coverslip (**Figure C.13**). The washers are large enough that the cells of interest should be in the hole of the washer and not in contact with the washer itself. A total of 4 layers of coverslips can fit inside the sample chamber.

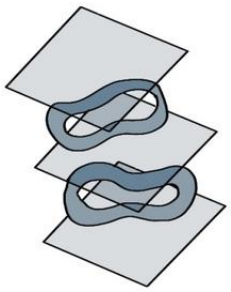

**Figure C.13. Using stainless steel crinkle washers to separate ITO coverslips during dehydration.** The washers prevent the coverslips from adhering to each other during the final dehydration steps.

    b. Use the critical point dryer to dehydrate the samples. On the Leica system,

we programmed the following dehydration conditions:

Stirring: 50%

Automatic exchanging: on

Speed of $CO_2$ injection: slow

Fillers: 1 stage (fillers are solid plastic pieces that are placed in the chamber to take up volume and minimize the drying volume)

Delay of $CO_2$ injection: 120 s

Speed of $CO_2$ exchange: 1 (out of 10)

Number of $CO_2$ exchange cycles: 25

Heating for $CO_2$ gassing out: slow

Speed of $CO_2$ gassing out: slow

11. Dried samples are now ready for mounting to pin stub specimen mounts (Procedure F).

**F. Mounting coverslips and carbon-coating for SEM imaging**

This procedure describes methods used to mount dehydrated ITO coverslips on SEM pin stub specimen mounts (Ted Pella, catalog number: 16144), referred to herein as “SEM mounting pins” or “pins”. It also describes the method used to carbon coat the samples. This procedure starts with dehydrated samples prepared in **Procedure E**.

1. Brush on a small amount of conductive silver paint around the edges of an SEM mounting pin.
   a. Apply the paint near to where the contours of the ITO coverslip will be when it is placed on the pin.
   b. The silver paint must fully off-gas and dry before it is placed under vacuum in the coating machine. Gluing coverslips by the edges rather than the center makes the drying process go faster in Step F3.
   c. The SEM mounting pin can be labeled with the sample identity by writing on the underside.
2. While the silver paint is wet, place the ITO coverslip with the cells facing up on the SEM mounting pin using fine point tweezers (**Figure C.14**).

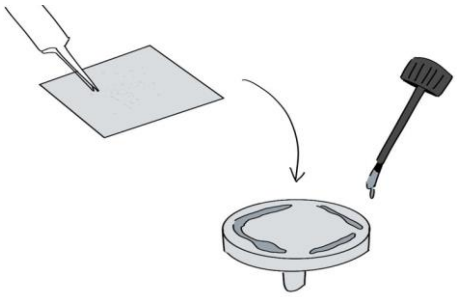

**Figure C.14. Gluing the ITO coverslip to the SEM mounting pin using conductive silver paint.** The paint is applied sparsely to the edges of the SEM mounting pin.

3. Store the pin-mounted ITO coverslips under desiccation and dry the silver paint overnight.

   **Note:** *We store pin-mounted coverslips in a desiccator cabinet with desiccant (i.e.,* Drierite™*).*

4. After the silver paint has dried, transfer samples to a high vacuum flash coating machine (Leica EM ACE600):
   a. Vent the chamber of the coating apparatus. When the chamber reaches atmospheric pressure (100 mbar), open the door.
   b. Place samples inside the chamber by seating the pins in the carousel holder. Do not overlap samples. Close the door.
   c. Load the carbon thread into the coating unit above the sample chamber.
   d. Place the coating unit back in the coating machine.
5. Coat the samples under vacuum:
   a. Run program “Pulse sgh coater”. Use these settings:
      Coat thickness: 10 nm
      Sample height: 3 nm
      Tilt: 0 degrees
6. Once the carbon coating is finished and the sample chamber is vented the samples can be removed and are ready for imaging by EM (Procedure G).

   **Note:** *SEM mounting pins can be reused by gently prying off the ITO coverslip and washing the pins with 100% ethanol. Let pins fully dry before adding silver paint.*

G. **Operating the FEI Helios Nanolab™ 660 SEM instrument for SEM imaging**. This procedure uses samples that were prepared through the end of Procedure F. These samples should contain cells on ITO coverslips that were mapped, dehydrated, glued to SEM mounting pins, and carbon coated.

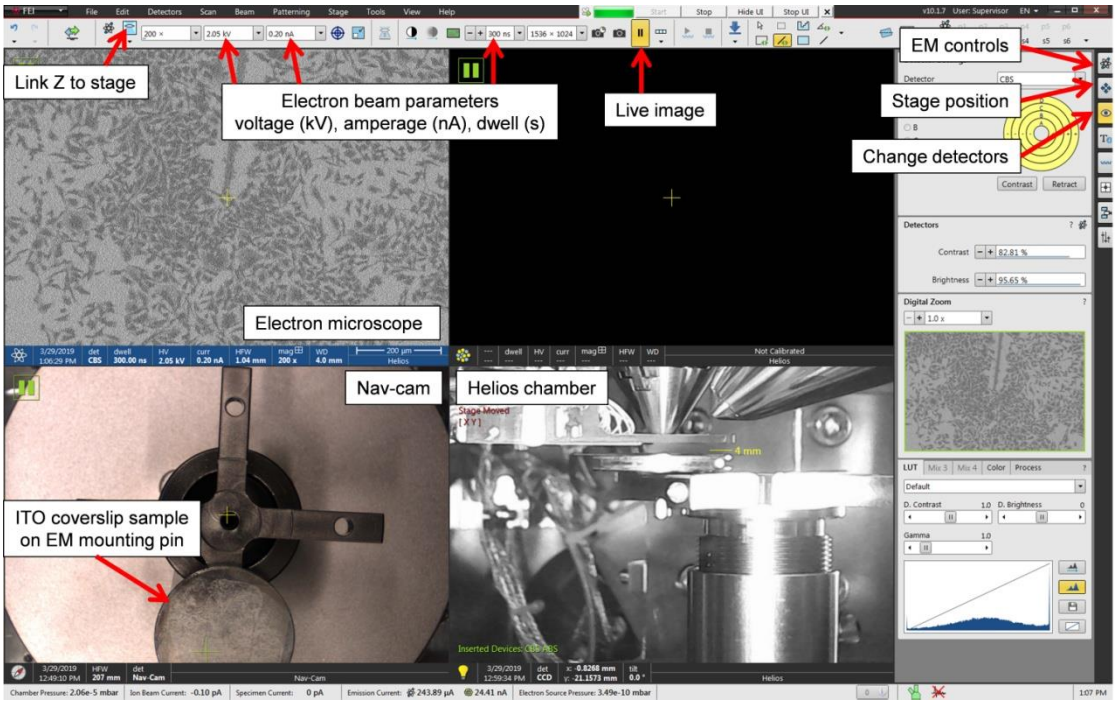


**Figure C.15. Annotated screen capture of the FEI Helios Nanolab™ xT Microscope Control software (version 10.1.7)**

1. Refer to **Figure C.15** for an annotated screen capture of the software controls. Additional information can be found in the FEI Helios Nanolab™ 660 user manual[38].
2. Vent the sample chamber of the FEI Helios Nanolab™ 660 SEM. A button labelled “Vent” is found in the panel labelled “EM controls.”
3. Once it is fully vented the chamber can be opened and the samples can be loaded onto the stage (up to 2 due to the size of the pins used). You will know when the chamber is fully vented when the SEM makes a hissing sound. You will also not be able to physically open the chamber door until it is fully vented.
4. Fasten the samples to the sample holder using the screw driver.
   a. Swing out the camera head (the “Nav-cam”) and take a photo of the stage

with the samples loaded. This is done by pressing the single button on the camera head.

b. Retract the Nav-cam head and close the chamber.
c. Pump down the chamber to reach optimal vacuum. This is done by pressing the button labelled “Pump” found in “EM controls”.

5. Open the FEI MAPS 3.0 software and load the MAPS files from the previous FEI CorrSight™ mapping session.
6. Prepare for operation of the SEM. The SEM is set to acquire on the Everhart-Thornley Detector (ETD) by default.
   a. Once the chamber is under vacuum, turn on the electron beam in “EM controls”. Set the beam voltage to 3.0 kV and 0.2 nA. These are conditions that balance sample preservation with image quality.
   b. Using the Nav-cam photograph of the stage (bottom left, **Figure C.15**), drive the microscope to the sample by double left-clicking on the sample.
   c. Zoom in on a feature at > 2,000x magnification and focus the microscope using the controller dashboard attached to the SEM. Click “Link Z to stage” in the software.
   d. Set the stage height to 4 mm in the panel labelled “Stage position” in preparation for Step G7.
7. Switch to the circular backscatter (CBS) detector in the panel labelled “Change detectors”. The live camera view of the chamber should show a metal detector arm (the CBS detector) swing under the electron gun.

   **Caution:** *Inappropriate stage height can damage your sample and the detector arm (see Step G6d).*
8. Use the Alignment Wizard to globally align the SEM to the coverslip light image collected in Procedure D (**Figure C.10** and **Figure C.16**).
   a. Left click on “Global Alignment” in the FEI MAPS software.
   b. Drive the SEM to different landmarks of the “F” fiducial marker.
   c. Take snapshots by right-clicking the center marker in the FEI MAPS software and select “Snapshot here”. The snapshots will load into FEI MAPS.
   d. Use the global alignment panel to match the features of the fiducial “F” by

SEM to the “F” on the transmitted light image of the ITO coverslip.

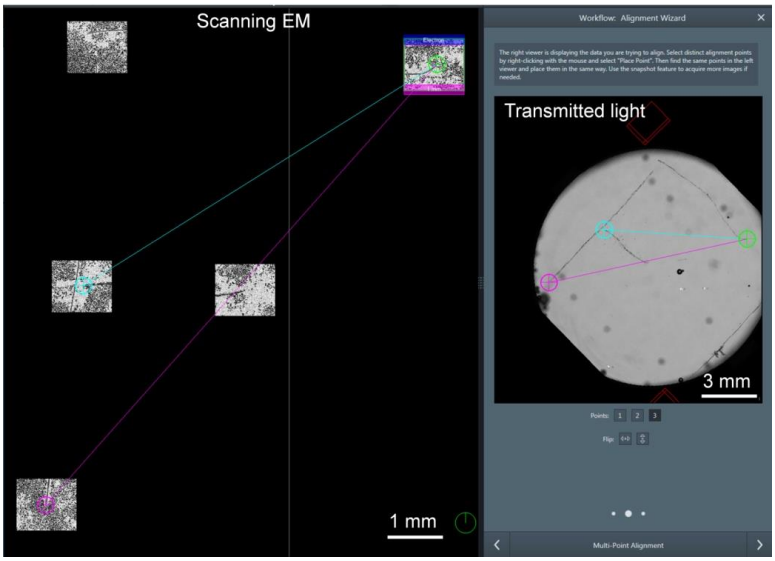


**Figure C.16. Aligning the FEI Helios Nanolab™ 660 SEM stage to the map generated by the FEI CorrSight™ using the Global Alignment tool.** Backscatter SEM snapshots of the fiducial marker “F” are aligned to the transmitted light image of the same “F” using a 3-point alignment. The user manually matches three landmarks on the “F” between the SEM and transmitted light image. The location marked by a green circle in the SEM is the same location as the green circle in the transmitted light view. The same process is repeated for the blue and pink circles.

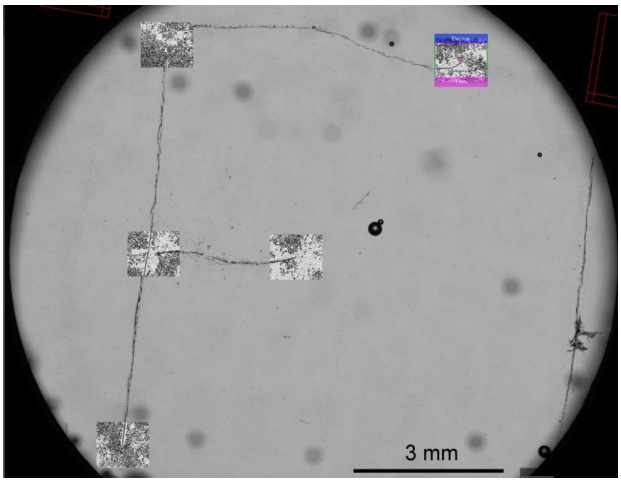


**Figure C.17. The FEI Helios Nanolab™ 660 SEM snapshots of the fiducial marker “F” aligned with the transmitted light image from the FEI CorrSight™.** After SEM image alignment with light-based images generated by the FEI CorrSight™, the FEI Helios Nanolab™ 600 SEM is now aligned with the FEI MAPS software. The user can now select anywhere on the micrographs collected by FM to drive the SEM stage to approximately the same location. Then the same cell can be imaged at high magnification by SEM.

e. Run the alignment command. If done correctly, the SEM images collected should now align perfectly with the “F” on the transmitted light image collected in Procedure D (**Figure C.17**).

9. After completing the global alignment, any cell from a prior fluorescent image can be selected in FEI MAPS and the SEM will drive to the location of the cell for high magnification SEM imaging.
   a. Due to the difficulty of aligning high magnification images, the cell will likely be off from the position selected by 10-100 microns.
   b. Use the shape of the cells or the 5x fluorescent images to locate the exact cell you want to image by SEM.
10. Image at 3,500x magnification (horizontal field width: 119 μm) to capture the entire cell in a single field-of-view.
    a. Similar to FEI CorrSight™ operation, create a new layer for each cell and each set of images. Samples can be grouped by creating Layer groups. Make layer names descriptive because they will be the folder names where your data is kept. All of the individual images collected by the FEI MAPS software are automatically named “Tile_000_0001” so descriptive layer names are important.
11. Image at 65,000x (horizontal field width: 6.37 μm) or 100,000x (horizontal field width: 4.14 μm) magnification to capture the cell surface and to resolve individual Qdots.
    a. The electron beam is destructive and will ablate cells (*i.e.* damage cells and introduce holes). While adjusting the imaging conditions (*i.e.*, focus, stigmatism), examine an area adjacent to the area containing the cell that will be imaged. This will help preserve cell morphology for SEM imaging at 65,000x or higher magnification. See **Figure C.18** for micrographs acquired at 3,500x, 63,000x, and 100,000x magnifications.
       b. Optionally, quantify the Qdots in the SEM micrographs as described in “**Data analysis**.”
12. Acquire multiple images per cell, and multiple cells per condition. We recommend at least 2 images per cell and at least 3 cells.

a. Transient transfection produces cell-cell variability in protein expression. Therefore, it is important to include replicates and image multiple cells to compensate for this variability.
b. For quantification of Qdots in SEM micrographs, we imaged 6 cells per condition with 2 images per cell, resulting in 12 images per condition.

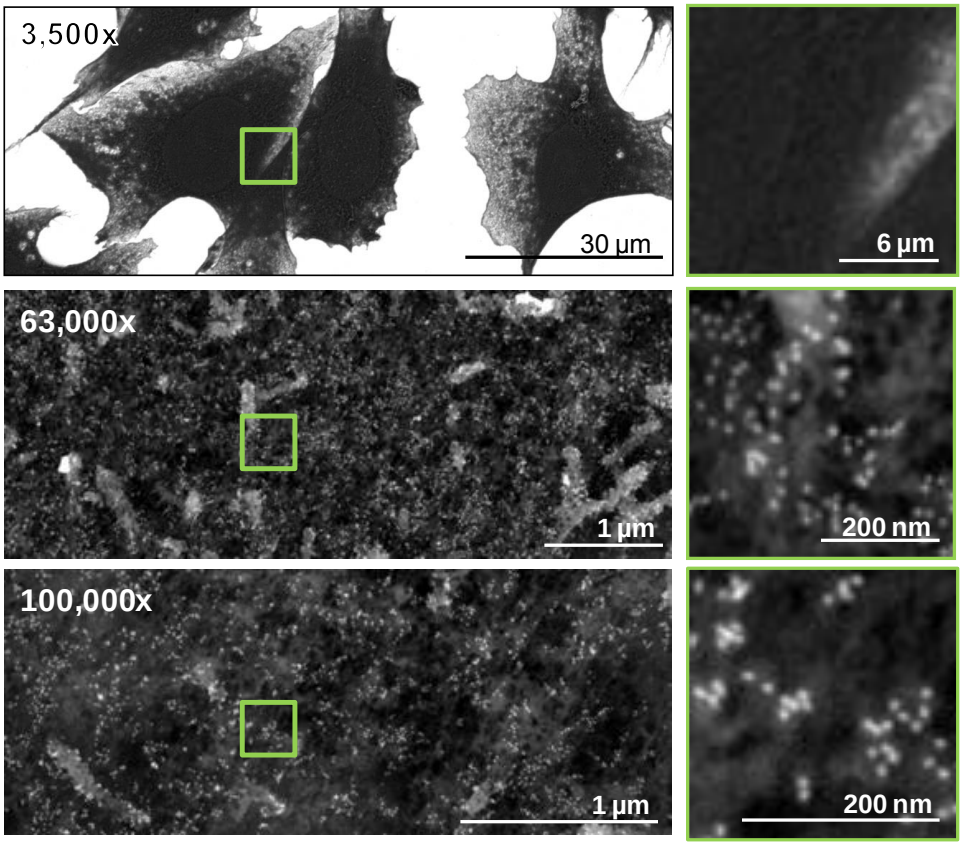


**Figure C.18. SEM micrographs of cells imaged at 3,500x (horizontal field width: 118 µm), 63,000x (horizontal field width: 6.38 µm) and 100,000X magnification (horizontal field width: 4.14 µm).** A 5x digital magnification of each capture is shown in the right column, highlighting the area outlined by a green box in the corresponding micrograph. Qdots are visible in the high-magnification micrographs as light gray circular particles.

## Data analysis: Quantification of particles in SEM images

VIPER labeling with Qdots is stoichiometric, meaning that there will be one Qdot per VIPER tag. This feature enables labeled proteins to be quantified by algorithmic

segmentation and counting of the Qdots. We recommend acquiring SEM images at high magnification (65,000x or 100,000x) for optimal particle detection and segmentation.

We developed a custom pipeline in Matlab (ver. R2017b) for automated detection and quantitation of particles in backscattered SEM images. We first detected bright objects of interest on a dark background by using morphological top-hat filtering. The object segmentation was performed using a succession of mathematical morphology operations. Briefly, automatic intensity thresholding was performed to detect Qdots. Clustered objects were separated using a seeded watershed transformation from the ultimate eroded results. Next, we counted the segmented single particles (n=1), dimers (n = 2), and multimers (n > 2). A representative micrograph before and after segmentation is provided in **Figure C.19**.

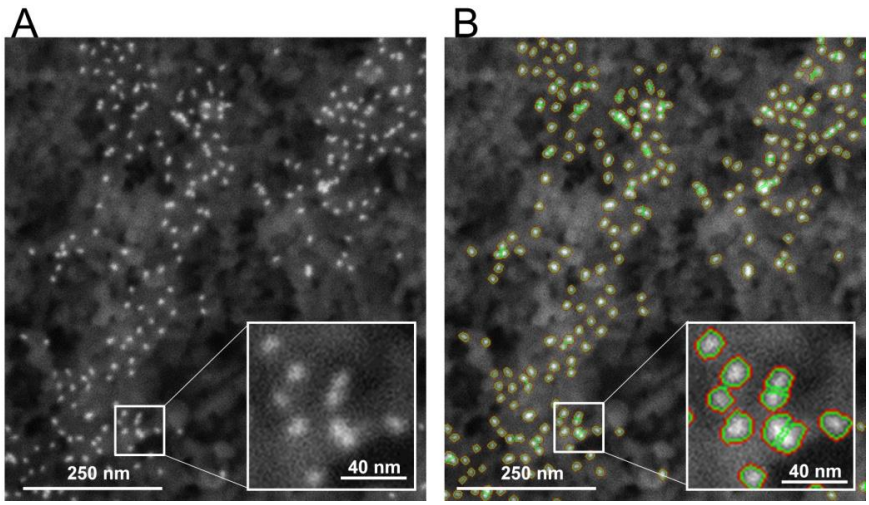


**Figure C.19. Algorithmic segmentation and automated counting of Qdots on the cell surface.** A. The original, unprocessed SEM micrograph acquired at 100,000x magnification is shown. Qdots appear as bright white dots on the cell surface, which appears dark gray. B. The micrograph in A was processed in Matlab to generate a counting mask. The red mask (red outline) indicates the objects detected by morphological top-hat filtering. The green mask (green outline) indicates the objects detected and separated using watershed transformation. Insets show a 3x magnification of the region indicated.

After the automated image processing, we visually inspected the segmentation to refine parameters and exclude objects falsely annotated as Qdots. False-annotations were rare, but typically result from irregular background, intensity variations,

background artifacts, or errors in segmentation overlooked by the automated procedure described above.

The parameter sets were optimized to quantify Qdot655 in SEM micrographs acquired at 65,000x-100,000x magnification on an FEI Helios Nanolab™ 660 SEM instrument using a CBS detector. These parameters may need to be adjusted to identify particles depending on the image quality, resolution, or type of particle (e.g., 10 nM gold or Qdot555). The “VIPER_object_detection.m" code requires two input parameters related to: (i) intensity (i.e., “int_threshold” in VIPER_object_detection.m) and (ii) object size (“obj_size”, “obj_size_filter” in VIPER_object_detection.m). The intensity-related parameter should be changed if there are variations in intensity across the images. The object size parameter (“obj_size”) will need to be adjusted if the detection particles are a different physical size (e.g., large gold particles) or if the resolution varies (i.e., pixel size). Also, the code includes filtering options for removing small objects. The “obj_size_filter” can be adjusted to remove undersized annotations. These are the parameters that we used for our analysis of Qdot655 particles:

```
int_threshold = 60; % intensity parameter;
obj_size = 10; % object size parameter;
obj_size_filter = 5; % filter for small size object;
```

Here is a brief tutorial that describes how to run our custom analysis pipeline to detect and count particles (*i.e.*, Qdots) and to count the segmented particles:

1. Copy the file 'VIPER_object_detection.m' into the desired computer directory.
2. Within the same computer directory, make a folder titled './img/'.
3. Copy SEM images ('tiff' file format) under './img/'.
4. Run 'VIPER_object_detection.m' in the command window in Matlab.
5. The program will start segmentation and count the objects.
6. The output file will provide the following information:
   qdot_count.csv: number of objects (single Qdots, dimers, multimers, N_total ≥ N_1 + N_2 x 2 + N_more x 3)
   [filename]-PTmask.mat: object mask

[filename]-Overlay.png: overlaid image with boundaries (red: objects, green: separated objects)

## Recipes

1. Live Cell Block solution

   10% v/v FBS, 6% w/v BSA, in Ham's F12 media

2. Qdot Block solution

   10% FBS and 6% BSA in DPBS

3. Qdot Labeling solution

   6% w/v BSA in DPBS

## Sequences

*The amino acid sequence of CoilR expressed from pET28b(+)_CoilR (7502.35 Da) is:*

MGGS **LEIR AAFLRQR NTALRTE VAELEQE VQRLENE VSQYETR YGPL**GGGAAALGCLAAALE*HHHHHH*

Sequence Key: linkers, **CoilR**, conjugation handle, *hexa-histidine*

*The pcDNA3.1_TfR1-CoilE vector encodes TfR1 with a C-terminal CoilE tag (TfR1-CoilE) [10]. The amino acid sequence is:*

MMDQARSAFSNLFGGEPLSYTRFSLARQVDGDNSHVEMKLAADEEENADNNMKASVRKPKRFNGRLCFAAIALVIFFLIGFMSGYLGYCKRVE
QKEECVKLAETEETDKSETMETEDVPTSSRLYWADLKTLLSEKLNSIEFADTIKQLSQNTYTPREAGSQKDESLAYYIENQFHEFKFSKVWRD
EHYVKIQVKSSIGQNMVTIVQSNGNLDPVESPEGYVAFSKPTEVSGKLVHANFGTKKDFEELSYSVNGSLVIVRAGEITFAEKVANAQSFNAI
GVLIYMDKNKFPVVEADLALFGHAHLGTGDPYTPGFPSFNHTQFPPSQSSGLPNIPVQTISRAAAEKLFGKMEGSCPARWNIDSSCKLELSQN
QNVKLIVKNVLKERRILNIFGVIKGYEEPDRYVVVGAQRDALGAGVAAKSSVGTGLLLKLAQVFSDMISKDGFRPSRSIIFASWTAGDFGAVG
ATEWLEGYLSSLHLKAFTYINLDKVVLGTSNFKVSASPLLYTLMGKIMQDVKHPVDGKSLYRDSNWISKVEKLSFDNAAYPFLAYSGIPAVSF
CFCEDADYPYLGTRLDTYEALTQKVPQLNQMVRTAAEVAGQLIIKLTHDVELNLDYEMYNSKLLSFMKDLNQFKTDIRDMGLSLQWLYSARGD
YFRATSRLTTDFHNAEKTNRFVMREINDRIMKVEYHFLSPYVSPRESPFRHIFWGSGSHTLSALVENLKLRQKNITAFNETLFRNQLALATWT
IQGVANALSGDIWNIDNEFGSGSGSTGM**LEIEAAFLERENTALETRVAELRQRVQRLRNRVSQYRTRYGPL**GGGCLETG

Key: **CoilE**, linker

## Acknowledgments

This work was funded by the OHSU School of Medicine and the National Institutes of Health (R01 GM122854). JKD was partially funded by the Portland Chapter of Achievement Rewards for College Scientists (ARCS). The protocols described herein were originally described in Doh et al. [33]. CHO TRVb cells were graciously provided by Prof. Timothy McGraw. EM and CLEM experiments were performed at the Multiscale Microscopy Core at OHSU and supported by the Advanced Multiscale Microscopy Shared Resource at the OHSU Knight Cancer Institute (NIH P30 CA069533). The aluminum coverslip holder was fabricated by Ingo Gestmann (FEI).

## Works Cited


1. Philimonenko, V. V. *et al.* Simultaneous detection of multiple targets for ultrastructural immunocytochemistry. *Histochem. Cell Biol.* **141**, 229-239, doi:10.1007/s00418-013-1178-6 (2014).
2. Giepmans, B. N. G., Deerinck, T. J., Smarr, B. L., Jones, Y. Z. & Ellisman, M. H. Correlated light and electron microscopic imaging of multiple endogenous proteins using Quantum dots. *Nat. Meth.* **2**, 743-749 (2005).
3. Lucas, M. S., Gunthert, M., Gasser, P., Lucas, F. & Wepf, R. Bridging microscopes: 3D correlative light and scanning electron microscopy of complex biological structures. *Methods Cell Biol.* **111**, 325-356, doi:10.1016/b978-0-12-416026-2.00017-0 (2012).
4. Johnson, E. *et al.* Correlative in-resin super-resolution and electron microscopy using standard fluorescent proteins. *Sci. Rep.* **5**, doi:10.1038/srep09583 (2015).
5. Kim, D. *et al.* Correlative Stochastic Optical Reconstruction Microscopy and Electron Microscopy. *PLoS ONE* **10**, e0124581, doi:10.1371/journal.pone.0124581 (2015).
6. Hildebrand, D. G. C. *et al.* Whole-brain serial-section electron microscopy in larval zebrafish. *Nature* **545**, 345-349, doi:10.1038/nature22356 (2017).
7. Ou, H. D. *et al.* ChromEMT: Visualizing 3D chromatin structure and compaction in interphase and mitotic cells. *Science* **357**, doi:10.1126/science.aag0025 (2017).
8. Sochacki, K. A., Dickey, A. M., Strub, M.-P. & Taraska, J. W. Endocytic proteins are partitioned at the edge of the clathrin lattice in mammalian cells. *Nat Cell Biol* **19**, 352-361, doi:10.1038/ncb3498 (2017).
9. Lucocq, J. M., Mayhew, T. M., Schwab, Y., Steyer, A. M. & Hacker, C. Systems biology in 3D space – enter the morphome. *Trends Cell Biol.* **25**, 59-64, doi:http://dx.doi.org/10.1016/j.tcb.2014.09.008 (2015).
10. Megason, S. G. & Fraser, S. E. Imaging in Systems Biology. *Cell* **130**, 784-795, doi:10.1016/j.cell.2007.08.031.
11. Plaza, S. M., Scheffer, L. K. & Chklovskii, D. B. Toward large-scale connectome reconstructions. *Curr. Opin. Neurobiol.* **25**, 201-210, doi:http://dx.doi.org/10.1016/j.conb.2014.01.019 (2014).
12. Lichtman, J. W., Livet, J. & Sanes, J. R. A technicolour approach to the connectome. *Nat. Rev. Neurosci.* **9**, 417-422 (2008).
13. Romain, F. L., Gabriele, S. K. S., Sebastian van de, L. & Clemens, F. K. From single-molecule spectroscopy to super-resolution imaging of the neuron: a review. *Methods Appl. Fluoresc.* **4**, 022004 (2016).
14. Müller, B. & Heilemann, M. Shedding new light on viruses: super-resolution microscopy for studying human immunodeficiency virus. *Trends Microbiol.* **21**, 522-533, doi:http://dx.doi.org/10.1016/j.tim.2013.06.010 (2013).
15. Romero-Brey, I. & Bartenschlager, R. Viral Infection at High Magnification: 3D Electron Microscopy Methods to Analyze the Architecture of Infected Cells. *Viruses* **7**, 6316-6345, doi:10.3390/v7122940 (2015).
16. Milne, J. L. S. & Subramaniam, S. Cryo-electron tomography of bacteria: progress, challenges and future prospects. *Nat. Rev. Micro.* **7**, 666-675, doi:http://www.nature.com/nrmicro/journal/v7/n9/suppinfo/nrmicro2183_S1.html (2009).

17. Kremer, A. *et al.* Developing 3D SEM in a broad biological context. *J. Microsc.* **259**, 80-96, doi:10.1111/jmi.12211 (2015).
18. Karreman, M. A. *et al.* Fast and precise targeting of single tumor cells in vivo by multimodal correlative microscopy. *J. Cell Sci.* **129**, 444-456, doi:10.1242/jcs.181842 (2016).
19. Berglund, L. *et al.* A Genecentric Human Protein Atlas for Expression Profiles Based on Antibodies. *Mol. Cell. Proteomics* **7**, 2019-2027, doi:10.1074/mcp.R800013-MCP200 (2008).
20. Bradbury, A. & Pluckthun, A. Reproducibility: Standardize antibodies used in research. *Nature* **518**, 27-29, doi:10.1038/518027a (2015).
21. Bordeaux, J. *et al.* Antibody validation. *Biotechniques* **48**, 197-209, doi:10.2144/000113382 (2010).
22. Baker, M. Reproducibility crisis: Blame it on the antibodies. *Nature* **521**, 274-276, doi:10.1038/521274a (2015).
23. Hinner, M. J. & Johnsson, K. How to obtain labeled proteins and what to do with them. *Curr. Opin. Biotechnol.* **21**, 766-776, doi:http://dx.doi.org/10.1016/j.copbio.2010.09.011 (2010).
24. Sunbul, M. & Yin, J. Site specific protein labeling by enzymatic posttranslational modification. *Org. Biomol. Chem.* **7**, 3361-3371 (2009).
25. Ellisman, M. H., Deerinck, T. J., Shu, X. & Sosinsky, G. E. in *Methods in cell biology* Vol. 111 (eds Müller-Reichert Thomas & Verkade Paul) 139-155 (Academic Press, 2012).
26. Lam, S. S. *et al.* Directed evolution of APEX2 for electron microscopy and proximity labeling. *Nat. Meth.* **12**, 51-54, doi:10.1038/nmeth.3179 (2015).
27. Martell, J. D. *et al.* Engineered ascorbate peroxidase as a genetically encoded reporter for electron microscopy. *Nat. Biotech.* **30**, 1143-1148, doi:http://www.nature.com/nbt/journal/v30/n11/abs/nbt.2375.html#supplementary-information (2012).
28. Shu, X. *et al.* A Genetically Encoded Tag for Correlated Light and Electron Microscopy of Intact Cells, Tissues, and Organisms. *PLoS Biol.* **9**, e1001041 (2011).
29. Gaietta, G. *et al.* Multicolor and electron microscopic imaging of connexin trafficking. *Science* **296**, 503-507 (2002).
30. Kuipers, J. *et al.* FLIPPER, a combinatorial probe for correlated live imaging and electron microscopy, allows identification and quantitative analysis of various cells and organelles. *Cell Tissue Res.* **360**, 61-70, doi:10.1007/s00441-015-2142-7 (2015).
31. Liss, V., Barlag, B., Nietschke, M. & Hensel, M. Self-labelling enzymes as universal tags for fluorescence microscopy, super-resolution microscopy and electron microscopy. *Sci. Rep.* **5**, 17740, doi:10.1038/srep17740 (2015).
32. Takizawa, T., Powell, R. D., Hainfeld, J. F. & Robinson, J. M. FluoroNanogold: an important probe for correlative microscopy. *J. Chem. Biol.* **8**, 129-142, doi:10.1007/s12154-015-0145-1 (2015).
33. Doh, J. K. *et al.* VIPER is a genetically encoded peptide tag for fluorescence and electron microscopy. *Proc. Natl. Acad. Sci. U.S.A.* **115**, 12961-12966, doi:10.1073/pnas.1808626115 (2018).

34. Zane, H. K., Doh, J. K., Enns, C. A. & Beatty, K. E. Versatile interacting peptide (VIP) tags for labeling proteins with bright chemical reporters. *ChemBioChem* **18**, 470-474 (2017).
35. McGraw, T. E., Greenfield, L. & Maxfield, F. R. Functional expression of the human transferrin receptor cDNA in Chinese hamster ovary cells deficient in endogenous transferrin receptor. *J Cell Biol* **105**, 207-214 (1987).
36. (ed Life Technologies) (Life Technologies 2013).
37. (ed FEI) (FEI, Graefelfing, Germany, 2015).
38. Kral, Z., Routh, R., Schmidt, M. & Brogden, V. (ed FEI) (FEI, Hillsboro, OR, USA, 2014).

# Appendix D: Initial progress investigating iron biology with VIP tags

**Julia K. Doh**, Shall Jue, Katie Kulp, Kimberly E. Beatty, Caroline A. Enns

*This appendix is a summary of in-progress work studying **HFE**'s localization and its interactions with Transferrin Receptor 2 (**TfR2**). Appendix D describes work completed as a collaboration between the Beatty and Enns group employing VIP tags to study iron biology. Shall Jue generated the stable cell lines and validated expression by western blot. Katie Kulp performed molecular biology experiments, including co-immunoprecipitations. I was responsible for imaging experiments and collected the micrographs.*

*This appendix discusses both human and mouse proteins. When referring to human proteins and discussing background knowledge, the proteins discussed are stylized as "TfR1", "TfR2", and "HFE". When discussing mouse receptors, which are used in this appendix experimentally, "Tfr1", "Tfr2", and "Hfe" are used.*

## Abstract

HFE is responsible for regulating iron levels, however its mechanism for sensing iron is unknown. Transferrin receptor 2 (**TfR2**) is speculated to be an iron sensor that drives iron-uptake regulation through binding with HFE. A model has been proposed where, in conditions of high iron, TfR2 and HFE are bound and co-traffick together. The goal of this project is to use in vitro methods and fluorescence imaging to determine TfR2 and HFE's subcellular localization in low and high iron and whether the two proteins interact. Interaction partners and receptor trafficking pathways will help devise the molecular mechanism by which HFE drives iron regulation. HFE, lacking a good antibody, was imaged using CoilE, a Versatile Interacting Peptide (**VIP**) tag. We have conducted an initial validation of stable AML12 cell lines generated to study proteins implicated in iron sensing. AML12, an immortalized hepatocytic cell line, were transduced to express CoilE-Hfe-myc-FLAG and Tfr2-CoilZ . Cells were determined to have maintained expression of Tfr1 and overexpressed Hfe. Tfr2, by comparison, showed little to no fluorescent VIP labeling on the cell surface but was detectable by western blot using an anti-TfR2 antibody. Co-immunoprecipitation of CoilE-Hfe-myc-

FLAG pulled down Tfr2-CoilZ in the presence and absence of Tf. These results indicate the feasibility of using this cell line to investigate HFE localization at the cell surface and in the endo-lysosomal pathway.

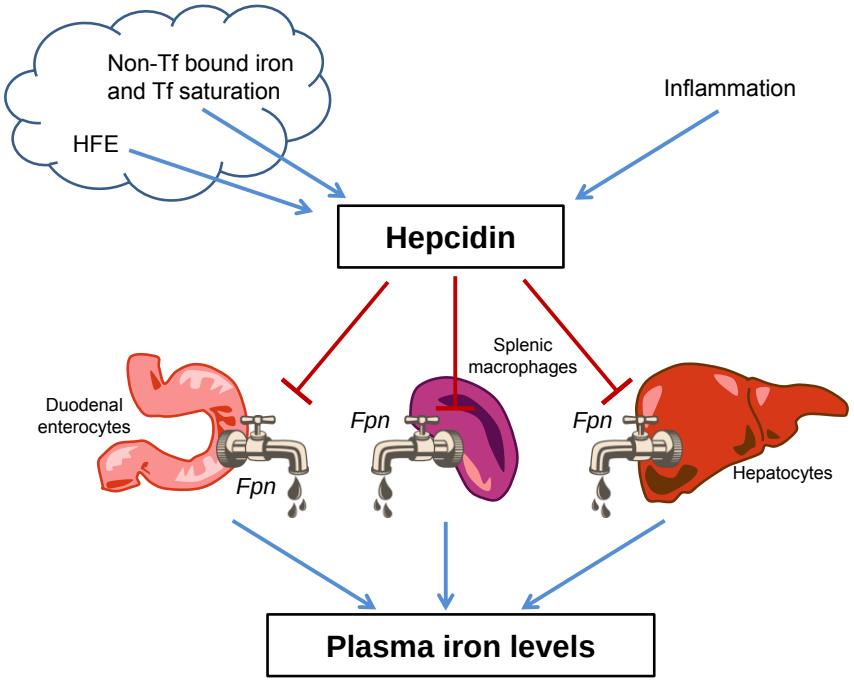


**Scheme D.1. How hepcidin regulates plasma iron levels.** Figure adapted from Ganz and Nemeth (2012)[1]. Fpn = ferroportin.

## Introduction

Iron is a critical metal for human health because it enables oxygen-transport in the blood and electron transport in the cell. However, an excess of iron causes oxidative damage to cells[2]. Iron overload diseases, also known as hemochromatosis, impair key organs such as the heart, liver, pancreas, and joints, resulting in heart arrhythmia, cirrhosis of the liver, diabetes, and arthritis[2]. While hemochromatosis is a polygenic disease, 90% of cases are caused by mutations in human hemochromatosis protein[3], also known as **HFE** ("high Fe" protein). HFE upregulates the HAMP gene, which encodes hepcidin[4], a peptide hormone. Hepcidin lowers serum iron levels by downregulating ferroportin (Fpn), an iron transporter responsible for exporting iron to the

bloodstream[5]. Deleterious HFE mutations thus result in heightened systemic iron levels, which causes dysfunction and oxidative damage to various organs (**Scheme D.1**).

Despite strong evidence for HFE's role in controlling hepcidin and tissue iron levels[6], the molecular mechanism of how HFE regulates iron remains poorly understood. HFE cannot bind iron and is thus believed to be interacting with other proteins to detect and lower iron levels in the cell. HFE's localization in the cell is also unknown. The mechanism of trafficking and location of proteins dictate their regulatory behaviors[7]. This is due to the fact that a number of adaptor proteins associated with cellular trafficking are responsible for coordinating cell signaling pathways[7].

HFE is major histocompatibility class 1 (MHC 1)-like protein. It is structurally similar to MCH 1, as it has an α1, α2, and α3 domain and complexes with β-2 microglobulin (β2M) for stability[8]. HFE binds Transferrin Receptor 1 (**TfR1**)[9–12], the major receptor for Tf-mediated iron uptake[13]. The transferrin (Tf) binding site on TfR1 overlaps with the HFE-TfR1 binding interface (**Scheme D.2**).

Transferrin Receptor 2 (**TfR2**) also binds HFE[12]. TfR2 is related to TfR1 by sequence homology (66%[14] in the ectodomain) and is proposed to be an iron sensor[15–17]. TfR2 binds Tf, but with 30-fold lower affinity than that of TfR1[14,18]. A lowered affinity makes TfR2 more sensitive to Tf saturation than TfR1, supporting TfR2's theoretical role as an iron sensor. In conditions of high iron, TfR2 binds Tf and this interaction stabilizes TfR2 on the cell surface[19,20]. Tf binding changes TfR2's trafficking behavior and redirects it from lysosomal degradation to the recycling pathway[19,20].

A model offered by the Enns group and Fleming group proposes that HFE and the TfR2 homodimer form a ternary complex that drives hepcidin signaling[21]. In co-immunoprecipitation pull downs, when HFE was precipitated in the absence of Tf, it pulled down TfR1. In the presence of 25 μM Tf, HFE pulled down TfR2 and Tf, but no longer pulled down TfR1[22]. This binary result was the basis of the model proposed in **Scheme D.2** and confirmed crystal structure evidence[12] that HFE occupies the same site as Tf on TfR1.

The proposed studies in this appendix aim to test this model by determining the interactions of TfR1, HFE, and TfR2 along with their localization as they internalize. Two key goals of this research project are: i) identify the proteins that HFE interacts with; and

ii) determine where HFE is localized in cells. Once these features are discovered, we can build a mechanistic understanding of HFE's role in iron regulation.

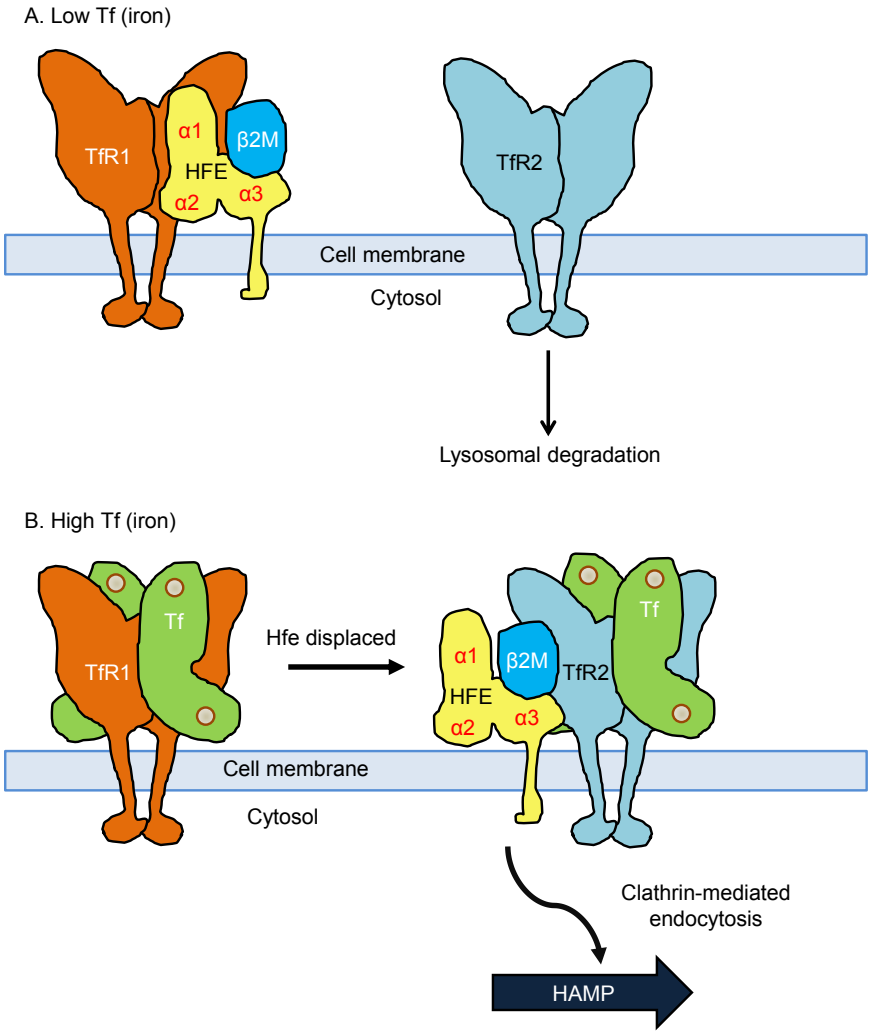


**Scheme D.2. Proposed model for iron sensing via a HFE-TfR2 binding interaction. (A)** Under low iron conditions (0 μM holo-Tf), HFE is bound to the TfR1 homodimer in a 1:2 [HFE:(TfR1-TfR1)] trimer[22]. The α1 and α2 domain of HFE bind TfR1 at the Tf binding domain[12]. TfR2, also a homodimer, is expressed on the cell surface but, in absence of Tf, is degraded in the lysosome. **(B)** Under high iron conditions (25 μM holo-Tf), Tf binds TfR1, displacing HFE. This allows HFE to complex with TfR2, via binding at the α3 domain. We hypothesize that TfR2 and Tf are also bound in this condition, stabilizing the TfR2-HFE-Tf complex on the cell surface and redirecting it to endosomal recycling. This would allow TfR2 to fulfill its "iron-sensing" role by transcriptional activation of HAMP, increasing hepcidin expression. *Models are drawn to approximate scale and depict binding orientations from published 3D crystal structure data (PDB: 1DE4)*[12]. The TfR2-HFE protein structure has not been solved and is inferred from in vitro interaction studies.

The interactions between TfR1-HFE and TfR2-HFE will be evaluated under high (25 μM) and low (0 μM) Tf levels. We hypothesize that in low iron conditions (absence of Tf), TfR1 and HFE are associated and HFE co-trafficks into the cell with TfR1 via clathrin-mediated endocytosis. Under these conditions, ligand-free TfR2 is lysosomally degraded. In conditions of high iron, we hypothesize TfR2 is bound to Tf and HFE. This Tf-TfR2-HFE complex would be stabilized by Tf-binding, and we predict that we would observe all three proteins trafficking together into the cell via clathrin-mediated endocytosis before recycling back to the cell surface.

## Proposed Studies

Investigation of TfR2-HFE interactions will be carried out with in vitro studies (western blotting and co-immunoprecipitation) and cell studies (e.g., microscopy) of mouse receptors: **Tfr1**, **Tfr2**, and **Hfe**. In vitro methods will help us detect interactions between Tfr1, Tfr2, and Hfe in a total protein population context. Co-immunoprecipation will recapitulate the original discovery[22] of the TfR2-HFE complex and confirm that the addition of VIP tags has not changed protein behavior.

In contrast, imaging will allow us to observe abundance, distribution, interactions and localization of proteins in cells. These studies cannot be done by immunolabeling because no sensitive antibody to Hfe is available. Previous work has relied on genetically-encoded tags, such as the FLAG epitope for detection[22,23].

In order to carry out the proposed work, we will use Versatile Interacting Peptide (**VIP**) tags[24,25]. Compared to ~30 kDa fluorescent proteins (**FP**) and other large tags[26–28], VIP tags are small (4.3-6.2 kDa) and compatible with various imaging modalities. Their small size makes them less likely to perturb protein function. Imaging of Tfr1, Tfr2, and Hfe will be used to see where Hfe trafficks in the cell in conditions of high and low iron, and whether Tfr1 or Tfr2 interact with Hfe in each condition.

## Results and Discussion

## Design of genetic constructs

We proposed to use VIPER[25] to tag and image Hfe and VIP Y/Z[24] to tag and image Tfr2. A summary of genetic constructs is provided in **Table D.1**. Tfr1 will be imaged by immunolabeling and was not genetically-tagged for these studies.

We used mouse proteins in our studies with the intent of creating a stable cell line in a mouse background in the future. These initial constructs were generated and cloned into pcDNA3 vectors, which allowed them to be expressed in mammalian cells via liposome transfection. For stable cell line generation, these genes were cloned out of mammalian expression vectors into retroviral vectors for virus generation and cell line transduction.

Hfe's N-terminus is extracellular so we opted to place the VIP tag at the N-terminal region between the signal sequence (SS) and the α1 domain, facing away from the Tfr1 binding interface. The VIP tag is also placed away from the β2M-binding interface (in the α3 domain). We expected that this is a favorable location for a genetic fusion. This VIP-tagged construct was inserted into an Hfe construct that also carries a C-terminal myc and FLAG tag[22]. The SS-CoilE-Hfe-myc-FLAG construct will be referred to as **CoilE-Hfe-myc-FLAG** for ease of reading.

We tagged Tfr2 at the extracellular C-terminus with CoilZ (Tfr2-CoilZ). This location is analogous to where we successfully tagged Tfr1 with CoilE[25], MiniE, and MiniR[29].

## Stable cell line generation

We selected AML12 cells to generate stable cell lines of these VIP-tagged Hfe and Tfr2 constructs (CoilE-Hfe-myc-FLAG Tfr2-CoilZ). AML12 is an immortalized mouse liver cell line. Much of the existing knowledge of TfR2 and HFE was derived from mouse liver or liver cell lines and so we opted to study these receptors in this cell background. AML12 cells would also enable follow-up work in live mice.

The cell lines were generated by retroviral transduction. Antibiotic selection was used to isolate clonal populations of transduced cells. A summary of stable cell lines is provided in **Table D.2**. This table includes cell lines that have been generated but not

discussed in this appendix, including CHO TRVb (Tfr1, Tfr1-CoilE or Tfr1-MiniE) and HEK 293 (CoilE-Hfe-myc-FLAG).

## Analysis of protein expression in AML12 clones

The clonal AML12 cell lines were analyzed to determine the amount of Tfr2 (endogenous Tfr2 and Tfr2-CoiZ) and Hfe (CoilE-Hfe-myc-FLAG; not endogenous Hfe) expressed in each line. Cell lysates were prepared from each clone, resolved by SDS-PAGE, and transferred to a membrane for Western blot analysis. Lysates from untransduced wild type AML12 was also analyzed as a control (**Figure D.1**). We probed for Tfr2-CoilZ with an anti-Tfr2 antibody (rabbit host, #25257) and CoilE-Hfe-myc-FLAG by an anti-FLAG (mouse host, M2) antibody. Secondary anti-mouse and anti-rabbit antibodies conjugated to horse radish peroxidase were used to detect proteins via chemiluminescence. Tfr2 was probed and imaged first, and then CoilE-Hfe-myc-FLAG was probed afterwards without stripping the blot.

All transduced clones showed an expected Tfr2 and Hfe band. Tfr2 has a calculated molecular weight of 88 kDa, while TfR2-CoilZ is 96 kDa. However, the apparent weight of TfR2 by SDS-PAGE is ~100 kDa, which is what we observed[30]. CoilE-Hfe-myc-FLAG has a predicted molecular weight of 50 kDa (48 kDa with the cleaved signal peptide), and we observed two closely spaced bands near 55 kDa on the blot.

Wild type AML12 showed lower levels of wild type Tfr2 relative to the clones. Since the 25257 antibody also detects Tfr2 without the additional tag, one can conclude that AML12 cells have low levels of endogenous Tfr2. Wild type cells had no detectable signal for the FLAG epitope because they don't express this epitope tag. Since we did not use an Hfe-specific antibody (M2 only detects FLAG), the endogenous presence of Hfe could not be determined from this data.

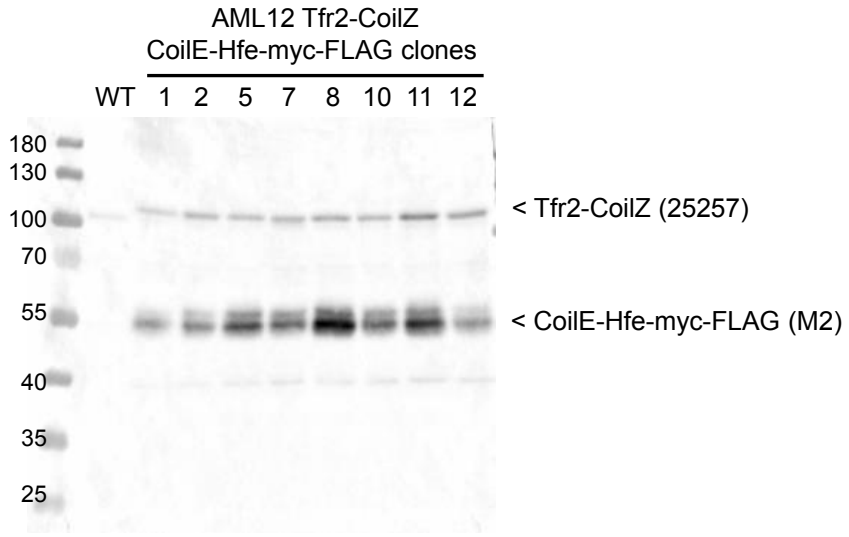


**Figure D.1. Western blot validation of AML12 Tfr2-CoilZ CoilE-Hfe-myc-FLAG clones.** Cell lysates (25 µg/well) of transduced AML12 cells were probed for Tfr2-CoilZ using #25257 (anti-mTfr2), then detected using anti-rabbit secondary antibody conjugated to HRP. After initial imaging of Tfr2-CoilZ, the blot was probed a second time for CoilE-Hfe-myc-FLAG using M2 (anti-FLAG) and detected using anti-mouse secondary antibody conjugated to HRP. Clones (denoted by numbers) were compared to wild type (WT) AML12 lysate. *Data collected and prepared by Shall Jue.*

The measured stoichiometry of TfR1, TfR2, and HFE in human liver samples indicated that Tfr2 was ~5-6 times more abundant than TfR1 and HFE levels were not measurable[31] in mouse liver. In all of the clones we assessed, Tfr2-CoilZ generated less signal than CoilE-Hfe-myc-FLAG. This could possibly be due to Tfr2 being expressed less than Hfe, which is incongruent with what was measured in liver. However, unless a quantitative western blot is conducted, this difference can only be speculated. The exact ratios of Tfr2 and Hfe in the clones could not be accessed accurately because different antibodies were used to detect the proteins. The efficiency of transfer in Western blots and the relative sensitivities of the antibodies are also not known. As long as we keep this caveat in mind, we can still continue to look for Hfe interactions and trafficking using these clones. Alternatively, more clones could be screened for the correct ratio.

We wanted to select a clone that had the highest Tfr2-CoilZ expression, while balancing the overexpression of Hfe. In other words, we looked for clones that showed a distinct band for TfR2-CoilZ, but with a weaker band for CoilE-Hfe-myc-FLAG relative to other clones. After assessing multiple clones, Clone 2, 7, 10 and 12 fit this criteria.

We selected Clone 10 to move forward with initial experiments but in the future it would be useful to assess multiple clones to determine if there is any experimental variability between clones. The AML12 Tfr2-CoilZ CoilE-Hfe-myc-FLAG (Clone 10) cell line is referred to herein as **AML12 VIP-Tfr2/Hfe**.

## Co-Immunoprecipitation studies

A co-immunoprecipitation (co-IP) experiment was conducted using AML12 VIP-Tfr2/Hfe line in order to repeat experiments demonstrated by Gao et al. (2009)[22]. In this work, when HepG2 (human liver carcinoma) cells were grown in the absence of Tf and HFE-FLAG was precipitated with anti-FLAG resin, TfR1 was recovered bound to HFE. When the cells were incubated with 25 μM holo-Tf and HFE was precipitated, TfR1 was lost but Tf and TfR2 was pulled down.

Repeating this experiment with AML12 VIP-Tfr2/Hfe accomplishes two goals: ensure the reproducibility of the previous findings and confirm that the addition of VIP tags to these receptors does not change interactions detected by co-IP. As the TfR2-HFE binding interface is currently unknown, it is not possible to predict if the location of the VIP tag will interfere with this binding interface, thus highlighting the importance of testing this interaction experimentally.

This initial experiment was conducted by Katie Kulp in AML12 VIP-Tfr2/Hfe. Only CoilE-Hfe-myc-FLAG and Tfr2-CoilZ were assessed by western blot. Tfr1 and Tf detection were absent from this experiment but should be included in follow up studies. We tested whether the addition of VIP tags interfered with the ability of Hfe and Tfr2 to interact. This was conducted in vitro using co-immunoprecipation of these receptors in cell lysates of AML12 Tfr2/Hfe (**Figure D.2.**). Cell lysates were incubated with anti-myc agarose beads in order to pull down CoilE-Hfe-myc-FLAG. That fraction was then assessed by western blot for Tfr2 (using anti-Tfr2 antibody 25257) and CoilE-Hfe-myc-FLAG (using the anti-FLAG M2 antibody).

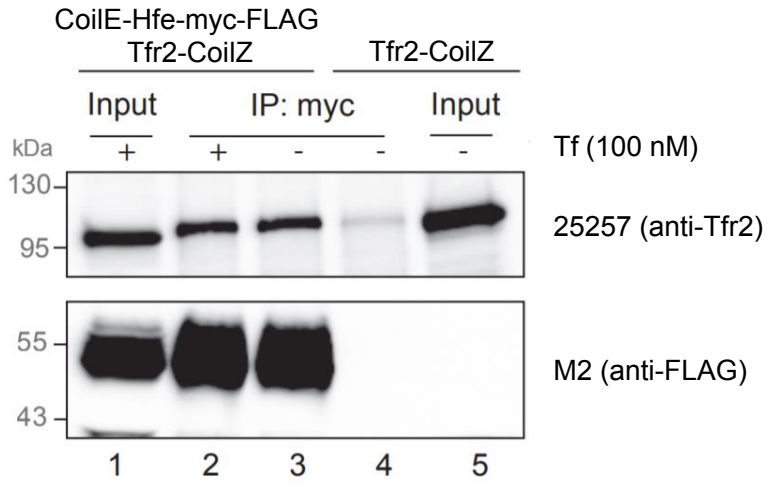


**Figure D.2. Tfr2-CoilZ interacts with Hfe-CoilE in presence and absence of transferrin.** Lanes 1-3 represent AML12 VIP-Tfr2/Hfe cell lysates. Lane 1 represents input (10% of IP volume). Lanes 2 and 3 represent pulldown of Hfe with 20 µL anti-myc agarose beads (Sigma Cat. No. E6654) without and with addition of 100 nM holo Tf respectively (each ½ of confluent 10 cm dish). Lanes 4 and 5 show control for Tfr2 nonspecific interactions using AML-12 Tfr2-CoilZ cell line that does not contain Hfe. Lane 4 shows a pulldown of Hfe via anti-myc agarose beads. Lane 5 represents input (10% of IP volume) of cells expressing Tfr2-CoilZ but not CoilR-Hfe-myc-FLAG. Tfr2-CoilZ was detected with rabbit #25257 anti-mouse antibody targeting the protein's ectodomain and CoilE-Hfe-myc-FLAG was detected with mouse M2 anti-FLAG antibody. All IP volumes represent ½ of a confluent 10cm dish, inputs represent 10%. *Data collected and prepared by Katie Kulp.*

This analysis showed that the AML12 VIP-Tfr2/Hfe cells express both Tfr2 and Hfe (**Figure D.2.** lane 1). The Tfr2-Hfe interaction was demonstrated using immunoprecipitation of CoilE-Hfe-myc-FLAG and detection of Tfr2 in absence of added Tf (**Figure D.2.** lane 2). The addition of CoilZ to the C-terminal of Tfr2 and CoilE to the N-terminal of Hfe does not prevent the interaction of Tfr2 with Hfe. Tf does not compete with Hfe for binding to Tfr2 as demonstrated in **Figure D.2.** (lane 2 versus 3). This is in contrast to our hypothesis and results found in Gao et al. 2009[22], where in the absence of Tf, HFE did not pull down TfR2. In our case, Tfr2 was pulled down by Hfe whether Tf was present or not, when we had hypothesized that Tfr2 would not bind Hfe in low iron conditions. This difference could possibly be due to differences in receptor behavior between HepG2 and AML12 cells, an effect of CoilZ or CoilE tagging creating a Tf-independent interaction, or a result of nonspecific protein-protein adhesion.

Nonspecific sticking of Tfr2 to the anti-myc beads was assessed with AML12 cells expressing Tfr2-CoilZ flowed over anti-myc resin in **Figure D.2.** (lane 4). Some signal in lane 4 could be detected. This signal could either reflect nonspecific protein sticking or overexposure of the western blot. Signal in lane 4 does appear distinctly fainter than signal in the input lanes (1 and 5) or lanes 2 and 3.

The main conclusion from this initial experiment is that the addition of VIP tags to Hfe and Tfr2 do not prevent the receptors from interacting in vitro. As this is an initial validation, this experiment will requires some changes when it is repeated. A follow up experiment will need to assess for Tf and Tfr1 in addition to Tfr2-CoilZ and CoilE-Hfe-myc-FLAG, in order to compare to previous work conducted by Gao et al. (2009)[22]. HepG2 cells and wild type AML12 transduced with Hfe-myc-FLAG (no VIP tag) should also be assessed alongside the AML12 VIP-Tfr2/Hfe cell line in order to determine the cause of Tfr2 and Hfe interacting in the absence of Tf. Lastly, cells should be incubated with 25 μM instead of 100 nM Tf to better match conditions previously outlined by Gao et al. (2009)[22]

## Secondary Antibody Validation

Prior to any imaging assessment of Tfr2 or Hfe, the secondary imaging antibodies used in this appendix were tested for nonspecific or off-target labeling. The antibodies assessed were anti-mouse-AF488, anti-rabbit-AF488, anti-rat-AF488, anti-rabbit-AF555, and anti-rat-AF555. See **Table D.3** for a summary of antibodies available for this work.

Cells were fixed and permeabilized and then treated with secondary antibodies (**Figure D.3**). This labeling was done without prior treatment with primary antibody. In this initial test, cells were permeabilized with .1% saponin in DPBS and blocked in 10% FBS, 5% sucrose, 2% BSA in DPBS. Following treatment with the secondary antibody, cells were imaged and processed so that the brightness and contrast settings were analogous to those used to image positive signal (see subsequent **Figures D.4-D.7**).

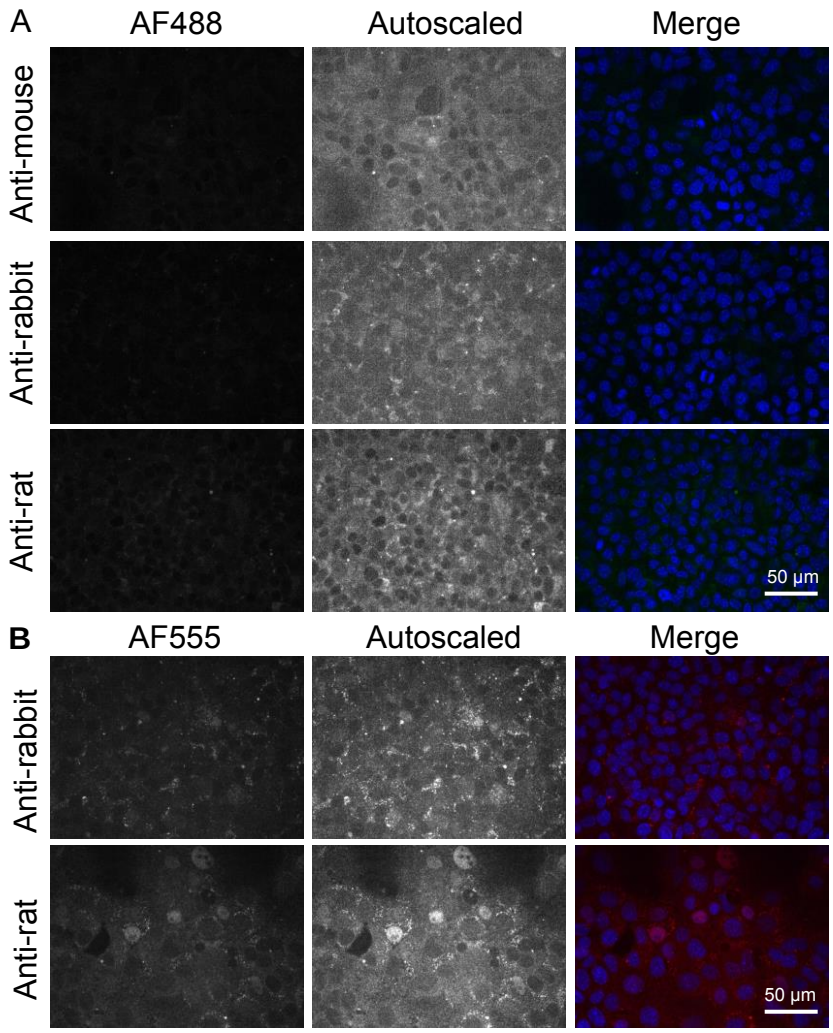


**Figure D.3. No primary controls of secondary antibodies used in this work.** AML12 VIP-Tfr2/Hfe cells were fixed and permeabilized with 0.1% saponin. AF488 (**A**) or AF555 (**B**) secondary antibodies were applied to cells to assess non-specific or off-target labeling. Cells were imaged at 40X (0.9 NA) after treatment and a standard view (normalized to positive signal from **Figures D.4-D.7**) and an autoscaled view are provided. Merged channels are false colored: AF488 is green, AF555 is red, and Hoechst (nuclei) is blue.

Under these conditions, fluorescent signal in the first column indicates non-specific labeling by the secondary antibody. The AF488-conjugated secondary antibodies overall had low signal and were deemed acceptable for usage. Of the antibodies assessed, the anti-mouse-AF488 secondary had the least amount of non-specific fluorescent signal. AF555-conjugated antibodies had more non-specific and off-target labeling as evidenced by brighter cell-associated signal. Anti-rat-AF555 had

the greatest non-specific signal of the secondary antibodies assessed. These antibodies were still used in absence of other options but with the caveat that labeling signal would have to be much brighter than the non-specific labeling in order to be significant.

Antibodies will need to be validated prior to conducting these experiments by performing a titration series of primary antibody and secondary antibody to ensure that labeling methods minimize background and do not show off-target or nonspecific labeling. Additionally, sample preparation methods can be tested to increase the signal to noise ratio, including using different fixatives, permeabilization agents, and blocking components.

## Imaging tagged receptors in AML12 VIP-Tfr2/Hfe

AML12 cells, including the clonal cell lines, express Tfr1 endogenously. Following in vitro assessment of protein expression, we used fluorescence microscopy to assess the cell surface expression of Tfr1, Tfr2, and Hfe in the AML12 VIP-Tfr2/Hfe cells. For labeling, cells were cooled to 4 °C to halt endocytosis and labeled cold with either fluorescent CoilR-Cy5, CoilY-Cy5, Tf-AF488, or (non-fluorescent) 8D3 (anti-Tfr1) antibody (**Figure D.4**). CoilR-Cy5 labels CoilE-Hfe-myc-FLAG and CoilY-Cy5 labels Tfr2-CoilZ. Tf and 8D3 both bind to endogenous Tfr1. Tf is also a ligand for Tfr2, and will bind tagged or untagged TfR2. After live cell labeling, the cells were fixed and any samples labeled with 8D3 were subsequently blocked with 6% BSA and 10% FBS in PBS and treated with secondary anti-rat AF488 antibody to detect 8D3.

Given the results by western blot in cell lysates, the expected result for this experiment was to observe fluorescent signal from Tfr1, Tfr2-CoilZ, and CoilE-Hfe-myc-FLAG on the cell surface. Tf-AF488 binding was also expected on the cell surface as the AML12 cells have endogenous Tfr1 and TfR2, and transduced Tfr2-CoilZ.

Imaging showed that CoilE-Hfe-myc-FLAG was expressed on the cell surface, as highlighted by the signal on the cell outline (**Figure D.4A**). Labeling was bright and cells were uniformly fluorescent across the sample, confirming that this clonal stable cell line has similar expression levels across all cells.

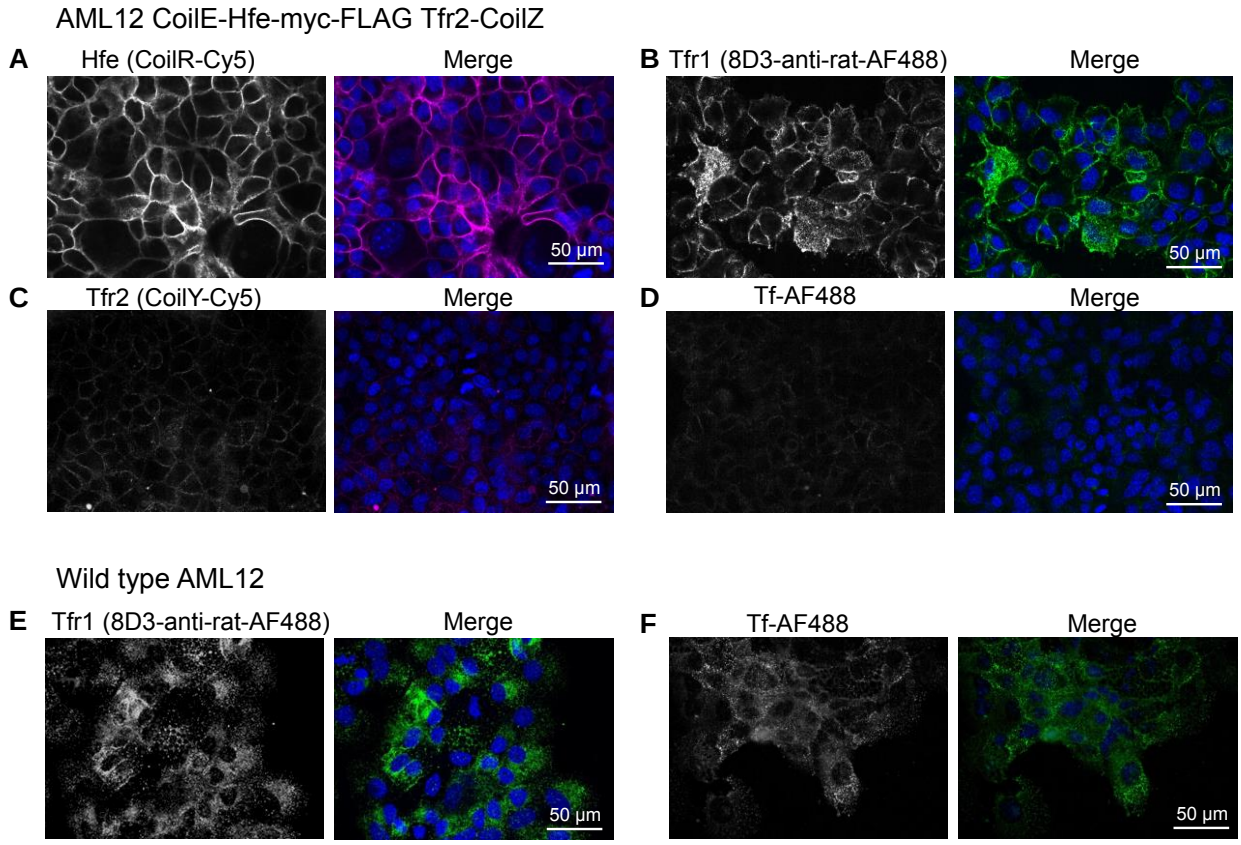


**Figure D.4. Assessment of receptors on the cell surface of live AML12 VIP-Tfr2/Hfe.** AML12 VIP-Tfr2/Hfe (**A-D**) or wild type AML12 cells (**E-F**) were cooled to 4 °C and labeled cold to halt endocytosis. Micrographs represent AML12 VIP-Tfr2/Hfe cells that are treated with only one of the following reagents: CoilR-Cy5 (**A**), 8D3 antibody (**B**), CoilY-Cy5 (**C**) or Tf-AF488 (**D**). After labeling, cells were fixed. Wild type AML12 cells were also labeled with 8D3 antibody (**E**) or Tf-AF488 (**F**). Antibody-labeled cells (**B** and **E**) were subsequently treated with anti-mouse-AF488 secondary for fluorescence imaging. Wild type AML12 were unintentionally warmed between labeling and fixing and this resulted in endocytosis of the fluorescent signal. Cells were imaged at 40X (0.9 NA). Merged channels are false colored (AF488 is green, Cy5 is magenta, and Hoechst/nuclei are blue).

Immunolabeling of Tfr1 by 8D3 was similarly bright and uniform as CoilE-Hfe-myc-FLAG labeling, highlighting the cell surface (**Figure D.4B**). However, unexpectedly, Tf-AF488 labeling was faint, despite the cells expressing both Tfr1 and Tfr2 (**Figure D.4D**).

Tfr2-CoilZ was only faintly detectable at the cell surface using CoilY-Cy5 (**Figure D.4C**). This was unexpected given the relative levels of protein demonstrated by the western blot of cell lysates in **Figure D.1**. This would suggest that the cells are

transduced with Tfr2-CoilZ, but the majority of the receptors are inside the cell and not on the cell exterior. This is in conflict with previous findings in mouse liver where Tfr2 was found to be 5.5 times more abundant in membranes versus the cell interior[31]. However, it is possible that the AML12 tissue culture cells are different from cells derived from mouse liver. The CoilY-Cy5 probe peptide has been used previously to label tagged proteins and we observed bright labeling[24]. Additionally, transiently transfected cells overexpressing Tfr2-CoilZ have been successfully labeled with CoilY-Cy5, making probe peptide quality or VIP Y/Z dimer formation an unlikely cause for this lack of labeling.

We did not observe Tf-AF488 labeling of AML12 VIP-Tfr2/Hfe cells (**Figure D.4D**), which was unexpected because these cells express both Tfr1 and Tfr2. The expectation was that the labeling by Tf would be localized to the cell surface, where it would encounter these receptors. This led us to hypothesize that Tf-binding had been impaired in AML12 VIP-Tfr2/Hfe. We hypothesized that overexpression of Hfe resulted in reduction of Tf binding through competition for the same binding site on Tfr1. The micrographs confirmed that the endogenous Tfr1 could be detected on the cell surface with immunolabeling, which confirmed that the receptor was being trafficked to the cell surface and would be accessible to Tf.

In order to test this hypothesis untransduced wild-type AML12 were labeled in a similar manner with 8D3 and Tf-AF488 (**Figure D.4E-F**). In wild-type AML12 cells, 8D3 labeling of endogenous Tfr1 was observed, confirming that Tfr1 is expressed in AML 12 cells. Tf-AF488 signal in untransduced wild type AML12 was brighter than in AML12 VIP-Tfr2/Hfe, indicating wild-type cells bound more Tf-AF488 than AML12 VIP-Tfr2/Hfe. This result supported the hypothesis that the cell line has reduced Tf-binding. An additional way to confirm this is to repeat the 8D3 and Tf fluorescent labeling experiment with AML12 transduced with Tfr2-CoilZ only. If the labeling matches the wild type AML12 it would support that the introduction of CoilE-Hfe-myc-FLAG caused the loss of Tf-binding.

The AML12 VIP-Tfr2/Hfe cell line generated is not ideal, given that it overexpresses CoilE-Hfe and expresses Tfr2-CoilZ at levels that will be difficult to detect in imaging experiments. From these results alone it may be worthwhile to

generate new cell lines, possibly using constructs with inducible promoters (e.g., doxycycline) in order to control for protein expression.

## Investigation of protein co-localization

It was expected that Tfr1 and Hfe would colocalize if imaged together, as this is an established interaction[9–12]. Based on the proposed iron sensing model[21], Tfr2 and Hfe would not interact in low iron conditions. This has already been challenged by our co-IP experiment in the previous section, and warrants further investigation as suggested in this appendix. For the imaging experiments low iron conditions were replicated by adding no holo-Tf to the media prior to imaging. We imaged two targets at once in live AML12 VIP-Tfr2/Hfe cells in order to assess if signal colocalization would provide evidence for the predicted interactions.

Cells were labeled and imaged as described above, with the change of adding two probes at once to look at pairwise combinations of labeled Tfr1, Tfr2-CoilZ, or CoilE-Hfe-myc-FLAG (**Figure D.5**). Cells were labeled with combinations of CoilR-Cy3 or -Cy5, CoilY-Cy5, or 8D3 (detected with anti-Rat-AF488). Since Tf binding was diminished in this cell line, fluorescent Tf was excluded from this experiment. These experiments were conducted on cells that did not have any holo-Tf added to the growth media.

First, AML 12 VIP-Tfr2/Hfe cells were treated live with CoilR-Cy5 to label tagged Hfe and 8D3 to label Tfr1 (Figure D.5B). After fixation, cells were blocked and labeled with anti-rat AF488 to detect 8D3 primary antibody. As previously observed in singly-labeled controls (Figure D.4A-B), Tfr1 and Hfe were both selectively labeled by immunolabeling and VIPER, respectively. Both showed signal at the cell surface, observed in the confocal slice as a fluorescent outline around each cell.

Tfr1 and Hfe showed many areas of fluorescence overlap, particularly in the cell membrane. This is observed as white signal in the green/magenta overlay. Colocalization analysis of the micrographs in ImageJ provided a initial means to quantify imaging results so that they could be compared32. Pearson's correlation assesses each pixel for overlap between two signals (yes/no) and how well the intensity matches for each signal. A value of 1.0 would indicate perfect co-localization and would indicate that

the images are identical. It should be noted that Pearson's correlation is limited by the resolution of the image, meaning the overlap can only be determined for the minimum distance that can be resolved. In typical confocal microscopy this value is greater than 250 nm. I found that the fluorescent signal corresponding to labeled Tfr1 and Hfe had good colocalization, with a Pearson's correlation value of 0.59.

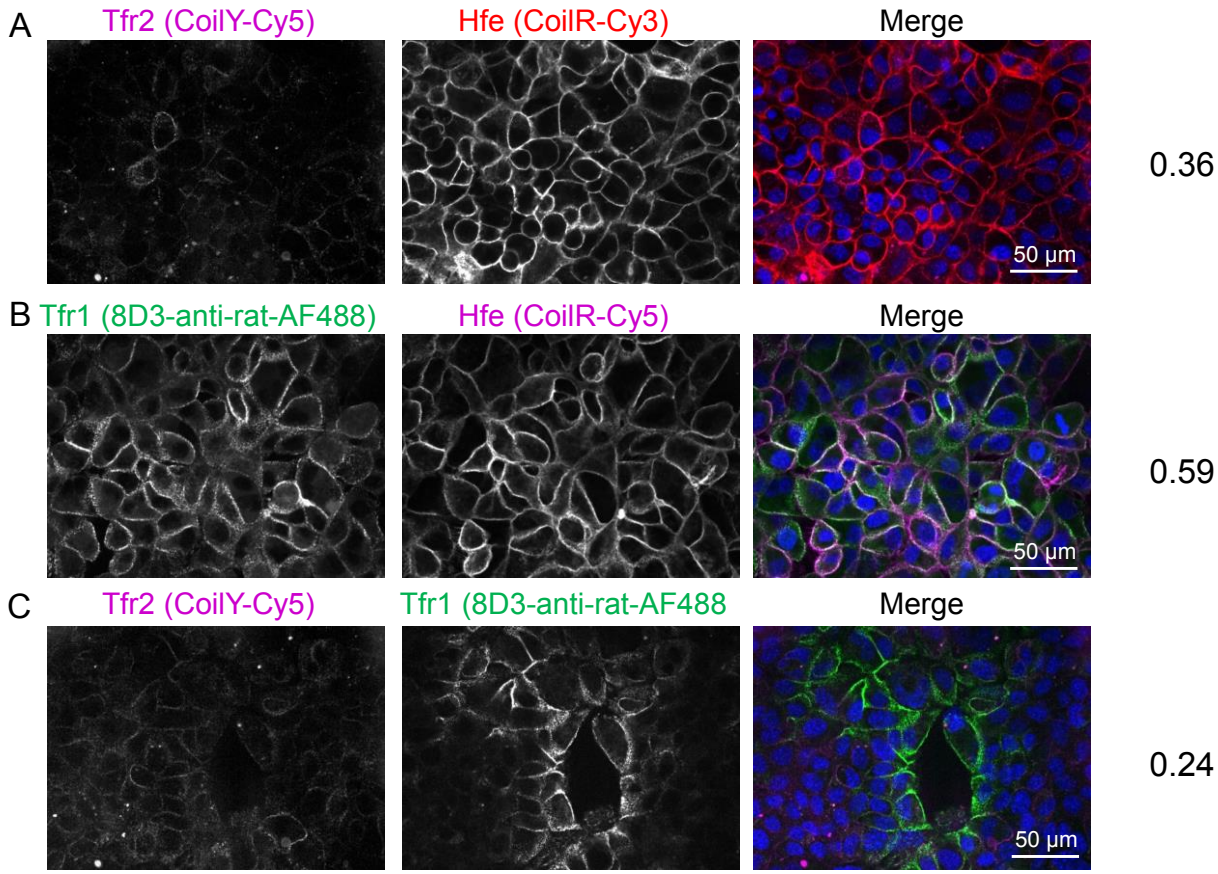


**Figure D.5. Two target imaging on the surface of live AML12 VIP-Tfr2/Hfe.** Cells were cooled to 4 °C and labeled cold to halt endocytosis. AML12 VIP-Tfr2/Hfe cells were treated with pairwise combinations of fluorescent CoilR, CoilY, or non-fluorescent 8D3 antibody (**A**: CoilR-Cy3+CoilY-Cy5, **B**: 8D3+CoilR-Cy5, **C:** CoilY-Cy5+8D3). After labeling cells were fixed, and antibody-labeled cells were subsequently treated with anti-mouse-AF488 secondary for fluorescence imaging. Cells were imaged at 40X (0.9 NA) after treatment. Merged channels are false colored where AF488 is green, AF555 is red, and Hoechst (nuclei) are blue. The Pearson's correlation value is reported to the right of each row.

Next, cells were prepared under conditions to label Tfr1 and Tfr2. AML 12 VIP-Tfr2/Hfe cells were treated live with CoilY-Cy5 to label tagged Tfr2 and 8D3 to label Tfr1

(**Figure D5.C**). After fixation, cells were blocked and labeled with anti-rat AF488 to detect 8D3. Separately, cells were prepared to label Tfr2 and Hfe (**Figure D5.A**). AML 12 VIP-Tfr2/Hfe cells were treated live with CoilR-Cy3 to label tagged Hfe and CoilY-Cy5 to label Tfr2. In either case, Cy5-labeled Tfr2 had a dim signal that made it difficult to observe colocalization with Tfr1 or Hfe. While Tfr2-CoilZ labeling was faint, it was noticeable that Tfr2-CoilZ was on the cell surface in some areas overlapping Tfr1 or Hfe signal. This resulted in a Pearson's correlation of 0.36 for Hfe:Tfr2 and 0.24 for Tfr1:Tfr2.

It is possible that Tfr2 and Hfe might still appear colocalized if the density of receptors was high enough. This is a limitation that results from the resolution limit of a standard confocal microscope. A more stringent imaging method, such as FRET microscopy, would be a proposed next step for imaging if colocalization was detected. This is due to FRET's dependence on fluorescently-labeled targets being within 10 nm of each other.

## Assessing intracellular protein targets

Following live, cell-surface assessment, I sought to determine if the tagged receptors were colocalized inside the cell. Intracellular labeling allowed me to assess the abundance of receptors within the cell, where they are located, and if they were colocalized with other partners. Tfr2-CoilZ and CoilE-Hfe-myc-FLAG were labeled after fixation and permeabilization to assess intracellular expression. VIPER labeling was used to detect CoilE-Hfe-myc-FLAG. Immunolabeling was used to detect CoilE-Hfe-myc-FLAG (M2), Tfr2-CoilZ (25257) and Tfr1 (8D3). Primary antibodies were subsequently detected by the appropriate fluorescent secondary antibodies.

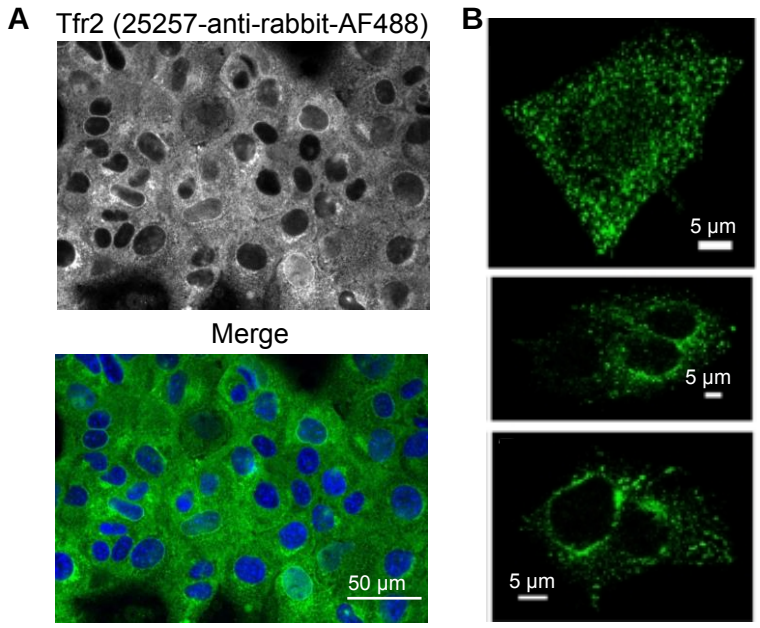


**Figure D.6. Labeling of Tfr2 inside fixed cells with 25257.** (**A**) AML12 VIP-Tfr2/Hfe cells were fixed and permeabilized with 0.1% saponin. Cells were then labeled with anti-Tfr2 (#25257), which detects mouse Tfr2. Following labeling, cells were treated with anti-rabbit-AF488 for fluorescence imaging. Cells were imaged at 40X (0.9 NA) after treatment. Merged channels are false colored (AF488 is green and Hoechst (nuclei) are blue). (**B**) Example immunofluorescence images of TfR2 reproduced from Johnson et al.[20] that show labeling of HepG2 cells with an anti-TfR2 antibody (9F81C11). It is of note that this immunolabeling was of human TfR2 in a human cell line.

Tfr2-CoilZ could not be labeled post-fixation with CoilY because VIP Y/Z is sensitive to amine-crosslinking. Therefore, I used an anti-mouse Tfr2 antibody, 25257. This antibody was produced in-lab in a rabbit host and was used as-is in serum. However, initial labeling with 25257 showed that labeling with 25257 followed by anti-rabbit secondary antibodies uniformly stained the interior of the cell (**Figure D.6**). This was theorized to be a result of other IgGs present in the rabbit serum that were detected by the anti-rabbit secondary antibodies. By comparison, published micrographs of immunolabeled Tfr2 with a different antibody (9F81C11) showed punctate staining consistent with TfR2 localized in endosomes[20]. In order to use 25257 antibody, it will have to be purified from the serum for future experiments. Another option is to locate a different commercial anti-Tfr2 antibody and validate it for fluorescence imaging.

Intracellular fixed-cell labeling proceeded for imaging Hfe and Tfr1. AML12 VIP-Tfr2/Hfe cells were first fixed and permeabilized and then blocked with 10% FBS, 5%

sucrose, 2% BSA in DPBS. Cells were then treated with pairwise combinations of CoilR-Cy5, M2, or 8D3 antibody (**Figure D.7**). M2 is an anti-FLAG primary antibody and detects CoilE-Hfe-myc-FLAG, which I used for counter-staining HFE alongside CoilR-Cy5. These two labels were expected to generate the most fluorescence overlap due to labeling the same CoilE-Hfe-myc-FLAG protein at both the N-terminus CoilE (with CoilR-Cy5) and C-terminus FLAG tag (with M2 antibody).

When cells were fixed and labeled with CoilR and M2, which should detect the same Hfe protein, a Pearson's correlation value of 0.73 was measured (**Figure D.7A**). When labeling with CoilR and 8D3 (**Figure D.7B**) to detect CoilE-Hfe-myc-FLAG and Tfr1, a correlation of 0.71 was determined. Lastly, when labeling cells with M2 and 8D3, which detects CoilE-Hfe-myc-FLAG and Tfr1 (**Figure D.7C**), a Pearson's correlation of 0.79 was determined.

Overall, there was good colocalization between Tfr1 and Hfe, as assessed by two different means of detecting CoilE-Hfe-myc-FLAG while detecting Tfr1 with the 8D3 antibody. These treatments labeled the same cellular features, albeit with variation in fluorescence intensity in some areas. An example of this is the perinuclear area of the cell where the Golgi and endoplasmic reticulum are found. This could be due to differences in fluorophore sensitivity or from a difference in labeling in these areas. For labeling the same molecule, CoilR-Cy5 and M2 signal did colocalize, but the labeling intensity in the interior of the cell was brighter for CoilR-Cy5. It could possibly be that CoilR, being significantly smaller than an antibody, can more readily access areas with a high density of targets, such as within organelles. This can be tested by using a stronger permeabilization than saponin, such as Triton-X-100 to allow for greater labeling access within the membrane-bound organelles. A smaller FLAG probe can be used, such as an antibody fragment specific for the FLAG tag[34], which is comparable in size to a VIP tag.

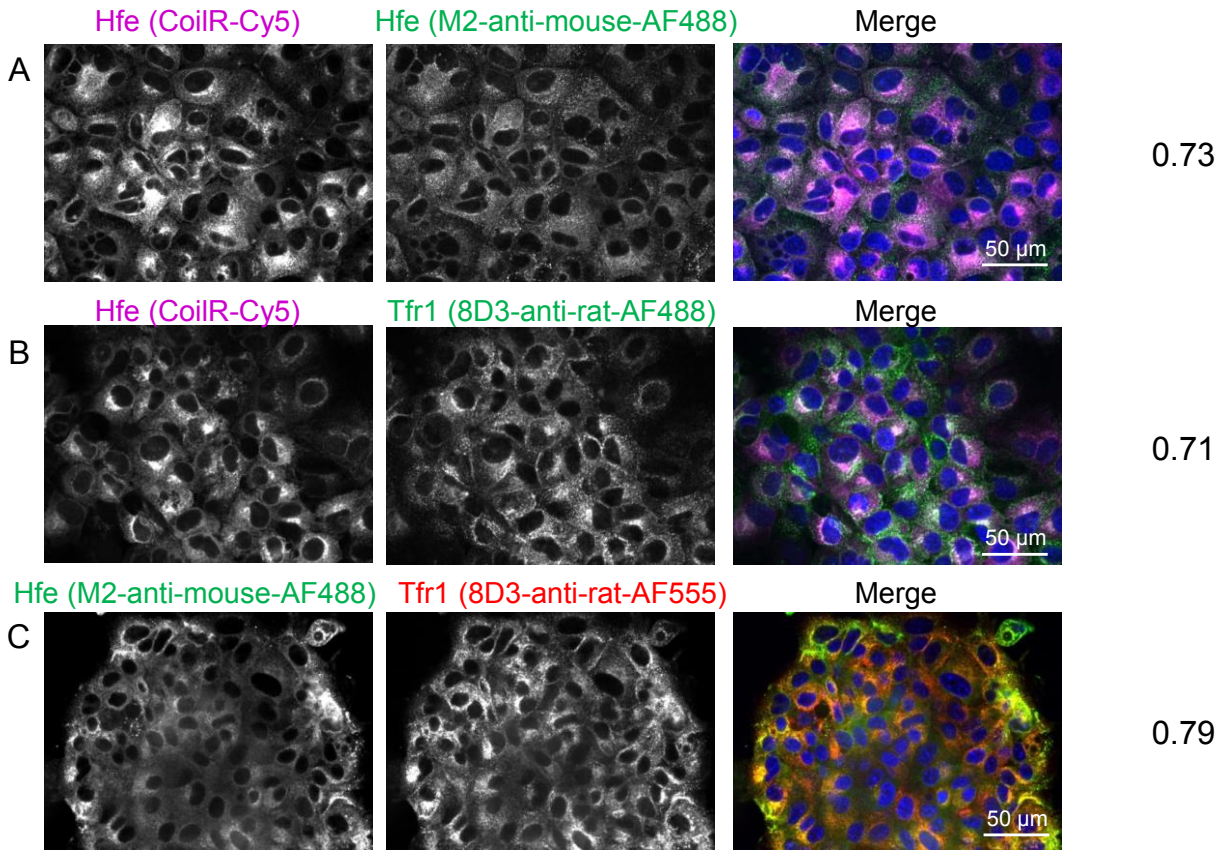


**Figure D.7. Assessment of Tfr1 and Hfe inside fixed AML12 VIP-Tfr2/Hfe.** AML12 VIP-Tfr2/Hfe cells were fixed and permeabilized with 0.1% saponin. Cells were then labeled with pairwise combinations of CoilR-Cy5, M2 or 8D3 (**A**: CoilR+M2, **B**: 8D3+CoilR, **C**: M2+8D3). CoilR and M2 both detect CoilE-Hfe-myc-FLAG and 8D3 detects Tfr1. Following labeling, primary antibodies were treated with secondary antibodies for fluorescence imaging. Cells were imaged at 40X (0.9 NA) after treatment. Merged channels are false colored: AF488 is green, AF555 is red, Cy5 is magenta, and Hoechst (nuclei) is blue. The Pearson's correlation value was reported to the right of each row.

## Conclusions

Western blot analysis of AML12 VIP-Tfr2/Hfe cell lysates demonstrated that this cell line is stably expressing CoilE-Hfe-myc-FLAG and Tfr2-CoilZ. In general, all clones assessed showed greater detection of CoilE-Hfe-myc-FLAG than Tfr2-CoilZ, which does not reflect the previously measured stoichiometry of 1:4 (Hfe:Tfr2)[31] in mouse liver.

When CoilE-Hfe-myc-FLAG was precipitated with anti-myc resin, Tfr2-CoilZ was pulled down in the presence and absence of Tf. This demonstrated that the addition of VIP tags did not interfere with the ability of Tfr2 and Hfe to bind.

Fluorescence imaging showed that AML12 VIP-Tfr2/Hfe cell line is stably expressing CoilE-Hfe-myc-FLAG on the cell surface. Tagged Hfe is over-expressed to the extent that it appears to be causing competition with Tf-binding for Tfr1 receptor, which needs to be explored further. A possible solution to this is to add saturating levels of holo-Tf to the cell media. As the formation of the Tfr2-Hfe iron sensing model is dependent on high iron levels, this would not experimentally conflict with the goals of the experiment. Ideally this stable cell line would be on an inducible promoter so that the tagged Hfe expression levels could be tuned to match levels found in mouse liver.

Endogenous Tfr1 can be readily detected with anti-Tfr1 immunolabeling. Tfr2-CoilZ on the other hand, is faintly detectable on the cell surface by VIP Y/Z labeling. This is in spite of Western blot analysis of cell lysates confirming Tfr2-CoilZ protein expression. This would suggest a lack of trafficking of Tfr2 to the cell surface or poor dimer formation. Further purification of the anti-Tfr2 antibody will be needed in order to assess the Tfr2 expression and distribution inside fixed cells. There is current ongoing work on making fixation-resistant VIP tags that are orthogonal to VIPER. These would make good candidates for tagging intracellularTfr2 and would circumvent the need for purified antibody.

While there were some mixed results with Tfr2-CoilZ expression levels, CoilE-Hfe-myc-FLAG is expressed at high levels in AML12 VIP-Tfr2/Hfe and is readily detectable with VIP labeling or immunolabeling (using an anti-FLAG antibody). This makes subsequent steps in investigating Hfe biology easier, particularly as it pertains to studying Hfe localization.

## Future Experiments: Sub-cellular localization and trafficking of Tfr2

Future experiments that can be pursued include combining VIP-labeling of Hfe with immunolabeling of cellular proteins involved in protein trafficking. These colocalization studies can be used to determine the localization of Hfe and Tfr2 within cells in conditions of high and low iron.

Previous analysis by Johnson, Enns, and coworkers of TfR2's sub-cellular distribution in HepG2 focused on EEA1 (early endosome), Rab7 (recycling endosome), LAMP1 (lysosome), and Golgin97 (trans-Golgi network)[20]. TfR2 was observed to

colocalize with EEA1, Rab7, and Golgin97 but not LAMP1. They suggested that TfR2 did not co-localize with LAMP1 due to rapid degradation of TfR2, causing loss of immunofluorescence. If TfR2 and HFE are indeed forming an iron-sensing complex, they are possibly co-trafficking in the cell. In future work, combining these trafficking markers with HFE can allow for a direct comparison with TfR2.

Experimentally, AML12 VIP-Tfr2/Hfe cells would be labeled live and cold with CoilR-Cy5 in order to label CoilE-Hfe-myc-FLAG in the cell surface. The cells would then be returned to 37 °C to allow VIP-labeled Hfe to traffic into the cell. A time series of 0, 5, 15, and 30 minutes post-labeling would capture the cell surface, early endocytosis, recycling endocytosis and degradation. After the allotted amount of time has passed the cells would be fixed and permeabilized. These cells could then be immunolabeled with a trafficking marker of choice, such as EEA1 to assess for Hfe colocalization with early endosome markers. HFE localization in early endoxomes could be expected to be seen at the 5 minute mark, but not the 30 minute mark. Meanwhile recycling (Rab7) and lysosomal (LAMP1) colocalization would be expected to be detected at later time points.

In addition to these experiments, companion studies will be conducted with Tfr1, which has a known trafficking pathway. TfR1 imaging would provide validation that the antibodies and methods used recapitulate known biology as well as allow Hfe's interactions with Tfr1 versus Tfr2 to be compared.

Based on these results and how they compare to published Tfr2 colocalization, a conclusion can be drawn about how Tfr2 and Hfe are localized in the cell. If the observations between Tfr2 and Hfe match in high iron conditions, but not low iron conditions, it provides further support that Tfr2 and Hfe are interacting together because they are also co-trafficking as an iron-sensing complex.

This will also be future opportunities to confirm known interactions between Tfr1 and Hfe by microscopy and high resolution methods such as electron microscopy or Forster resonance energy transfer imaging (FRET). Crystal structure data of Tfr1 and Hfe complex[12] indicated that the proteins were physically close enough in distance for this measurement.

## Materials and Methods

The Materials and Methods and Supplementary tables reflect work that I have conducted and described in this chapter. Stable cell line generation and in vitro methods were performed in the Enns group and will be described and reported by them.

A description of constructs used in the current work, including peptide and protein sequences, is provided in **Table D.1**. Cell line information is provided in Table **D.2**. Antibody reagent information is provided in Table **D.3**. I have also included details on the constructs and reagents not mentioned in this Appendix chapter but are relevant to the project.

### Cell culture maintenance and plating

AML12 cells were obtained from ATCC (Cat. No. CRL-2254). CHO TRVb cells were generously provided by Prof. Timothy McGraw (Weill Cornell Medical School).

AML12 cells were maintained in DMEM/F12 media (Gibco) supplemented with 10% fetal bovine serum (FBS), 10 µg/ml insulin, 5.5 µg/ml transferrin, 5 ng/ml selenium 40 ng/ml dexamethasone (AML12 media) in 10 cm polystyrene dishes. The insulin, transferrin and selenium are purchased as a 10X ITS supplement (Gibco). Dexamethasone was dissolved in ethanol to create 100X stocks (40 ug/mL). Cells were grown in a humidified incubator at 37 °C with 5% $CO_2$ and passaged when they reached 80-90% confluency. Cells were detached with 0.25% trypsin/1 mM EDTA (TRED) and seeded at a 1:4 dilution (5 x $10^6$ cells/dish).

Transduced cells were grown in AML12 media with supplemented antibiotics (see **Table D.2**) and passaged as described.

For imaging, cells were detached and plated at 1 x $10^5$ cells per well in an 8-chambered #1.5 coverglass (Cellvis).

### Live cell labeling of cell surface targets

AML12 cells plated to 8-chambered coverglass were blocked with 10% FBS, 6% BSA in AML12 media for 30 min at 37 °C in a humidified incubator with 5% CO2. Cells were cooled to 4 °C to pause endocytosis, then incubated (30 min) with labeling

reagents diluted in AML12 media. Labeling reagents were one of or a combination of the following:

100 nM VIP probe peptide
50 µg/ml Tf-AF488 (Thermofisher)
10 µg/ml primary antibody (such as 8D3)

After incubation, cells were washed three times with cold DPBS and then fixed with 4% PFA for 15 min at 4 °C. Cells were washed twice with DPBS. If cells were treated with primary antibody, cells were subsequently blocked with 10% FBS, 6% BSA in DPBS for 30 min at RT. Cells were then labeled with 10 µg/ml fluorescently labeled secondary antibody for 1 hour at RT in 10% FBS, 6% BSA in DPBS. After labeling cells were washed twice with DPBS and nuclei were stained with 10 µg/mL Hoechst 33342 (10 min), and washed twice more with DPBS before imaging.

Labeling concentrations for VIP tags were determined experimentally, while concentrations for antibodies was based off the manufacturer's instruction for immunofluorescence imaging (generally a 1:100 dilution of a 1 µg/ml stock).

**Fixed cell imaging of intracellular targets**

Prior to labeling AML12 cells were fixed with 4% PFA in DPBS for 15 min at RT. Cells were subsequently washed twice with DPBS and permeabilized with 0.1% saponin in DPBS for 10 min. Cells were washed twice with DPBS to remove detergent and blocked for 30 min in 10% FBS 5% sucrose 2% BSA in DPBS (Fixed Cell Blocking Solution). Cells were treated with labeling reagent in Fixed Cell Blocking Solution for 1 h at room temperature. Labeling reagents were one of or a combination of the following:

100 nM VIP probe peptide
10 µg/ml primary antibody (such as 8D3)

After labeling cells were washed twice with DPBS. Cells labeled with primary antibody were then labeled with 10 µg/ml fluorescently labeled secondary antibody for 1

hour. After labeling cells were washed twice with DPBS and nuclei were stained with 10 μg/mL Hoechst 33342 (10 min), and washed twice more with DPBS before imaging.

**Fluorescence Microscopy**

Cells were imaged on a Zeiss Yokogawa spinning disk confocal microscope. For **Figures D.3-D.7** a 40X (NA 0.9) objective lens was used. When imaging samples within the same experiment, the same acquisition settings (e.g., laser intensity and exposure time) were used for all samples. The following excitation (ex) laser lines and emission filters (em) were used for the indicated fluorophores:

Hoechst 33342 – ex: 405 nm; em: 405/50 nm
AF488 – ex: 488 nm; em: 525/50 nm
Cy3 or AF555– ex: 561 nm; em: 629/62 nm
Cy5 – ex: 638 nm; em: 690/50 nm

**Image Analysis**

Images were adjusted and false-colored for analysis using ImageJ. The ImageJ 'Channels' tool was used to false color individual channels and to create a multicolored merge image. Scale bars were added in ImageJ. For colocalization analysis, the Coloc2 analysis software packaged with ImageJ was used. Channel files were split into two images by using Image>Color>Split Channels. The nucleus channel was removed. With the two channels to be compared opened as separate images, Analyze>Colocalization>Coloc2 was run.

# Supplementary Tables

## Table D.1. Summary of genetic constructs

| Protein Name | **Sequence** (1-letter amino acid code)<br>Sequence annotation key: **Coil tag**; linker; myc; FLAG | MW (Da) | pI | Vector Name |
|---|---|---|---|---|
| **CoilY** | MGSS**NTVKELKNYIQELEERNAELKNLKEHLKFAKAELEFELAAHKFE**GGGAAACLG<br>KLAAALEHHHHHH | 7826.85 | 6.43 | pET28b(+)<br>_CoilY |
| **CoilE** | MGGS**LEIEAAFLERENTALETRVAELRQRVQRLRNRVSQYRTRYGPL**GGGCLEHHHH<br>H | 6737.56 | 9.29 | pET28b(+)<br>_CoilE |
| **CoilR** | MGGS**LEIRAAFLRQRNTALRTEVAELEQEVQRLENEVSQYETRYGPL**GGGAAALGCL<br>AAALEHHHHHH | 7502.35 | 6.00 | pET28b(+)<br>_CoilR |
| **MiniE** | MGSS**LEIEAAFLERENTALETRVAELRQRVQRLRNEYGPL**GGGAAAWGLCYPWVYGL<br>EHHHHHH | 7322.19 | 6.27 | pET28b(+)<br>_MiniE |
| **MiniR** | MGSS**LEIRVAFLRQRNTALRTEVAELEQEVQRLENRYGPL**GGGAAAWGLCYPWVYGL<br>EHHHHHH | 7349.26 | 6.57 | pET28b(+)<br>_MiniR |
| **Transferrin Receptor 1 (Tfr1)** | MMDQARSAFSNLFGGEPLSYTRFSLARQVDGDNSHVEMKLAADEEENADNNMKASVR<br>KPKRFNGRLCFAAIALVIFFLIGFMSGYLGYCKRVEQKEECVKLAETEETDKSETME<br>TEDVPTSSRLYWADLKTLLSEKLNSIEFADTIKQLSQNTYTPREAGSQKDESLAYYI<br>ENQFHEFKFSKVWRDEHYVKIQVKSSIGQNMVTIVQSNGNLDPVESPEGYVAFSKPT<br>EVSGKLVHANFGTKKDFEELSYSVNGSLVIVRAGEITFAEKVANAQSFNAIGVLIYM<br>DKNKFPVVEADLALFGHAHLGTGDPYTPGFPSFNHTQFPPSQSSGLPNIPVQTISRA<br>AAEKLFGKMEGSCPARWNIDSSCKLELSQNQNVKLIVKNVLKERRILNIFGVIKGYE<br>EPDRYVVVGAQRDALGAGVAAKSSVGTGLLLKLAQVFSDMISKDGFRPSRSIIFASW<br>TAGDFGAVGATEWLEGYLSSLHLKAFTYINLDKVVLGTSNFKVSASPLLYTLMGKIM<br>QDVKHPVDGKSLYRDSNWISKVEKLSFDNAAYPFLAYSGIPAVSFCFCEDADYPYLG<br>TRLDTYEALTQKVPQLNQMVRTAAEVAGQLIIKLTHDVELNLDYEMYNSKLLSFMKD<br>LNQFKTDIRDMGLSLQWLYSARGDYFRATSRLTTDFHNAEKTNRFVMREINDRIMKV<br>EYHFLSPYVSPRESPFRHIFWGSGSHTLSALVENLKLRQKNITAFNETLFRNQLALA<br>TWTIQGVANALSGDIWNIDNEF | 85731.40 | 6.13 | pcDNA3.1_<br>Tfr1 |
| **Tfr1-CoilZ** | MDQARSAFSNLFGGEPLSYTRFSLARQVDGDNSHVEMKLAADEEENADNNMKASVRK<br>PKRFNGRLCFAAIALVIFFLIGFMSGYLGYCKRVEQKEECVKLAETEETDKSETMET<br>EDVPTSSRLYWADLKTLLSEKLNSIEFADTIKQLSQNTYTPREAGSQKDESLAYYIE<br>NQFHEFKFSKVWRDEHYVKIQVKSSIGQNMVTIVQSNGNLDPVESPEGYVAFSKPTE<br>VSGKLVHANFGTKKDFEELSYSVNGSLVIVRAGEITFAEKVANAQSFNAIGVLIYMD<br>KNKFPVVEADLALFGHAHLGTGDPYTPGFPSFNHTQFPPSQSSGLPNIPVQTISRAA<br>AEKLFGKMEGSCPARWNIDSSCKLELSQNQNVKLIVKNVLKERRILNIFGVIKGYEE<br>PDRYVVVGAQRDALGAGVAAKSSVGTGLLLKLAQVFSDMISKDGFRPSRSIIFASWT<br>AGDFGAVGATEWLEGYLSSLHLKAFTYINLDKVVLGTSNFKVSASPLLYTLMGKIMQ<br>DVKHPVDGKSLYRDSNWISKVEKLSFDNAAYPFLAYSGIPAVSFCFCEDADYPYLGT<br>RLDTYEALTQKVPQLNQMVRTAAEVAGQLIIKLTHDVELNLDYEMYNSKLLSFMKDL<br>NQFKTDIRDMGLSLQWLYSARGDYFRATSRLTTDFHNAEKTNRFVMREINDRIMKVE<br>YHFLSPYVSPRESPFRHIFWGSGSHTLSALVENLKLRQKNITAFNETLFRNQLALAT<br>WTIQGVANALSGDIWNIDNEFGSGSGSTG**QKVAQLKNRVAYKLKENAKLENIVARLE<br>NDNANLEKDIANLEKDIANLERDVAR**TG | 92534.95 | 6.24 | pcDNA3.1_<br>Tfr1-CoilZ |
| **Tfr1-CoilE** | MMDQARSAFSNLFGGEPLSYTRFSLARQVDGDNSHVEMKLAADEEENADNNMKASVR<br>KPKRFNGRLCFAAIALVIFFLIGFMSGYLGYCKRVEQKEECVKLAETEETDKSETME<br>TEDVPTSSRLYWADLKTLLSEKLNSIEFADTIKQLSQNTYTPREAGSQKDESLAYYI<br>ENQFHEFKFSKVWRDEHYVKIQVKSSIGQNMVTIVQSNGNLDPVESPEGYVAFSKPT<br>EVSGKLVHANFGTKKDFEELSYSVNGSLVIVRAGEITFAEKVANAQSFNAIGVLIYM<br>DKNKFPVVEADLALFGHAHLGTGDPYTPGFPSFNHTQFPPSQSSGLPNIPVQTISRA<br>AAEKLFGKMEGSCPARWNIDSSCKLELSQNQNVKLIVKNVLKERRILNIFGVIKGYE<br>EPDRYVVVGAQRDALGAGVAAKSSVGTGLLLKLAQVFSDMISKDGFRPSRSIIFASW<br>TAGDFGAVGATEWLEGYLSSLHLKAFTYINLDKVVLGTSNFKVSASPLLYTLMGKIM<br>QDVKHPVDGKSLYRDSNWISKVEKLSFDNAAYPFLAYSGIPAVSFCFCEDADYPYLG<br>TRLDTYEALTQKVPQLNQMVRTAAEVAGQLIIKLTHDVELNLDYEMYNSKLLSFMKD<br>LNQFKTDIRDMGLSLQWLYSARGDYFRATSRLTTDFHNAEKTNRFVMREINDRIMKV<br>EYHFLSPYVSPRESPFRHIFWGSGSHTLSALVENLKLRQKNITAFNETLFRNQLALA<br>TWTIQGVANALSGDIWNIDNEFGSGSGSTGM**LEIEAAFLERENTALETRVAELRQRV<br>QRLRNRVSQYRTRYGPL**GGGCLETG | 92312.77 | 6.34 | pcDNA3.1_<br>Tfr1-<br>CoilE |
| **Tfr1-MiniE** | MMDQARSAFSNLFGGEPLSYTRFSLARQVDGDNSHVEMKLAADEEENADNNMKASVR<br>KPKRFNGRLCFAAIALVIFFLIGFMSGYLGYCKRVEQKEECVKLAETEETDKSETME<br>TEDVPTSSRLYWADLKTLLSEKLNSIEFADTIKQLSQNTYTPREAGSQKDESLAYYI<br>ENQFHEFKFSKVWRDEHYVKIQVKSSIGQNMVTIVQSNGNLDPVESPEGYVAFSKPT<br>EVSGKLVHANFGTKKDFEELSYSVNGSLVIVRAGEITFAEKVANAQSFNAIGVLIYM<br>DKNKFPVVEADLALFGHAHLGTGDPYTPGFPSFNHTQFPPSQSSGLPNIPVQTISRA<br>AAEKLFGKMEGSCPARWNIDSSCKLELSQNQNVKLIVKNVLKERRILNIFGVIKGYE<br>EPDRYVVVGAQRDALGAGVAAKSSVGTGLLLKLAQVFSDMISKDGFRPSRSIIFASW | 91049.28 | 6.06 | pcDNA3.1_<br>Tfr1-MiniE |

| | | | | |
|---|---|---|---|---|
| | TAGDFGAVGATEWLEGYLSSLHLKAFTYINLDKVVLGTSNFKVSASPLLYTLMGKIM<br>QDVKHPVDGKSLYRDSNWISKVEKLSFDNAAYPFLAYSGIPAVSFCFCEDADYPYLG<br>TRLDTYEALTQKVPQLNQMVRTAAEVAGQLIIKLTHDVELNLDYEMYNSKLLSFMKD<br>LNQFKTDIRDMGLSLQWLYSARGDYFRATSRLTTDFHNAEKTNRFVMREINDRIMKV<br>EYHFLSPYVSPRESPFRHIFWGSGSHTLSALVENLKLRQKNITAFNETLFRNQLALA<br>TWTIQGVANALSGDIWNIDNEFGSGSGSTGM**LEIEAAFLERENTALETRVAELRQRV<br>QRLRNEYGPL**GGGTG | | | |
| **Tfr1-MiniR** | MMDQARSAFSNLFGGEPLSYTRFSLARQVDGDNSHVEMKLAADEEENADNNMKASVR<br>KPKRFNGRLCFAAIALVIFFLIGFMSGYLGYCKRVEQKEECVKLAETEETDKSETME<br>TEDVPTSSRLYWADLKTLLSEKLNSIEFADTIKQLSQNTYTPREAGSQKDESLAYYI<br>ENQFHEFKFSKVWRDEHYVKIQVKSSIGQNMVTIVQSNGNLDPVESPEGYVAFSKPT<br>EVSGKLVHANFGTKKDFEELSYSVNGSLVIVRAGEITFAEKVANAQSFNAIGVLIYM<br>DKNKFPVVEADLALFGHAHLGTGDPYTPGFPSFNHTQFPPSQSSGLPNIPVQTISRA<br>AAEKLFGKMEGSCPARWNIDSSCKLELSQNQNVKLIVKNVLKERRILNIFGVIKGYE<br>EPDRYVVVGAQRDALGAGVAAKSSVGTGLLLKLAQVFSDMISKDGFRPSRSIIFASW<br>TAGDFGAVGATEWLEGYLSSLHLKAFTYINLDKVVLGTSNFKVSASPLLYTLMGKIM<br>QDVKHPVDGKSLYRDSNWISKVEKLSFDNAAYPFLAYSGIPAVSFCFCEDADYPYLG<br>TRLDTYEALTQKVPQLNQMVRTAAEVAGQLIIKLTHDVELNLDYEMYNSKLLSFMKD<br>LNQFKTDIRDMGLSLQWLYSARGDYFRATSRLTTDFHNAEKTNRFVMREINDRIMKV<br>EYHFLSPYVSPRESPFRHIFWGSGSHTLSALVENLKLRQKNITAFNETLFRNQLALA<br>TWTIQGVANALSGDIWNIDNEFGSGSGSTGMGSS**LEIRVAFLRQRNTALRTEVAELE<br>QEVQRLENRYGPL**TG | 91136.41 | 6.14 | pcDNA3.1_<br>Tfr1-MiniR |
| **Transferrin Receptor 2 (Tfr2)** | MEQRWGLLRRVQQWSPRPSQTIYRRVEGPQLEHLEEEDREEGAELPAQFCPMELKGP<br>EHLGSCPGRSIPIPWAAAGRKAAPYLVLITLLIFTGAFLLGYVAFRGSCQACGDSVL<br>VVDEDVNPEDSGRTTLYWSDLQAMFLRFLGEGRMEDTIRLTSLRERVAGSARMATLV<br>QDILDKLSRQKLDHVWTDTHYVGLQFPDPAHANTLHWVDADGSVQEQLPLEDPEVYC<br>PYSATGNATGKLVYAHYGRSEDLQDLKAKGVELAGSLLLVRVGITSFAQKVAVAQDF<br>GAQGVLIYPDPSDFSQDPHKPGLSSHQAVYGHVHLGTGDPYTPGFPSFNQTQFPPVE<br>SSGLPSIPAQPISADIADQLLRKLTGPVAPQEWKGHLSGSPYRLGPGPDLRLVVNNH<br>RVSTPISNIFACIEGFAEPDHYVVIGAQRDAWGPGAAKSAVGTAILLELVRTFSSMV<br>SNGFRPRRSLLFISWDGGDFGSVGATEWLEGYLSVLHLKAVVYVSLDNSVLGDGKFH<br>AKTSPLLVSLIENILKQVDSPNHSGQTLYEQVALTHPSWDAEVIQPLPMDSSAYSFT<br>AFAGVPAVEFSFMEDDRVYPFLHTKEDTYENLHKMLRGRLPAVVQAVAQLAGQLLIR<br>LSHDHLLPLDFGRYGDVVLRHIGNLNEFSGDLKERGLTLQWVYSARGDYIRAAEKLR<br>KEIYSSERNDERLMRMYNVRIMRVEFYFLSQYVSPADSPFRHIFLGQGDHTLGALVD<br>HLRMLRADGSGAASSRLTAGLGFQESRFRRQLALLTWTLQGAANALSGDVWNIDNNF | 88402.12 | 5.72 | pcDNA3_Tf<br>r2 |
| **Tfr2-CoilZ** | MEQRWGLLRRVQQWSPRPSQTIYRRVEGPQLEHLEEEDREEGAELPAQFCPMELKGP<br>EHLGSCPGRSIPIPWAAAGRKAAPYLVLITLLIFTGAFLLGYVAFRGSCQACGDSVL<br>VVDEDVNPEDSGRTTLYWSDLQAMFLRFLGEGRMEDTIRLTSLRERVAGSARMATLV<br>QDILDKLSRQKLDHVWTDTHYVGLQFPDPAHANTLHWVDADGSVQEQLPLEDPEVYC<br>PYSATGNATGKLVYAHYGRSEDLQDLKAKGVELAGSLLLVRVGITSFAQKVAVAQDF<br>GAQGVLIYPDPSDFSQDPHKPGLSSHQAVYGHVHLGTGDPYTPGFPSFNQTQFPPVE<br>SSGLPSIPAQPISADIADQLLRKLTGPVAPQEWKGHLSGSPYRLGPGPDLRLVVNNH<br>RVSTPISNIFACIEGFAEPDHYVVIGAQRDAWGPGAAKSAVGTAILLELVRTFSSMV<br>SNGFRPRRSLLFISWDGGDFGSVGATEWLEGYLSVLHLKAVVYVSLDNSVLGDGKFH<br>AKTSPLLVSLIENILKQVDSPNHSGQTLYEQVALTHPSWDAEVIQPLPMDSSAYSFT<br>AFAGVPAVEFSFMEDDRVYPFLHTKEDTYENLHKMLRGRLPAVVQAVAQLAGQLLIR<br>LSHDHLLPLDFGRYGDVVLRHIGNLNEFSGDLKERGLTLQWVYSARGDYIRAAEKLR<br>KEIYSSERNDERLMRMYNVRIMRVEFYFLSQYVSPADSPFRHIFLGQGDHTLGALVD<br>HLRMLRADGSGAASSRLTAGLGFQESRFRRQLALLTWTLQGAANALSGDVWNIDNNF<br>GEFGGGSEFMRS**QKVAQLKNRVAYKLKENAKLENIVARLENDNANLEKDIANLEKDI<br>ANLERDVAR** | 95830.49 | 5.74 | pcDNA3_Tf<br>r2-CoilZ |
| **CoilE-Hfe-myc-FLAG** | MSLSAGLPVRPLLLLLLLLWSVAPM**LEIEAAFLERENTALETRVAELRQRVQRLRNR<br>VSQYRTRYGPL**GGGCLEAAAQALPPRSHSLRYLFMGASEPDLGLPLFEARGYVDDQL<br>FVSYNHESRRAEPRAPWILEQTSSQLWLHLSQSLKGWDYMFIVDFWTIMGNYNHSKV<br>TKLGVVSESHILQVVLGCEVHEDNSTSGFWRYGYDGQDHLEFCPKTLNWSAAEPGAW<br>ATKVEWDEHKIRAKQNRDYLEKDCPEQLKRLLELGRGVLGQQVPTLVKVTRHWASTG<br>TSLRCQALDFFPQNITMRWLKDNQPLDAKDVNPEKVLPNGDETYQGWLTLAVAPGDE<br>TRFTCQVEHPGLDQPLTASWEPLQSQAMIIGIISGVTVCAIFLVGILFLILRKRKAS<br>GGTMGGYVLTDCETRTRPLEQKLISEEDLAANDILDYKDDDDK | 50083.15<br>(signal<br>peptide,<br>residue<br>1-22 is<br>2405.07) | 5.58 | pcDNA3_S<br>S-CoilE-<br>Hfe-myc-<br>FLAG |

## Table D.2. Summary of stable cell lines

| Construct | Cell line background | Method of integration | Antibiotics | Generated by | Date generated |
|---|---|---|---|---|---|
| pcDNA3.1_Tfr1 | CHO TRVb | Lipofectamine2000 transfection | 800 µg/ml G418 | Julia Doh | 06/2018 (JKD Notebook 5 pg. 58) |
| pcDNA3.1_Tfr1-CoilE | CHO TRVb | Lipofectamine2000 transfection | 800 µg/ml G418 | Julia Doh | 06/2018 (JKD Notebook 5 pg. 58) |
| pcDNA3.1_Tfr1-MiniE | CHO TRVb | Lipofectamine2000 transfection | 800 µg/ml G418 | Julia Doh | 06/2018 (JKD Notebook 5 pg. 58) |
| SS-CoilE-Hfe-myc-FLAG | HEK 293 | Lipofectamine2000 transfection | 400 µg/ml G418 | Shall Jue | 01/2019 |
| Tfr2-CoilZ | AML12 | Retroviral transduction | 400 µg/ml G418 | Shall Jue | 10/2019 |
| SS-CoilE-Hfe-myc-FLAG | AML12 | Retroviral transduction | 1 µg/ml puromycin | Shall Jue | 11/2019 |
| Tfr2-CoilZ SS-CoilE-Hfe-myc-FLAG | AML12 | Retroviral transduction | 400 µg/ml G418 1 µg/ml puromycin | Shall Jue | 01/2020 |

## Table D.3. Summary of Antibodies

| Name | Target | Supplier | Catalog # | Host | Validation |
|---|---|---|---|---|---|
| H68.4 | Tfr1 (cytosolic) | Thermofisher Scientific | 13-6800 | Mouse | CHO TRVb (knock-out) cell line (Doh) |
| 8D3 | Tfr1 (extracellular) | Novus Biologics | NB100-64979 | Rat | CHO TRVb (knock-out) cell line (Doh) |
| 25257 | Mouse Tfr2 | Purified rabbit serum | NA (Enns lab antibody) | Rabbit | CHO TRVb (knock-out) cell line (Doh) |
| 9F8 1C11 | Human Tfr2 | Santa Cruz Biotechnology | sc-32271 | Mouse | Johnson et. al[20] |
| M2 | FLAG epitope | Sigma Aldrich | F3165 | Mouse | WT AML12 |
| CDF4 | Golgin97 | Thermofisher Scientific | A21270 | Mouse | ND |
| R4779 | Rab7 | Sigma Aldrich | R4779 | Rabbit | ND |
| H4A3 | LAMP1 | Abcam | ab25630 | Mouse | ND |
| Ab2900 | EEA1 | Abcam | ab2900 | Rabbit | ND |
| Secondary anti-mouse-AF488 | Mouse Fc | Thermofisher Scientific | A-11001 | Goat | No primary control |
| Secondary anti -rabbit-AF488 | Rabbit Fc | Thermofisher Scientific | A-11008 | Goat | No primary control |
| Secondary anti-rabbit-AF555 | Rabbit Fc | Thermofisher Scientific | A-21428 | Goat | No primary control |
| Secondary anti -rat-AF488 | Rat Fc | Thermofisher Scientific | A-11006 | Goat | No primary control |
| Secondary anti -rat-AF555 | Rat Fc | Thermofisher Scientific | A-21434 | Goat | No primary control |

## Works Cited


1. Ganz, T. & Nemeth, E. Hepcidin and iron homeostasis. *Biochim. Biophys. Acta BBA - Mol. Cell Res.* **1823**, 1434–1443 (2012).
2. Liu, P. & Olivieri, N. Iron overload cardiomyopathies: new insights into an old disease. *Cardiovasc. Drugs Ther.* **8**, 101–110 (1994).
3. Greer, J. P. *et al. Wintrobe's clinical hematology*. (Wolters Kluwer Lippincott Williams & Wilkins Health, 2014).
4. Gao, J. *et al.* Hepatocyte-targeted HFE and TFR2 control hepcidin expression in mice. *Blood* **115**, 3374–3381 (2010).
5. De Domenico, I., Lo, E., Ward, D. M. & Kaplan, J. Hepcidin-induced internalization of ferroportin requires binding and cooperative interaction with Jak2. *Proc. Natl. Acad. Sci. U. S. A.* **106**, 3800–3805 (2009).
6. Zhou, X. Y. *et al.* HFE gene knockout produces mouse model of hereditary hemochromatosis. *Proc. Natl. Acad. Sci. U. S. A.* **95**, 2492–2497 (1998).
7. Sorkin, A. & von Zastrow, M. Endocytosis and signalling: intertwining molecular networks. *Nat. Rev. Mol. Cell Biol.* **10**, 609–622 (2009).
8. Lebrón, J. A. *et al.* Crystal structure of the hemochromatosis protein HFE and characterization of its interaction with transferrin receptor. *Cell* **93**, 111–123 (1998).
9. Parkkila, S. *et al.* Association of the transferrin receptor in human placenta with HFE, the protein defective in hereditary hemochromatosis. *Proc. Natl. Acad. Sci. U. S. A.* **94**, 13198–13202 (1997).
10. Feder, J. N. *et al.* The hemochromatosis gene product complexes with the transferrin receptor and lowers its affinity for ligand binding. *Proc. Natl. Acad. Sci.* **95**, 1472–1477 (1998).
11. Waheed, A. *et al.* Association of HFE protein with transferrin receptor in crypt enterocytes of human duodenum. *Proc. Natl. Acad. Sci. U. S. A.* **96**, 1579–1584 (1999).
12. Bennett, M. J., Lebrón, J. A. & Bjorkman, P. J. Crystal structure of the hereditary haemochromatosis protein HFE complexed with transferrin receptor. *Nature* **403**, 46–53 (2000).
13. Zhao, N. & Enns, C. A. Iron Transport Machinery of Human Cells: Players and Their Interactions. *Curr. Top. Membr.* **69**, 67–93 (2012).
14. Kawabata, H. *et al.* Transferrin Receptor 2-α Supports Cell Growth Both in Iron-chelated Cultured Cells and in Vivo. *J. Biol. Chem.* **275**, 16618–16625 (2000).
15. Ganz, T. Is TfR2 the iron sensor? *Blood* **104**, 3839–3840 (2004).
16. Goswami, T. & Andrews, N. C. Hereditary hemochromatosis protein, HFE, interaction with transferrin receptor 2 suggests a molecular mechanism for mammalian iron sensing. *J. Biol. Chem.* **281**, 28494–28498 (2006).
17. Chen, J., Wang, J., Meyers, K. R. & Enns, C. A. Transferrin-directed internalization and cycling of transferrin receptor 2. *Traffic Cph. Den.* **10**, 1488–1501 (2009).
18. West, A. P. *et al.* Comparison of the Interactions of Transferrin Receptor and Transferrin Receptor 2 with Transferrin and the Hereditary Hemochromatosis Protein HFE. *J. Biol. Chem.* **275**, 38135–38138 (2000).
19. Johnson, M. B. & Enns, C. A. Diferric transferrin regulates transferrin receptor 2 protein stability. *Blood* **104**, 4287–4293 (2004).

20. Johnson, M. B., Chen, J., Murchison, N., Green, F. A. & Enns, C. A. Transferrin Receptor 2: Evidence for Ligand-induced Stabilization and Redirection to a Recycling Pathway. *Mol. Biol. Cell* **18**, 743–754 (2006).
21. Fleming, R. E. Iron Sensing as a Partnership: HFE and Transferrin Receptor 2. *Cell Metab.* **9**, 211–212 (2009).
22. Gao, J. *et al.* Interaction of the Hereditary Hemochromatosis Protein HFE with Transferrin Receptor 2 Is Required for Transferrin-Induced Hepcidin Expression. *Cell Metab.* **9**, 217–227 (2009).
23. Hopp, T. P. *et al.* A Short Polypeptide Marker Sequence Useful for Recombinant Protein Identification and Purification. *Bio/Technology* **6**, 1204–1210 (1988).
24. Zane, H. K., Doh, J. K., Enns, C. A. & Beatty, K. E. Versatile interacting peptide (VIP) tags for labeling proteins with bright chemical reporters. *ChemBioChem* (2017) doi:10.1002/cbic.201600627.
25. Doh, J. K. *et al.* VIPER is a genetically encoded peptide tag for fluorescence and electron microscopy. *Proc. Natl. Acad. Sci.* 201808626 (2018) doi:10.1073/pnas.1808626115.
26. Gronemeyer, T., Chidley, C., Juillerat, A., Heinis, C. & Johnsson, K. Directed evolution of O6-alkylguanine-DNA alkyltransferase for applications in protein labeling. *Protein Eng. Des. Sel.* **19**, 309–316 (2006).
27. Gautier, A. *et al.* An engineered protein tag for multiprotein labeling in living cells. *Chem. Biol.* **15**, 128–136 (2008).
28. Los, G. V. *et al.* HaloTag: A Novel Protein Labeling Technology for Cell Imaging and Protein Analysis. *ACS Chem. Biol.* **3**, 373–382 (2008).
29. Doh, J. K., Tobin, S. & Beatty, K. E. MiniVIPER is a peptide tag for imaging and translocating proteins in cells. (2020).
30. Forejtnikovà, H. *et al.* Transferrin receptor 2 is a component of the erythropoietin receptor complex and is required for efficient erythropoiesis. *Blood* **116**, 5357–5367 (2010).
31. Chloupková, M., Zhang, A.-S. & Enns, C. A. Stoichiometries of Transferrin Receptors 1 and 2 in Human Liver. *Blood Cells. Mol. Dis.* **44**, 28 (2010).
32. Entzminger, K. C. *et al.* De novo design of antibody complementarity determining regions binding a FLAG tetra-peptide. *Sci. Rep.* **7**, 1–11 (2017).

# Appendix E: Assessment of transfection and expression effects of VIP tagging by flow cytometry

*This appendix details an experiment to determine if VIP tags changed the expression or transfection efficiency of tagged proteins compared to the untagged wild type using flow cytometry.*

## Quantitative assessment of transfection efficiency of VIP-tagged constructs

We sought to evaluate the effect of the genetically-encoded tag on transfection and protein expression. First, we used flow cytometry to analyze U-2 OS cells transiently transfected with VIP-tagged or untagged H2B-mEmerald. We gated for single cells and determined the transfection efficiency based on the fluorescent protein signal (green fluorescence). The difference in transfection efficiency (13-16%) by introduction of a CoilE, MiniE, or MiniR tag onto this protein was statistically non-significant (**Figure E.1**). The mean fluorescence intensity of transfected cells was comparable for MiniR- and CoilE-tagged constructs compared to the untagged (H2B-mEmerald) construct, while the MiniE-tagged construct was slightly more fluorescent ($p<0.05$). This suggests that the MiniE-tagged construct expressed more protein per cell than the other fusion proteins. The same analysis was done with U-2 OS cells transfected with TOMM20-mCherry variants. For this protein, addition of the tag significantly improved the transfection efficiency (38% for untagged, 47-51% for tagged, $p<0.05$); the mean fluorescence levels varied slightly between samples with the CoilE-tagged construct being slightly more fluorescent ($p<0.05$). For these two targets, we conclude that the VIP tags showed no detrimental effect on either transfection or protein expression, both of which were estimated based on fluorescent protein fluorescence.

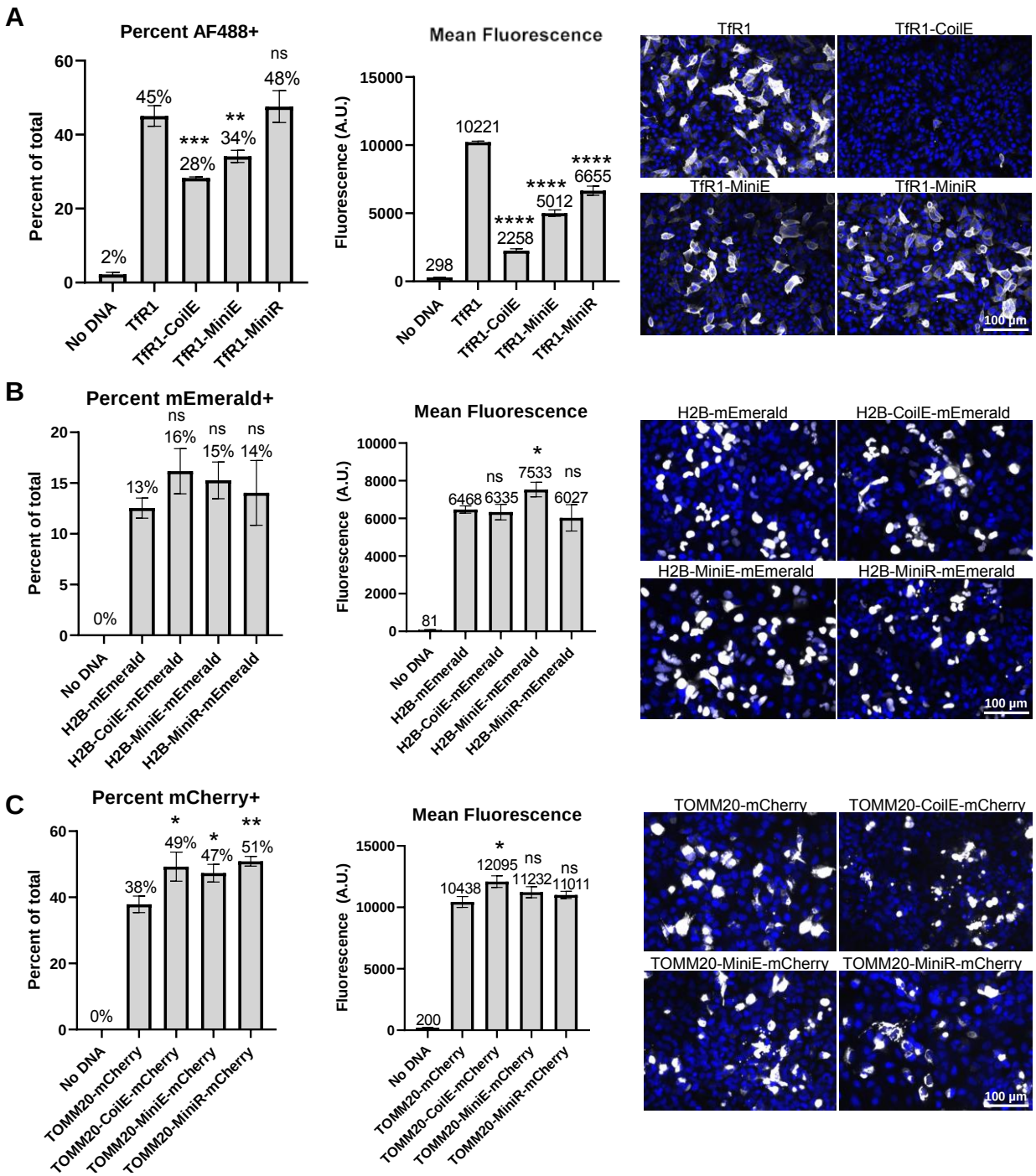


**Figure E.1: MiniVIPER has an increased or non-perturbative effect on transfection efficiency.** (**A**) CHO TRVb cells were transfected with no DNA, TfR1, TfR1-CoilE, TfR1-MiniE, or TfR1-MiniR and labeled live with Tf-AF488 and then fixed. Cells analyzed by flow cytometry, and the percent transfected cells out of total cells counted was determined by AF488+ signal (left), indicative of Tf binding. Of the transfected (AF488+) cells, the mean AF488 fluorescence was assessed (middle). A 20X micrograph is provided for all constructs where white represents the fluorophore assessed by flow cytometry and Hoechst 33342 highlights the cell nuclei in blue (right). (**B**) Percent transfection for U2-OS cells transfected with no DNA,

H2B-mEmerald, H2B-CoilE-mEmerald, H2B-MiniE-mEmerald, or H2B-MiniR-mEmerald as analyzed by flow cytometry (left). Of the transfected cells, the mean mEmerald fluorescence was assessed (middle) and a representative micrograph is shown for each construct (right). (**C**) Percent transfection for U2-OS cells transfected with no DNA, TOMM20-mCherry, TOMM20-CoilE-mCherry, TOMM20-MiniE-mCherry or TOMM20-MiniR-mCherry as analyzed by flow cytometry (left). Of the transfected cells, the mean mCherry fluorescence was assessed (middle). Each construct was assessed with 3 transfection replicates. * = $p < 0.05$, ** = $p < 0.01$, *** = $p < 0.001$, **** = $p < 0.0001$.

Next we evaluated CHO TRVb cells transfected with Transferrin Receptor 1 (TfR1) constructs. CHO TRVb cells do not express any endogenous TfR1 or TfR2[1]. Untransfected cells would thus not bind any transferrin (Tf). Transferrin binding therefore served as a marker for positive TfR1 transfection. Cells were treated with a saturating amount of Tf-AF488 to label surface-accessible TfR1 before analysis and gated for green fluorescence. For these constructs, we found that TfR1-CoilE had a significantly ($p < 0.001$) fewer TfR1-expressing cells compared to untagged TfR1 (28% versus 45% Tf-bound). TfR1-MiniE also had fewer expressing cells (34%, $p < 0.01$), while TfR1-MiniR was not significantly different from the untagged TfR1 (48%). Among (Tf-AF488)-binding cells, the highest mean fluorescence intensity was for untagged TfR1. Several factors could influence Tf-AF488 binding differences between cells and receptor constructs, including TfR1 expression, folding, trafficking, or ligand binding. Overall, the flow cytometry analysis suggests that VIP tags had a small influence on TfR1 expression or Tf-AF488 binding at the cell surface. Similar to other genetically-encoded tags[2,3], we recommend rigorous testing of new fusion proteins to ensure that they retain normal behavior and function.

## Materials and Methods

### Mammalian cell culture and maintenance

Chinese Hamster Ovary (CHO) TRVb (ΔTfR1 ΔTfR2) cells were generously provided by Prof. Timothy E. McGraw (Cornell University, New York). These cells do not express functional transferrin receptor 1 (TfR1) or transferrin receptor 2 (TfR2). CHO TRVb cells were maintained in Ham's F12 media (Gibco) supplemented with 5% fetal bovine serum (FBS) in 10 cm polystyrene dishes. Cells were grown in a humidified incubator at 37 °C with 5% $CO_2$ and passaged when they reached 80-90% confluency. Cells were detached with 0.25% trypsin/1 mM EDTA (TRED) and seeded at a 1:10 dilution (2 x $10^6$ cells/dish).

U-2 OS cells were purchased from ATCC (Cat #HTB-96). Cells were maintained in McCoy's 5A media (HyClone) with 10% FBS in 10 cm polystyrene dishes. Cells were grown in a humidified incubator at 37 °C with 5% $CO_2$ and passaged when they reached 80-90% confluency. They were detached with TRED and seeded at a 1:10 dilution (2 x $10^6$ cells/dish).

### Transfecting VIP-tagged proteins for flow cytometry

Transfection was performed using Lipofectamine 2000 (ThermoFisher) following the manufacturer's instructions. All constructs used for transfections can be found in **Table E.1**. A DNA:Lipofectamine ratio of 1:2 was used.

CHO TRVb cells were plated (2 x $10^6$ cells/well) in a 6-well dish and grown to 90% confluence in 6-well dishes. Cells were transfected with 2 µg of pcDNA3.1_TfR1, pcDNA3.1_TfR1-CoilE, pcDNA3.1_TfR1-MiniE, or pcDNA3.1_TfR1-MiniR and 4 µg of Lipofectamine 2000 in 1 mL of Opti-MEM. After 4 h, cells were returned to serum-containing media. After 24 h, cells were processed for flow cytometry.

U-2 OS cells were plated (2 x$10^6$ cells/well) in a 6-well dish and grown to 90% confluence in 6-well dishes. Cells were transfected with 2 µg of H2B-mEmerald or TOMM20-mCherry constructs (untagged, CoilE-, MiniE-, or MiniR-tagged) and 4 µg of Lipofectamine 2000 in 1 mL of Opti-MEM. After 4 h, cells were returned to serum-containing media. After 24 h, cells were processed for flow cytometry.

**Preparation of cells for flow cytometry**

**A. Tf-AF488 labeling of transfected CHO TRVb cells for flow analysis**

TfR1 is not fluorescent. However, it can be labeled with fluorescent transferrin such as Tf-AF488 and fixed for flow cytometry analysis. To do this, transfected CHO TRVb cells (TfR1, TfR1-CoilE, TfR1-MiniE, TfR1-MiniR) were detached with 10 mM EDTA in DPBS for 10 min. Cells were pelleted by spinning at 200 x g and resuspended in F12 with 50 µg/mL Tf-AF488. Cells were labeled for 30 min at 4 °C with agitation, before being pelleted and washed three times with F12. Cells were incubated at 37 °C for 5 min post-labeling to allow for receptor internalization. Cells were resuspended completely and fixed in 1% PFA for 15 min at room temperature. Cells were pelleted again, washed once with DPBS, and resuspended in DPBS for flow analysis.

**B. Detaching transfected U-2 OS cells for flow analysis**

U-2 OS cells transfected with H2B-mEmerald or TOMM20-mCherry constructs (untagged, CoilE-, MiniE-, or MiniR-tagged) were detached with 10 mM EDTA in DPBS for 10 min. Cells were pelleted by spinning at 200 x g and resuspended in DPBS. Cells were resuspended completely and fixed in 1% PFA for 15 min at room temperature. Cells were pelleted again, washed once with DPBS, and resuspended in DPBS for flow analysis.

**C. Flow cytometry and Flo-Jo analysis**

Cells were analyzed using a Fortessa Flow Cytometer (BD Biosciences) and gated for singlet cells using side scatter and forward scatter parameters. AF488 and mEmerald were excited by 488 nm laser light and detected through 530/30 nm emission filters. mCherry was excited by 561 nm laser light and detected through 610/20 nm emission filters. Flow data was analyzed using FlowJo software (Version X.07). A scatterplot of forward scatter area versus side scatter area (FSC-A/SSC-A) was used to gate cells from debris, and a scatterplot of forward scatter area versus side scatter width (FSC-A/ SSC-W) was used to gate for singlets.

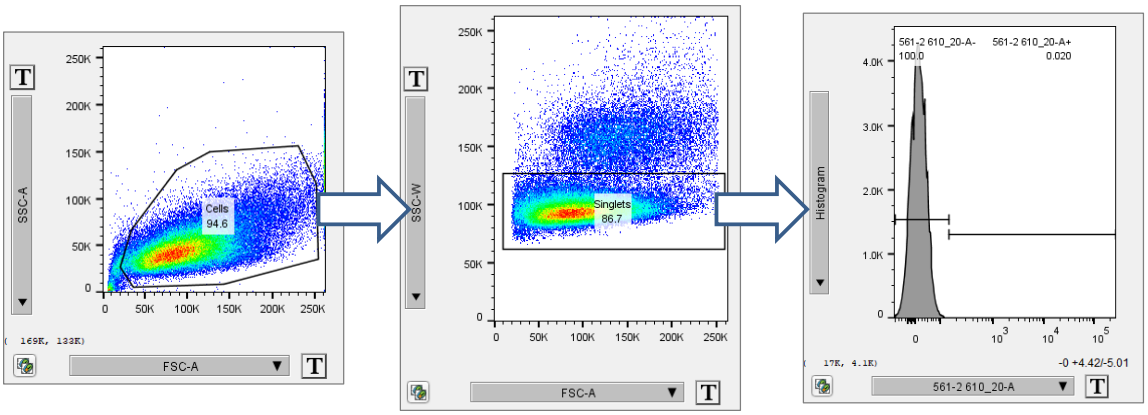


**Figure E.2 Gating strategy in FlowJO X.07 for flow analysis of transfected cells.**

For assessing transfection of H2B-mEmerald and TfR1 constructs (untagged, CoilE-, MiniE-, or MiniR-tagged), singlet cells were gated for green fluorescence (530/30 nm) intensity, and cells greater than 200 relative fluorescence units were deemed transfected. TOMM20-mCherry constructs were assessed analogously but for red fluorescence (610/20 nm).

Transfection efficiency (% transfection) was determined by dividing these cells by the total singlet cells analyzed. The median and mean green or red fluorescence was determined for these positive cells and replicates were graphed in GraphPad Prism 8.0.

For determining statistical significance, values were compared using an unpaired, two-tail t-test. We assumed a Gaussian distribution and unequal variances. Significance values were reported in the figure captions.

# Supplementary Tables

## Table E.1. Summary of genetic constructs.

| Protein Name | **Sequence** (1-letter amino acid code)<br>Sequence annotation key: **Coil tag**; linker; mEmerald; mCherry | Size (Da) | pI | Vector Name |
|---|---|---|---|---|
| **Transferrin Receptor 1 (TfR1)** | MMDQARSAFSNLFGGEPLSYTRFSLARQVDGDNSHVEMKLAADEEENADNNMKAS<br>VRKPKRFNGRLCFAAIALVIFFLIGFMSGYLGYCKRVEQKEECVKLAETEETDKS<br>ETMETEDVPTSSRLYWADLKTLLSEKLNSIEFADTIKQLSQNTYTPREAGSQKDE<br>SLAYYIENQFHEFKFSKVWRDEHYVKIQVKSSIGQNMVTIVQSNGNLDPVESPEG<br>YVAFSKPTEVSGKLVHANFGTKKDFEELSYSVNGSLVIVRAGEITFAEKVANAQS<br>FNAIGVLIYMDKNKFPVVEADLALFGHAHLGTGDPYTPGFPSFNHTQFPPSQSSG<br>LPNIPVQTISRAAAEKLFGKMEGSCPARWNIDSSCKLELSQNQNVKLIVKNVLKE<br>RRILNIFGVIKGYEEPDRYVVVGAQRDALGAGVAAKSSVGTGLLLKLAQVFSDMI<br>SKDGFRPSRSIIFASWTAGDFGAVGATEWLEGYLSSLHLKAFTYINLDKVVLGTS<br>NFKVSASPLLYTLMGKIMQDVKHPVDGKSLYRDSNWISKVEKLSFDNAAYPFLAY<br>SGIPAVSFCFCEDADYPYLGTRLDTYEALTQKVPQLNQMVRTAAEVAGQLIIKLT<br>HDVELNLDYEMYNSKLLSFMKDLNQFKTDIRDMGLSLQWLYSARGDYFRATSRLT<br>TDFHNAEKTNRFVMREINDRIMKVEYHFLSPYVSPRESPFRHIFWGSGSHTLSAL<br>VENLKLRQKNITAFNETLFRNQLALATWTIQGVANALSGDIWNIDNEF | 85731.40 | 6.13 | pcDNA3.1_ TfR1 |
| **TfR1-CoilE** | MMDQARSAFSNLFGGEPLSYTRFSLARQVDGDNSHVEMKLAADEEENADNNMKAS<br>VRKPKRFNGRLCFAAIALVIFFLIGFMSGYLGYCKRVEQKEECVKLAETEETDKS<br>ETMETEDVPTSSRLYWADLKTLLSEKLNSIEFADTIKQLSQNTYTPREAGSQKDE<br>SLAYYIENQFHEFKFSKVWRDEHYVKIQVKSSIGQNMVTIVQSNGNLDPVESPEG<br>YVAFSKPTEVSGKLVHANFGTKKDFEELSYSVNGSLVIVRAGEITFAEKVANAQS<br>FNAIGVLIYMDKNKFPVVEADLALFGHAHLGTGDPYTPGFPSFNHTQFPPSQSSG<br>LPNIPVQTISRAAAEKLFGKMEGSCPARWNIDSSCKLELSQNQNVKLIVKNVLKE<br>RRILNIFGVIKGYEEPDRYVVVGAQRDALGAGVAAKSSVGTGLLLKLAQVFSDMI<br>SKDGFRPSRSIIFASWTAGDFGAVGATEWLEGYLSSLHLKAFTYINLDKVVLGTS<br>NFKVSASPLLYTLMGKIMQDVKHPVDGKSLYRDSNWISKVEKLSFDNAAYPFLAY<br>SGIPAVSFCFCEDADYPYLGTRLDTYEALTQKVPQLNQMVRTAAEVAGQLIIKLT<br>HDVELNLDYEMYNSKLLSFMKDLNQFKTDIRDMGLSLQWLYSARGDYFRATSRLT<br>TDFHNAEKTNRFVMREINDRIMKVEYHFLSPYVSPRESPFRHIFWGSGSHTLSAL<br>VENLKLRQKNITAFNETLFRNQLALATWTIQGVANALSGDIWNIDNEFGSGSGST<br>GM**LEIEAAFLERENTALETRVAELRQRVQRLRNRVSQYRTRYGPL**GGGCLETG | 92312.77 | 6.34 | pcDNA3.1_ TfR1-CoilE |
| **TfR1-MiniE** | MMDQARSAFSNLFGGEPLSYTRFSLARQVDGDNSHVEMKLAADEEENADNNMKAS<br>VRKPKRFNGRLCFAAIALVIFFLIGFMSGYLGYCKRVEQKEECVKLAETEETDKS<br>ETMETEDVPTSSRLYWADLKTLLSEKLNSIEFADTIKQLSQNTYTPREAGSQKDE<br>SLAYYIENQFHEFKFSKVWRDEHYVKIQVKSSIGQNMVTIVQSNGNLDPVESPEG<br>YVAFSKPTEVSGKLVHANFGTKKDFEELSYSVNGSLVIVRAGEITFAEKVANAQS<br>FNAIGVLIYMDKNKFPVVEADLALFGHAHLGTGDPYTPGFPSFNHTQFPPSQSSG<br>LPNIPVQTISRAAAEKLFGKMEGSCPARWNIDSSCKLELSQNQNVKLIVKNVLKE<br>RRILNIFGVIKGYEEPDRYVVVGAQRDALGAGVAAKSSVGTGLLLKLAQVFSDMI<br>SKDGFRPSRSIIFASWTAGDFGAVGATEWLEGYLSSLHLKAFTYINLDKVVLGTS<br>NFKVSASPLLYTLMGKIMQDVKHPVDGKSLYRDSNWISKVEKLSFDNAAYPFLAY<br>SGIPAVSFCFCEDADYPYLGTRLDTYEALTQKVPQLNQMVRTAAEVAGQLIIKLT<br>HDVELNLDYEMYNSKLLSFMKDLNQFKTDIRDMGLSLQWLYSARGDYFRATSRLT<br>TDFHNAEKTNRFVMREINDRIMKVEYHFLSPYVSPRESPFRHIFWGSGSHTLSAL<br>VENLKLRQKNITAFNETLFRNQLALATWTIQGVANALSGDIWNIDNEFGSGSGST<br>GM**LEIEAAFLERENTALETRVAELRQRVQRLRNEYGPL**GGGTG | 91049.28 | 6.06 | pcDNA3.1_ TfR1-MiniE |
| **TfR1-MiniR** | MMDQARSAFSNLFGGEPLSYTRFSLARQVDGDNSHVEMKLAADEEENADNNMKAS<br>VRKPKRFNGRLCFAAIALVIFFLIGFMSGYLGYCKRVEQKEECVKLAETEETDKS<br>ETMETEDVPTSSRLYWADLKTLLSEKLNSIEFADTIKQLSQNTYTPREAGSQKDE<br>SLAYYIENQFHEFKFSKVWRDEHYVKIQVKSSIGQNMVTIVQSNGNLDPVESPEG<br>YVAFSKPTEVSGKLVHANFGTKKDFEELSYSVNGSLVIVRAGEITFAEKVANAQS<br>FNAIGVLIYMDKNKFPVVEADLALFGHAHLGTGDPYTPGFPSFNHTQFPPSQSSG<br>LPNIPVQTISRAAAEKLFGKMEGSCPARWNIDSSCKLELSQNQNVKLIVKNVLKE<br>RRILNIFGVIKGYEEPDRYVVVGAQRDALGAGVAAKSSVGTGLLLKLAQVFSDMI<br>SKDGFRPSRSIIFASWTAGDFGAVGATEWLEGYLSSLHLKAFTYINLDKVVLGTS<br>NFKVSASPLLYTLMGKIMQDVKHPVDGKSLYRDSNWISKVEKLSFDNAAYPFLAY<br>SGIPAVSFCFCEDADYPYLGTRLDTYEALTQKVPQLNQMVRTAAEVAGQLIIKLT<br>HDVELNLDYEMYNSKLLSFMKDLNQFKTDIRDMGLSLQWLYSARGDYFRATSRLT<br>TDFHNAEKTNRFVMREINDRIMKVEYHFLSPYVSPRESPFRHIFWGSGSHTLSAL<br>VENLKLRQKNITAFNETLFRNQLALATWTIQGVANALSGDIWNIDNEFGSGSGST<br>GMGSS**LEIRVAFLRQRNTALRTEVAELEQEVQRLENRYGPL**TG | 91136.41 | 6.14 | pcDNA3.1_ TfR1-MiniR |
| **H2B-mEmerald** | MPEPAKSAPAPKKGSKKAVTKAQKKGGKKRKRSRKESYSIYVYKVLKQVHPDTGI<br>SSKAMGIMNSFVNDIFERIAGEASRLAHYNKRSTITSREIQTAVRLLLPGELAKH<br>AVSEGTKAITKYTSAKDPPVATMVSKGEELFTGVVPILVELDGDVNGHKFSVSGE | 41320.19 | 9.26 | H2B-6-mEmerald Addgene: |

| | | | | |
|---|---|---|---|---|
| | GEGDATYGKLTLKFICTTGKLPVPWPTLVTTLTYGVQCFARYPDHMKQHDFFKSA MPEGYVQERTIFFKDDGNYKTRAEVKFEGDTLVNRIELKGIDFKEDGNILGHKLE YNYNSHKVYITADKQKNGIKVNFKTRHNIEDGSVQLADHYQQNTPIGDGPVLLPD NHYLSTQSALSKDPNEKRDHMVLLEFVTAAGITLGMDELYK | | | 54111 |
| **H2B-CoilE** | MPEPAKSAPAPKKGSKKAVTKAQKKGGKKRKRSRKESYSIYVYKVLKQVHPDTGI SSKAMGIMNSFVNDIFERIAGEASRLAHYNKRSTITSREIQTAVRLLLPGELAKH AVSEGTKAITKYTSAKDPM**LEIEAAFLERENTALETRVAELRQRVQRLRNRVSQY RTRYGPL** | 19388.45 | 10.42 | H2B-6-CoilE |
| **H2B-CoilE-mEmerald** | MPEPAKSAPAPKKGSKKAVTKAQKKGGKKRKRSRKESYSIYVYKVLKQVHPDTGI SSKAMGIMNSFVNDIFERIAGEASRLAHYNKRSTITSREIQTAVRLLLPGELAKH AVSEGTKAITKYTSAKDPPVM**LEIEAAFLERENTALETRVAELRQRVQRLRNRVS QYRTRYGPL**GGGGPVATMVSKGEELFTGVVPILVELDGDVNGHKFSVSGEGEGDA TYGKLTLKFICTTGKLPVPWPTLVTTLTYGVQCFARYPDHMKQHDFFKSAMPEGY VQERTIFFKDDGNYKTRAEVKFEGDTLVNRIELKGIDFKEDGNILGHKLEYNYNS HKVYITADKQKNGIKVNFKTRHNIEDGSVQLADHYQQNTPIGDGPVLLPDNHYLS TQSALSKDPNEKRDHMVLLEFVTAAGITLGMDELYK | 47060.74 | 9.39 | H2B-6-CoilE-mEmerald |
| **H2B-MiniE-mEmerald** | MPEPAKSAPAPKKGSKKAVTKAQKKGGKKRKRSRKESYSIYVYKVLKQVHPDTGI SSKAMGIMNSFVNDIFERIAGEASRLAHYNKRSTITSREIQTAVRLLLPGELAKH AVSEGTKAITKYTSAKDPM**LEIEAAFLERENTALETRVAELRQRVQRLRNEYGPL** PVATMVSKGEELFTGVVPILVELDGDVNGHKFSVSGEGEGDATYGKLTLKFICTT GKLPVPWPTLVTTLTYGVQCFARYPDHMKQHDFFKSAMPEGYVQERTIFFKDDGN YKTRAEVKFEGDTLVNRIELKGIDFKEDGNILGHKLEYNYNSHKVYITADKQKNG IKVNFKTRHNIEDGSVQLADHYQQNTPIGDGPVLLPDNHYLSTQSKLSKDPNEKR DHMVLLEFVTAAGITLGMDELYK | 45775.31 | 9.24 | H2B-6-MiniE-mEmerald |
| **H2B-MiniR-mEmerald** | MPEPAKSAPAPKKGSKKAVTKAQKKGGKKRKRSRKESYSIYVYKVLKQVHPDTGI SSKAMGIMNSFVNDIFERIAGEASRLAHYNKRSTITSREIQTAVRLLLPGELAKH AVSEGTKAITKYTSAKDPM**LEIRVAFLRQRNTALRTEVAELEQEVQRLENRYGPL** PVATMVSKGEELFTGVVPILVELDGDVNGHKFSVSGEGEGDATYGKLTLKFICTT GKLPVPWPTLVTTLTYGVQCFARYPDHMKQHDFFKSAMPEGYVQERTIFFKDDGN YKTRAEVKFEGDTLVNRIELKGIDFKEDGNILGHKLEYNYNSHKVYITADKQKNG IKVNFKTRHNIEDGSVQLADHYQQNTPIGDGPVLLPDNHYLSTQSKLSKDPNEKR DHMVLLEFVTAAGITLGMDELYK | 45802.38 | 9.29 | H2B-6-MiniR-mEmerald |
| **TOMM20-mCherry** | MVGRNSAIAAGVCGALFIGYCIYFDRKRRSDPNFKNRLRERRKKQKLAKERAGLS KLPDLKDAEAVQKFFLEEIQLGEELLAQGEYEKGVDHLTNAIAVCGQPQQLLQVL QQTLPPPVFQMLLTKLPTISQRIVSAQSLAEDDVEGGSGDPPVATMVSKGEEDNM AIIKEFMRFKVHMEGSVNGHEFEIEGEGEGRPYEGTQTAKLKVTKGGPLPFAWDI LSPQFMYGSKAYVKHPADIPDYLKLSFPEGFKWERVMNFEDGGVVTVTQDSSLQD GEFIYKVKLRGTNFPSDGPVMQKKTMGWEASSERMYPEDGALKGEIKQRLKLKDG GHYDAEVKTTYKAKKPVQLPGAYNVNIKLDITSHNEDYTIVEQYERAEGRHSTGG MDELYK | 43840.92 | 6.08 | TOMM20-mCherry-N-10 Addgene: 55146 |
| **TOMM20-CoilE-mCherry** | MVGRNSAIAAGVCGALFIGYCIYFDRKRRSDPNFKNRLRERRKKQKLAKERAGLS KLPDLKDAEAVQKFFLEEIQLGEELLAQGEYEKGVDHLTNAIAVCGQPQQLLQVL QQTLPPPVFQMLLTKLPTISQRIVSAQSLAEDDVEGGSGM**LEIEAAFLERENTAL ETRVAELRQRVQRLRNRVSQYRTRYGPL**DPPVATMVSKGEEDNMAIIKEFMRFKV HMEGSVNGHEFEIEGEGEGRPYEGTQTAKLKVTKGGPLPFAWDILSPQFMYGSKA YVKHPADIPDYLKLSFPEGFKWERVMNFEDGGVVTVTQDSSLQDGEFIYKVKLRG TNFPSDGPVMQKKTMGWEASSERMYPEDGALKGEIKQRLKLKDGGHYDAEVKTTY KAKKPVQLPGAYNVNIKLDITSHNEDYTIVEQYERAEGRHSTGGMDELYK | 49157.01 | 6.71 | TOMM20-CoilE-mCherry |
| **TOMM20-MiniE-mCherry** | MVGRNSAIAAGVCGALFIGYCIYFDRKRRSDPNFKNRLRERRKKQKLAKERAGLS KLPDLKDAEAVQKFFLEEIQLGEELLAQGEYEKGVDHLTNAIAVCGQPQQLLQVL QQTLPPPVFQMLLTKLPTISQRIVSAQSLAEDDVEGGSGM**LEIEAAFLERENTAL ETRVAELRQRVQRLRNEYGPL**DPPVATMVSKGEEDNMAIIKEFMRFKVHMEGSVN GHEFEIEGEGEGRPYEGTQTAKLKVTKGGPLPFAWDILSPQFMYGSKAYVKHPAD IPDYLKLSFPEGFKWERVMNFEDGGVVTVTQDSSLQDGEFIYKVKLRGTNFPSDG PVMQKKTMGWEASSERMYPEDGALKGEIKQRLKLKDGGHYDAEVKTTYKAKKPVQ LPGAYNVNIKLDITSHNEDYTIVEQYERAEGRHSTGGMDELYK | 48238.94 | 5.96 | TOMM20-MiniE-mCherry |
| **TOMM20-MiniR-mCherry** | MVGRNSAIAAGVCGALFIGYCIYFDRKRRSDPNFKNRLRERRKKQKLAKERAGLS KLPDLKDAEAVQKFFLEEIQLGEELLAQGEYEKGVDHLTNAIAVCGQPQQLLQVL QQTLPPPVFQMLLTKLPTISQRIVSAQSLAEDDVEGGSGM**LEIRVAFLRQRNTAL RTEVAELEQEVQRLENRYGPL**DPPVATMVSKGEEDNMAIIKEFMRFKVHMEGSVN GHEFEIEGEGEGRPYEGTQTAKLKVTKGGPLPFAWDILSPQFMYGSKAYVKHPAD IPDYLKLSFPEGFKWERVMNFEDGGVVTVTQDSSLQDGEFIYKVKLRGTNFPSDG PVMQKKTMGWEASSERMYPEDGALKGEIKQRLKLKDGGHYDAEVKTTYKAKKPVQ LPGAYNVNIKLDITSHNEDYTIVEQYERAEGRHSTGGMDELYK | 48266.01 | 6.10 | TOMM20-MiniR-mCherry |

## Works Cited


1. McGraw, T. E., Greenfield, L. & Maxfield, F. R. Functional expression of the human transferrin receptor cDNA in Chinese hamster ovary cells deficient in endogenous transferrin receptor. *J. Cell Biol.* **105**, 207–214 (1987).
2. Costantini, L. M. & Snapp, E. L. Fluorescent proteins in cellular organelles: serious pitfalls and some solutions. *DNA Cell Biol.* **32**, 622–627 (2013).
3. Doh, J., Enns, C. & Beatty, K. Implementing VIPER for Imaging Cellular Proteins by Fluorescence Microscopy. *BIO-Protoc.* **9**, (2019).